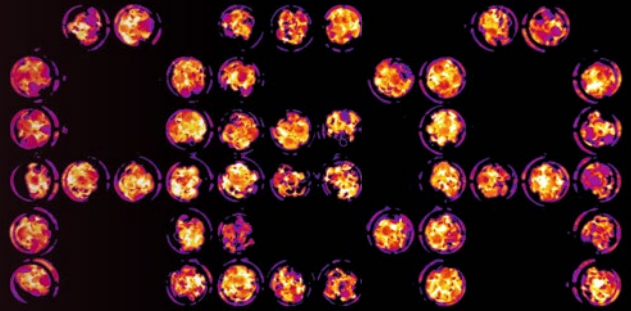


Methods in
Molecular Biology 2213

Springer Protocols



Glenn R. Hicks
Chunhua Zhang *Editors*

Plant Chemical Genomics

Methods and Protocols

Second Edition

 Humana Press

METHODS IN MOLECULAR BIOLOGY

Series Editor

John M. Walker

**School of Life and Medical Sciences,
University of Hertfordshire
Hatfield, Hertfordshire, UK**

For further volumes:

<http://www.springer.com/series/7651>

For over 35 years, biological scientists have come to rely on the research protocols and methodologies in the critically acclaimed *Methods in Molecular Biology* series. The series was the first to introduce the step-by-step protocols approach that has become the standard in all biomedical protocol publishing. Each protocol is provided in readily-reproducible step-by-step fashion, opening with an introductory overview, a list of the materials and reagents needed to complete the experiment, and followed by a detailed procedure that is supported with a helpful notes section offering tips and tricks of the trade as well as troubleshooting advice. These hallmark features were introduced by series editor Dr. John Walker and constitute the key ingredient in each and every volume of the *Methods in Molecular Biology* series. Tested and trusted, comprehensive and reliable, all protocols from the series are indexed in PubMed.

Plant Chemical Genomics

Methods and Protocols

Second Edition

Edited by

Glenn R. Hicks

*Department of Botany and Plant Sciences, Institute of Integrative Genome Biology,
University of California, Riverside, CA, USA*

Chunhua Zhang

*Department of Botany and Plant Pathology, Center for Plant Biology, Purdue University,
West Lafayette, IN, USA*

 **Humana Press**

Editors

Glenn R. Hicks
Department of Botany
and Plant Sciences
Institute of Integrative
Genome Biology
University of California
Riverside, CA, USA

Chunhua Zhang
Department of Botany
and Plant Pathology
Center for Plant Biology
Purdue University
West Lafayette, IN, USA

ISSN 1064-3745

Methods in Molecular Biology

ISBN 978-1-0716-0953-8

<https://doi.org/10.1007/978-1-0716-0954-5>

ISSN 1940-6029 (electronic)

ISBN 978-1-0716-0954-5 (eBook)

© Springer Science+Business Media, LLC, part of Springer Nature 2014, 2021

This work is subject to copyright. All rights are reserved by the Publisher, whether the whole or part of the material is concerned, specifically the rights of translation, reprinting, reuse of illustrations, recitation, broadcasting, reproduction on microfilms or in any other physical way, and transmission or information storage and retrieval, electronic adaptation, computer software, or by similar or dissimilar methodology now known or hereafter developed.

The use of general descriptive names, registered names, trademarks, service marks, etc. in this publication does not imply, even in the absence of a specific statement, that such names are exempt from the relevant protective laws and regulations and therefore free for general use.

The publisher, the authors, and the editors are safe to assume that the advice and information in this book are believed to be true and accurate at the date of publication. Neither the publisher nor the authors or the editors give a warranty, expressed or implied, with respect to the material contained herein or for any errors or omissions that may have been made. The publisher remains neutral with regard to jurisdictional claims in published maps and institutional affiliations.

This Humana imprint is published by the registered company Springer Science+Business Media, LLC, part of Springer Nature.

The registered company address is: 1 New York Plaza, New York, NY 10004, U.S.A.

Preface

The first edition of *Plant Chemical Genomics: Methods and Protocols* was published in 2014. At that time, the use of chemical genomics was rapidly developing with critical success stories leading to an enhanced understanding of plant stress, pathogen responses, endomembrane trafficking, hormone signaling, and other areas in plant biology. As a result, the focus of that edition was on sharing with the scientific community approaches to screen synthetic small molecule libraries for novel compounds affecting a broad range of plant processes. Along with this emphasis were methods necessary for successful screening campaigns including automation and imaging, cheminformatics, and protocols for examining hormones and metabolites using mass spectroscopy, NMR, and HPLC. All of these technologies enabled chemical screening. Target identification and validation were critical as well, but only several chapters were included as this reflected where the plant chemical genomics community was at the time. There were still relatively few examples in academia where small molecule protein targets were identified successfully. This has changed as the community of plant biologists utilizing small molecule approaches has increased along with increased sophistication of screening and target protein identification.

The field has now evolved to the point that finding a novel bioactive chemical *and* its cognate target is important or even required for scientific impact. For the basic research community, it is critical that a small molecule and its target(s) contribute new insights into plant biology. At the time of the first edition, the primary means of target identification in plants was the use of *Arabidopsis* genetics and genomics approaches, primarily forward EMS and reverse genetic strategies. Yeast and other model systems were also employed. We termed the field chemical genomics because of the genomics emphasis. Today it is probably more encompassing to term our field as chemical biology because we utilize chemistry including synthetic (and native) small molecules and a variety of tools to understand biological processes.

This latest volume contains some of the latest methods for the screening of plants for novel bioactive chemicals including areas not previously covered such as lipid signaling, a photoreceptor, and assaying drug efficacy in plant cells. In addition, there are contributions that highlight approaches that expand our vision of small molecule screens to include peptide ligands to generate new variation that can be exploited for discovery. An area of great interest in plant chemical biology that has and continues to be important is using novel chemicals to affect and dissect hormone signaling as reflected in chapters on small molecules impacting the perception of the hormones ABA, ethylene, and auxin.

Another recent development is the application of simpler microscale methods to simplify target identification and validation. This permits the use of more than one method to provide evidence of ligand-target interaction increasing confidence in our conclusions. We have emphasized these approaches with a section devoted to examples of these methods. Along with these microscale methods are examples of chemical proteomics in which proteomics is used to identify chemical targets. It should be noted that these methods have mostly been employed for target identification and validation in mammalian systems and are only now becoming more common practice in plants and thus reflected in the content of this volume. In addition, the emergence of sophisticated automated phenotyping and *in vivo*

photoaffinity labeling combined with chemical proteomics is on the horizon for perhaps a future edition of this series.

Plant Chemical Genomics: Methods and Protocols, Second Edition is an extension and companion to the first volume. We hope that both editions will provide a foundation in methodologies for novices to the field as well as experts within the plant chemical biology community.

Riverside, CA, USA
West Lafayette, IN, USA

Glenn R. Hicks
Chunhua Zhang

Contents

<i>Preface</i>	<i>v</i>
<i>Contributors</i>	<i>ix</i>

PART I SCREENING FOR NOVEL SMALL MOLECULES

1 Chemical Genetics to Uncover Mechanisms Underlying Lipid-Mediated Signaling Events in Plants	3
<i>Bibi Rafeiza Khan, Kent D. Chapman, and Alison B. Blancaflor</i>	
2 Method for Phenotypic Chemical Screening to Identify Cryptochrome Inhibitors	17
<i>Emiko Okubo-Kurihara, Wen-Dee Ong, Yukio Kurihara, Natsumaro Kutsuna, and Minami Matsui</i>	
3 Whole-Seedling-Based Chemical Genetic Screens in <i>Arabidopsis</i>	29
<i>Shuai Huang and Xin Li</i>	
4 Identification of Type III Secretion Inhibitors for Plant Disease Management	39
<i>Roger de Pedro Jové, Pau Sebastià, and Marc Valls</i>	
5 Investigation of Drug Efficacy by Screening Bioactive Chemical Effects on Plant Cell Subcellular Architecture	49
<i>Gian Pietro Di Sansebastiano</i>	

PART II NEW APPROACHES TO VARIATION: PEPTIDE SCREEN FOR NOVEL EFFECTORS

6 In Vivo Chemical Genomics with Random Cyclized Peptides	61
<i>Tautvydas Shuipys, Maureen Clancy, Elizabeth Estrada-Johnson, and Kevin M. Folta</i>	
7 Interfering Peptides Targeting Protein–Protein Interactions in the Ethylene Plant Hormone Signaling Pathway as Tools to Delay Plant Senescence	71
<i>Alexander Hofmann, Alexander Minges, and Georg Groth</i>	

PART III CHEMICAL GENOMICS IN HORMONE SIGNALING

8 The Screening for Novel Inhibitors of Auxin-Induced Ca ²⁺ Signaling	89
<i>Kjell De Vriese, Long Nguyen, Simon Stael, Dominique Audenaert, Tom Beeckman, and Steffen Vanneste</i>	
9 Identification of ABA Receptor Agonists Using a Multiplexed High-Throughput Chemical Screening	99
<i>Jorge Lozano-Juste, Irene García-Maquilón, José Brea, Rocío Piña, Armando Albert, Pedro L. Rodríguez, and María Isabel Loza</i>	

10	A Luciferase Reporter Assay to Identify Chemical Activators of ABA Signaling	113
	<i>Irene García-Maquilón, Pedro L. Rodríguez, Aditya S. Vaidya, and Jorge Lozano-Juste</i>	
11	Identification of Novel Molecular Regulators Modulating Ethylene Biosynthesis Using EMS-Based Genetic Screening.....	123
	<i>Chanung Park, Dong Hye Seo, Joseph Buckley, and Gyeong Mee Yoon</i>	
12	Investigation of Auxin Biosynthesis and Action Using Auxin Biosynthesis Inhibitors	131
	<i>Kazuo Soeno, Akiko Sato, and Yukihisa Shimada</i>	
PART IV TARGET IDENTIFICATION AND CONFIRMATION APPROACHES		
13	Target Profiling of an Anticancer Drug Curcumin by an In Situ Chemical Proteomics Approach.....	147
	<i>Dan-dan Liu, Chang Zou, Jianbin Zhang, Peng Gao, Yongping Zhu, Yuqing Meng, Nan Ma, Ming Lv, Chengchao Xu, Qingsong Lin, and Jigang Wang</i>	
14	Label-Free Target Identification and Confirmation Using Thermal Stability Shift Assays	163
	<i>Cecilia Rodríguez-Furlan and Glenn R. Hicks</i>	
15	Drug Affinity Responsive Target Stability (DARTS) Assay to Detect Interaction Between a Purified Protein and a Small Molecule.....	175
	<i>Lei Huang, Diwen Wang, and Chunhua Zhang</i>	
16	Using Differential Scanning Fluorimetry (DSF) to Detect Ligand Binding with Purified Protein	183
	<i>Xiaohui Li and Chunhua Zhang</i>	
17	Microscale Thermophoresis (MST) to Detect the Interaction Between Purified Protein and Small Molecule	187
	<i>Lei Huang and Chunhua Zhang</i>	
	<i>Index</i>	195

Contributors

- ARMANDO ALBERT • *Instituto de Química Física Rocasolano, Consejo Superior de Investigaciones Científicas (IQFR-CSIC), Madrid, Spain*
- DOMINIQUE AUDENAERT • *Screening Core, VIB, Ghent, Belgium; Centre for Bioassay Development and Screening (C-BIOS), Ghent University, Ghent, Belgium*
- TOM BEECKMAN • *Department of Plant Biotechnology and Bioinformatics, Ghent University, Ghent, Belgium; VIB Center for Plant Systems Biology, Ghent, Belgium*
- ELISON B. BLANCAFLOR • *Noble Research Institute LLC, Ardmore, OK, USA*
- JOSÉ BREA • *Innopharma Screening Platform, BioFarma Research Group, Centro de Investigación en Medicina Molecular y Enfermedades Crónicas (CiMUS), Universidad de Santiago de Compostela, Santiago de Compostela, Spain*
- JOSEPH BUCKLEY • *Department of Biological Science, Purdue University, West Lafayette, IN, USA*
- KENT D. CHAPMAN • *Department of Biological Sciences, BioDiscovery Institute, University of North Texas, Denton, TX, USA*
- MAUREEN CLANCY • *Horticultural Sciences Department, University of Florida, Gainesville, FL, USA*
- ROGER DE PEDRO JOVÉ • *Department of Genetics, University of Barcelona, Barcelona, Catalonia, Spain; Centre for Research in Agricultural Genomics (CSIC-IRTA-UAB-UB), Bellaterra, Catalonia, Spain*
- KJELL DE VRIESE • *Department of Plant Biotechnology and Bioinformatics, Ghent University, Ghent, Belgium; VIB Center for Plant Systems Biology, Ghent, Belgium*
- GIAN PIETRO DI SANSEBASTIANO • *Department of Biological and Environmental Sciences and Technologies (DiSTeBA), University of Salento, Lecce, Italy*
- ELIZABETH ESTRADA-JOHNSON • *Horticultural Sciences Department, University of Florida, Gainesville, FL, USA*
- KEVIN M. FOLTA • *Genetics and Genomics Graduate Program, University of Florida, Gainesville, FL, USA; Horticultural Sciences Department, University of Florida, Gainesville, FL, USA; Plant Molecular and Cellular Biology Program, University of Florida, Gainesville, FL, USA*
- PENG GAO • *Institute of Chinese Materia Medica, and Artemisinin Research Center, China Academy of Chinese Medical Sciences, Beijing, China*
- IRENE GARCÍA-MAQUILÓN • *Instituto de Biología Molecular y Celular de Plantas, Consejo Superior de Investigaciones Científicas, Universidad Politécnica de Valencia (IBMCP-CSIC-UPV), Valencia, Spain*
- GEORG GROTH • *Institute of Biochemical Plant Physiology, Heinrich Heine University Düsseldorf, Düsseldorf, Germany*
- GLENN R. HICKS • *Department of Botany and Plant Sciences, Institute of Integrative Genome Biology, University of California, Riverside, CA, USA; Uppsala Bio Center, Swedish University of Agricultural Sciences, Uppsala, Sweden*
- ALEXANDER HOFMANN • *Institute of Biochemical Plant Physiology, Heinrich Heine University Düsseldorf, Düsseldorf, Germany*
- LEI HUANG • *Department of Botany and Pathology, Purdue University, West Lafayette, IN, USA; Center for Plant Biology, Purdue University, West Lafayette, IN, USA*

- SHUAI HUANG • *Department of Microbial Pathogenesis, Howard Hughes Medical Institute, Yale University School of Medicine, New Haven, CT, USA; Yale Systems Biology Institute, Yale University, West Haven, CT, USA*
- BIBI RAFEIZA KHAN • *Department of Biology, Turkeyen Campus, University of Guyana, Greater Georgetown, Guyana*
- YUKIO KURIHARA • *RIKEN, Center for Sustainable Resource Science, Yokohama, Kanagawa, Japan*
- NATSUMARO KUTSUNA • *LPixel Inc., Kanagawa, Japan*
- XIAOHUI LI • *Department of Botany and Plant Pathology, Purdue University, West Lafayette, IN, USA; Purdue Center for Plant Biology, Purdue University, West Lafayette, IN, USA*
- XIN LI • *Michael Smith Laboratories, University of British Columbia, Vancouver, BC, Canada; Department of Botany, University of British Columbia, Vancouver, BC, Canada*
- QINGSONG LIN • *Department of Biological Sciences, Faculty of Science, National University of Singapore, Singapore, Singapore*
- DAN-DAN LIU • *Institute of Chinese Materia Medica, and Artemisinin Research Center, China Academy of Chinese Medical Sciences, Beijing, China*
- MARÍA ISABEL LOZA • *Innopharma Screening Platform, BioFarma Research Group, Centro de Investigación en Medicina Molecular y Enfermedades Crónicas (CiMUS), Universidad de Santiago de Compostela, Santiago de Compostela, Spain*
- JORGE LOZANO-JUSTE • *Instituto de Biología Molecular y Celular de Plantas, Consejo Superior de Investigaciones Científicas, Universidad Politécnica de Valencia (IBMCP-CSIC-UPV), Valencia, Spain*
- MING LV • *Institute of Chinese Materia Medica, and Artemisinin Research Center, China Academy of Chinese Medical Sciences, Beijing, China*
- NAN MA • *Institute of Chinese Materia Medica, and Artemisinin Research Center, China Academy of Chinese Medical Sciences, Beijing, China*
- MINAMI MATSUI • *RIKEN, Center for Sustainable Resource Science, Yokohama, Kanagawa, Japan*
- YUQING MENG • *Institute of Chinese Materia Medica, and Artemisinin Research Center, China Academy of Chinese Medical Sciences, Beijing, China*
- ALEXANDER MINGES • *Institute of Biochemical Plant Physiology, Heinrich Heine University Düsseldorf, Düsseldorf, Germany*
- LONG NGUYEN • *Screening Core, VIB, Ghent, Belgium; Centre for Bioassay Development and Screening (C-BIOS), Ghent University, Ghent, Belgium*
- EMIKO OKUBO-KURIHARA • *RIKEN, Center for Sustainable Resource Science, Yokohama, Kanagawa, Japan*
- WEN-DEE ONG • *Zhejiang A & F University, School of Forestry and Biotechnology, Hangzhou, China*
- CHANUNG PARK • *Department of Botany and Plant Pathology, Purdue University, West Lafayette, IN, USA; Center for Plant Biology, Purdue University, West Lafayette, IN, USA*
- ROCÍO PIÑA • *Innopharma Screening Platform, BioFarma Research Group, Centro de Investigación en Medicina Molecular y Enfermedades Crónicas (CiMUS), Universidad de Santiago de Compostela, Santiago de Compostela, Spain*

- PEDRO L. RODRIGUEZ • *Instituto de Biología Molecular y Celular de Plantas, Consejo Superior de Investigaciones Científicas, Universidad Politécnica de Valencia (IBMCP-CSIC-UPV), Valencia, Spain*
- CECILIA RODRIGUEZ-FURLAN • *Department of Botany and Plant Sciences, Institute of Integrative Genome Biology, University of California, Riverside, CA, USA*
- AKIKO SATO • *Yokohama City University, Kihara Institute for Biological Research, Yokohama, Kanagawa, Japan*
- PAU SEBASTIÀ • *Centre for Research in Agricultural Genomics (CSIC-IRTA-UAB-UB), Bellaterra, Catalonia, Spain*
- DONG HYE SEO • *Department of Botany and Plant Pathology, Purdue University, West Lafayette, IN, USA; Center for Plant Biology, Purdue University, West Lafayette, IN, USA*
- YUKIHISA SHIMADA • *Yokohama City University, Kihara Institute for Biological Research, Yokohama, Kanagawa, Japan*
- TAUTVYDAS SHUIPYS • *Genetics and Genomics Graduate Program, University of Florida, Gainesville, FL, USA*
- KAZUO SOENO • *Western Region Agricultural Research Center (WARC), National Agriculture and Food Research Organization (NARO), Kagawa, Japan*
- SIMON STAEL • *Department of Plant Biotechnology and Bioinformatics, Ghent University, Ghent, Belgium; VIB Center for Plant Systems Biology, Ghent, Belgium*
- ADITYA S. VAIDYA • *Department of Botany and Plant Sciences, Institute for Integrative Genome Biology, University of California, Riverside, Riverside, CA, USA*
- MARC VALLS • *Department of Genetics, University of Barcelona, Barcelona, Catalonia, Spain; Centre for Research in Agricultural Genomics (CSIC-IRTA-UAB-UB), Bellaterra, Catalonia, Spain*
- STEFFEN VANNESTE • *Department of Plant Biotechnology and Bioinformatics, Ghent University, Ghent, Belgium; VIB Center for Plant Systems Biology, Ghent, Belgium; Lab of Plant Growth Analysis, Ghent University Global Campus, Incheon, Republic of Korea*
- DIWEN WANG • *Department of Botany and Pathology, Purdue University, West Lafayette, IN, USA; Center for Plant Biology, Purdue University, West Lafayette, IN, USA*
- JIGANG WANG • *Institute of Chinese Materia Medica, and Artemisinin Research Center, China Academy of Chinese Medical Sciences, Beijing, China; Clinical Medical Research Center, The First Affiliated Hospital of Southern University of Science and Technology, The Second Clinical Medical College of Jinan University, Shenzhen Public Service Platform on Tumor Precision Medicine and Molecular Diagnosis, Shenzhen People's Hospital, Shenzhen, China*
- CHENGCHAO XU • *Institute of Chinese Materia Medica, and Artemisinin Research Center, China Academy of Chinese Medical Sciences, Beijing, China; Clinical Medical Research Center, The First Affiliated Hospital of Southern University of Science and Technology, The Second Clinical Medical College of Jinan University, Shenzhen Public Service Platform on Tumor Precision Medicine and Molecular Diagnosis, Shenzhen People's Hospital, Shenzhen, China*
- GYEONG MEE YOON • *Department of Botany and Plant Pathology, Purdue University, West Lafayette, IN, USA; Center for Plant Biology, Purdue University, West Lafayette, IN, USA*
- CHUNHUA ZHANG • *Department of Botany and Plant Pathology, Center for Plant Biology, Purdue University, West Lafayette, IN, USA*

- JIANBIN ZHANG • *Department of Oncology, Clinical Research Institute, Zhejiang Provincial People's Hospital, People's Hospital of Hangzhou Medical College, Hangzhou, China*
- YONGPING ZHU • *Institute of Chinese Materia Medica, and Artemisinin Research Center, China Academy of Chinese Medical Sciences, Beijing, China*
- CHANG ZOU • *Clinical Medical Research Center, The First Affiliated Hospital of Southern University of Science and Technology, The Second Clinical Medical College of Jinan University, Shenzhen Public Service Platform on Tumor Precision Medicine and Molecular Diagnosis, Shenzhen People's Hospital, Shenzhen, China*

Part I

Screening for Novel Small Molecules



Chapter 1

Chemical Genetics to Uncover Mechanisms Underlying Lipid-Mediated Signaling Events in Plants

Bibi Rafeiza Khan, Kent D. Chapman, and Elison B. Blancaflor

Abstract

Like animals, plants use various lipids as signaling molecules to guide their growth and development. The focus of our work is on the *N*-acylethanolamine (NAE) group of lipid mediators, which have been shown to play important physiological roles in plants. However, mechanisms by which NAEs modulate plant function remain elusive. Chemical genetics has emerged as a potent tool to elucidate signaling pathways in plants, particularly those orchestrated by plant hormones. Like plant hormones, exogenous application of NAEs elicits distinct plant growth phenotypes that can serve as biological readouts for chemical genetic screens. For example, *N*-lauroylethanolamide (NAE 12:0) inhibits seedling development in the model plant *Arabidopsis thaliana*. Thus, a library of small synthetic chemical compounds can be rapidly screened for their ability to reverse the inhibitory effect of NAE 12:0 on seedling development. Chemicals identified through such screens could be potential agonists/antagonists of NAE receptors or signaling pathways and therefore serve as additional tools for understanding NAE function in plants. In this chapter, we describe general protocols for NAE 12:0-based chemical genetic screens in *Arabidopsis*. Although such screens were designed primarily for NAE 12:0, they could potentially be applied for similar work with other NAE species or plant lipid mediators.

Key words *N*-Acylethanolamines, *N*-Lauroylethanolamide, Fatty acid amide hydrolase, *Arabidopsis*, Lipids, Chemical genetics, Growth inhibition

1 Introduction

In eukaryotes, *N*-acylethanolamines (NAEs) are a ubiquitous group of conserved fatty acid amides [1, 2]. NAEs were first isolated in animals, where they regulate several physiological and behavioral responses primarily through the endocannabinoid signaling pathway [3, 4]. The synthesis and degradation of NAEs are highly conserved [5, 6]. They are produced through the action of phospholipase D on a minor membrane lipid, *N*-acylphosphatidylethanolamine (NAPE) [7, 8].

The NAE species generated by *NAPE* hydrolysis differ in the length of their acyl chain and the degree of saturation. In just the last two decades, a combination of pharmacological studies and

genetic analysis has provided insights into several functional roles for NAEs in plants. Studies revealed that NAEs are most abundant and ubiquitous in desiccated seeds where during germination and early seedlings establishment, their levels rapidly decline [2, 9]. NAEs also elicit physiological responses during early seedling development, flowering, and bacterial pathogen infection [10–12]. Specifically, NAEs may act as negative regulators of seedling growth and stress responses, and emerging studies revealed cross talk with stress hormones such as abscisic acid (ABA) and salicylic acid (SA) [5, 11, 13–16]. Pharmacological analysis with *N*-lauroylethanolamide (NAE 12:0) revealed that it has negative effects on cell walls, cytoskeletal organization, endomembrane trafficking, and cell shape [5, 13].

The physiological responses elicited by NAEs are terminated by the action of the enzyme, fatty acid amide hydrolase (FAAH) [12, 17–22]. Recently, malonylation of NAE 12:0 by a phenolic glucoside malonyltransferase (PMAT1) was implicated in modulating NAE biological activity [23]. In both animals and plants, FAAH has broad substrate specificity and it catalyzes the hydrolysis of NAEs to ethanolamine and free fatty acid. In animals, FAAH is a target for the development of drugs for therapeutic treatment of physiological disorders linked to endocannabinoid signaling [24].

The distinct and rapid effects of exogenous NAE12:0 on *Arabidopsis* seedling development [10] pave the way for the application of chemical genetics to studies of NAE function in plants. A simple approach would be to screen a library of small synthetic molecules that mitigate the inhibitory effects of NAE12:0 on seedling development. Chemicals identified through such a screen could be potential NAE receptor antagonists or activators and inhibitors of NAE degradation/conjugation (e.g., FAAH, PMAT1) and synthesis, respectively. Using chemical genetics, we previously identified a small synthetic molecule called 6-(2-methoxyphenyl)-1,3-dimethyl-5-phenyl-1*H*-pyrrolo[3,4-*d*]pyrimidine-2,4(3*H*,6*H*)-dione (MDPD), which mitigates NAE12:0's inhibitory effect on seedling growth in part by enhancing FAAH activity [25]. In this chapter, we describe general procedures for deployment of chemical genetics in studies of NAE signaling with the expectation that such approaches could generate novel pharmacological tools to help dissect NAE function in plants.

2 Materials

2.1 Preparing *Arabidopsis* Seeds for Screening

1. Dry *Arabidopsis thaliana* Columbia-0 seeds.
2. 1.5-ml Eppendorf tubes.
3. 30% Clorox bleach.
4. 0.1% Triton X-100.

5. Vortex.
6. Sterilized double-distilled water.
7. Pipette (100–1000 μl).
8. Pipette (0.2–2 μl).
9. Mini tabletop centrifuge.

2.2 Preparing Media for Screening

1. 0.5 \times Murashige and Skoog (MS) salt with micronutrients and 1% sucrose, pH 5.7.
2. Autoclave.

2.3 Preparing for Chemical Screening

1. 96-well plates with lids.
2. 24-well plates with lids.
3. Parafilm.
4. Multichannel pipettes (2–20 μl and 20–200 μl).
5. Laminar flow hood.
6. Dimethyl sulfoxide (DMSO).
7. *N*-Lauroylethanolamide (NAE 12:0) powder.
8. Chembridge library of 10,000 small synthetic molecules.
9. 200-ml and 500-ml Erlenmeyer flasks.
10. Orbital shaker.
11. 50-ml Falcon tubes.
12. 500-ml and 100-ml graduated cylinders.
13. Sterile disposable reagent reservoir.
14. Square Petri plates.
15. Round Petri plates.
16. Sterile toothpicks.
17. Round filter papers.
18. Forceps.
19. Balance.
20. 4 $^{\circ}\text{C}$ refrigerator.
21. Growth room with 16-h-light/8-h-dark cycle ($60 \mu\text{mol m}^{-2} \text{s}^{-1}$) at 20–22 $^{\circ}\text{C}$.

2.4 Imaging

1. Camera.
2. Camera stand.

3 Method

3.1 Primary Chemical Screen

3.1.1 Preparation of Seeds and Growth Media

1. To synchronize germination and ensure uniformity in seedling development, use recently harvested *Arabidopsis* Col-0 seeds (*see Note 1*). Aliquot seeds to the 0.2-ml mark in 1.5-ml microcentrifuge tubes and surface sterilize in 1 ml of 30% bleach with 0.1% triton X-100 surfactant by vortexing vigorously for 10 min. Collect seeds by centrifuging briefly in a mini tabletop centrifuge and slowly aspirate off the supernatant with a 100–1000- μ l pipette. Rinse the seeds by adding 1 ml of sterilized double-distilled water, vortex for 1 min, briefly centrifuge, and aspirate the supernatant. Repeat this rinsing step three more times to remove all traces of the Clorox. Add 1 ml of sterilized double-distilled water to the seeds and store for 2 days in the dark at 4 °C.
2. Weigh 121.7 mg of *N*-lauroylethanolamide (NAE 12:0) (MW 243.391 g/mol) powder and dissolve by vortexing vigorously in 5 ml of dimethyl sulfoxide (DMSO) to make a 100 mM NAE 12:0 stock solution. Keep vortexing until the powder is completely dissolved; this will take a few minutes.
3. Prepare the seedling growth media with $\frac{1}{2}$ Murashige and Skoog (MS) salt with micronutrients and 1% sucrose, pH 5.7. Allow the $\frac{1}{2}$ MS media to cool to room temperature in a laminar flow hood. Measure 300 ml of the media with a graduated cylinder and pour into an Erlenmeyer flask. Add 105 μ l of the 100 mM NAE 12:0 stock solution to make a 35 μ M NAE 12:0 $\frac{1}{2}$ MS media. Place a lid on the flask and swirl gently to make the media homogeneous. Use the graduated cylinder to measure 150 ml of $\frac{1}{2}$ MS media and pour the solution into another Erlenmeyer flask. Add 45 μ l DMSO and swirl. This will serve as the nontreated control (*see Note 2*).
4. Under a laminar flow hood, pour some of the $\frac{1}{2}$ MS media plus DMSO into a sterile reservoir and use a 20–200- μ l microchannel pipette to add 150 μ l of the media to each of the wells in the first rows (A1–H1) of the 96-well plates with lids (Fig. 1a, b). Pour some of the $\frac{1}{2}$ MS media plus 35 μ M NAE 12:0 into another sterile reservoir and use the 20–200- μ l microchannel pipette to add 150 μ l of this media to all the remaining wells (11 rows) of the 96-well plates (Fig. 1a) (*see Note 3*).
5. Use a 100–1000- μ l pipette to aspirate off the water in which the surface-sterilized seeds were stratified in for 2 days at 4 °C in the dark, and add 1 ml of fresh sterilized double-distilled water. Use the same 100–1000- μ l pipette to suck up a small amount to the seeds and add 4–5 seeds to each of the wells in the first rows (A1–H1) of the 96-well plates (*see Note 4*).

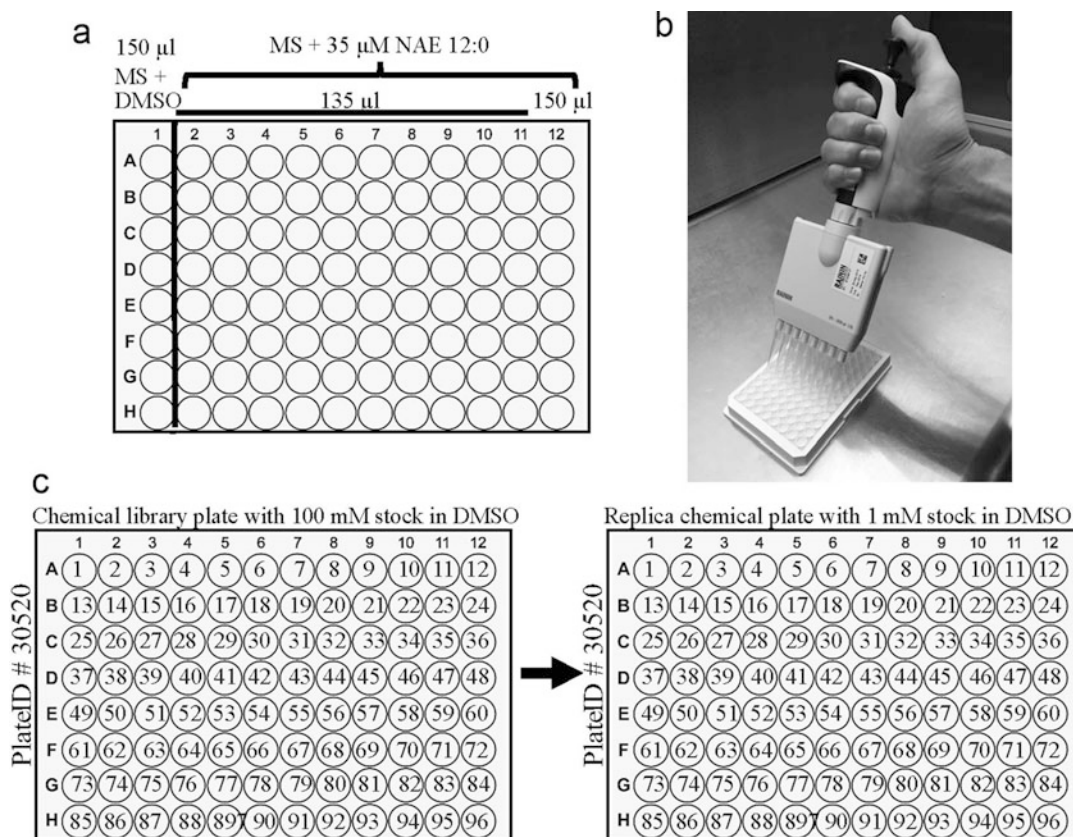


Fig. 1 Preparing replica plates with working solutions of small molecules for antagonistic effects on NAE 12:0. (a) Organization of a 96-well plate with $\frac{1}{2}$ MS media supplemented with DMSO or 35 μ M NAE 12:0. Row 1 (A1–H1) contains 150 μ l, $\frac{1}{2}$ MS plus DMSO. The remaining 11 rows (A2–H2–A12–H12) contain 150 μ l $\frac{1}{2}$ MS plus 35 μ M NAE 12:0. (b) Microchannel pipette used for diluting and distributing small-molecule stock solutions. (c) A representative 96-well chemical library plate with 100-mM stock concentration and the corresponding 96-well dilution replica plate with 1-mM working concentrations

Change the pipette tip and add 4–5 seeds to all the other wells, one row at a time (11 rows) (*see Note 5*).

- After adding seeds to all the plates, cover the plates with lids and seal around the edges where the lid and plate overlap with parafilm. Transfer the plates to a growth room with 16-h-light/8-h-dark cycle ($60 \mu\text{mol m}^{-2} \text{s}^{-1}$) at 20–22 $^{\circ}\text{C}$ and incubate on an orbital shaker at 200 rpm for 4 days (*see Note 6*).

3.1.2 Dilution of Chemicals in the Library

- The Chembridge library of 10,000 small synthetic molecules was supplied in 96-well plates, dissolved in DMSO to a stock concentration of 100 mM. The library was diluted to 1 mM in DMSO to obtain optimal working concentrations (*see Note 7*).

2. Prepare new 96-well replica plates for the dilutions by labeling the plates with the identification numbers (ID #) of the original plates. While making the dilutions, keep plates with the chemical compounds and replica dilution plates on ice. Pour 5 ml of DMSO into a sterile reservoir and use a 20–200- μ l multichannel pipette to add 99 μ l of DMSO to each of the wells in the 96-well replica plates. Use the 0.2–2- μ l pipette to add 1 μ l of each of the chemical compounds from the library to their matching replica plates one row at a time to make a 1-mM working concentration (Fig. 1c). Seal the chemical library plates with parafilm and store at -80°C . The chemical replica plates with the 1-mM working concentration will be used to treat the seedlings in the screen.

3.1.3 Treating Seedlings with the Chemical Compounds

1. After 4 days of incubation, remove plates from the growth room and unwrap in a laminar flow hood. One should notice that seedlings in $\frac{1}{2}$ MS media plus 35 μM NAE 12:0 will be smaller compared to seedlings grown in media with DMSO (i.e., solvent controls) only (Fig. 2a).
2. Use a permanent marker to label the 96-well 4-day-old seedling treatment plates with the chemical ID # of the chemical replica plates so that they match the treatment (Fig. 2b). Use a 2–20- μ l microchannel pipette to add 15 μ l of chemical compounds from the chemical replica plates to the 4-day-old seedlings in the 96-well treatment plates to a final concentration of 100 μM . Add the chemical compounds by matching row 1 (A1–H1) of the chemical replica plate 1 to row 2 (A2–H2) of treatment plate 1, ending at row 10 (A10–H10) of chemical replica plate 1 to row 11 (A11–H11) of treatment plate 1 (Fig. 2b) (see **Note 8**). No chemical compounds will be added to row 1 (A1–H1) with $\frac{1}{2}$ MS media plus DMSO, or row 12 (A12–H12) with $\frac{1}{2}$ MS media plus 35 μM NAE 12:0 of the treatment plates (Fig. 2b). These two rows are the positive and negative controls for the screen. Cover both treatment plate 1 and chemical replica plate 1 and place them in a corner of the laminar flow hood for later. Add the chemical compounds from the chemical replica plate to the treatment plate by matching rows 1–10 (A1–H1–A10–H10) of chemical replica plate 2 to rows 2–11 (A2–H2–A11–H11) of treatment plate 2 (Fig. 2b). Again, cover both chemical replica plate and treatment plate and set aside for later. Repeat this step with four other chemical replica plates and treatment plates (see **Note 9**). Label a sixth treatment plate, add the chemical compounds from chemical replica plate 1 rows 11 and 12 (A11–H11–A12–H12) to treatment plate 6 rows 2 and 3 (A2–H2–A3–H3) (Fig. 3). Repeat this same procedure by matching chemical compounds from chemical replica plates 2, 3, 4, and 5, rows

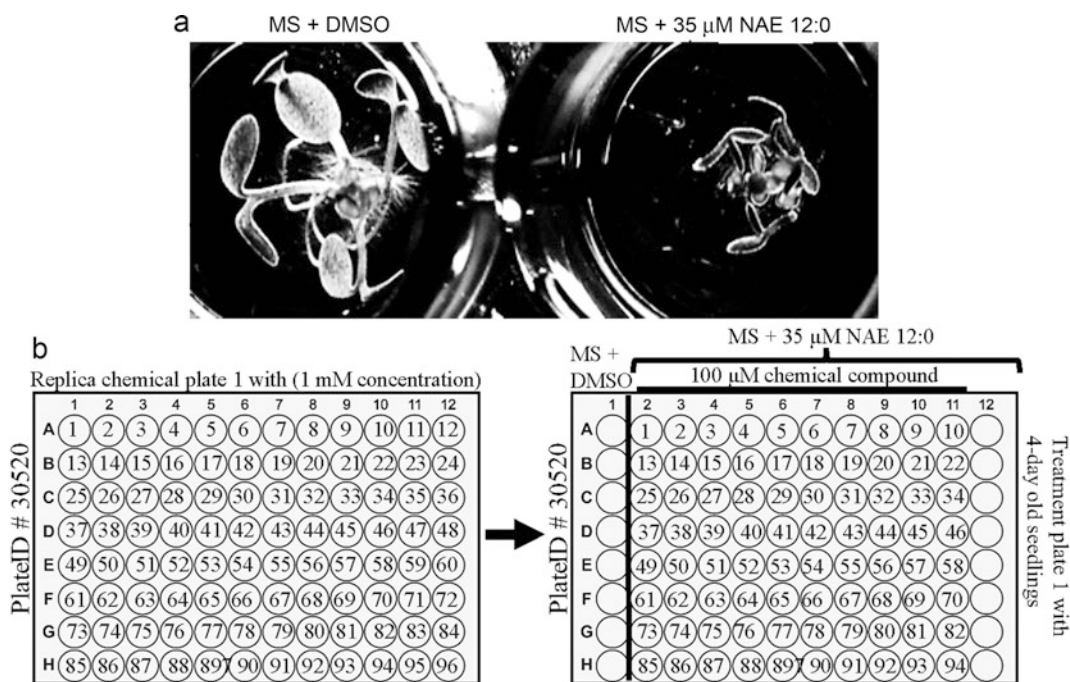


Fig. 2 Organization of a representative treatment plate with screening chemicals from a replica plate (a). Two representative wells from a 96-well plate with 4-day-old seedlings grown in media without (MS+DMSO) or with 35 μ M NAE 12:0. (b) Strategy for screening working chemical compounds on 4-day-old seedlings. The diluted stock solution (1 mM) is represented by the plate on the left and the seedling treatment plate is on the right. Each replica plate contains 96 chemicals dissolved in DMSO to a 1-mM working concentration. For the seedling treatment plate, row 1 (A1–H1) of each plate contains seedlings grown in media with DMSO, while rows 2 to 12 (A2–H2–A12–H12) contain seedlings grown in media with 35 μ M NAE 12:0. Chemical compounds from the chemical replica plates are added in rows 2 to 11 (A2–H2–A11–H11) in the order shown by the number in each well. Row 12 (A12–H12) of the treatment plates was not treated with any of the chemical compounds. Both rows 1 (A1–H1) and 12 (A12–H12) served as positive and negative controls

11 and 12 (A11–H11–A12–H12) to treatment plate 6 rows 4 and 5 (A4–H4–A5–H5), rows 6 and 7 (A6–H6–A7–H7), rows 8 and 9 (A8–H8–A9–H9), and rows 10 and 11 (A10–H10–A11–H11), respectively (Fig. 3).

3. Repeat the procedure in **step 2** until all 10,000 of chemical compounds have been applied (*see Note 10*).
4. Seal the treatment plates with parafilm around the edges where the lid and plate overlap and incubate for 4 days on an orbital shaker at 200 rpm in a growth room with 16-h-light/8-h-dark cycle ($60 \mu\text{mol m}^{-2} \text{s}^{-1}$) at 20–22 $^{\circ}\text{C}$ (*see Note 11*).

3.1.4 Scoring Treatment Plates for Putative “Hits”

1. Move plates from growth room to lab bench for visual scoring. Unwrap treatment plate 1 and compare seedlings treated with 35 μ M NAE12:0 plus 100 μ M of the chemical compounds to nontreated seedlings in row 1 (A1–H1) and seedlings treated with 35 μ M NAE12:0 in row 12 (A12–H12).

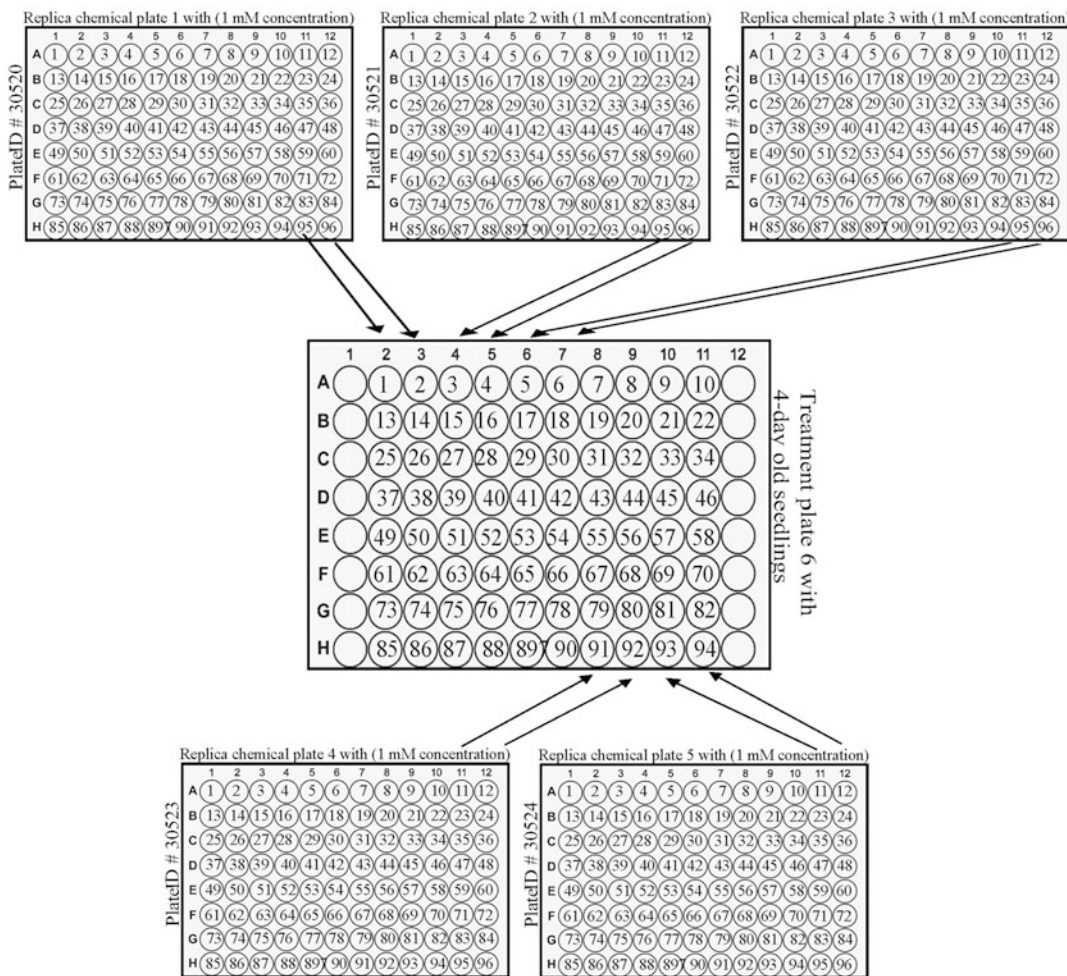


Fig. 3 Screening chemical compounds from rows 11 and 12 (A11–H11–A12–H12) of chemical replica plates 1–5 on 4-day-old seedlings in treatment plates 6. Row 1 (A1–H1) of each plate contains seedlings grown in media with DMSO, while rows 2 to 12 (A2–H2–A12–H12) contain seedlings grown in media with 35 μ M NAE 12:0. Chemical compounds from the chemical replica plates were added in rows 2 to 11 (A2–H2–A11–H11) in the order shown by the number in each well. Row 12 (A12–H12) of the treatment plate was not treated with any of the chemical compounds. Both rows 1 (A1–H1) and 12 (A12–H12) serve as positive and negative controls

- Seedling development is inhibited with NAE 12:0 treatment (Fig. 2a); therefore, seedlings treated with 35 μ M NAE12:0 plus 100 μ M of the chemical compounds that develop better than seedlings treated with 35 μ M NAE12:0 alone in row 12 (A12–H12) or similar to nontreated seedlings in row 1 (A1–H1) can be scored as possible “hits.” These “hits” are putative chemical compounds that impact the functional roles of NAE or terminate NAE responses (Fig. 4). In a notebook, record the plate ID # and the positions on the plate where the chemical compounds or “hits” are located.

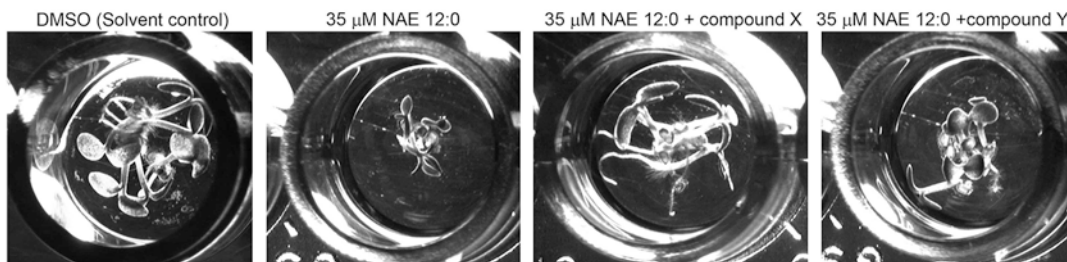


Fig. 4 Representative individual wells showing how small molecules antagonistic to NAE 12:0 are identified. Note that compound X and Y appear to reverse the inhibitory effect of NAE 12:0 on seedling development

3.2 Secondary Chemical Screen

1. After putative “hits” are identified, the chemical compounds must be rescreened to verify the phenotype and eliminate false positives. Prepare $\frac{1}{2}$ MS media with micronutrients and 1% sucrose, pH 5.7. Cool media in a laminar flow hood, measure 300 ml with a graduated cylinder, pour into an Erlenmeyer flask, and add 105 μ l of 100 mM NAE 12:0 to a final concentration of 35 μ M. For the nontreated control media, measure another 100 ml of the media and add 35 μ l of DMSO.
2. Use the 100–1000- μ l pipette to add 0.5 ml of the media with DMSO and 35 μ M NAE 12:0 to 24-well plates. Add 10 stratified *Arabidopsis* Col-0 seeds to the wells and seal the plates with parafilm.
3. Incubate the plates on an orbital shaker at 200 rpm in a growth room with 16-h-light/8-h-dark cycle ($60 \mu\text{mol m}^{-2} \text{s}^{-1}$) at 20–22 $^{\circ}\text{C}$ for 4 days.
4. Transfer plates from the growth room to a laminar flow hood for treatment. Unwrap the plates and rescreen the putative “hits” on the 4-day-old seedlings at 50- μ M and 100- μ M concentrations. Seal the plates with parafilm and incubate for an additional 4 days on an orbital shaker at 200 rpm in a growth room with 16-h-light/8-h-dark cycle ($60 \mu\text{mol m}^{-2} \text{s}^{-1}$) at 20–22 $^{\circ}\text{C}$.
5. Score plates visually to confirm the phenotype by comparing seedlings treated with 35 μ M NAE 12:0 plus the chemical compounds to nontreated seedlings and seedlings treated with 35 μ M NAE 12:0 alone (Fig. 4).
6. Image seedlings in the 24-well plates of the secondary screen with a camera mounted on a stand and remove any false positives identified in the primary screen from your notebook.

3.3 Third Chemical Screen

1. Purchase the compounds confirmed in the secondary screen from Chembridge and dissolve them in glass vials with DMSO to make a 100-mM concentration. Test these compounds in solid media with 50 μ M NAE 12:0 at 35- μ M and 50- μ M concentrations on seedlings in square Petri plates.

2. Prepare solid $\frac{1}{2}$ MS media with 0.5% agar, micronutrients, and 1% sucrose. Cool the media under a laminar flow hood until about 60 °C.
3. Label square Petri plates with the chemical ID # and concentrations of the chemical compounds to be added to the plates.
4. Use a graduated cylinder to measure 300 ml of the media and pour into an Erlenmeyer flask. Add 150 μ l of the 100-mM NAE 12:0 stock concentration dissolved in DMSO to 300 ml of media to make a 50- μ M concentration and gently swirl to mix. Measure 35 ml of the $\frac{1}{2}$ MS media plus 50 μ M NAE 12:0 with a falcon tube, add 10.5 μ l of chemical compound A to make a 35- μ M concentration, shake gently to mix, and pour into the appropriately labeled Petri plate. To make the 50- μ M concentration, measure another 35 ml of $\frac{1}{2}$ MS media plus 50 μ M NAE 12:0 with another falcon tube, add 17.5 μ l of the chemical compound A, shake gently to mix, and pour into the appropriately labeled Petri plate. Prepare a nontreated control plate by measuring 35 ml of $\frac{1}{2}$ MS media with a falcon tube, add 35 μ l of DMSO, shake gently, and pour. Prepare a control plate with 35 ml of $\frac{1}{2}$ MS media plus 50 μ M NAE 12:0. Cover plates and allow to solidify under the laminar flow hood. Repeat this step to prepare plates for all the other confirmed chemical compounds.
5. Surface sterilize freshly harvested *Arabidopsis* Col-0 seeds in 1.5-ml microcentrifuge tubes in 1 ml of 30% bleach with 0.1% Triton X-100 surfactant vortexing vigorously for 10 min. Collect seeds by centrifuging briefly in a mini tabletop centrifuge and gently aspirate off supernatant. Rinse seeds with 1 ml of sterilized double-distilled water, vortex for 1 min, briefly centrifuge, and aspirate off supernatant. Repeat this rinsing step three more times to remove all traces of the Clorox. Under a laminar flow hood, use a sterile forceps to place sterile round filter papers into round Petri plates and pipette the sterilized seeds onto the filter paper-lined plates. Leave the plates open under the hood to allow the seeds to dry.
6. After the seeds dry, use a sterile toothpick to pick up the seeds, one at a time, and embed them in the media on the control and treatment plates. Seal the plates with parafilm and store for 2 days in the dark at 4 °C to allow for stratification and synchronize germination.
7. Remove plates after 2 days and incubate vertically in a growth room with 16-h-light/8-h-dark cycle ($60 \mu\text{mol m}^{-2} \text{s}^{-1}$) at 20–22 °C for 8 days.
8. Unwrap plates and image with a camera mounted on a stand (Fig. 5). Analyze images with ImageJ software by quantifying root length and cotyledon area (Fig. 5).

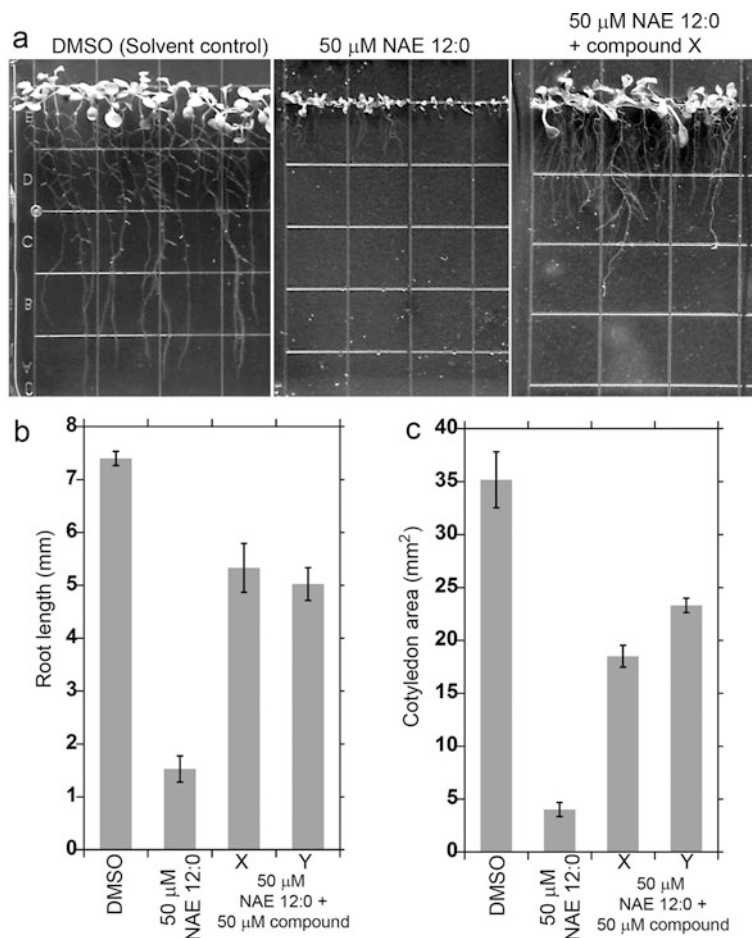


Fig. 5 Validation of chemicals identified from the primary and secondary screen. (a) Seedlings grown for 8 days on DMSO (solvent controls), 50 μM NAE 12:0, and 50 μM NAE 12:0 plus 50 μM compound X. Quantification of root length (b) and cotyledon area (c) on DMSO (solvent controls), 50 μM NAE 12:0, and 50 μM NAE 12:0 plus 50 μM compounds X and Y. Error bars represent the standard error of the means ($n \geq 16$ for cotyledon area and primary root)

4 Notes

1. Harvest seeds from *Arabidopsis thaliana* Col-0 plants planted at the same time and grown under the same conditions. Store the seeds for 1 week on a clean filter paper in a sterile Petri dish to allow for after-ripening. Use this one-week-old after-ripened seeds for the screen.
2. Avoid using solid agar media for screening in 96-well plates because if you do not work quickly, the media will solidify during pipetting of the media into the 96-well plates. Furthermore, we observed that the effects of the chemical compounds

from the library on the seedling phenotype are more potent in liquid media compared to when they are added to the surface of the solid media.

3. For accuracy in measurement and to avoid bubbles during pipetting of the media into the 96-well plates, place the tips of the multichannel pipette at the side of the rows in the 96-well plate and then slowly dispense the media to the first stop of the multichannel pipette.
4. If it is difficult to control the 100–1000- μ l pipette to add the 4–5 seeds to the wells, then a 1-ml glass pipette dropper with a rubber bulb can be used. Some individuals find the 1-ml glass pipette dropper easier to control in dispensing a small number of seeds. To dispense the seeds from the pipette, touch the tip of the pipette tip to the corner of the well without touching the media and carefully dispense the seeds. Do not add more than 5 seeds to a 96-well plate. We observed more false positives when the seed number per well is greater than 5.
5. To avoid contamination, periodically change the pipette tip when you are adding the seeds to the wells. This procedure is tedious and should not be done if you are in a rush.
6. Since the volume of the media in the wells is only 150 μ l, it is important to seal the lids on the plates tightly with parafilm to prevent the media in the wells at the edges of the plates from drying out. The phenotype of the seedlings in the wells at the edge of the plates will be affected if they dry out.
7. The chemical compounds should be diluted in an appropriate solvent. If the chemical library you obtained is already dissolved in a solvent, then to obtain the optimal working concentrations, the compounds should be diluted in the same solvent as the original stock. Before starting the screen, check the effects of the solvent in which the chemical compounds are dissolved on seedling development for any undesirable effects.
8. When adding the chemical compounds to the treatment plates, it is important to place the tips of the multichannel pipette on the surface of the media in the 96-well treatment plates to (1) protect the seedlings from damage by the pipette tip (the response of the seedlings to the chemical compounds may differ if they are damaged since this may alter how the compounds are perceived by the seedlings) and (2) be certain that the seedlings are receiving the full effects of the chemical compounds by eliminating the possibility of the compounds adhering to the walls of the wells. With this screening procedure, you will not be able to determine in which part of the seedling (i.e., leaves, hypocotyl, roots) the compound is perceived.

9. Since rows 1 and 12 of the seedling treatment plates contained the positive and negative controls for the screens, chemicals from rows 11 and 12 (A11–H11–A12–H12) of the replica plates could not be screened on these plates. Therefore, seedling treatment plate 6 was used to screen the chemicals from rows 11 and 12 of replica plates 1–5. The layout of seedling treatment plate 6 with the chemicals from rows A11–H11 and A12–H12 of replica plates 1–5 is shown in (Fig. 3). This step was repeated after every fifth replica plate in the screen.
10. If you are planning to screen all 10,000 chemical compounds on the same day, start treating the seedlings with the chemical compounds early in the morning since this is a tedious task. Seedlings older than 4 days should also be avoided. Alternatively, screening can be spread out over several days by growing the seedlings at different times.
11. Avoid incubating the seedlings for longer than 8 days in 96-well plates since the media will dry out and the seedling phenotype will be affected.

Acknowledgments

The authors' work on plant lipid signaling is supported by the Department of Energy, Office of Science, Basic Energy Sciences Program grant DEFG02-05ER15647 (to KDC and EBB) and the National Science Foundation, Division of Integrative Organismal Systems, IOS1656263 (to KDC). The chemical genetics work is partly supported by the Oklahoma Center for the Advancement of Science and Technology grant PS15-012 (to EBB).

References

1. Schmid HHO, Schmid PC, Natarajan V (1996) The N-acylation-phosphodiesterase pathway and cell signalling. *Chem Phys Lipids* 80:133–142
2. Chapman KD (2004) Occurrence, metabolism, and prospective functions of N-acylethanolamines in plants. *Prog Lipid Res* 43:302–327
3. Pagotto U, Marsican G, Cota D, Lutz B, Pasquali R (2006) The emerging role of the endocannabinoid system in endocrine regulation and energy balance. *Endocr Rev* 27:73–100
4. Butler H, Korbonsits M (2009) Cannabinoids for clinicians: the rise and fall of the cannabinoid antagonists. *Eur J Endocrinol* 5:655–662
5. Kilaru A, Blancaflor EB, Venables BJ, Tripathy S, Mysore KS, Chapman KD (2007) The N-acylethanolamine-mediated regulatory pathway in plants. *Chem Biodivers* 4:1933–1955
6. Kim SC, Chapman KD, Blancaflor EB (2010) Fatty acid amide lipid mediators in plants. *Plant Sci* 178:411–419
7. Okamoto Y, Morishita J, Tsuboi K, Tonai T, Ueda N (2004) Molecular characterization of a phospholipase D generating anandamide and its congeners. *J Biol Chem* 279:5298–5305
8. Pappan K, Austin-Brown S, Chapman KD, Wang X (1998) Substrate selectivities and lipid modulation of plant phospholipase D alpha, -beta, and -gamma. *Arch Biochem Biophys* 353:131–140
9. Venables BJ, Waggoner CA, Chapman KD (2005) N-acylethanolamines in seeds of selected legumes. *Phytochemistry* 66:1913–1918

10. Blancaflor EB, Hou G, Chapman KD (2003) Elevated levels of N-lauroylethanolamine, an endogenous constituent of desiccated seeds, disrupt normal root development in *Arabidopsis thaliana* seedlings. *Planta* 217:206–217
11. Kang L, Wang YS, Uppalapati SR, Wang K, Tang Y, Vadapalli V, Venables BJ, Chapman KD, Blancaflor EB, Mysore KS (2008) Overexpression of a fatty acid amide hydrolase compromises innate immunity in Arabidopsis. *Plant J* 56:336–349
12. Teaster ND, Keereetaweep J, Kilaru A, Wang YS, Tang Y, Tran CN, Ayre BG, Chapman KD, Blancaflor EB (2012) Overexpression of fatty acid amide hydrolase induces early flowering in *Arabidopsis thaliana*. *Front Plant Sci* 3:32
13. Cotter MQ, Teaster ND, Blancaflor EB, Chapman KD (2011) N-acylethanolamine (NAE) inhibits growth in *Arabidopsis thaliana* seedlings via ABI3-dependent and independent pathways. *Plant Signal Behav* 6:671–679
14. Kim SC, Kang L, Nagaraj S, Blancaflor EB, Mysore KS, Chapman KD (2009) Mutations in Arabidopsis fatty acid amide hydrolase reveal that catalytic activity influences growth but not sensitivity to abscisic acid or pathogens. *J Biol Chem* 284:34065–34074
15. Teaster ND, Motes CM, Tang Y, Wiant WC, Cotter MQ, Wang YS, Kilaru A, Venables BJ, Hasenstein KH, Gonzalez G, Blancaflor EB, Chapman KD (2007) N-Acylethanolamine metabolism interacts with abscisic acid signaling in *Arabidopsis thaliana* seedlings. *Plant Cell* 19:2454–2469
16. Wang YS, Shrestha R, Kilaru A, Wiant W, Venables BJ, Chapman KD, Blancaflor EB (2006) Manipulation of Arabidopsis fatty acid amide hydrolase expression modifies plant growth and sensitivity to N-acylethanolamines. *Proc Natl Acad Sci U S A* 103:12197–12202
17. Cravatt BF, Demarest K, Patricelli MP, Bracey MH, Giang DK, Martin BR, Lichtman AH (2001) Supersensitivity to anandamide and enhanced endogenous cannabinoid signaling in mice lacking fatty acid amide hydrolase. *Proc Natl Acad Sci U S A* 98:9371–9376
18. McKinney MK, Cravatt BF (2005) Structure and function of fatty acid amide hydrolase. *Annu Rev Biochem* 74:411–432
19. Schmid HH (2000) Pathways and mechanisms of N-acylethanolamine biosynthesis: can anandamide be generated selectively? *Chem Phys Lipids* 108:1–87
20. Shrestha R, Dixon RA, Chapman KD (2003) Molecular identification of a functional homologue of the mammalian fatty acid amide hydrolase in *Arabidopsis thaliana*. *J Biol Chem* 278:34990–34997
21. Shrestha R, Kim SC, Dyer JM, Dixon RA, Chapman KD (2006) Plant fatty acid (ethanol) amide hydrolases. *Biochim Biophys Acta* 1761:324–334
22. Otrubova K, Ezzili C, Boger DL (2011) The discovery and development of inhibitors of fatty acid amide hydrolase (FAAH). *Bioorg Med Chem Lett* 21:4674–4685
23. Khan BR, Wherret DJ, Huhman D, Sumner LW, Chapman KD, Blancaflor EB (2016) Malonylation of glucosylated N-lauroylethanolamine a new pathway that determines N-acylethanolamine metabolic fate in plants. *J Biol Chem* 291:27112–27121
24. Drakakaki G, Robert S, Szatmari AM, Brown MQ, Nagawa S, Van Damme D, Leonard M, Yang Z, Girke T, Schmid SL et al (2011) Clusters of bioactive compounds target dynamic endomembrane networks in vivo. *Proc Natl Acad Sci U S A* 108:17850–17855
25. Khan BR, Faure L, Chapman KD, Blancaflor EB (2017) A chemical genetic screen uncovers a small molecule enhancer of the N-acylethanolamine degrading enzyme, fatty acid amide hydrolase, in Arabidopsis. *Sci Rep* 7:41121



Method for Phenotypic Chemical Screening to Identify Cryptochrome Inhibitors

Emiko Okubo-Kurihara, Wen-Dee Ong, Yukio Kurihara,
Natsumaro Kutsuna, and Minami Matsui

Abstract

After germination, plants determine their morphogenesis, such as hypocotyl elongation and cotyledon opening, by responding to various wavelengths of light (photomorphogenesis). Cryptochrome is a blue-light photoreceptor that controls de-etiolation, stomatal opening and closing, flowering time, and shade avoidance. Successful incorporation of these phenotypes as indicators into a chemical screening system results in faster selection of candidate compounds. Here, we describe phenotypic screening for the blue-light response of *Arabidopsis thaliana* seedling and the resulting process that clarifies that the compound obtained in the screening is an inhibitor of cryptochromes.

Key words Phenotypic screen, photomorphogenesis, Photoreceptor, Cryptochrome, Image processing

1 Introduction

Phenotypic chemical screening involves the selection of chemicals based on phenotypic changes that occur in treated samples [1–3]. Its advantage is that noninvasive analysis is possible, and the images obtained contain a lot of information on morphology, localization, membrane permeability, and cytotoxicity [4]. Since the phenotype appears as a result of a chemical effect, it can be analyzed even if the mechanism of the chemical action is unknown. However, it is necessary to find a characteristic phenotype for the screening index and identify the target of the identified compound, which is often challenging. To help overcome these problems, we describe how phenotype-based chemical screening should be performed, how images obtained during the screening should be processed and evaluated without observer bias, and how to identify the target protein of the compound obtained.

Light plays an important role in successful growth and morphogenesis [5–7]. Light-induced morphological development is

called photomorphogenesis [8]. Under light, young *Arabidopsis* seedlings develop expanded cotyledons and short hypocotyls [9]. Blue light controls hypocotyl elongation, stomatal opening, flowering time, and the synthesis of anthocyanin through blue-light receptors called cryptochromes [10, 11]. If the blue-light-signaling pathway is inhibited by a compound, cotyledon expansion and hypocotyl elongation inhibition does not occur. When an inhibitor of this signaling is identified, it can be used not only as a tool for revealing unknown aspects of blue-light signaling but also for agricultural applications. Some genes acting in the pathway and their corresponding mutant plants have been isolated. Checking differences in the chemically induced phenotype between wild-type and mutant plants enables us to predict a specific target protein. Previously we performed phenotypic chemical screening to investigate blue-light signal transduction and identified 3-bromo-7-nitroindazole (3B7N) as a novel cryptochrome inhibitor [12]. Furthermore, Orth et al. reported that 3B7N competes for the ATP-binding cassette of the cryptochrome [13]. Here, we present the principles of high-throughput chemical screening and introduce how to identify a molecule (cryptochrome) targeted by the compound (3B7N).

2 Materials

2.1 Plant Material

1. Seeds of *Arabidopsis thaliana* wild-type Columbia (Col-0) or Wassilewskija (Ws) and other blue-light-signaling mutant lines (*see Note 1*).
2. Sterilizing solution: 20% (v/v) concentrated sodium hypochlorite solution (or bleach), 0.05% (v/v) Tween-20.
3. 70% EtOH
4. Sterile deionized water.

2.2 Culture Media and Growth Conditions

1. Culture media: half-strength Murashige and Skoog (1/2 MS) media [14], 1× Gamborg's vitamin solution, and 0.05% (w/v) 2-(*N*-morpholino)ethanesulfonic acid (MES) (*see Note 2*). Adjust pH to 5.8 with KOH. Autoclave solution and store at 4 °C.
2. Light conditions: *Arabidopsis* seedlings need to be irradiated with monochromatic LEDs (light-emitting diodes) of blue, red, or far-red light in growth chambers. In the light chambers, the LED panels can be set to a wavelength with a main peak at 450 nm for blue light, 660 nm for red light, and 730 nm for far-red light. Blue and red light with an intensity of 10 $\mu\text{mol m}^{-2} \text{s}^{-1}$ and far-red light with an intensity of 1 $\mu\text{mol m}^{-2} \text{s}^{-1}$ can be used. Incubate sample plates in the

growth chambers at 22 °C with a humidity of 40–60%. Conduct incubation in blue and far-red light chambers for 6 days and in red light for 4 days.

3. Solid media for mutant analysis: 1/2 MS media contains 1× Gamborg’s vitamin solution, 0.05% (w/v) 2-(*N*-morpholino) ethanesulfonic acid (MES), and 1% agar. Adjust pH to 5.8 with KOH and autoclave. After autoclave, cool the medium below 65 °C. Add 2.5 μM 3B7N or 1% dimethyl sulfoxide (DMSO) and pour into plates.

2.3 Chemical Library

1. 96-well polypropylene plates.
2. Dimethyl sulfoxide (DMSO).
3. Aluminum microplate sealing tape.
4. Microplate sealing tape (*see Note 3*).
5. Chemical library, for example, the chemical library LATCA, which is an acronym for “*Library of AcTive Compounds on Arabidopsis*” [15]. This library contains 4086 small chemical compounds (*see Note 4*). The library is arrayed in a 96-well plate format at a concentration of 2.5 mM pre-dissolved in 100% DMSO and is stored at –20 °C. Use the 2.5-mM chemical plates as master plates. Prepare 250-μM plates by diluting the master plates with 100% DMSO and store at –20 °C.

2.4 Image Acquisition

1. Fluorescence microscope equipped with a cooled CCD camera head system and a motorized stage is required for screening. Images of the wells can be semi-automatically acquired using software.
2. Digital camera.

2.5 Cell-Free Protein Synthesis

1. pEU-E01-His-MCS-N2 vector.
2. WEPRO7240H Expression Kit that includes reagents for SP6 promoter-mediated in vitro transcription and protein synthesis in wheat germ extract.
3. Protomist-DT II, which is an automatic machine for in vitro transcription and protein synthesis in wheat germ extract.
4. Storage buffer: 1× phosphate-buffered saline (PBS; 137 mM NaCl, 2.7 mM KCl, 10 mM Na₂HPO₄, 1.76 mM KH₂PO₄) pH 7.4, 10% glycerol, 5 mM EDTA.
5. Ultracentrifuge Filters with 10K cutoff.
6. DC Protein Assay Reagents.

2.6 In Vitro Beads Binding Assay

1. Binding buffer A: 10 mM Tris-HCl (pH 7.6), 50 mM KCl, 5 mM MgCl₂, 1 mM EDTA.
2. Binding buffer B: 10 mM Tris-HCl (pH 7.6), 50 mM KCl, 5 mM MgCl₂, 1 mM EDTA, 10% glycerol, and 0.025% Triton X-100.
3. Precast gel (10–20% gradient SDS-PAGE gel).
4. PVDF membrane.
5. TBS buffer: 50 mM Tris-HCl (pH 7.6), 150 mM NaCl.
6. TBST: TBS, 0.125% Tween-20.
7. Anti-HA antibody from mouse.
8. Anti-mouse IgG antibody conjugating HRP from goat.
9. ECL Advance Western Blotting Detection Kit.
10. Chemical beads: 3B7N (positive compound), 3-bromoindazole (negative compound), and no compound derivative-photoaffinity linker-coated agarose beads (control) are prepared as described in Supporting Information Methods in [16].

3 Methods

3.1 Prepare Plant Material

1. Place an appropriate amount of wild-type (WT) Columbia (Col-0) seeds in a 1.5-ml microtube with a medical spoon.
2. In a laminar flow cabinet, add 1 ml of 70% ethanol, stir quickly, and discard the supernatant.
3. Add 1 ml of sterilizing solution, mix and incubate for 1 min, and then discard the supernatant.
4. Add sterile water, mix by inverting, and discard the supernatant.
5. Repeat **step 4**, wash with sterile water three times, and add 1 ml of sterile water.
6. Wrap the microtube in aluminum foil and stand upright at 4 °C for 2 days to vernalize.
7. Remove the supernatant and add 1 ml of growth medium, mix by inverting, and then discard the supernatant.
8. Add 1 ml of growth medium and expose for 1 h under white light (*see Note 5*).

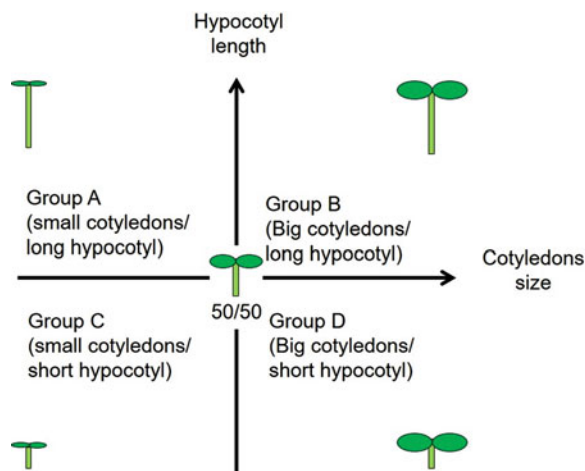


Fig. 1 Criteria of seedlings based on hypocotyl length and cotyledon size. The X-axis indicates cotyledon size and the Y-axis hypocotyl length. The center (0/0) indicates average seedling morphology. The upper left quadrant (Group A) contains light-signal inhibitors. Group B contains growth enhancers and early germination and Group C contains growth inhibitors and also late germination. Group D contains light-signal enhancers that cause hypersensitivity to light

3.2 Chemical Screening

3.2.1 First Screening for Blue-Light-Signaling Inhibitors

In the first screening, select chemicals inducing long hypocotyls and small cotyledons under blue-light irradiation (Fig. 1 Group A).

1. Mix plant growth media and the seeds in the tube with gentle pipetting and aliquot into 96-well plates. The volume of the liquid medium dispensed with the seeds is 50 μl . The number of seeds is limited to 4–6 seeds (*see Note 6*).
2. For each plate, the first column of wells is treated with 1% DMSO as a control, and Columns 2 to 11 contain the treatments of LATCA chemicals (2.5 μM). Since the 12th column is used as a background at the time of image processing, dispense culture medium without seeds into it.
3. Apply a clear 96-well plate seal.
4. Grow for 6 days under monochromatic blue light ($10 \mu\text{mol m}^{-2} \text{s}^{-1}$) at 22 $^{\circ}\text{C}$.
5. Take images with a microscope under bright-field optics, 10 \times magnification, 3 \times 3 tiling (Fig. 2) (*see Note 7*).

3.2.2 Phenotype Quantification by Image Processing

Simultaneously extract morphological data from the images of the seedlings using an image processing program, for example, the program developed by LPIXEL Inc (*see Note 8*).

1. Quantify images by following the process showed in Fig. 3. Reverse the 96-well sample image to white-dark contrast. Then, adjust the brightness of the white-dark image to intensify the image of the samples. Next, erase the well numbers and the

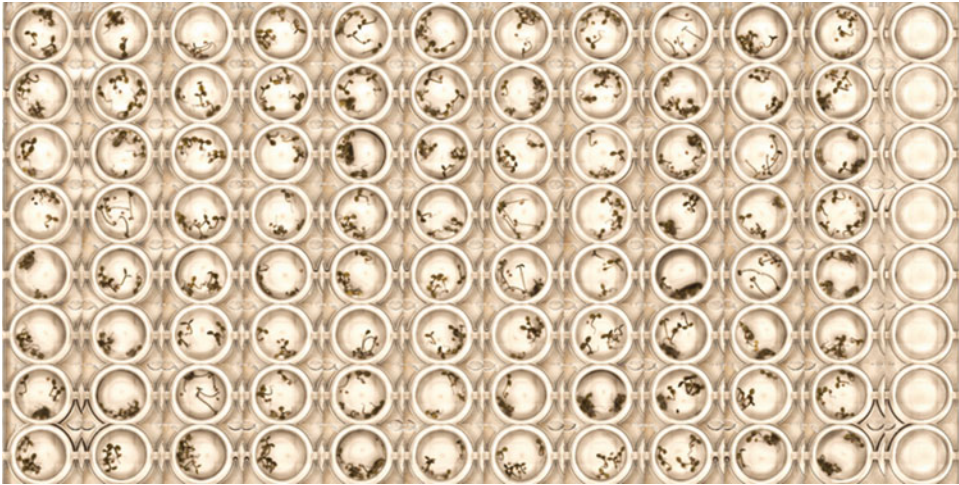
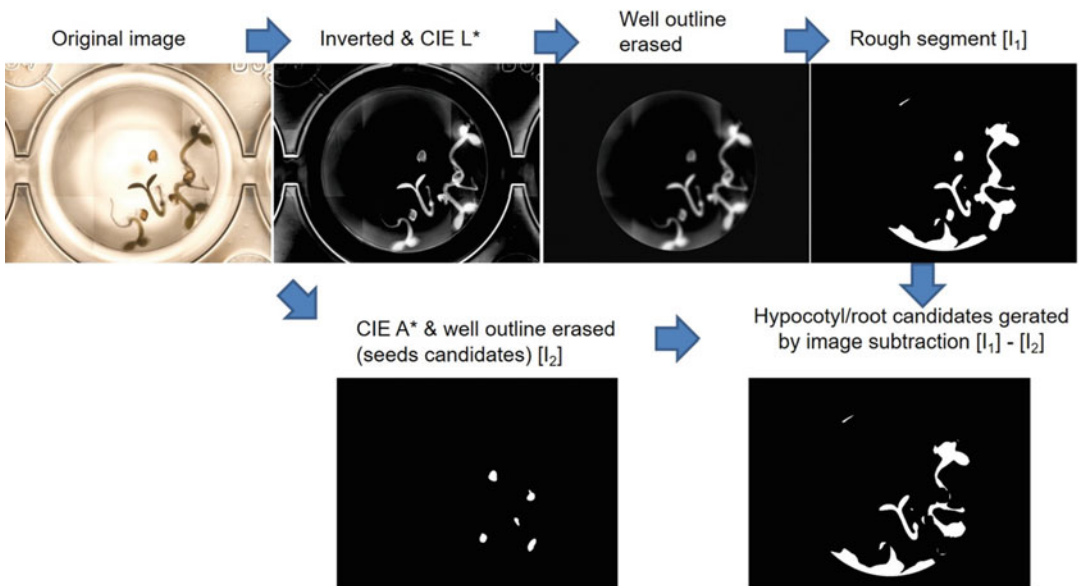


Fig. 2 Example images of seedlings taken by an automatic microscope



CIE L*: Lightness defined in International Commission on Illumination (CIE)

CIE A*: From Greenness (-1) to redness (+1) defined in International Commission on Illumination (CIE)

Fig. 3 Outline of methodology for extracting seedling morphological measurements from image data

outlines of the titer wells. Measure the length of the seedlings for each sample treatment.

- From the extracted image data of hypocotyl/root candidates, measure 22 types of quantitative values such as area, circumference, complexity, and deformation.

- To understand the phenotype, use a standard score, the T-score, to analyze the morphological data extracted from images of the seedlings. For each 96-well plate, 8 control samples and 80 LATCA chemicals can be screened. Calculate the T-score by multiplying the Z-score by 10 and adding 50. Obtain the Z-score by subtracting the mean value of 86 samples (N) from the actual value (A) and dividing by the standard deviation (s) of the 86 samples. A T-score of 50 represents the mean and a difference of 10 from the mean indicates a difference of one standard deviation.

$$T - \text{score} = (10 \times (A - N))/s + 50$$

Most of the chemicals are plotted along this trend line crossing the center of this map (50/50) that represents the average morphology of a WT seedling.

- In this example experiment, by showing the hypocotyl length and the leaf size in a scatter plot, candidates that are significantly different from those plotted in Group A of Fig. 1 are selected using visual confirmation (*see Note 9*).

3.2.3 Second Screening of Compounds That Specifically Inhibit Seedling Growth Only Under Blue-Light Irradiation

A secondary screening needs to be performed to verify whether the positive compounds obtained in the first screening specifically act in blue-light signaling (Fig. 4).

- Mix plant growth medium and seeds in the tube with gentle pipetting and aliquot into 96-well plates. The volume of the liquid medium to be aliquoted with the seeds should be 50 μl . The number of seeds is limited to 4–6 seeds.
- Treat with the positive compounds from the first screening to a final concentration of 2.5 μM .
- Apply a clear 96-well plate seal.
- Prepare four sets of 96-well plates and place them separately in LED chambers with monochromatic blue, red light, and far-red light, and a chamber under dark conditions. The compounds that induce differences only under blue light are considered as final candidates.

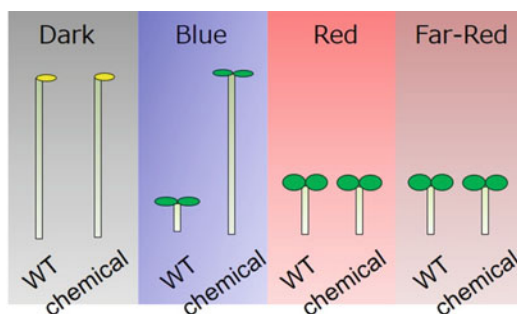


Fig. 4 Outline of second screening

3.3 Target Identification

The target is predicted through expression analysis of blue-light-signaling genes and phenotypic analysis of light-signaling mutants when their seedlings are treated with the compound.

3.3.1 Prediction of the Action Pathway or Target of a Compound Using Light-Signaling Mutant Lines

1. Sow seeds of wild type and the light-signaling mutant lines on 3B7N and DMSO plates.
2. Grow for 6 days under monochromatic blue light ($10 \mu\text{mol m}^{-2} \text{s}^{-1}$) at 22 °C.
3. Lay the growing hypocotyl on the surface of the agar medium using tweezers, and take images with a digital camera.
4. Measure the length of each hypocotyl in an image using ImageJ (<https://imagej.nih.gov/ij/index.html>). Those that show no difference between the 3B7N plate and the DMSO plate are considered to be targets (*see* **Note 10**).

3.3.2 Recombinant Protein Synthesis Using Wheat Germ Extract

1. Clone the gene candidate for the chemical-targeted protein into the pEU-E01-His-MCS-N2 vector to make N-terminal His-tagged proteins.
2. Use the plasmid as a template for in vitro transcription. The in vitro transcription, protein synthesis in wheat germ, and purification of the products are performed using the Protomist-DT II, an automatic machine, according to the manufacturer's instructions (Cell Free Science). Perform protein synthesis in a 6-ml volume of wheat germ extract (*see* **Note 11**).
3. After purification of the N-terminal His-tagged proteins, replace the solvent (20 mM sodium phosphate (pH 7.5), 0.3 M NaCl, 0.5 M imidazole) with storage buffer (1× phosphate-buffered saline (PBS; 137 mM NaCl, 2.7 mM KCl, 10 mM Na_2HPO_4 , 1.76 mM KH_2PO_4) pH 7.4, 10% glycerol, 5 mM EDTA) using Ultra Centrifugal Filters with 10K cutoff to a final volume of 250 μl .
4. Determine the concentration of the synthesized proteins using DC Protein Assay Reagents.

3.3.3 In Vitro Binding Assay and Immunoblot Analysis

1. Dispense 20 μl of 3B7N, the negative compounds, and no compound derivative-photoaffinity linker-coated agarose beads into each microtube.
2. Add 1 ml of binding buffer A and centrifuge at $500 \times g$ for 1 min. Discard the supernatant.
3. Incubate the recombinant proteins (75 μg) and 250 μl of binding buffer A with 20 μl of 3B7N beads or control derivative-photoaffinity linker-coated agarose beads, from 4 h to overnight at 4 °C.

4. Wash the reacted beads with 250 μ l of binding buffer B four times and then wash with 250 μ l of binding buffer A two times.
5. Elute bound proteins with SDS-PAGE buffer by incubation at 95 °C for 5 min and separate by electrophoresis on a 10–20% gradient SDS-polyacrylamide gel (Wako, Japan).
6. After electrophoresis, electrophoretically transfer the proteins to a PVDF transfer membrane in blotting buffer.
7. Block the membrane with 5% skimmed milk in TBS for 30 min, incubate the membrane with anti-HA antibodies conjugated with horseradish peroxidase for 1 h at room temperature, and wash three times with TBST with 10 min for each wash. Visualize protein bands using chemiluminescence.

4 Notes

1. Seed stocks of the *A. thaliana* photomorphogenic mutants including phyAphyB, cry1, cry2, cry1cry2, hy5, cop1-4, cop1-6, hfr1, and laf1 can be obtained from the Arabidopsis Biological Resource Center (Ohio State University). Seeds of the overexpressor lines CRY1-OX and CRY2-OX [17, 18] can be requested from Dr. Chentao Lin, while the hy5hyh seeds can be requested from Dr. Xing-Wang Deng [19]. Mutants are either in the Columbia (Col-0) or Wassilewskija (Ws) background.
2. In experiments involving the light response, it is preferable not to put sucrose in the medium because the response is easier to observe when it is absent.
3. As light irradiation plays an important role in these experiments, we used a tape with high transparency.
4. The LATCA library is not commercially available, but several chemical libraries such as the DIVERSet™ libraries (Chembridge Corporation, https://www.chembridge.com/screening_libraries/diversity_libraries/index.php) are available.
5. The germination rate is remarkably low when cultured under blue-light irradiation immediately after adding the chemical. Leaving the seeds under white light for several hours and then transferring them to blue light give a good germination rate.
6. If the number of seeds is too small, statistical analysis cannot be carried out. If it is too large, the seeds overlap, and it is not possible to obtain an image that is easy to analyze. To avoid clusters of seedlings in each well, tape the plate gently to scatter the seeds before incubation in the growth chamber.
7. To measure numerical values for hypocotyls and cotyledons in the image analysis, it is desirable that individual seedlings are

photographed, and it is recommended that an image of the whole well is taken.

8. It is possible to instruct LPixel INC. (<https://lpixel.net/>) to undertake image deformation processing for chemical evaluation and toxicity assessment. There is a charge for this service, but it is a useful way to evaluate a large number of images quickly.
9. Image analysis is a powerful tool, but in the case of plants that grow too much or overlap in one place, accurate numerical values may not be obtained from image analysis. Therefore, be sure to check the results by visual inspection.
10. For target prediction, gene expression analysis may be performed when any changes occur when a candidate compound is added to the light-signaling mutant and the wild type.
11. See https://www.cfsciences.com/images/synthesizer/Protomist_DT_II_reagent_manual_ver.2.3.pdf for details.

Acknowledgments

This work was funded partly by a grant-in-aid for Challenging Exploratory Research from the Japan Society for the Promotion of Science with grant No. 25560421 to E.O.-K.

References

1. Khersonsky SM, Chang YT (2004) Strategies for facilitated forward chemical genetics. *Chem Bio Chem* 5:903–908
2. Zheng W, Thorne N, McKew JC (2013) Phenotypic screens as a renewed approach for drug discovery. *Drug Discov Today* 18:1067–1073
3. Choi H, Kim JY, Chang YT, Nam HG (2014) Forward chemical genetic screening. *Methods Mol Biol* 1062:393–404
4. Futamura Y, Yamamoto K, Osada H (2017) Phenotypic screening meets natural products in drug discovery. *Biosci Biotechnol Biochem* 81:28–31
5. Jiao Y, Lau OS, Deng XW (2007) Light-regulated transcriptional networks in higher plants. *Nat Rev Genet* 8:217–230
6. Fankhauser C, Chory J (1997) Light control of plant development. *Annu Rev Cell Dev Biol* 13:203–229
7. Kami C, Lorrain S, Hornitschek P, Fankhauser C (2010) Light-regulated plant growth and development. *Curr Top Dev Biol* 91:29–66
8. Kendrick RE, Kronenberg GHM (1994) *Photomorphogenesis in plants*, 2nd edn. Kluwer, Dordrecht
9. Boyes DC, Zayed AM, Ascenzi R, McCaskill AJ, Hoffman NE, Davis KR, Grolach J (2001) Growth stage-based phenotypic analysis of *Arabidopsis*: a model for high throughput functional genomics in plants. *Plant Cell* 13:1499–1510
10. Wang X, Wang Q, Nguyen P, Lin C (2014) Cryptochrome-mediated light responses in plants. *Enzyme* 35:167–189
11. Ahmed M, Cashmore AR (1997) The blue light receptor cryptochrome 1 shows functional dependence on phytochrome A or phytochrome B in *Arabidopsis thaliana*. *Plant J* 11:421–427
12. Ong WD, Okubo-Kurihara E, Kurihara Y, Shimada S, Makita Y, Kawashima M, Honda K, Kondoh Y, Watanabe N, Osada H, Cutler SR, Sudesh K, Matsui M (2017) Chemical-induced inhibition of blue light-mediated seedling development caused by disruption of upstream signal transduction involving cryptochromes in *Arabidopsis thaliana*. *Plant Cell Physiol* 58:95–105
13. Orth C, Niemann N, Hennig L, Essen LO, Batschauer A (2017) Hyperactivity of the *Arabidopsis* cryptochrome (cry1) L407F mutant is

- caused by a structural alteration close to the cry1 ATP-binding site. *J Biol Chem* 292:12906–12920
14. Murashige T, Skoog F (1962) A revised medium for rapid growth and bio assays with tobacco tissue cultures. *Physiol Plant* 15:473–497
 15. Zhao Y, Chow TF, Puckrin RS, Alfred SE, Korir AK, Larive CK, Cutler SR (2007) Chemical genetic interrogation of natural variation uncovers a molecule that is glycoactivated. *Nat Chem Biol* 3:716–721
 16. Kawatani M, Okumura H, Honda N, Kanoh N, Muroi M, Dohmae N, Takami M, Kitagawa M, Futamura Y, Imoto M, Osada H (2008) The identification of an osteoclastogenesis inhibitor through the inhibition of glyoxalase I. *Proc Natl Acad Sci U S A* 105:11691–11696
 17. Lin C, Ahmad M, Cashmore AR (1996) Arabidopsis cryptochrome 1 is a soluble protein mediating blue light-dependent regulation of plant growth and development. *Plant J* 10:893–902
 18. Lin C, Yang H, Guo H, Mockler T, Chen J, Cashmore AR (1998) Enhancement of blue-light sensitivity of Arabidopsis seedlings by a blue light receptor cryptochrome 2. *Proc Natl Acad Sci U S A* 95:2686–2690
 19. Holm M, Ma LG, Qu LJ, Deng XW (2002) Two interacting bZIP proteins are direct targets of COP1-mediated control of light-dependent gene expression in Arabidopsis. *Genes Dev* 16:1247–1259



Whole-Seedling-Based Chemical Genetic Screens in *Arabidopsis*

Shuai Huang and Xin Li

Abstract

Forward genetics has been extremely powerful for dissecting biological pathways in various model organisms. However, it is limited by the fact that redundant gene families and essential genes cannot be readily uncovered through such methods. Chemical genetics, on the other hand, provides a valuable complementary approach to probe biological processes and is suitable for not only genetic model organisms but also genetically less tractable species. We describe here a high-throughput chemical genetic screening method simply based on plant growth and developmental phenotypes in *Arabidopsis*. It was successfully utilized to study plant immunity and can be easily adapted for dissecting other plant signal transduction pathways.

Key words Chemical genetic screen, Suppressor screen, *Arabidopsis*, Small molecule, Small-molecule libraries

1 Introduction

Humanity has been benefiting from small molecules, such as natural products, for millennia. Although high-throughput screening (HTS) of small molecules is widely used in the pharmaceutical and biotechnology industry for drug discovery, its implementation for functional studies is more recent.

Chemical genetic screens exploit small molecules to perturb gene functions in specific biological pathways [1]. Forward chemical genetics (phenotype-based screening) searches for compounds from diverse small-molecule libraries that can affect the phenotype of interest. Further identification of the molecular target of the specific molecule is usually necessary for revealing the mechanism of the chemical. In reverse chemical genetics (target-based screening), the target of interest (e.g., a protein) is often known. By screening for compounds that can bind to the target, the consequences and phenotypes caused by the small molecules can be determined (Fig. 1).

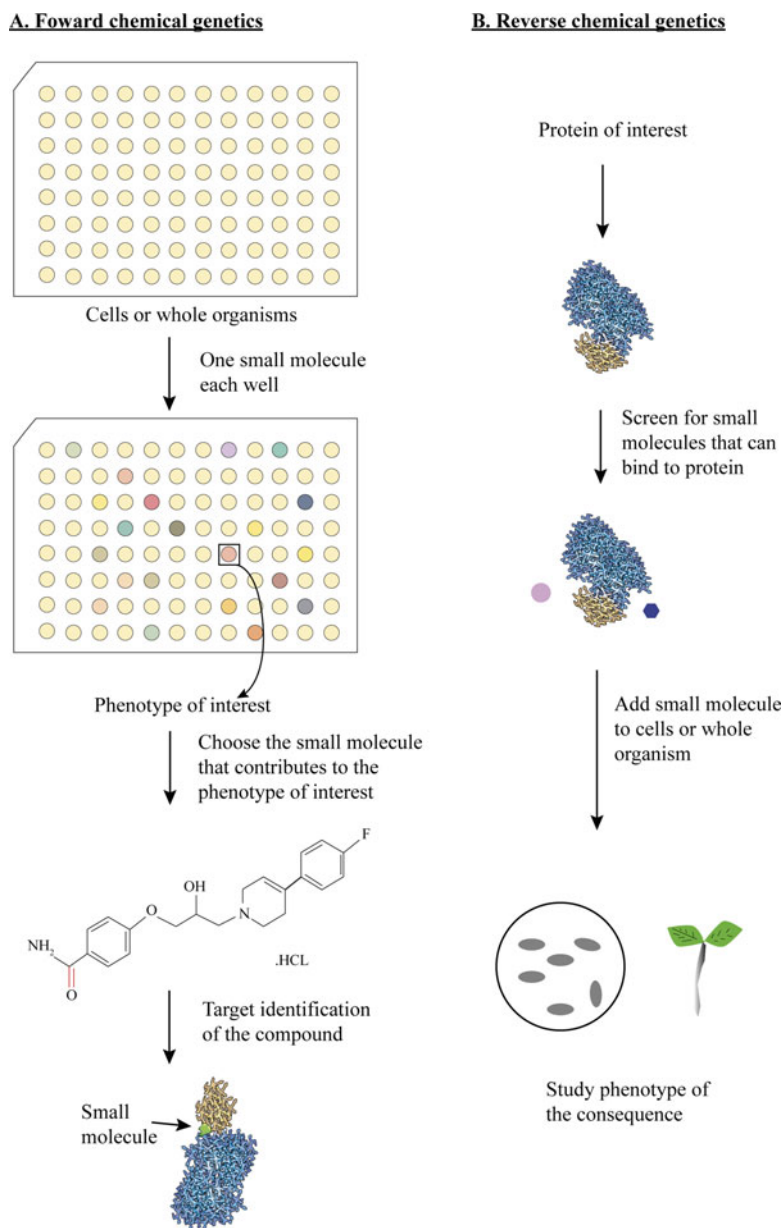


Fig. 1 Comparison of forward and reverse chemical genetics. **(a)** Phenotype-based forward chemical genetics. **(b)** Target-based reverse chemical genetics

Compared with classical genetics, chemical genetics enables antagonists with low selectivity to inhibit the function of redundant gene families. Chemicals targeting essential genes can also be used at lower concentrations to avoid lethality. In addition, chemicals can be added or removed at will, and HTS methods enable a large quantity of chemicals to be tested in a relatively short time period with the availability of liquid handling robots. Over the decades,

chemical genetics has shown its power in illustrating various biological processes in plants [2–5]. Using chemical genetics to study plant–microbe interactions and dissect plant immune pathways has also emerged in recent years [6–9].

Multiple chemical genetic screening protocols have been previously described in *Arabidopsis* with either reporter lines or cell cultures to study plant signaling pathways [6, 7, 10, 11]. Here, we describe a whole-seedling-based high-throughput chemical genetic screening method simply exploiting plant growth and developmental phenotype as the readout, which greatly simplifies and accelerates the general screening procedure. Using this approach, we successfully identified a small molecule involved in resistance protein-mediated plant immune responses in *Arabidopsis* [12]. Our protocol is easy to establish and should also be applicable to other plant biology fields.

2 Materials

1. Murashige and Skoog (MS) medium, premixed.
2. 96-well culture plates.
3. Small-molecule libraries commercially available from different suppliers.
4. Ethyl methanesulfonate (EMS).
5. Agar.
6. Phytigel.
7. Sucrose.
8. Commercial bleach.
9. Tween-20.
10. Parafilm.
11. Razor blades.

3 Methods

3.1 Search for an Optimum Screening Condition

Mutants displaying phenotypes observable by a human’s naked eyes are probably geneticists’ most cherished pets. Scientists have been harnessing such mutants to understand some of the very fundamental questions in biology [13–15]. In *Arabidopsis*, the morphological phenotypes of seedlings grown in culture medium can be dramatically different from those grown in soil, which is influenced by multiple parameters, such as mutant background, types of culture plates, temperature, composition of growth media, light intensity, and diurnal cycles. Therefore, to ensure the success of the screen, it is critical to search for optimal conditions under which

the mutant plants are morphologically the most distinguishable from wild-type (WT) plants. Here, we specifically discuss the first three parameters that showed the most significant effects in our research.

3.1.1 Choice of Mutant Lines

Mutants disturbing the same signaling pathways are often morphologically alike. For example, autoimmune mutants often exhibit dwarf phenotypes when grown on soil [16–19]. We are interested in identifying components downstream of TIR-NB-LRR type immune receptors using chemical genetics [12]. Multiple mutant lines are available to us including *chs3-2D*, *snc1*, and *SNC1-GFP* (a *SNC1* overexpression line). The *chs3-2D* mutant consistently exhibits the most striking phenotypic differences in both soil and culture media compared with WT, whereas the growth dissimilarity is largely diminished for *snc1* mutant plants when grown in solid media. Interestingly, the *SNC1-GFP* OX line shows some differential phenotypes under certain conditions (see below), suggesting that mutants affecting the same gene can alter the growth output as reflected by the strength of the corresponding mutation. Therefore, when multiple mutant lines involved in the same signaling pathway are available, it is essential to determine the most suitable mutant line for the screen via comparative and parallel studies (*see Note 1*).

3.1.2 Types of Screening Plate

To suit for HTS, 96-well or 384-well culture plates should be used. The types of screening plate can affect plant growth via affecting the amount of nutrients, space for plant expansion, availability of air, and size of the plant populations. For example, in 96-well plates at 16 °C growth condition, *chs3-2D* was consistently the smallest on different volumes of medium (75 µL, 100 µL, and 125 µL). Interestingly, with increasing temperature (22 °C), both *chs3-2D* and *snc1-GFP* showed the most dwarf morphology compared with WT (Fig. 2).

3.1.3 Temperature

The optimal growth temperature for *Arabidopsis* is 22–23 °C. However, it can tolerate nonharming low (15 °C) and high (30 °C) temperatures, although sterility can be challenging at higher temperatures. Changing growth temperatures within the permissive regime can maximize the phenotypic differences of weak alleles or further enhance the altered morphology caused by robust gain-/loss-of function mutations. For example, temperature can profoundly influence plant immunity and the subsequent growth phenotype of some mutant lines [20]. To enhance the autoimmune mutant phenotype, we decreased the growth temperature to 16 °C in our study [12].

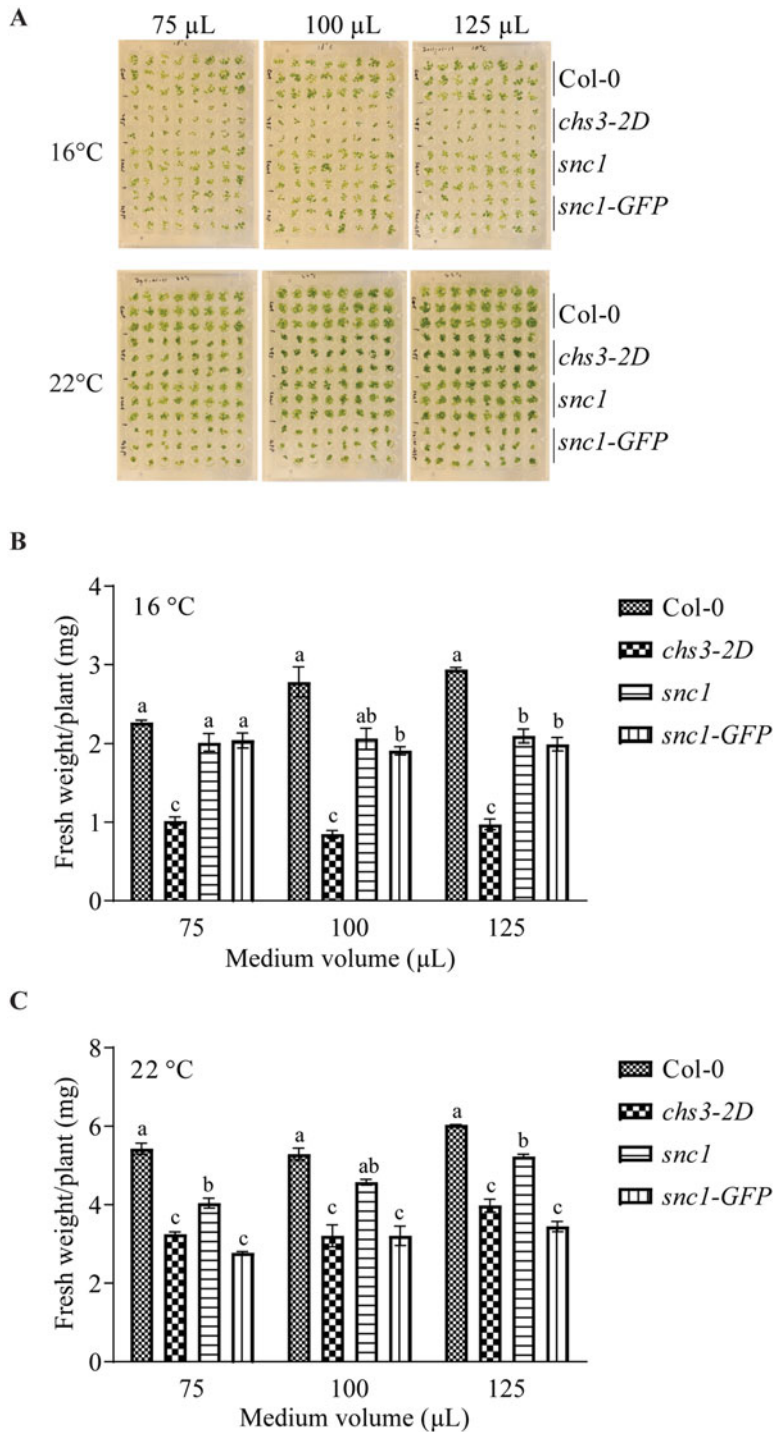


Fig. 2 Growth of autoimmune mutants on 96-well screening plates. (a) Morphology of two-week-old plants grown at 16 °C on 96-well plates containing different volumes of $\frac{1}{2}$ strength MS medium for 2 weeks. (b) and (c) Fresh weight of two-week-old plants grown under indicated conditions on 96-well screening plates. Error bars represent mean \pm SE ($n = 3$ with 10 plants each). Stars indicate statistical difference (one-way ANOVA followed by Bonferroni post-test; $P < 0.01$) within each medium volume (not between medium volume). The experiment was repeated once with similar results

3.2 Preparation of Seeds and Culture Media

To suit for HTS, we describe here the protocol with 96-well tissue culture plates since they are compatible with our chemical library-handling robotic system. Since medium volume did not affect the phenotypes of our selected mutants, we used 100 μL $\frac{1}{2}$ MS media in the screen [12].

Perform all procedures under sterile conditions:

1. Use the formula below to calculate the total volume of $\frac{1}{2}$ Murashige and Skoog (MS) media (0–1% sucrose, 0.3–0.5% phytigel, pH 5.7 at 25 °C adjusted with 1 M KOH, also *see Note 2*) needed for the screen.

$$100 \mu\text{L}/\text{well} \times 96 \text{ wells} \times \text{NO. of plates} = \text{Total volume of media}$$

2. Sterilize the media in a flask containing a stir bar for 20 min.
3. Allow the media to cool to ~60 °C with constant stirring on a heating magnetic stirrer.
4. Allocate 100 μL of culture media to each well of the 96-well culture plates using an electronic repeater pipette in a biosafety cabinet.
5. Allow the media to solidify with the lids covered at RT for at least 2 h. Solidification can be performed overnight.
6. Plates can now be stored at 4 °C for months without loss of activity, or proceed to **step 7**.
7. Sterilize the seeds in 15% bleach +0.1% Tween-20.
8. Wash the seeds twice with sterile water.
9. Resuspend the seeds in 0.1% sterile agar in sterile ultrapure water.
10. Stratify the seeds at 4 °C for 2–3 days.
11. During **step 10**, prepare seed-spotting tips by cutting off the end (~5 mm) of the 200- μL pipette tips using a razor blade and sterilize the tips before usage. This allows easy passage of the seeds through the pipette tips onto the media.
12. Spot 2–4 vernalized seeds into each well of the 96-well plates to ensure germination of the seeds (*see Note 3*).

3.3 Chemical Genetic Screen

1. Thaw small-molecule libraries at room temperature (RT) for 1 h before starting each batch of the screen.
2. Add desired concentration of small molecules into the 96-well culture plates using a robot-controlled 96-well pin tool (*see Note 4*). For a typical 10,000 compounds library, this step can be readily finished within 1 week. A positive control, if known, is highly recommended to be included in each batch of the screen. A negative control could be a well without adding any chemical or solvent alone used to dissolve the compounds (e.g., DMSO) in the library.

3. Seal the plates with parafilm to maintain humidity.
4. Place the screening plates in an *Arabidopsis* growth chamber under desired diurnal cycles and temperature. Placing plates in a typical growth room is not recommended since the poor ventilation often leads to water condensation on the lids.
5. Constantly monitor the growth phenotypes of the plants for up to 4 weeks (*see Note 5*). Depending on the stringency of the screen, the number of hits to be identified also varies. Mutants with weak or mild phenotypes tend to result in a large number of candidate hits and false positives. Therefore, it is recommended to start with mutants with strong, consistent, and clear phenotypes to reduce the number of false positives. For example, we utilized autoimmune mutants as the screening materials to dissect immune pathways. Only compounds that could revert the stunted growth of the mutants to near wild-type levels were kept for further studies (*see Note 6*).
6. Once a candidate compound is identified, perform a secondary screen with the small molecule at various concentrations to confirm the effects of the chemical, if any, and to determine the dosage responses of the compound. In our hands, over 95% of candidates uncovered from the primary screen were false positives though we set up relatively stringent screening criteria.
7. Further characterize the candidate compound by performing additional experiments such as gene expression analysis and pathogen infection assays.
8. A final validation step is to test the specific compound acquired from a different source. It is not rare that compounds may have undergone structural modifications, decomposition, or cross-contamination during storage or handling. An NMR analysis to confirm the identity of the candidate compound is sometimes required.
9. If available, similar chemicals with modified structures can be tested to determine the structural requirement of the identified molecule.

Finding a lead compound is usually only the beginning of the study. Convincing conclusions depicting the molecular mechanisms of the small molecule often requires the identification of the chemical target. Both biochemical and genetic approaches have been deployed to successfully identify the targets of small-molecule compounds [21–23]. Here, we briefly describe our genetic approach to isolate chemical-insensitive mutants, which has provided useful insights into the mechanism of the identified small molecule [12].

1. Mutagenize the background mutant seeds with EMS (for a detailed protocol on EMS mutagenesis, please see ref. 24).
2. Plant the M2 population on $\frac{1}{2}$ MS media containing the candidate chemical at desired concentrations. It is recommended here to use 10-cm or 15-cm culture dishes for expensive chemicals.
3. Transplant chemical-insensitive mutants to soil and harvest seeds.
4. Characterize the mutants and molecularly clone the mutant genes as previously described [24].

4 Notes

1. The protocol described above primarily uses plant size as the screening output in *Arabidopsis*. It is generally also applicable to other visible phenotypes and other plant species with small size.
2. We used $\frac{1}{2}$ strength MS media containing 1% sucrose and 0.5% phytigel in our screen. Other concentrations of the components and additional additives should be adjusted according to the screen.
3. The rate limiting step in our screen was spotting seeds in culture plates. We found that resuspending the seeds in 0.1% agar prevents the seeds sinking to the bottom of the tube and denser seed suspensions (10 mg seeds in 1 mL liquid) greatly aided the spotting process. Spotting of small amount of seeds (2–4) in each 96-well can be achieved via gentle pressure exerted on the pipette.
4. If an automatic chemical library-handling system is not available, a multichannel pipet can be considered for a medium-throughput screen.
5. Contamination caused by bacteria or fungi in the culture media was not an issue in our study, which is <0.05% out of 13,600 compounds.
6. Leaving the seedlings in the culture plates for more than 3 weeks will cause gradual depletion of the media and stress conditions, leading to false positives.

Acknowledgments

The authors thank NSERC-Discovery, CFI-JELF, CSC, and UBC Cooper Memorial fund for their financial support. Mr. Paul Kapos is sincerely thanked for careful reading of the manuscript.

References

1. Stockwell BR (2000) Chemical genetics: ligand-based discovery of gene function. *Nat Rev Genet* 1:116–125
2. Park SY, Fung P, Nishimura N, Jensen DR, Fujii H, Zhao Y, Lumba S, Santiago J, Rodrigues A, Chow TF et al (2009) Abscisic acid inhibits type 2C protein phosphatases via the PYR/PYL family of START proteins. *Science* 324:1068–1071
3. Zhao Y, Dai X, Blackwell HE, Schreiber SL, Chory J (2003) SIR1, an upstream component in auxin signaling identified by chemical genetics. *Science* 301:1107–1110
4. Hayashi K, Ogino K, Oono Y, Uchimiya H, Nozaki H (2001) Yokonolide A, a new inhibitor of auxin signal transduction, from *Streptomyces diastatochromogenes* B59. *J Antibiot* 54:573–581
5. Min YK, Asami T, Fujioka S, Murofushi N, Yamaguchi I, Yoshida S (1999) New lead compounds for brassinosteroid biosynthesis inhibitors. *Bioorg Med Chem Lett* 9:425–430
6. Serrano M, Robatzek S, Torres M, Kombrink E, Somssich IE, Robinson M, Schulze-Lefert P (2007) Chemical interference of pathogen-associated molecular pattern-triggered immune responses in *Arabidopsis* reveals a potential role for fatty-acid synthase type II complex-derived lipid signals. *J Biol Chem* 282:6803–6811
7. Serrano M, Hubert DA, Dangl JL, Schulze-Lefert P, Kombrink E (2010) A chemical screen for suppressors of the *avrRpm1*-RPM1-dependent hypersensitive cell death response in *Arabidopsis thaliana*. *Planta* 231:1013–1023
8. Abdel-Hamid H, Chin K, Moeder W, Yoshioka K (2011) High throughput chemical screening supports the involvement of Ca^{2+} in cyclic nucleotide-gated ion channel-mediated programmed cell death in *Arabidopsis*. *Plant Signal Behav* 6:1817–1819
9. Noutoshi Y, Okazaki M, Kida T, Nishina Y, Morishita Y, Ogawa T, Suzuki H, Shibata D, Jikumaru Y, Hanada A et al (2012) Novel plant immune-priming compounds identified via high-throughput chemical screening target salicylic acid glucosyltransferases in *Arabidopsis*. *Plant Cell* 24:3795–3804
10. Dinh TT, Chen X (2015) Chemical genetic screens using *Arabidopsis thaliana* seedlings grown on solid medium. *Methods Mol Biol* 1263:111–125
11. Bjornson M, Song X, Dandekar A, Franz A, Drakakaki G, Dehesh K (2015) A chemical genetic screening procedure for *Arabidopsis thaliana* seedlings. *Bio Protoc* 5:e1519
12. Huang S, Balg A, Pan Y, Li M, Zhang X, Du L, Zhou M, Roberge M, Li X (2016) Identification of Methylosome components as negative regulators of plant immunity using chemical genetics. *Mol Plant* 9:1620–1633
13. Forsburg SL (2001) The art and design of genetic screens: yeast. *Nature Rev Genetics* 2:659–668
14. Jorgensen EM, Mango SE (2002) The art and design of genetic screens: *caenorhabditis elegans*. *Nat Rev Genet* 3:356–369
15. Page DR, Grossniklaus U (2002) The art and design of genetic screens: *Arabidopsis thaliana*. *Nat Rev Genet* 3:124–136
16. Zhang Y, Goritschnig S, Dong X, Li X (2003) A gain-of-function mutation in a plant disease resistance gene leads to constitutive activation of downstream signal transduction pathways in suppressor of *npr1-1*, constitutive 1. *Plant Cell* 15:2636–2646
17. Bi D, Johnson KCM, Zhu Z, Huang Y, Chen F, Zhang Y, Li X (2011) Mutations in an atypical TIR-NB-LRR-LIM resistance protein confer autoimmunity. *Front Plant Sci* 2:71
18. Zhang Y, Yang Y, Fang B, Gannon P, Ding P, Li X (2010) *Arabidopsis* *snc2-1D* activates receptor-like protein-mediated immunity transduced through WRKY70. *Plant Cell* 22:3153–3163
19. Bi D, Cheng YT, Li X, Zhang Y (2010) Activation of plant immune responses by a gain-of-function mutation in an atypical receptor-like kinase. *Plant Physiol* 153:1771–1779
20. Alcázar R, Parker JE (2011) The impact of temperature on balancing immune responsiveness and growth in *Arabidopsis*. *Trends Plant Sci* 16:666–675
21. Burdine L, Kodadek T (2004) Target identification in chemical genetics: the (often) missing link. *Chem Biol* 11:593–597
22. Ziegler S, Pries V, Hedberg C, Waldmann H (2013) Target identification for small bioactive molecules: finding the needle in the haystack. *Angew Chem Int Ed Engl* 52:2744–2792
23. Jost M, Weissman JS (2018) CRISPR approaches to small molecule target identification. *ACS Chem Biol* 13:366–375
24. Li X, Zhang Y (2016) Suppressor screens in *Arabidopsis*. *Methods Mol Biol* 1363:1–8



Identification of Type III Secretion Inhibitors for Plant Disease Management

Roger de Pedro Jové, Pau Sebastià, and Marc Valls

Abstract

Bacterial plant pathogens are among the most devastating threats to agriculture. To date, there are no effective means to control bacterial plant diseases due to the restrictions in the use of antibiotics in agriculture. A novel strategy under study is the use of chemical compounds that inhibit the expression of key bacterial virulence determinants. The type III secretion system is essential for virulence of many Gram-negative bacteria because it injects into the plant host cells bacterial proteins that interfere with their immune system. Here, we describe the methodology to identify bacterial type III secretion inhibitors, including a series of protocols that combine *in planta* and *in vitro* experiments. We use *Ralstonia solanacearum* as a model because of the number of genetic tools available in this organism and because it causes bacterial wilt, one of the most threatening plant diseases worldwide. The procedures presented can be used to evaluate the effect of different chemical compounds on bacterial growth and virulence.

Key words Bacterial plant pathogens, Type III secretion system, *Ralstonia solanacearum*, Chemical inhibitors, Plants, Protocols, Immunodetection, *In vitro* inhibitory test

1 Introduction

Bacteria can cause a range of diseases in economically important crops, leading to important losses. *Ralstonia solanacearum*, the causal agent of bacterial wilt, is one of the most devastating plant pathogens worldwide. The lack of effective means to control bacterial diseases and block the spread of these pathogens urge for new control strategies. The use of antibiotics and copper-based compounds is nowadays banned or tightly regulated in many countries [1, 2]. Using compounds that inhibit specific bacterial virulence factors is a promising and sustainable strategy.

The type III secretion system (T3SS) is one of the most distinctive hallmarks of Gram-negative bacterial pathogens. These pathogens use the T3SS to inject small molecules called effectors

Roger de Pedro Jové and Pau Sebastià contributed equally to this work.

inside the plant cell. Bacterial type III effectors (T3Es) hijack plant defense mechanisms and manipulate different metabolic pathways to successfully colonize the host [3]. Mutant bacteria devoid of the T3SS are totally nonpathogenic so that a possible strategy to inhibit bacterial virulence is to use chemical compounds that block the expression of this secretion system and impede bacterial colonization throughout the plant [4–6].

In this protocol, we present a stepwise guide to assess the ability of different chemical compounds to transcriptionally downregulate the expression of key T3SS genes and to test if they could be used as a means to decrease the virulence of the tested pathogens *in planta*.

2 Materials

2.1 Plant Growth

1. *Nicotiana benthamiana*; *Nicotiana tabacum*; and *Solanum lycopersicum* cv. Marmande.
2. Soil mix: Peat soil substrate n°2 + vermiculite + perlite (see **Note 1**).
3. Plant growth chambers with temperature, humidity, and photoperiod control.

2.2 Bacterial Strains and Growth

1. *Ralstonia solanacearum* GMI1000 reporter strains for transcription of *hrpB* (*PhrpB::luxCDABE*), *psbA* (*PpsbA::luxCDABE*), and *hrpY* (*PhrpY::luxCDABE*). *R. solanacearum* GMI1000 *PpsbA::avrA*-HA.
2. B medium: 10 g/L bacteriological peptone, 1 g/L yeast extract, and 1 g/L casamino acids. Add 1.5% agar for solid media before autoclaving. Before plating, add 0.5% glucose and 0.005% triphenyltetrazolium chloride (TTC). Supplement with the appropriate antibiotics (see **Notes 2** and **3**).
3. Boucher's minimal medium [7]: To prepare 1 L of 2× Boucher's medium, mix 100 mL of 5× M63 medium (10 g/L (NH₄)₂SO₄, 68 g/L KH₂PO₄, and 2.5 mg/L FeSO₄·7H₂O, pH 7 with KOH) with 405 µL of 1 M MgSO₄·7H₂O and adjust to 1 L with sterile distilled water. Before use, dilute to 1× with sterile distilled water (or 2× agar on water for plates). Supplement with 20 mM glutamate and appropriate antibiotics.

2.3 T3SS Inhibition Test In Vitro

1. Potential type III secretion inhibitory compound to test.
2. DMSO.
3. Incubator at 28 °C with rotor.
4. Luminometer.
5. Spectrophotometer.

2.4 Effect of the Tested Compound on Bacterial T3E Secretion

1. Sucrose.
2. Congo red.
3. 0.22- μ M filter.
4. 10-mL syringe.
5. 25% trichloroacetic acid.
6. 90% acetone.
7. Phosphate-buffered saline (PBS) 1 \times : 8 g/L NaCl, 0.201 g/L KCl, 1.42 g/L Na₂HPO₄, 0.272 g/L KH₂PO₄.
8. 4 \times Laemmli buffer.
9. Digital sonifier.
10. Primary anti-HA rat monoclonal antibody conjugated to horseradish peroxidase (HRP) in Tris-buffered saline (TBS) with 0.1% Tween-20 and 1% skimmed milk (*see Note 4*).
11. Coomassie blue.
12. LAS-4000 mini system.

2.5 In Planta Experiments

1. Blunt-end syringe.
2. 100% ethanol.
3. Leaf disk puncher.
4. Potter S homogenizer.

3 Methods

3.1 Plant and Bacterial Growth

3.1.1 *N. benthamiana*/ *N. tabacum*

1. Sow *N. benthamiana* or *N. tabacum* seeds in a pot at 26 °C and 14 h light/10 h darkness.
2. After 10 days, transfer each seedling to individual pots.
3. After 10 days, transfer each individual plant to single big pots. These plants will be ready for assays after 3 weeks (*see Notes 5 and 6*).

3.1.2 *Solanum lycopersicum* *cv. Marmande*

1. Sterilize Marmande tomato seeds with a sterile solution containing 1:3.33 of commercial bleach (4.7% concentrated) and 0.05% triton. Keep the seeds in the solution for 10 min. Wash with sterile distilled water at least five times.
2. Sow the sterilized seeds and cover with plastic film.
3. Keep the plants in the growth chamber at 22 °C, 16 h light and 8 h darkness for 1 week, until tomato seedlings emerge and touch the plastic film on top.
4. Transfer each tomato seedling to individual soil pots with the soil mix and let them grow for 3 weeks in a chamber at 22 °C and 16 h light and 8 h darkness (*see Note 5*).

3.1.3 *Ralstonia solanacearum*

1. Streak the bacterial strain from a glycerol stock at $-80\text{ }^{\circ}\text{C}$ on B medium supplemented with antibiotics for 2 days at $28\text{ }^{\circ}\text{C}$.
2. Pick a single colony and incubate in liquid B or minimal media.

3.2 In Vitro T3SS Inhibitor Screening in *Ralstonia solanacearum*

1. Grow an overnight pre-culture in liquid B media supplemented with antibiotics (*see* **Notes 7 and 8**).
2. Centrifuge the overnight pre-culture in 2-mL Eppendorf tubes at RT for 1 min at maximum speed, discard the supernatant, and resuspend the bacterial pellet in 1 mL of sterile distilled H_2O .
3. Measure the OD_{600} with a spectrophotometer (*see* **Note 9**).
4. Adjust to a final OD_{600} of 0.3 adding the right pre-culture volume to a culture tube containing 1.5 mL of fresh Boucher's minimal medium supplemented with 20 mM glutamate, antibiotic, and 100 mM inhibitory test compound/DMSO (*see* **Note 10**).
5. Mix by vortexing for a few seconds and incubate in a shaker.
6. Measure luminescence at times 0, 4, 6, 8 and 24 h transferring 200 μL from each tube into a 1.5-mL Eppendorf tube and quantifying light emission from the reporter in the luminometer. For each time point, measure as well OD_{600} in a spectrophotometer by transferring the 200 μL into a cuvette containing 800 μL of distilled water (*see* **Notes 11–13**).

3.3 Effect of the Tested Compound on Bacterial T3E Secretion

1. From an overnight culture of liquid B medium supplemented with antibiotics, adjust to a final OD_{600} of 0.2 (2×10^8 CFUs/mL) in a final volume of 10 mL of minimal medium supplemented with antibiotics, 10 mM glutamate, 10 mM sucrose, 100 $\mu\text{g}/\text{mL}$ congo red (*see* **Note 14**), and 100 $\mu\text{g}/\text{mL}$ of the test inhibitor compound (or 10 μL of DMSO as a control).
2. Incubate at room temperature for 12–14 h (or until OD_{600} reaches 1).
3. Transfer the culture to a 50-mL falcon tube and centrifuge at $4000 \times g$ for 10 min.
4. Filter the supernatant through a 0.22- μm filter with a syringe in order to remove any bacteria. The bacterial pellet is also kept at $-20\text{ }^{\circ}\text{C}$ for further analysis.
5. Add 10 mL of cold 25% TCA to the filtered supernatant and let it precipitate all night long at $4\text{ }^{\circ}\text{C}$.
6. Centrifuge at $6000 \times g$ for 30 min at $4\text{ }^{\circ}\text{C}$ and discard the supernatant.
7. Wash the protein pellet (it will contain all secreted proteins in the medium) twice with cold 90% acetone and let it dry at RT.

8. Resuspend the protein pellet in 100 μL of PBS 1 \times . Mix 15 μL of this solution with 15 μL of Laemmli buffer.
9. Recover the frozen bacterial pellet, freeze–thaw 3–4 times ($-80\text{ }^{\circ}\text{C}$ –RT cycles), resuspend in 1 mL of 1 \times PBS, and sonicate the cells using a sonifier (*see Note 15*). Mix 15 μL of the mixture with 15 μL of Laemmli buffer.
10. Boil the samples for 5 min and load it on SDS-PAGE (it will be a 100 \times concentration from initial culture).
11. The presence of particular proteins in the extracts can be analyzed by immunoblot using an antibody against the protein of interest. Coomassie-stained sodium dodecylsulfate-polyacrylamide gel electrophoresis (SDS-PAGE) membranes (used in the western blotting) can be visualized using a LAS-4000 mini system (*see Fig. 1*).

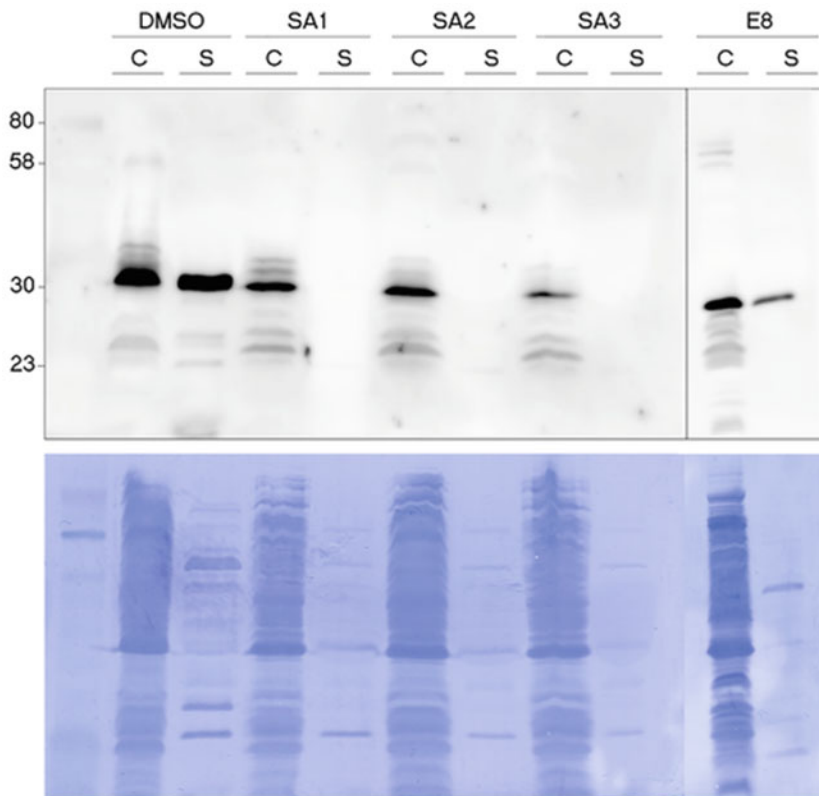


Fig. 1 Immunoblot of the secreted T3 effector (in this case, AvrA-HA) after treatment with four different inhibitory compounds (SA1-3 and E8) or the control (DMSO). The cytosolic (C) and secreted (S) fractions were separated by centrifugation. The protein of interest was detected with anti-HA antibody. Coomassie blue-stained membranes (below) used in the western blotting are also shown. (Reproduced from [9] with permission of John Wiley and Sons)



Fig. 2 *N. benthamiana* leaves infiltrated with serial dilutions of *R. solanacearum* preincubated with inhibitory compounds (in this case, SA1, SA2, SA3) or with a control solution (DMSO). Leaves were photographed 2 days post-infiltration. (Reproduced from [9] with permission of John Wiley and Sons)

3.4 *In Vivo* T3E Translocation Test Using Hypersensitive Response Assays

1. To the overnight culture of the desired bacterial strain (e.g., *R. solanacearum* GMI1000) in Boucher's minimal medium supplemented with 20 mM glutamate and antibiotic, add the tested inhibitory compound at 100 μ M (or with DMSO for the nontreated condition) and incubate for 8 h.
2. Centrifuge at maximum speed for 8 min and discard the supernatant.
3. Resuspend bacterial pellet with sterile distilled water and measure the OD₆₀₀. Make serial dilutions ranging from 10⁷ to 10⁵ CFUs/mL (see Note 16).
4. Leaf-infiltrate *N. benthamiana* and *N. tabacum* plants with a blunt-end syringe following a predesigned scheme (see Note 17 and Fig. 2).
5. The first signs of hypersensitive responses are visible 12 h post-infiltration, but they can be better appreciated when the dead tissue is totally dry, so the pictures are taken 2 days post-infiltration in *N. tabacum*, and 5 days post-infiltration in *N. benthamiana* (see Note 18).

3.5 Compound Effect on Bacterial Fitness In Planta

1. Grow an overnight pre-culture in liquid B medium supplemented with antibiotics.
2. Measure the OD₆₀₀ of the pre-culture and adjust a bacterial suspension to 10⁵ CFU/mL (OD₆₀₀ = 0.0001) with autoclaved tap water supplemented with each test compound at 100 μ M (or DMSO alone for control condition).

3. Hand-infiltrate 4 tomato leaves per tested compound with a blunt-end syringe (*see Note 19*).
4. Place the infiltrated plants in the growth chamber for 1 h at 27 °C and 60% relative humidity.
5. At time 0 (just after infiltration) and at 4 days post-infiltration (d.p.i.), collect 2 leaf discs (5 mm diameter) from the infiltrated area of six independent leaves. Combine in a 1.5-mL Eppendorf tube the disks from 2 leaves (4 disks total) to generate three biological replicates.
6. Homogenize the plant material with a Potter S homogenizer in 200 μ L of sterile distilled water (*see Note 20*).
7. Add 800 μ L of sterile distilled water to each Eppendorf tube.
8. Place the plants back in the growth chamber.
9. Prepare tenfold dilutions from the leaf homogenates (*see Note 21*).
10. Plate 10 μ L drops of the 4 dilutions on plates of B medium (containing TTC and glucose) supplemented with antibiotics and incubate at 28 °C for 1–2 days to count colonies (*see Note 22*).

3.6 Effect of the T3 Secretion Inhibitor on Bacterial Virulence to Plants

1. Grow an overnight pre-culture in liquid B medium supplemented with antibiotics.
2. For each treatment, wound the roots of 12 plants grown in independent pots with a 1-mL pipette tip by making 4 holes in the soil around the stem. Water each plant with 40 mL of a bacterial suspension containing 10^8 CFUs/mL supplemented with 100 μ M of the compound to test or DMSO (*see Note 23*).
3. Record wilting symptoms during 9 days after infection for each plant using a semiquantitative scale ranging from 0 (no wilting) to 4 (death) (*see Note 24*).

4 Notes

1. For 24 individual square pots mix: 7 L of peat soil, 0.2 L of vermiculite, and 0.2 L of perlite.
2. For gentamicin and tetracycline, use half of the recommended concentration in liquid media (e.g., 10 μ g/mL gentamicin in solid medium and 5 μ g/mL in liquid medium).
3. Keep the TTC solution and tetracycline away from direct light contact. Glucose strongly enhances exopolysaccharide production and TTC turns red through bacterial metabolism, so wild-type *R. solanacearum* colonies appear red with a thick mucus halo in this medium. Spontaneous nonmucous mutants (usually rare) are nonpathogenic and can be discarded.

4. The anti-HA antibody (clone 3F10) from Roche, Switzerland, works well for us at 1:4000 dilution. Anti-HA antibodies from our resources might work as well, and we recommend testing for ideal dilutions before use.
5. To acclimate the plants, 2 days prior to bacterial inoculation, transfer them to the infection growth chamber (27 °C and 60% humidity).
6. For HR assays, plants should not be stressed. Clear signs of stress are chlorotic leaves and flowering. To avoid this, do not water in excess, and always use high-intensity light. Plants can be grown at 24–26 °C without any difference.
7. Minimal medium is appropriate when type III secretion gene expression has to be induced (e.g., *PhrpY::lux*). B medium is appropriate when high growth is desired, or expression of the type III secretion genes has to be repressed.
8. Normally, 10 mL of overnight culture should be enough to prepare 20 tubes for the inhibition test.
9. We recommend measuring OD₆₀₀ from 1/10 dilutions of overnight cultures to avoid saturation, as spectrophotometers usually measure linearly between 0.01 and 2.
10. To ease the experiment, prepare these minimal media culture tubes the day before and store at 4 °C. Pre-warm the media before use.
11. Use a cuvette with the same growth medium as blank to calibrate the spectrophotometer.
12. This protocol can be scaled up to 96-well plates in case a larger set of inhibitors has to be tested. For growth measurements, a transparent bottom plate must be used. For luminescence measurements, use white opaque plates, which help reflecting luminescence and amplify the signal. The 96-well plates can be measured using a Spectramax M3 from Molecular Devices.
13. Luminescence measurements allow quantification of the transcriptional output at different time points, and OD₆₀₀ measurements quantify bacterial growth to normalize luminescence per cell and rule out eventual inhibitory or bacteriostatic effects of the tested compounds.
14. Congo red enhances bacterial protein secretion through the type III secretion system [8].
15. We normally sonicate for 90s at 30% amplification and 10s ON/OFF intervals using a digital sonifier, Model 250/450 (BRANSON, USA). The required sonication time and intervals can vary for different sonifiers.
16. In *R. solanacearum*, an OD₆₀₀ = 1 usually corresponds to 10⁹ CFUs/mL.

17. It is recommended to randomize the infiltration of the bacterial dilutions in different leaves in order to get rid of eventual position effects. Infiltrate in the inter-vein areas to avoid a mixture of treatments.
18. For a better HR cell death visualization, the treated leaves can be bleached using 100% ethanol in a water bath at 60 °C for 20 min.
19. Tomato plants can be vacuum-infiltrated instead using Silwett as an adjuvant to facilitate infiltration (80 µL/L). Usually, 20–30 s of vacuum infiltration is enough per tomato plant, but timings might change in other plant species depending on the hardness of their leaves. A change in the leaf color to dark green indicates proper vacuum infiltration.
20. We use the mechanic drill with a plastic pestle, but a tissue lyser with beads or a classical mortar can also be used.
21. To ease manipulation, it is advisable to perform dilutions in 96-well plates using a multichannel pipette by transferring 10 µL into 90 µL of sterile distilled H₂O consecutively. Make sure to mix well each dilution.
22. For colony count, make sure that colonies are well separated. Bacterial growth is calculated as recovered CFU/cm² (area depends on the size of the leaf disk puncher).
23. In order to facilitate plant infection, it is better to stop watering them 2 days prior to inoculation.
24. Wilting symptoms are recorded based on a scale from 0 to 4: 0 = no wilting, 1 = 25% of the leaves wilted, 2 = 50% of the leaves wilted, 3 = 75% of the leaves wilted, and 4 = 100% of the leaves wilted. It is recommended that the same person carries out the whole symptom recording to avoid biases.

References

1. Duffy B, Schärer HJ, Bünter M et al (2005) Regulatory measures against *Erwinia amylovora* in Switzerland. *EPPPO Bull* 35:239–244. <https://doi.org/10.1111/j.1365-2338.2005.00820.x>
2. MacKie KA, Müller T, Kandler E (2012) Remediation of copper in vineyards—a mini review. *Environ Pollut* 167:16–26. <https://doi.org/10.1016/j.envpol.2012.03.023>
3. Büttner D (2016) Behind the lines—actions of bacterial type III effector proteins in plant cells. *FEMS Microbiol Rev* 40:894–937. <https://doi.org/10.1093/femsre/fuw026>
4. Hudson DL, Layton AN, Field TR et al (2007) Inhibition of type III secretion in *Salmonella enterica* serovar typhimurium by small-molecule inhibitors. *Antimicrob Agents Chemother* 51:2631–2635. <https://doi.org/10.1128/AAC.01492-06>
5. Kauppi AM, Nordfelth R, Uvell H et al (2003) Targeting bacterial virulence: inhibitors of type III secretion in *Yersinia*. *Chem Biol* 10:241–249. [https://doi.org/10.1016/s1074-5521\(03\)00046-2](https://doi.org/10.1016/s1074-5521(03)00046-2)
6. Muschiol S, Bailey L, Gylfe A et al (2006) A small-molecule inhibitor of type III secretion inhibits different stages of the infectious cycle of *Chlamydia trachomatis*. *Proc Natl Acad Sci U S A* 103:14566–14571. <https://doi.org/10.1073/pnas.0606412103>
7. Boucher CA, Barberis PA, Demery DA (1985) Transposon mutagenesis of *Pseudomonas*

- solanacearum: isolation of Tn5-induced Avirulent mutants. *Microbiology* 131:2449–2457. <https://doi.org/10.1099/00221287-131-9-2449>
8. Bahrani FK, Sansonetti PJ, Parsot C (1997) Secretion of Ipa proteins by *Shigella flexneri*: inducer molecules and kinetics of activation. *Infect Immun* 65:4005–4010
9. Solé M, Puigvert M, Davis RA et al (2018) Type III secretion inhibitors for the management of bacterial plant diseases. *Mol Plant Pathol* 20:20–32. <https://doi.org/10.1111/mpp.12736>



Investigation of Drug Efficacy by Screening Bioactive Chemical Effects on Plant Cell Subcellular Architecture

Gian Pietro Di Sansebastiano

Abstract

New biologically active compounds are regularly discovered through screening procedures using micro-organisms. This very cheap procedure is followed by drug discovery that is usually seen as a highly focused approach, testing new compounds on animals or cell lines. In vivo assays of candidate drugs in mammals are expensive and sometimes not affordable at the preliminary stages of drug development. Early screening approaches in transgenic plants would allow chemotherapeutic drug candidates further selection before their characterization in expensive biological models. The proposed screening approach is based on cell subcellular architecture observations in transgenic plants within a short time of treatment, which is better than observing the effects of compounds on growth.

Key words Screening, Transgenic plant, *Arabidopsis*, Chemotherapeutics, Cytoskeleton, Endomembranes, Green fluorescent protein

1 Introduction

The twentieth century saw the introduction of pure small-molecule drug treatments, such as antibiotics, including penicillin (natural product) and ciprofloxacin (synthetic), and an understanding of the biological basis for their activity. New molecules are continuously discovered or synthesized and require efficient screening methods for their functional characterization [1].

An original screening method for chemotherapeutic drugs was recently proposed, based on solid knowledge of tumorigenesis and plant endomembrane biology [2]. It is difficult to draw a picture of the state of the art on this topic because of the novelty of the approach bringing together very distant aspects of cell biology research. What is evident is that the application of small molecules has played a crucial role in identifying novel components involved in the plant secretory system and that the bioactive molecules identified *in planta* were also found to be active in different species, owing to evolutionary conservation [1, 3–6].

New active compounds are regularly discovered through screening procedures using microorganisms. This very cheap procedure does not reveal the full potential of each compound but allows a first selection of the most interesting ones. Chemotherapeutic drug discovery follows this approach temporally and is usually seen as a highly focused approach where new compounds are tested on animals or animal and human cell lines. To reduce costs for selecting the best candidate molecules, new screening procedures on small animals such as *Drosophila* [7, 8] and zebrafish [9, 10] have been developed. The use of plants was also proposed [2, 5, 11], and at least one patent application was deposited [12]. Regardless, despite the great impact of drug discovery on human health, the coverage of innovative approaches in the life sciences is not clear [13]. Early screening approaches using transgenic plants would reduce the number of selected drug candidates to be characterized in later, more expensive, biological models as chemotherapeutics.

Since plant cells are divergent from animal cells, the use of growth as a reporter of small-molecule effects may not translate to chemotherapeutics even if growth inhibition can be observed [14]. The screening approach proposed here is based on subcellular architecture observation [15] within a short time of treatment [2, 16].

Chemotherapeutics interfere with cell vitality, affecting different metabolic and traffic pathways. One of their main targets is cytoskeleton, but they also influence directly membrane organization and traffic such as autophagy. This last process could act as a survival mechanism since it was shown that upregulation of autophagy can reduce the sensitivity to treatment of osteosarcoma cells to cisplatin-based chemotherapy [17]. Autophagy inhibition can thus enhance the efficacy of chemotherapy [18].

Our method proposes to observe a few selected *Arabidopsis* transgenic lines covering both cytoskeleton and endomembranes. As a suggestion, we propose three lines: the first expressing the tagged microtubule-protein TUA6 (GFP-TUA6) decorating cell cytoskeleton with GFP fused to α -tubulin, and the second and third expressing two different vacuolar markers, AleuGFP and GFPChi, selected to label the entire secretory pathway and its compartments but not the autophagic compartments in particular [2]. AleuGFP sorting follows the pathway through the Golgi and prevacuolar compartment to the central vacuole, generally with lytic characteristics [16, 19, 20]. GFPChi sorting to vacuole occurs through different pathways but mainly through direct ER-to-vacuole traffic [16, 19, 20] and is expected to be influenced by autophagy defects because of the cross talk of the two mechanisms. Other markers with similar distribution may be used. Direct observation of the fluorescent pattern perturbation can suggest the subcellular target of drugs and their most probable synergistic combinations.

2 Materials

2.1 Chemicals

Compounds can be dissolved in double distilled water or dimethylsulfoxide (DMSO) to be diluted no less than 1:500 for final use. The definition of an appropriate set of concentrations for screening has to be based on previous experimental data; alternatively, the assessment must be based on practical considerations such as the maximum concentration compatible with a therapeutic use. The use of higher concentrations would be unsustainable, and the effect of smaller concentrations could later be tested directly in animal models if the compound is selected as a candidate drug.

2.2 Transgenic Plants

Transgenic *Arabidopsis thaliana* plants have to stably express chimerical GFP-tagged markers in all tissues. At least two transgenic lines have to be analyzed in parallel, one expressing a GFP-tagged marker decorating cytoskeleton, and the other expressing a soluble vacuolar marker (to visualize all steps of intracellular membrane traffic).

Cytoskeleton composition is conserved among eukaryotes, and differences are restricted only to some organization aspects and specialized functions [21, 22]. To visualize the *Arabidopsis* cytoskeleton, we use GFP-tagged α -tubulin TUA6 (GFP-TUA6) expressed in transgenic *Arabidopsis* ecotype Columbia under the control of the CaMV 35S promoter [23]. Transgenic *Arabidopsis* (cv. Wassilewskaja) lines expressing soluble GFPs (AleuGFP; GFPChi) [24] have been shown to label several membranous compartments: the endoplasmic reticulum (ER), prevacuolar compartments (PVCs), small vacuoles (SVs), and central vacuole (CV).

Transgenic plantlets are grown from T2 seeds on sterile solid Murashige and Skoog basal medium under continuous light at 24 °C. Observed samples consist of plantlets transferred to liquid medium, supplemented with drugs in a range of concentrations that is used to treat human cancer cells in vitro or that would be sustainable in a therapeutic formulation, from 1 μ M to 100 μ M. Plantlets are placed into multiwell plates 14 days after germination and monitored in the following 1–36 h. It is important to start observation within 6 h since strong toxic effects made evident by chlorophyll bleaching (Fig. 1a) mask the initial subcellular targets.

2.3 Microscopy

For microscopic observation, whole plantlets should be mounted in water under glass coverslips and imaged using a confocal laser microscope (for figures, LSM 710 (Carl Zeiss MicroImaging GmbH, Germany) was used). GFP markers can be detected in the wavelength range 505–530 nm, assigning the green color; chlorophyll autofluorescence can be detected above 650 nm, assigning the blue color. Excitation wavelength of 488 nm should be used.

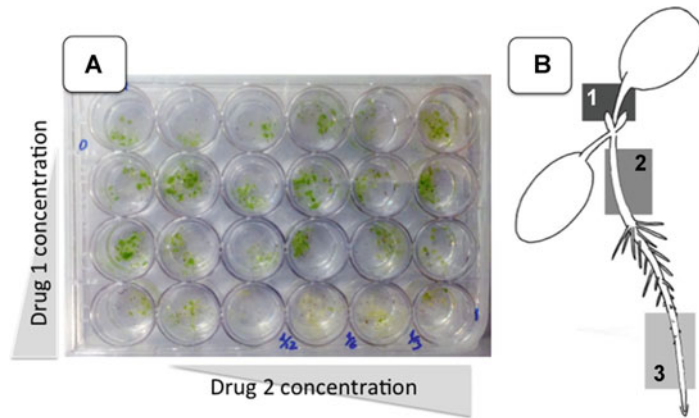


Fig. 1 (a) Suggested organization of samples in a multiwell plate to test one or two drugs; (b) schematic representation of *Arabidopsis* plantlet parts to be observed

Three different portions of plant organs are observed. Cytoskeleton is better observed in petiole and hypocotyl (Fig. 1b, areas 1 and 2), and endomembranes are observed in hypocotyl and root differentiation regions with emerging root hairs (Fig. 1b, areas 2 and 3).

3 Methods

3.1 Plantlet Treatment and Observation

1. Sterilize seeds from T2 transgenic plants transformed with cytoskeleton markers and place them on sterile solid Murashige and Skoog basal medium (MS, 3% sucrose, pH 5.7 adjusted with KOH, 0.8% agar); vernalize incubating 36 h at 8 °C in the dark.
2. Move seeds to a growth chamber for germination and grow plantlets under continuous light (about 120 $\mu\text{E m}^{-2} \text{s}^{-1}$) at 24 °C for about 10 days.
3. 10–14 days after germination, when primary leaves start to be visible, transfer plantlets to liquid medium supplemented with drugs in a range of concentrations that is normally used to treat human cancer cells in vitro; prepare multiple testing solutions using multiwell plates incubating several plantlets (*see Note 1*) in each well.
4. Monitor plantlets in the following 6–36 h. It is important to start observation as early as possible (*see Note 2*) since strong toxic effects made evident by chlorophyll bleaching would mask effects on specific subcellular targets.

5. For fluorescence microscopic observation, mount whole plantlets in water under glass coverslips and image them using a confocal laser microscope, revealing fluorescence of the marker used, with the appropriate wavelength.
6. Observe petiole and hypocotyl elongated cells and visualize cytoskeleton alignment and labeling of microtubules around plastids under control conditions; verify deformation of filaments and detachment from plastids (typical effects of Taxol (paclitaxel) and similar drugs) or destructuration of filaments (often observed with high doses of platinated molecules or sorafenib (BAY43-9006)). Interesting situations were previously described [2] (*see Note 3*).
7. Define a new set of drug concentrations below the dose sufficient to visualize the first effects on cytoskeleton for testing endomembrane traffic markers (*see Note 4*).
8. Repeat **steps 1–5** using transgenic lines expressing secretory markers.
9. Observe hypocotyl elongated cells corresponding to Fig. 1b area 2 (*see Note 5*) and root epidermal cells in the differentiation area corresponding to Fig. 1b area 3, where root hairs start to be formed (*see Note 6*). Verify if root epidermal cell vacuoles appear as under control conditions; verify if compartments of hypocotyl elongated cells are altered, starting from the highest drug concentration tested. Interesting situations were described previously [16].
10. Interpret the data considering that alteration of cytoskeleton implies membrane traffic alteration. The observation of endomembrane traffic alteration in the absence of cytoskeleton defects may indicate off-target undesirable effects. On the contrary, the generation of vesiculation and starting of an apoptotic process may indicate interesting subcellular traffic.

In conclusion, effects on cytoskeleton not anticipated by endomembrane alteration or early vesiculation induction without disruption of ER and CV might indicate interesting drug candidates that may have limited off-target effects on endomembrane traffic (*see Note 7*).

4 Notes

1. Plantlets used for observations are sacrificed. Multiple mechanical stresses should be avoided as much as possible. For this reason, one plantlet should be available to allow the observation at each time point planned. Five to seven plantlets can be incubated in each well.

2. Subcellular effects start immediately, but their interpretation can be difficult; therefore, it is better to wait 1 h to start observation. It is anyhow necessary to perform observations within 6 h.
3. Observation of microtubules (MTs). Hypocotyl and petiole elongated cells have to be observed to establish the conditions of the cytoskeleton labeled by GFP-TUA6. MTs are usually well visible and show a predominant orientation (Fig. 2a); nonetheless, it is possible to note variability in the shape of cells, more or less elongated (Fig. 2a and b) and fluorescent pattern with a less evident orientation of MTs (Fig. 2b). Transition of MT distribution seen in Fig. 2a to distribution seen in Fig. 2b can already reveal an effect of cytoskeleton, but alterations usually appear more distinct. The deformation of MTs due to de-polymerization defects can produce abnormal mixed orientations and multiple curvatures of the same MT (Fig. 2c). Detachment from plastids can also be observed (typical effects of Taxol (paclitaxel) and similar drugs). A more severe effect of drugs on polymerization or turnover can cause deconstruction of MTs. It is often observed with high doses of platinated molecules or sorafenib (BAY43-9006) (Fig. 2d).
4. If cytoskeleton is affected, the alteration of endomembrane will be likely dependent on the cytoskeleton defect. As a consequence, it is not advisable to analyze specific effects on endomembranes since they will be indirect and represent unnecessary costs to evaluate chemotherapeutic drug efficacy in the early screening.

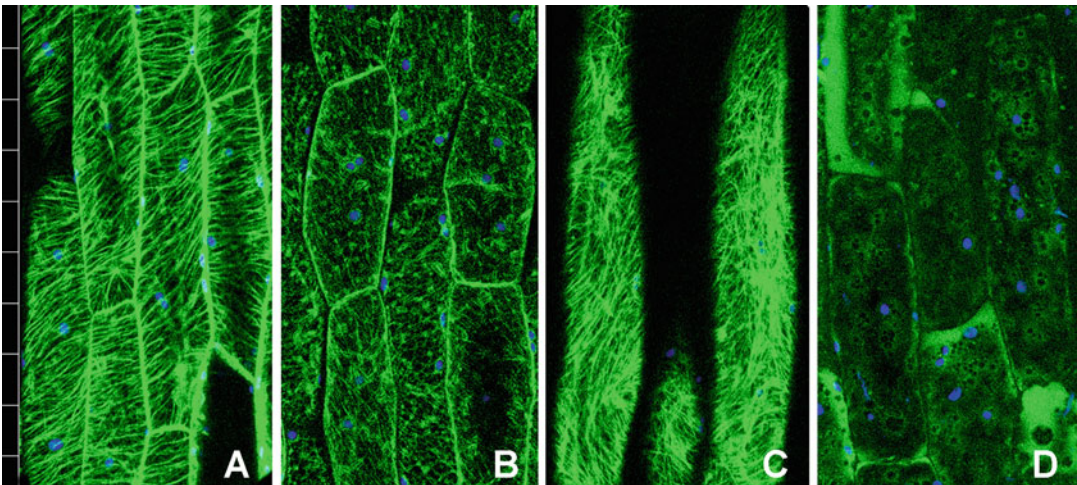


Fig. 2 Z-stack confocal projections of hypocotyl cells from transgenic plants expressing GFP-TUA6 (a, b) under control conditions; (c) treated 1 h with 60 μ M paclitaxel; (d) treated 6 h with 15 μ M sorafenib (BAY43-9006). Scale unit on the left side is 20 μ m

5. The observation of the hypocotyl shows that cells do not stably accumulate GFP in the central vacuole. Differences in vacuolar accumulation of GFP can be observed in transgenic lines from different cultivars of Col0 and the Wassilevskaja used here [24, 25]. The fluorescent distribution of GFPChi is limited to ER and, in particular, ER bodies (Fig. 3a). Alterations can take many forms. In the case of GFPChi, it could be less concentrated in the ER bodies and more distributed in the ER network including nuclear envelope and dotted compartments (Fig. 3b), or it could be exported from the ER but blocked in dotted structures and small aberrant round-shaped vacuoles (Fig. 3c). The pattern may also look essentially unchanged, but the fluorescence in the central vacuole may increase dramatically because of the alteration of central vacuole luminal characteristics (Fig. 3d). Finally, a combination of such alterations may be observed (Fig. 3e). The AleuGFP sorting pathway is shared with proteases [26], and the protein is then unstable in the central vacuole (Fig. 3f). Even if it labels ER bodies, ER labeling is not strong and the signal in the central vacuole may

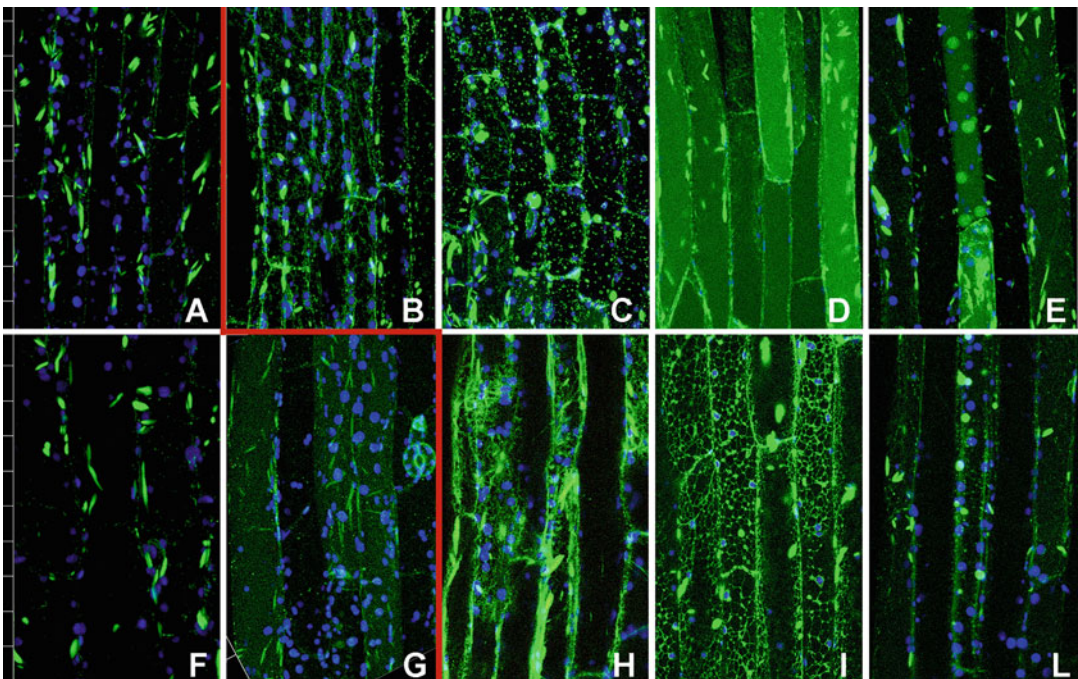


Fig. 3 Z-stack confocal projections of hypocotyl cells from transgenic plants expressing GFPChi (upper row) or AleuGFP (lower row). (a) GFPChi distribution under control conditions or (b–e) treated for 24 h with several Pt-based molecules; (f) AleuGFP distribution under control conditions looks similar to the distribution of GFPChi (a) but under some-not-yet-determined conditions, it may label more dotted structures and central vacuole (g). (h–l) Treated for 24 h with diverse Pt-based molecules, its distribution is altered, labeling more the ER or aberrant small vacuoles. The red line separates images under control conditions from treatments. Scale unit on the left side is 20 μm

occasionally be detectable above background (Fig. 3g). Drug effects can induce a more evident retention of this marker in the ER bodies (Fig. 3h), its distribution in an altered ER network (Fig. 3i) or in aberrant round-shaped small vacuoles (Fig. 3l).

6. Observation of the root epidermis shows different patterns for the two vacuolar GFPs [24]. GFPChi is still distributed in the ER and in small vacuoles (Fig. 4a). Drugs may delay the fusion of small vacuoles inducing the increase of their size (Fig. 4b) or delay the export from the ER itself (Fig. 4c). In some cases, the heterotypic fusion of small vacuoles and the central vacuole can be accelerated (Fig. 4d). AleuGFP is exported from the ER more efficiently [26] and labels directly the central vacuole (Fig. 4e). Since deeper layers of cells belong to different cell types, vacuolar labeling may look different from root epidermal cells under control conditions (Fig. 4f). Drugs may cause retention in small aberrant vacuoles and delay fusion to the central vacuole (Fig. 4g), producing fluorescent patterns similar to those observed with the alternative vacuolar marker (Fig. 4h).

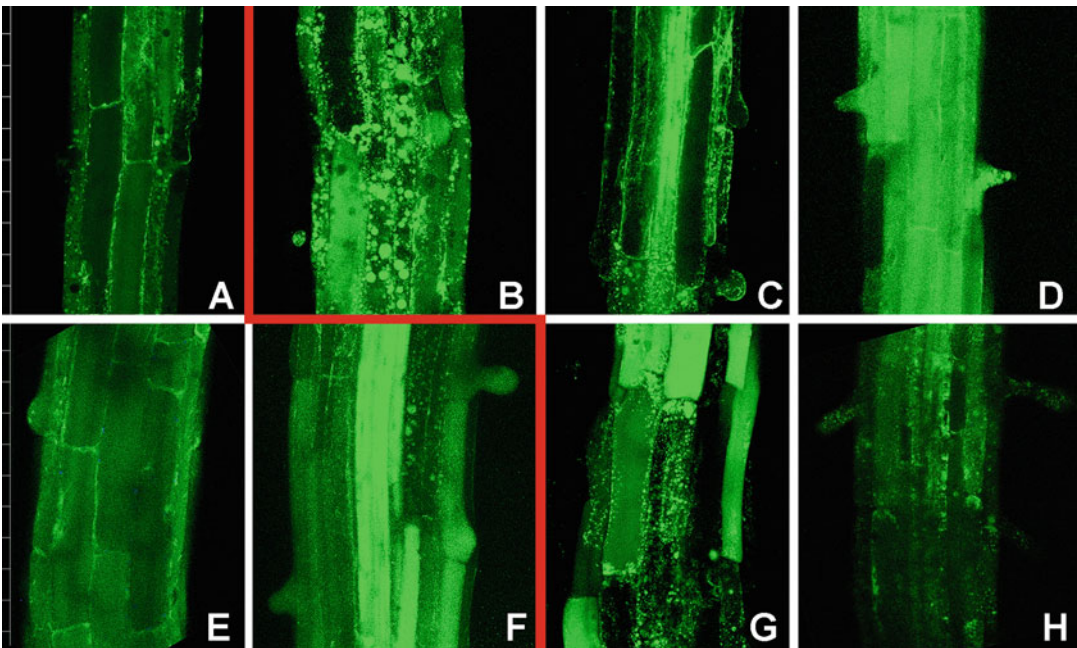


Fig. 4 Z-stack confocal projections of root cells in the differentiation zone of plants expressing GFPChi (upper row) or AleuGFP (lower row). (a) GFPChi distribution under control conditions or (b–d) treated for 24 h with several Pt-based molecules that induce a delay in vacuolar fusions (b), retention in the ER (c), or a more rapid confluence in the central vacuole (d); (e, f) AleuGFP distribution under control conditions labels the central vacuole in root's epidermis (e) but may appear variable in the internal cell layers (f); (g, h) Treatments with drugs (here 24 h with diverse Pt-based molecules) affect arrival to the central vacuole. The red line separates images under control conditions from treatments. Scale unit on the left side is 20 μ m

7. The interpretation of altered patterns has to be done case by case. A suggestion about the interpretation of some of the possible patterns can be extrapolated from previous literature [15, 16].

Acknowledgments

This work was supported by Italian Ministero dell'Università e della Ricerca and Regione Puglia with project n!14 "Reti di Laboratori Pubblici di ricerca, SELGE". A special thanks to Dr. Fabrizio Barozzi for his technical assistance and usefull discussion of the method and to Prof. Daniele Vergara for the critical reading of the manuscript.

References

1. Spring DR (2005) Chemical genetics to chemical genomics: small molecules offer big insights. *Chem Soc Rev* 34:472–482. <https://doi.org/10.1039/b312875j>
2. Vergara D, de Domenico S, Maffia M, Piro G, Di Sansebastiano GP (2015) Transgenic plants as low-cost platform for chemotherapeutic drugs screening. *Int J Mol Sci* 16(1):2174–2186. <https://doi.org/10.3390/ijms16012174>
3. Lobikin M, Wang G, Xu J et al (2012) Early, nonciliary role for microtubule proteins in left-right patterning is conserved across kingdoms. *Proc Natl Acad Sci U S A* 109(31):12586–12591. <https://doi.org/10.1073/pnas.1202659109>
4. Tóth R, Gerding-Reimers C, Deeks MJ et al (2012) Prieurianin/endosidin I is an actin-stabilizing small molecule identified from a chemical genetic screen for circadian clock effectors in *Arabidopsis thaliana*. *Plant J* 71:338–352. <https://doi.org/10.1111/j.1365-3113X.2012.04991.x>
5. Zhang C, Brown MQ, van de Ven W et al (2016) Endosidin2 targets conserved exocyst complex subunit EXO70 to inhibit exocytosis. *Proc Natl Acad Sci U S A* 13(1):E41–E50. <https://doi.org/10.1073/pnas.1521248112>
6. Rodriguez-Furlan C, Raikhel NV, Hicks GR (2017) Merging roads: chemical tools and cell biology to study unconventional protein secretion. *J Exp Bot* 69(1):39–46. <https://doi.org/10.1093/jxb/erx261>
7. Enomoto M, Siow C, Igaki T (2018) Drosophila as a cancer model. *Adv Exp Med Biol* 1076:173–194. https://doi.org/10.1007/978-981-13-0529-0_10
8. Tsuda L, Lim YM (2018) Alzheimer's disease model system using drosophila. *Adv Exp Med Biol* 1076:25–40. https://doi.org/10.1007/978-981-13-0529-0_3
9. Letrado P, de Miguel I, Lamberto I, Díez-Martínez R, Oyarzabal J (2018) Zebrafish: speeding up the cancer drug discovery process. *Cancer Res* 78(21):6048–6058. <https://doi.org/10.1158/0008-5472.CAN-18-1029>
10. Kithcart AP, MacRae CA (2018) Zebrafish assay development for cardiovascular disease mechanism and drug discovery. *Prog Biophys Mol Biol* 138:126–131. <https://doi.org/10.1016/j.pbiomolbio.2018.07.002>
11. Kolkusaoglu U, Thurow K (2010) Future and frontiers of automated screening in plant sciences. *Plant Sci* 178:476–484. <https://doi.org/10.1016/j.plantsci.2010.03.006>
12. Choe S, Puna M M, Park S, Cha R (2017) Method of discovering bioactive substance using plants based on efficacy. Patent application US2017/0218445A1
13. Smith JA, Arshad Z, Thomas H, Carr AJ, Brindley DA (2017) Evidence of insufficient quality of reporting in patent landscapes in the life sciences. *Nat Biotechnol* 35(3):210–214. <https://doi.org/10.1038/nbt.3809>
14. Marti L, Lia A, Reca IB, Roversi P, Santino A, Zitzmann N (2018) In planta preliminary screening of ER glycoprotein folding quality control (ERQC) modulators. *Int J Mol Sci* 19(7):E2135. <https://doi.org/10.3390/ijms19072135>
15. Brown MQ, Ung N, Raikhel NV, Hicks GR (2014) High-throughput identification of chemical endomembrane cycling disruptors

- utilizing tobacco pollen. *Methods Mol Biol* 1056:111–114. https://doi.org/10.1007/978-1-62703-592-7_11
16. Papadia P, Barozzi F, Hoeschele JD, Piro G, Margiotta N, Di Sansebastiano GP (2017) Cisplatin, Oxaliplatin, and Kiteplatin subcellular effects compared in a plant model. *Int J Mol Sci* 18(2):E306. <https://doi.org/10.3390/ijms18020306>
 17. Miao XD, Cao L, Zhang Q, Hu XY, Zhang Y (2015) Effect of PI3K-mediated autophagy in human osteosarcoma MG63 cells on sensitivity to chemotherapy with cisplatin. *Asian Pac J Trop Med* 8(9):731–738. <https://doi.org/10.1016/j.apjtm.2015.07.024>
 18. Friedhuber AM, Chandolu V, Manchun S, Donkor O, Sriamornsak P, Dass CR (2015) Nucleotropic doxorubicin nanoparticles decrease cancer cell viability, destroy mitochondria, induce autophagy and enhance tumour necrosis. *J Pharm Pharmacol* 67(1):68–77. <https://doi.org/10.1111/jphp.12322>
 19. Stigliano E, Faraco M, Neuhaus JM, Montefusco A, Dalessandro G, Piro G, Di Sansebastiano GP (2013) Two glycosylated vacuolar GFPs are new markers for ER-to-vacuole sorting. *Plant Physiol Biochem* 73:337–343. <https://doi.org/10.1016/j.plaphy.2013.10.010>
 20. Barozzi F, Papadia P, Stefano G, Renna L, Brandizzi F, Migoni D, Fanizzi FP, Piro G, Di Sansebastiano GP (2019) VARIATION in membrane trafficking linked to SNARE AtSYP51 interaction with aquaporin NIP1;1. *Front Plant Sci* 9:1949. <https://doi.org/10.3389/fpls.2018.01949>
 21. Yubuki N, Leander BS (2013) Evolution of microtubule organizing centers across the tree of eukaryotes. *Plant J* 75(2):230–244. <https://doi.org/10.1111/tpj.12145>
 22. Brandizzi F, Wasteneys GO (2013) Cytoskeleton-dependent endomembrane organization in plant cells: an emerging role for microtubules. *Plant J* 75(2):339–349. <https://doi.org/10.1111/tpj.12227>
 23. Ueda K, Matsuyama T, Hashimoto T (1999) Visualization of microtubules in living cells of transgenic *Arabidopsis thaliana*. *Protoplasma* 206:201–206. <https://doi.org/10.1007/BF01279267>
 24. Fluckiger R, De Caroli M, Piro G, Dalessandro G, Neuhaus JM, Di Sansebastiano GP (2003) Vacuolar system distribution in *Arabidopsis* tissues, visualized using GFP fusion proteins. *J Exp Bot* 54(387):1577–1584. <https://doi.org/10.1093/jxb/erg160>
 25. Di Sansebastiano GP, Renna L, Gigante M, De Caroli M, Piro G, Dalessandro G (2007) Green fluorescent protein reveals variability in vacuoles of three plant species. *Biol Plant* 51:49–55
 26. Di Sansebastiano GP, Paris N, Marc-Martin S, Neuhaus JM (2001) Regeneration of a lytic central vacuole and of neutral peripheral vacuoles can be visualized by green fluorescent proteins targeted to either type of vacuoles. *Plant Physiol* 126(1):78–86

Part II

New Approaches to Variation: Peptide Screen for Novel Effectors



In Vivo Chemical Genomics with Random Cyclized Peptides

Tautvydas Shuipys, Maureen Clancy, Elizabeth Estrada-Johnson,
and Kevin M. Folta

Abstract

We have developed and applied a novel strategy that can best be described as *in vivo chemical genomics*, a concept where populations of any transformable organism may be screened for consequences of novel RNAs or peptides. We created a library of ~800,000 random DNA sequences biased only by third-position nucleotide substitutions that suppress the frequency of termination codons. The sequences may be shuttled to any plant, microbial, or animal expression vector with recombination cloning. We then generated large populations of *Arabidopsis thaliana* plants, each expressing a randomized DNA sequence, presumably giving rise to synthetic RNA species and/or the peptides they encode. These novel molecules are produced within the context of the cell and have been shown to affect plant biology with a relatively high frequency, as evidenced by diverse phenotypes. This chapter provides the protocols necessary to construct the libraries and isolate plants expressing randomized DNA sequences.

Key words In vitro chemical genomics, Random peptides, Random DNA sequence, *Arabidopsis thaliana*

1 Introduction

Chemical genomics is the emerging field that queries large numbers of small molecules for potential intersection with biological processes. In these screens, extensive libraries of chemical compounds are examined for gain- or loss-of-function effects on discrete aspects of growth, development, or physiology. Synthetic or natural small molecules connect with resident cellular chemistry, leading to a phenotypic variation that can be explored further to understand fundamental biological questions or possibly inform drug design.

These principles have been applied to plants. Chemical genomics screens overcome some of the limitations of standard genetic screens, such as functional genetic redundancy and lethal mutations [1]. These approaches have mostly been used in the model plant *Arabidopsis thaliana* to identify chemistries that affect key processes. Notable examples are inducers of phosphate starvation

signaling [2, 3], ABA signaling in water stress [4], and strigolactone receptor agonists [3]. Such approaches are increasingly valuable in complementing genetic efforts to explore basic plant biology.

It is also clear that peptides have an increasingly visible role in plant processes [5], acting primarily as small signaling entities. Our laboratory has united chemical genomics, peptide ligand biology, and the disruptive potential of random chance using plants [6]. The model plant *Arabidopsis thaliana* is an outstanding system to screen for biologically active peptides. It is easily transformable and transitions through many developmental states where a defect may be exposed. We demonstrated the ability to create phenotypic variation from the introduction of a virtually-random DNA sequence via transgenesis, leading to the production of novel cyclized peptides (or potentially just their nascent RNAs) that affect specific biological processes. Random DNA sequences were identified that delayed flowering, changed plant stature, or were lethal when expressed [6]. Abnormal phenotypes were observed at a surprisingly high frequency.

One particular peptide demonstrated the specific nature of the interaction. It was important to determine if the phenotypes observed were just an artifact of hyper-accumulation of a peptide or if the sequence was directly integrating into a specific process. One of the sequences caused transgenic seedlings to show symptoms consistent with defects in red-light sensing. Seedlings presented long hypocotyls and poorly expanded cotyledons in response to red light, but the effects were not as severe under blue or far-red light [6]. The seedlings were normal in darkness. These observations suggested that the peptide was affecting light sensing, signaling, or response through the red-light photoreceptor phytochrome B.

To narrow down the precise mechanism of action, Shuipys et al. [7] examined other red-light responses and found them to be normal in response to red light. Red light, through phytochrome B, also affects early gene expression, seedling growth relative to gravity, and ultimately flowering time. All of these responses were normal, indicating that the peptide was exerting its effect in the process of red-light-mediated suppression of seedling hypocotyl elongation and cotyledon expansion, two reciprocal responses of cellular expansion in response to light. This work also showed that the peptide could induce the response when applied exogenously, albeit at a lower magnitude. Further study of localization and biochemical interaction is ongoing.

The process is chemical genomics, yet it critically contrasts with previously published methods in several ways. Primarily, the plant generates the novel chemistry in vivo. Also, the peptides created arise from almost-random DNA sequences, leading to production of novel chemistry that biology is forced to reconcile for the very first time. This technique is basically a way to disrupt or enhance

any process of interest through introduction of a completely foreign chemistry cluster that articulates with extant cellular machinery.

Creation of novel peptides within plant populations is a useful approach because it is another way to introduce biological variation for mechanistic analysis of fundamental plant traits. The findings may translate well to application, as novel peptides may inform the development of mimetic compounds that can control plant development or perhaps act as herbicides. The peptides may also identify previously unknown vulnerabilities that may be exploited for herbicide design, potentially giving rise to the next generation of environmentally safe crop protection strategies.

The goal of this chapter is to outline the process of creating the peptide-encoding libraries, their introduction to plants, and noting some of the not-necessarily-obvious considerations in library preparation, screening, and reproducibility.

2 Materials

2.1 Library Construction

1. Custom primer with partial attB sequences:
 5' AAAAAGCAGGCTCC ATG (NNN)_x TAG ACCCAGC TTTCT
 Translational start and stop codons are underlined, and (NNN)_x denotes codons within the open reading frame (*see Note 1*).
2. Universal attB amplification primers:
 attB1: 5' G GGG ACA AGT TTG TAC AAA AAA GCA GGC T 3'
 attB2: 5' GGG GAC CAC TTT GTA CAA GAA AGC TGG GT 3'.
3. Molecular biology grade (MBG) water (e.g., MilliQ 18 MΩcm at 25 °C).
4. Taq DNA polymerase.
5. Thermocycler.
6. Agarose gel and electrophoresis unit.

2.2 Gateway Cloning

1. Gateway-cloning entry vector pDONR222 and destination vector pK7WG2D.
2. BP and LR Clonase enzymes (Invitrogen).
3. Chemically competent cells from *E. coli* host strain.
4. Liquid and solid selective medium: Luria Broth (10 g tryptone, 5 g yeast extract, 10 g NaCl/L), 15 g/L agar for solid medium with addition of kanamycin (50 µg/mL after autoclaving, for

pDONR222 vector) or spectinomycin (75 µg/mL, for destination vector).

5. Sterile microfuge tubes and screw top vials or cryovials.
6. SOC medium (2% w/v tryptone, 0.5% yeast extract, 8.56 mM NaCl, 2.5 mM KCl, ddH₂O, 10 mM MgCl₂).
7. Shaking and stationary incubators at 37 °C.
8. 42 °C water bath .
9. Large square Petri plates (245 mm × 245 mm × 25 mm).
10. Sterile spreader.
11. Culture flasks.
12. Sterile 80% glycerol and –80 °C freeze.
13. Plasmid isolation kit or appropriate reagents.
14. Electro-competent *Agrobacterium tumefaciens* strain GV3101.
15. Liquid and solid selective medium for *Agrobacterium*: LB with 15 g/L agar for solid medium and 10 µg/mL rifampicin, 50 µg/mL gentamycin, and 75 µg/mL spectinomycin.
16. Shaking and stationary incubators at 28–30 °C.

2.3 Floral Dip Transformation of *Arabidopsis thaliana*

1. Wildtype *Arabidopsis thaliana* seeds (Col-0).
2. 4" square pots, 10 × 20 flats, tall humidity domes to fit.
3. Your *Agrobacterium tumefaciens* expression clone or expression library stock.
4. Liquid Agro selective medium: LB containing 10 µg/mL rifampicin, 50 µg/mL gentamycin, and 75 µg/mL spectinomycin.
5. 5% sucrose solution.
6. Silwet-77 reagent.
7. Foil or other light-blocking materials.

2.4 Transgenic Seed Selection

1. 70% ethanol.
2. 50-mL sterile conical tube.
3. Freshly prepared 0.8% sodium hypochlorite (~10% dilution of commercial bleach).
4. Sterile MBG water.
5. Laminar flow cabinet.
6. Top agarose: 0.4% sterile agarose solution at 50–55 °C.
7. 5-mL pipet and tips.
8. Deep Petri plates (100 mm × 15 mm).

9. Selective plating medium: one-half strength MS basal medium, 0.5 g/L MES, adjust to pH 5.8 with KOH, 0.5% Phyto Agar, supplemented after autoclaving with 50 µg/mL kanamycin.
10. Gauze micropore tape.
11. Growth chamber or other controlled temperature light environments.

3 Methods

3.1 Library Construction

1. Amplify the sequence of the random primer template using PCR with the attB1 and attB2 universal primers mentioned above.

PCR reaction composition		
5× Buffer		10 µL
dNTP	10 mM	1.0 µL
MgCl ₂	25 mM	3.0 µL
attB1	10 µM	1.5 µL
attB2	10 µM	1.5 µL
Custom primer	10 µM	0.75 µL
Taq DNA polymerase	5 U/µL	0.25 µL
MBG water		32 µL
<i>Total</i>		<i>50 µL</i>

Prepare four identical reactions, terminating one reaction after 20, 25, 30, and 35 cycles.

<i>PCR program:</i>
2 min @ 95 °C
<i>20—35 cycles:</i>
30 s @ 95 °C
30 s @ 66 °C
30 s @ 72 °C
5 min @ 72 °C
Hold @ 10 °C

2. Determine the optimal PCR cycle number by electrophoresis on ~2% agarose gels (*see Note 2*).
3. Optional: PCR products may be purified using commercial kits or reagents.

3.2 Gateway Cloning

1. Clone the PCR products into Gateway entry vector pDONR222 using a full reaction of BP Clonase enzyme and overnight incubation according to Invitrogen's protocol.
2. On ice, mix quarter-aliquots of the BP entry vector reaction products with four 50- μ L aliquots of chemically competent *E. coli* cells in microfuge tubes and incubate for 30 min. Heat shock each tube for 30–45 s at 42 °C and return to ice briefly before adding 500 μ L of SOC. Incubate shaking at 37 °C for 60 min. Spread the entire transformation volume (~2.2 mL) on one 245 mm \times 245 mm \times 25 mm large Petri plate containing pDONR222 entry vector solid selective medium and incubate overnight at 37 °C (*see Note 3*).
3. Count the colonies in a measured portion of the plate to estimate the total number of entry vector bacterial transformants. A plate with almost confluent growth represents $\geq 10,000$ independent events (*see Note 4*).
4. Harvest bacterial transformants by flooding plate with pDONR222 entry vector liquid selective medium (LB plus 50 μ g/mL kanamycin) and scraping into a sterile bottle or flask using a sterile spreader.

Recommended volumes for harvesting a crowded plate are an initial 40 mL wash, followed by two successive washes of 30 mL. With each wash, use the sterile spreader to mix and recover the bacterial colonies.
5. Add additional medium if harvested culture is excessively thick and refresh by shaking at 37 °C for 1–2 h. Use a few mL to prepare several aliquots of the bacterial library stock in screw top vials or cryovials by adding sterile glycerol to 20–25%; store stocks at –80 °C (*see Note 5*).
6. At this stage, library plasmid DNA may be prepared directly from the harvested culture. We prefer to start an overnight culture (50–200 mL LB plus 50 μ g/mL kanamycin) for a library plasmid DNA prep on the following day and retain the remaining harvested culture at 4 °C until plasmid DNA has been prepared and quantified.
7. Transfer the pDONR222 library or clone to Gateway-compatible overexpression vector (e.g., pK7WG2D) by the LR reaction. Use a 2:1 molar ratio of entry to destination vector in a full reaction of LR Clonase II enzyme overnight according to Invitrogen's protocol.
8. Proceed with bacterial transformation, plating, harvest, and plasmid recovery according to the directions in **steps 2–6** using destination vector liquid and solid selective medium.
9. Transform electro-competent cells of *Agrobacterium tumefaciens* GV3101 with plasmid DNA of the destination vector

library. Plate on one 245 mm × 245 mm × 25 mm large Petri plate containing solid pK7WG2D-Agro selective medium and incubate for 1–2 days at 28 °C to 30 °C (*see Note 6*).

10. Harvest the destination library *Agrobacterium* transformants using pK7WG2D-Agro selective medium and prepare storage cultures (**steps 4 and 5**).

3.3 Floral Dip Transformation of *Arabidopsis thaliana*

1. Grow *Arabidopsis thaliana* seedlings (in our case Columbia-0; Col-0) under long-day illumination in multiple 4" pots (~10–30 plants per pot) until bolting. Plant 1 or more flats of 18 pots for each library transformation. To achieve maximum flowering, remove all inflorescences several times over about 2–3 weeks by cutting with scissors. Fertilize the plants to promote flowering during the cutting phase. Plants are generally receptive for floral dipping about 5–8 days after last cutting: check for abundant flower buds just opening.
2. From a storage culture of *Agrobacterium tumefaciens* containing the expression library, inoculate a 30-mL culture of liquid LB with appropriate antibiotic selection and grow overnight shaking at 28–30 °C. In the morning, dilute 25 mL of the overnight culture into 225 mL LB with appropriate antibiotic selection and incubate to OD600 of 0.8 (about 5 h) with constant shaking at 28–30 °C. Harvest the culture by centrifugation and resuspend the cell pellet in 250 mL of 5% sucrose by swirling and gentle pipetting. After resuspending the cells, add Silwet to 0.02% (50 µL per 250 mL), mixing gently to avoid foaming [8].
3. Pour the cell suspension into a small dish or shallow container. Immerse inflorescences of each pot in the *Agrobacterium* solution for 3–5 s.
4. Drain and then stand pots upright together in containment tray. Plants in pots dipped with the same library can be touching; plants dipped with different libraries should be separated from each other (*see Note 7*). Cover plants and tray with a tall dome to maintain humidity. Use foil or other light blockers and incubate in darkness overnight. After about 20 h, remove foil and humidity dome and continue to grow plants with long-day illumination.
5. To increase transformation efficiency, the floral dipping process can be repeated 1–3 additional times at 5–9 day intervals as new flowers form.
6. Collect seeds after plants have matured, senesced, and dried.

3.4 *Transgenic Seedling Selection*

3.4.1 *Surface Sterilization of Seeds*

1. Add 0.15 g seeds to a sterile 50-mL conical Falcon tube (*see Note 8*).
2. In a laminar flow cabinet, add 40 mL of 70% ethanol and soak seeds 3–5 min, inverting several times to mix; discard the liquid.
3. Soak 15–20 min in 40 mL of 0.8% sodium hypochlorite, occasionally mixing gently to disperse the seeds.
4. Wash seeds thoroughly with four changes of sterile MBG ddH₂O.

3.4.2 *Plating*

1. Add top agarose at 50–55 °C to about 25 mL in the Falcon tube with the seeds. Mix quickly and then use a 5-mL pipette tip to divide the suspension among six deep Petri plates containing solid selective plating medium.
2. Rock each plate to distribute agarose, avoiding pushing seeds all the way to edge.
3. After top agarose has set, apply gauze micropore tape to seal each plate.

3.4.3 *Germination*

1. Stratify plates for 2–3 days (dark, 4 °C).
2. Transfer plates to continuous white light for 4–6 h at room temperature (RT; 22–25 °C).
3. Wrap with foil or use other light blockers and incubate for 2 days at room temperature to synchronize germination and grow etiolated seedlings.
4. Unwrap plates and expose to white light (either continuous light or on long-day cycles).

3.4.4 *Selection*

Initially, all seedlings will be etiolated. Over the next 1–2 days, cotyledons of transgenic seedlings will become green while wild-type seedlings will remain yellow and fail to develop further.

Confirm transgenic seedlings by visualizing GFP expression and by the development of true leaves.

It is also critical to note that the most common phenotype observed is poor growth. It is critical to verify transgene presence using a visual marker in addition to antibiotic selection, as plants may be resistant to the selection agent yet performing poorly due to the peptide.

4 Phenotyping and Genotyping

4.1 *Phase I Screening*

GFP-positive plants and/or plants surviving on the selective media are then observed for developmental differences such as size, pigmentation, and root morphology. Once transplanted into soil,

additional observations on time to flower and rosette diameter can be made. While on media and in soil, GFP-positive plants that exhibit arrested development, alterations in morphology, or premature senescence potentially indicate the presence of biologically active peptides. Leaf material from these plants should be collected, and the sequence of the putatively causal sequence should be determined by PCR with flanking primers and sequencing of the product. All surviving plants are allowed to go to seed, and the seeds are harvested for use in subsequent screens.

4.2 Phase II Screening

Because the candidate sequence is under the control of the CaMV35S promoter, phenotypes arise that are not due to the random sequence but instead are related to excitation of genes adjacent to the T-DNA insert. Candidate sequences from plants exhibiting phenotypes are determined by sequencing and then re-installed into *Arabidopsis* plants to test for independent reproducibility of the phenotype.

4.3 Additional Activities

1. RNA or Peptide? The causative sequence may be recoded to conserve the peptide sequence but alter the RNA sequence. This step will provide additional evidence supporting that the effects arise from either the RNA or the peptide.
2. Conditional screens. All seeds collected may be screened for conditional phenotypes that are induced by the presence of the random peptide. Candidates have been identified, following screens on elevated NaCl, heat, and drought.

5 Notes

1. The experimenter may design codons representing a single specific sequence to produce a desired clone or incorporate random elements to produce a library of sequences.
2. PCR composition and cycling parameters may require adjustment to obtain optimal results based on the characteristics of the custom primer. Agarose gel electrophoresis of the PCR products allows the evaluation of specificity and yield. Select the number of cycles giving good incorporation of primers into a single gel band of the expected size.
Generally, we choose the lowest cycle number fitting these criteria to avoid over-amplification of any specific sequences within the library population.
3. Instead of the preferred large square Petri plates, multiple smaller Petri plates may be used to generate an equivalent surface area for plating.

4. If colony numbers are judged insufficient, repeat the BP entry vector cloning and plating (**steps 1 and 2**) additional times and pool until the desired number of potentially unique clones is obtained.
5. At this stage, the experimenter may wish to make a spot check of clone diversity in the entry vector population. Streak a selective plate with an aliquot of the bulked, harvested bacteria. Prepare plasmid or perform PCR from individual colonies and sequences.
6. Growth may be lightly visible after 24 h and should be maximal on day 2.
7. Some researchers prefer to lay plants horizontally overnight after floral dipping.

We have obtained good transformation results using either orientation, but space considerations lead us to favor upright placement.

8. Generally, about 0.15 g (range of 0.13–0.17 g) seeds, surface-sterilized and divided between six Petri plates, gave 5–20 GFP-positive seedlings per plate.

The seeds should be clean and free of debris, which will be the most likely cause of fungal contamination during selection on agar plates. CONTROLS: Use the corresponding nontransgenic ecotype (e.g., Col-0) on plates with and without kanamycin to verify the efficacy of KAN-selection. *Also:* compare the growth of COL on KAN-minus plates to putative transformants on KAN-plus plates after germination.

References

1. Raikhel N, Pirrung M (2005) Adding precision tools to the plant biologists' toolbox with chemical genomics. *Plant Physiol* 138(2):563–564
2. Bonnot C, Nussaume L, Desnos T (2018) Identification of chemical inducers of the phosphate-starvation signaling pathway in *A. thaliana* using chemical genetics. *Methods Mol Biol* 1795:65–84
3. Holbrook-Smith D, McCourt P (2018) Chemical screening for strigolactone receptor antagonists using *Arabidopsis thaliana*. *Methods Mol Biol* 1795:117–126
4. Okamoto M, Cutler SR (2018) Chemical control of ABA receptors to enable plant protection against water stress. *Methods Mol Biol* 1795:127–141
5. Sarethy IP (2017) Plant peptides: bioactivity, opportunities and challenges. *Protein Pept Lett* 24(2):102–108. <https://doi.org/10.2174/0929866523666161220113632>
6. Bao Z, Clancy MA, Carvalho RF, Elliott K, Folta KM (2017) Identification of novel growth regulators in plant populations expressing random peptides. *Plant Physiol* 175(2):619–627. <https://doi.org/10.1104/pp.17.00577>
7. Shuipys T, Carvalho RF, Clancy MA, Bao Z, Folta KM (2019) A synthetic peptide encoded by a random DNA sequence inhibits discrete red light responses. *Plant Direct* 3(10):e00170. <https://doi.org/10.1002/pld3.170>
8. Clough SJ, Bent AF (1998) Floral dip: a simplified method for agrobacterium-mediated transformation of *Arabidopsis thaliana*. *Plant J* 16(6):735–743



Interfering Peptides Targeting Protein–Protein Interactions in the Ethylene Plant Hormone Signaling Pathway as Tools to Delay Plant Senescence

Alexander Hofmann, Alexander Minges, and Georg Groth

Abstract

Interfering peptides (iPs) have been recognized as valuable substances to specifically target protein–protein interactions (PPIs) in senescence and disease. Although the concept of iPs has been validated for several PPIs in medical and pharmaceutical research, little attention so far has been paid to the enormous potential iPs that may provide to target and control plant growth and developmental processes or plant environmental responses. However, recent research on PPIs in the ethylene signaling pathway has identified the synthetic peptide NOP-1 derived from the nuclear localization signal of ethylene regulator EIN2 as an efficient inhibitor of typical ethylene responses such as ripening, aging, and senescence. Biophysical and biochemical studies on purified recombinant proteins of the ethylene receptor family from various plant species demonstrate that the synthetic peptide binds in the nM– μ M range at the plant target. Here, we describe methods to evaluate and quantify the effect of the NOP-1 peptide on flower senescence as a typical ethylene response in the intact plant system. This approach will help to systematically advance our technological capability to delay plant ethylene responses and to expand shelf-life or vase life of fruits and flowers.

Key words Interfering peptides, Protein–protein interactions, Ethylene signaling, Plant senescence

1 Introduction

Peptides have been shown to play pivotal roles in plant development and plant environmental responses. Based on their biological role, length, and sequence, plant peptides group into different families. These include nonsecreted intracellular peptides such as PEP1 (23 aa) [1] that are released by N-terminal processing from an inactive precursor, posttranslationally modified small peptides (5–20 aa), e.g., of the CLE family [2] requiring proline hydroxylation for biological activity [3] and cysteine-rich peptides (50–100 aa) containing intramolecular disulfide bonds crucial for their biological function. Most of these peptides act locally, but some of them such as CEP have been shown to function as a root-to-

shoot mobile signal and are transported in the vasculature [4]. According to our current knowledge, all known plant peptides bind to specific pockets at target receptors where they initiate plant responses to the peptide. Some of these highly specific and selective binding sites have been resolved in atomic resolution, helping to understand receptor signaling or to identify small molecule mimetics for receptors and related plant responses.

In contrast to these natural peptide ligands targeting soluble or membrane-bound receptor proteins, synthetic peptides may modulate plant signaling and response by interfering with protein–protein interactions (PPIs) at any point in the signaling pathway. These peptides often target large and flat protein surfaces rather than well-defined ligand-binding pockets formed by a few residues with the remaining protein structure acting as a framework for the correct orientation of binding residues [5].

The first peptide described in pursuit of the idea of interfering with plant PPIs was identified in our lab [6]. Studies on the ethylene signaling pathway uncovered that the highly conserved nuclear localization signal (NLS) sequence of the central ethylene signaling regulator EIN2 provides tight interaction with the plant hormone receptors located at the ER membrane. Synthetic peptides mimicking the NLS sequence were shown to interfere with this PPI, thereby destabilizing or disrupting the EIN2-ethylene receptor complex [6, 7]. Subsequent work from our lab demonstrated that these NLS peptides, in particular, the octapeptide NOP-1 (H2N-LKRYKRRL-COOH), have the potential to reduce diverse ethylene-specific developmental processes in plants [8–10]. The findings opened up a novel route to control plant ethylene responses such as fruit ripening or flower senescence.

Here, we describe a quantitative and highly parallel method for the phenotypic analysis of carnation plants—an established model system to study flower senescence—upon application of the inhibitory peptide NOP-1. More specifically, this method extends traditional plant senescence studies by temporal and spatial digital RGB tracing, aiming to visualize and quantify floral senescence at high resolution. The technology for acquiring high-quality RGB data in an automated manner has become more affordable and manageable in recent years in terms of instrument size, paving the way for a scientific use in small-to-medium-sized controlled environments. To be more precise, a modular setup with an RGB camera (Raspberry Pi Camera Module v2), controlled by a Raspberry Pi single-board computer, is used in our approach to evaluate and quantify the effect of inhibitory peptides on floral senescence. Plants treated with the senescence inhibitory peptide and control plants are placed in custom-designed containers in a controlled environment below the camera and are monitored throughout their vase life. At an interval of 20 min, high-resolution images are recorded inside a phyto-chamber. This vast amount of image data can be readily

analyzed by the open-source platform PlantCV [11], which is used here to track mean RGB values and the diameter of each carnation's inflorescence throughout the experiment.

2 Materials

Prepare all buffers and solutions using ultrapure water. Reagents used should be of analytical grade/high quality. Prepare and store all reagents at room temperature if not stated otherwise.

2.1 Plant Material

For vase-life experiments, use untreated freshly cut carnation flowers preferentially of cv. Delphi. The white color of this line gives the best contrast for RGB picture tracking and background subtraction. Additionally, this line is not among the carnation lines specifically bred to have a high ethylene tolerance [12], proving them receptacle for NOP-1 treatment. The average vase life of this cultivar is 10 days [13], but this value is subject to high plasticity and vase life up to 21 days has been observed.

2.2 Instrumentation

1. Analytical scales (with a range of 82 g—0.01 g).
2. Peptide concentration determination: Use either a plate reader with a NanoQant function for 2 μ L drops or a spectrometer as an alternative.
3. Phyto-chamber, for example, a Percival AR41L2.
4. Color palette, for example, SpyderCHEKR[®] 24 from Datacolor AG Europe, Dietlikon, Switzerland.
5. Raspberry Pi (RPi) single-board computer and Raspberry Pi Camera Module v2 (PiCam) for automatic image acquisition and sensor readout (*see Note 1*).
6. Sensors: A broad variety of sensor modules can be directly controlled by the RPi and may be used to log additional data such as temperature, humidity, or illumination. Common choices include BME280- (temperature/humidity/pressure) or DHT22-based (temperature/humidity) modules, e.g., Adafruit BME280-SPI/I2C (Adafruit, New York, USA).
7. (a) Standard container for cut flowers: 15-mL screw cap tubes may be used for initial tests. However, reservoir volume is limited in this case and frequent watering is required (*see Note 2*).
 - (b) Customized container (vase) for cut flowers: To allow for continuous medium and water supply of cut flowers, customized triplicate containers that include a reservoir compartment holding up to 50 mL of liquid shared between the triplicate vase containers were designed. This setup allows reservoir refilling without moving plants, which helps to maintain consistent orientation of flowers throughout the experiment.

Triplicate vases can be 3D-printed using food-safe black polyethylene terephthalate (PETG) filament (*see Note 3*). The model has been designed to be printable without support structures. Design files and meshed models can be prepared using FreeCAD Version 1.18 [14] and are available for download [15]. Check printed containers for water tightness before usage (*see Note 4*).

2.3 Software Stack for Data Analysis

1. Image processing: PlantCV [11] library used with the Python programming language. Initial workflow development can be performed in an interactive manner using the Jupyter Notebook software [16]. The PlantCV documentation [17] provides excellent information on how to set up a working environment of Python, PlantCV, and Jupyter (*see Note 5*).
2. Data obtained from image processing can be further analyzed using the R programming language (*see Note 6*).

3 Methods

3.1 Preparation of Peptide Stock for Senescence Studies

1. Prepare peptide solutions immediately before use. Make sure that the buffer used is suitable for the peptide used. Typically, ion strength and pH of the buffer have to be adjusted according to the peptide characteristics. Choose a pH that differs by at least 1.5 units from the isoelectric point (IEP) of the peptide. If the peptide is sensitive to oxidation, the addition of reducing agents such as dithiothreitol (DTT) or β -mercaptoethanol (BME) is recommended to preserve peptide activity. NOP-1, the peptide used in this study, has a molecular weight of 1132.42 Da and a theoretical *pI* of 11.73. The peptide is used at a final concentration of 500 μ M in 10 mL in a buffer at pH 8.0.
2. Prepare 3 mL of a 5 mM peptide stock solution by weighing in 17 mg of lyophilized peptide and solubilize in 3 mL of 50 mM Tris-HCl at pH 8.
3. Determine peptide concentration by measuring absorption at 280 nm or by infrared (IR)-based spectrometry, e.g., by using a Millipore Direct Detect™ (Merck, Darmstadt, Germany). For peptides such as NOP-1 containing only low amounts or even single aromatic amino acids, quantification on IR-based detection is recommended.
4. Add 1 mL of the stock solution to 8 mL of buffer in a 15-mL screw-cap tube.
5. Readjust pH to the desired value (pH 8 for NOP-1).
6. Prepare buffer without peptide but otherwise identical to the peptide solution prepared in **step 4** for the mock treatment.

3.2 Setup of Senescence Studies

The principle setup of the phenotyping analysis of senescence processes in cut flowers is illustrated in Fig. 1.

1. Buy plants freshly, preferentially from the direct distributor. Three replicates for each treatment should be selected and kept in tap water until use.
2. *Time critical step*: Cut stalks to 9 cm from the bottom of the receptacle with a disposable scalpel to increase the surface area for uptake in a reproducible fashion. A paper template with a 45° angle, drawn in a square, can be used to cut the stalk at this angle (*see* Fig. 1b for illustration). This step is critical and has to be done quickly to lower the chance of xylem cavitation and embolisms, both of which lead to premature senescence and lowered transpiration [18].
3. Incubate the processed plants in 10 mL of the treatment solution, by placing them in 15-mL screw-cap tubes. This step should be performed in the morning, for the uptake of the treatment solution will take place in the course of day 0.
4. When the treatment solution is completely used up, transfer plants to the 3D printed triplicate container, filled with tap water. Be careful not to have inflorescence overlaps from the top view, in order to allow automatic area detection of the inflorescence. Use a black piece of cloth or plastic to provide high contrast between plants and background.

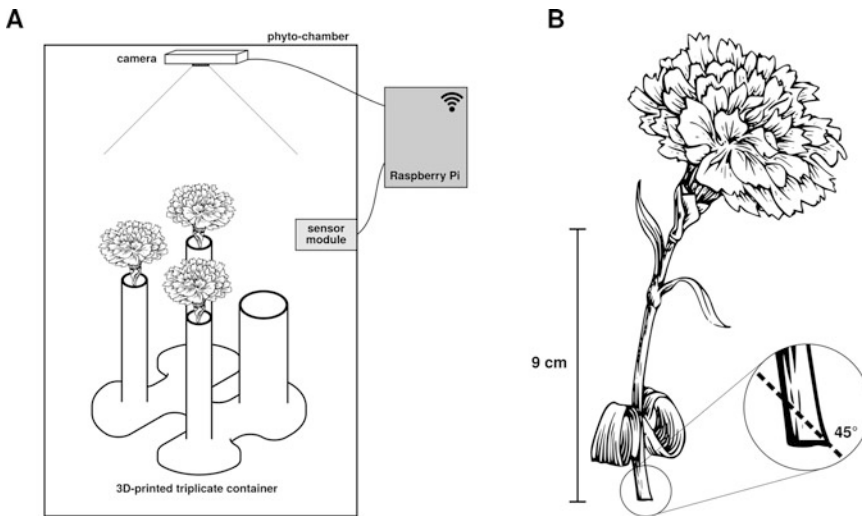


Fig. 1 Schematic representation of the phenotyping platform. (a) With carnations positioned under the PiCam in a triplicate container. The camera module is positioned right above the plants inside the phyto-chamber. Additional sensors, like the humidity sensor, are also attached inside the chamber at the level of the inflorescence. All modules are linked to the Raspberry Pi 3 single-board computer, which controls image acquisition. The carnations are cut to a stalk length of 9 cm from the receptacle (b) with an angle of 45° to increase the water-absorbing surface

5. Position the color palette next to the triplicate container and check if the complete color palette is visible in each picture.
6. Place the camera in a way that all plants and the color palette are within the imaged area. Position any sensors (e.g., humidity) at the level of the inflorescence.
7. Operate the phyto-chamber at 20 °C, permanent illumination (~150 PAR at canopy level), and ~50% air humidity. The permanent illumination serves the image tracking, to produce identical light patterns throughout each picture.

3.3 Continuous Monitoring of Senescence Studies

1. Login locally using keyboard and screen attached to the RPi or via SSH network access into the RPi. The procedure outlined below will work from the command line under GNU/Linux or Mac OS. The recommended SSH client to use in conjunction with Windows is PuTTY[19].

```
# ssh pi@rpi.ip.address
```

2. Verify that sufficient memory is allocated to the graphical processing unit (GPU) as this is required for the camera module to work properly in the highest resolution. Start the raspi-config tool:

```
# sudo raspi-config
```

Navigate to the ‘Advanced Options’ using the arrow keys and confirm by pressing [ENTER]. Select ‘Memory Split’ and set to 256 MB.

3. Move back to the main menu and select ‘Interface Options’. Select ‘Camera’ and choose ‘Enable’.
4. Navigate back to the main menu and exit the raspi-config tool. Reboot the system:

```
# sudo reboot
```

5. After rebooting, log in again as described in **step 1**. Verify that the camera is properly attached and detected by the operating system:

```
# raspistill -v -o test.jpg
```

This command should give no errors and yield a JPEG image with nonzero size:

```
# ls -lh test.jpg
-rw-r--r-- 1 pi pi 518K Mar 11 2019 test.jpg
```

6. Copy the image to your workstation for inspection:

```
# scp pi@rpi.ip.address:/home/pi/test.jpg ./test.jpg
```

If using Windows, open a command line (cmd.exe) and run the command above but replace “scp” with “pscp”.

If you are not connected via network, but logged in locally with keyboard and screen attached to the RPi, you can access a live preview of the camera:

```
# raspistill --preview -t0
```

To terminate the preview, close the program by pressing [CTRL+C] on the keyboard.

7. Adjust the viewport by using either test images transferred to your workstation or the local preview as described in **step 6**.

8. Create a directory to store the time-lapse images (*see Note 7*):

```
# mkdir ~/time_lapse
```

9. Time-lapse images can then be captured using the following command:

```
# raspistill -t 1209600 -tl 1200000 -o ~/time_lapse/image%06d.jpg
```

The total run-time of the time-lapse is specified in seconds following the parameter “-t”. Images will be taken every 20 min, which is determined by the parameter “-tl” that requires the interval to be given in ms. Images will be written to the filename and path given by the “-o” parameter. File-names will be suffixed with a 6-digit frame number including leading zeros. To switch, e.g., to four digits, change “%06d” to “%04d” in the filename. When using the raspistill program to capture time-lapse images as stated above, image parameters such as white balance, shutter, and exposure time may vary from image to image. In this case, preprocessing of all images to correct colors and white balance in relation to a reference picture is mandatory. White balance and exposure time can be specified by passing the ‘--awb’ and ‘--shutter’ options. However, these parameters have to be adjusted empirically. Please refer to the raspistill documentation [20] on valid values for these options. Alternatively, a simple python script that captures a time-lapse with fixed camera settings provided at

[15] may be used. Settings are automatically optimized before taking the first picture and kept constant for all subsequent images. When using this script, correction of color and/or white balance is not necessary if illumination is kept constant. If illumination changes during the experiment or image acquisition is interrupted and restarted, color correction and adjustment of white balance is strictly required.

10. To terminate the capturing process before the specified time (14 days in this example) has passed, press [CTRL+C].

3.4 Processing of Image Files Acquired in Senescence Studies

1. Copy images to the workstation used for data analysis. This can be done via network access (*see* Subheading 3.3, step 6) or locally using external USB drives.
2. To process the images captured during a time-lapse, a set of filters needs to be defined that will reliably distinguish plant material (e.g., petals) from the background (*see* Note 8) and the other items that are visible on the pictures. Optionally, images may be color corrected in relation to a reference picture (usually the first picture of the dataset) to ensure the comparability of color values across the dataset (*see* Note 9). Install Python, PlantCV, Jupyter, and their dependencies (*see* Note 10). Refer to the PlantCV documentation [17] for an in-depth description of the installation procedure.
3. Start the Jupyter notebook server from a command line:

```
# jupyter notebook
```

4. The default web browser will start automatically, presenting an overview of running notebook sessions. Alternatively, a URL pointing to the page is shown in the command line output and can be copy-pasted to a web browser of choice.
5. Open a new notebook by selecting “New”. Choose either “Python 2” or “Python 3” depending on the Python version installed in step 2. An example notebook is included in the dataset for this article [15]. For further details, refer to the PlantCV documentation and tutorials on setting up a VIS workflow and/or a multiplant workflow [17]. Start by loading the necessary libraries and turn on visual debugging information:

```
import sys
from plantcv import plantcv as pcv
pcv.params.debug='plot'
```

Execute the commands by pressing [SHIFT + ENTER]. A new cell will be created after these commands have been run successfully.

6. Load a single picture from the dataset to test filters and object recognition parameters (test image):

```
img, path, filename = pcv.readimage("/path/to/image.jpg")
```

7. If necessary, use the `pcv.shift_img` and `pcv.rotate` functions to correct misalignment of the (color corrected) test image and to remove unwanted objects that might disturb object recognition (e.g., color checker card or reflections) from the image:

```
# image will be shifted 880 pixels from right to left;
# original image size is maintained
shifted = pcv.shift_img(img, 880, 'right')
```

Use the rotated/shifted image for subsequent analysis steps instead of the originally loaded and color-corrected one.

8. Convert image to grayscale-color space. Here, HSV (Hue, Saturation, Value) and LAB (Lightness, Green-Magenta, Blue-Yellow) color spaces are used. We combine value (v) and lightness (l) channels to generate a threshold mask and isolate flowers from the background of the pictures. However, any single channel or a combination of multiple channels may be used to construct a working filter for image recognition depending on the plant material used and imaging conditions. Additional filter algorithms may be applied to further improve the mask. In the following example, small false-positive regions will be filled.

```
# convert to HSV and LAB grayscale
v = pcv.rgb2gray_hsv(shifted, 'v')
l = pcv.rgb2gray_lab(shifted, 'l')
# generate binary masks; channel values above 180 (v) or
100 (l)
# will be kept
v_thresh = pcv.threshold.binary(v, 180, 255, 'light')
l_thresh = pcv.threshold.binary(l, 100, 255, 'light')
# filter out small (< 200 px) false-positive regions of the
mask
v_thresh_fill = pcv.fill(v_thresh, 200)
l_thresh_fill = pcv.fill(l_thresh, 200)
# combine both masks
combined = pcv.logical_or(l_thresh_fill, v_fill)
# filter black and white noise
filled = pcv.fill(combined, 400)
final_mask = pcv.closing(filled)
```


9. Inspect the generated mask (`final_mask`) for correctness: Petal area should be completely covered without gaps or missing parts. Background and objects should not be included. Take special care to identify potential overlaps between individual flowers (*see Note 11*).
10. Extract objects (individual flowers) from the original image using the generated mask and cluster them.

```
id_objects, obj_hierarchy = pcv.find_objects(shifted, combined)
# optionally a region of interest may be defined to limit
# analysis to certain areas
roi_objects, roi_obj_hierarchy, kept_mask, obj_area = pcv.
roi_objects(shifted, 'partial', roi_contour, roi_hierarchy,
            id_objects, obj_hierarchy)

# cluster objects based on a defined grid; adjust grid
# parameters (6, 6) in a way that ideally one flower is present
# per grid square
clusters_i, contours, hierarchies = pcv.cluster_contours(
    shifted, roi_objects, roi_obj_hierarchy, 6, 6,
    show_grid=True)
```

11. Inspect the clusters generated. Colors should be different for all individual flowers, which will indicate the absence of overlaps and proper alignment to the grid specified in **step 10**.
12. Split the original image to show individual flowers and generate masks for them. Write them to a specified output directory:

```
out = "/path/to/output/"
output_path, imgs, masks = pcv.cluster_contour_splitimg(
    shifted, clusters_i, contours,
    hierarchies, out, file=filename)
```

13. Use generated masks to re-process the original image and analyze color values and petal area for individual flowers. A separate result file is saved for each identified flower:

```
for i in range(0, len(masks)):
    o, h = pcv.find_objects(shifted, masks[i])
    # merge if holes in mask generate multiple contours
    o, m = pcv.object_composition(shifted, o, h)
    # analysis of area and color values
    size_img = pcv.analyze_object(imgs[i], o, m)
    color_hist = pcv.analyze_color(imgs[i], m, 'all')
    # output results to text file
    pcv.print_results(filename="{}/{}_{}_result.json".format(
        out, basename, str(i)))
```

14. The result file in JSON format can then be inspected using text editors or imported into data analysis programs such as R or Origin for further processing and visualization.
15. Convert the Jupyter notebook to a Python script for batch processing of images (*see* **Note 12**).

3.5 Analysis of Processed Image Data

Generated results can be processed using commercially available data analysis software (e.g., Origin) or freely available tools such as R (*see* **Note 13**). To import data into R, the jsonlite [21] package is needed to map the data structure from the result files to appropriate data types within R. Blue color frequencies from the detected flower area are used in the example below:

```
install.packages("jsonlite")
install.packages("ggplot2")
library(jsonlite)
library(ggplot2)
# load data from file
json <- fromJSON("/path/to/result/file")
# move blue color frequency values to data frame for plotting
data <- as.data.frame(json$observations$blue_frequencies)
# visualize data
p <- ggplot(data, aes(label, value))
p + geom_col() + labs(x="color value", y="frequency (blue channel)")
```

This will plot a histogram of frequency distribution of blue color value within the flower area. To extract the most populated color value:

```
index <- which.max(data$value)
most_populated <- data$label[index]
```

This value can be averaged for each replicate. By iterating over all result files, variation of recorded parameters over time can be resolved (*see* Fig. 2).

3.6 Troubleshooting

1. If AgNO₃ is used as a positive control, it is essential to use acetate for pH adjustment since HCl will lead to insoluble AgCl precipitate.
2. Coprecipitated salts after HPLC peptide purification may lead to varying results of peptide concentrations in comparison to the mass of lyophilized powder used. An accurate determination of the final concentration is essential. If possible, use Direct Detect™ for a final assessment.

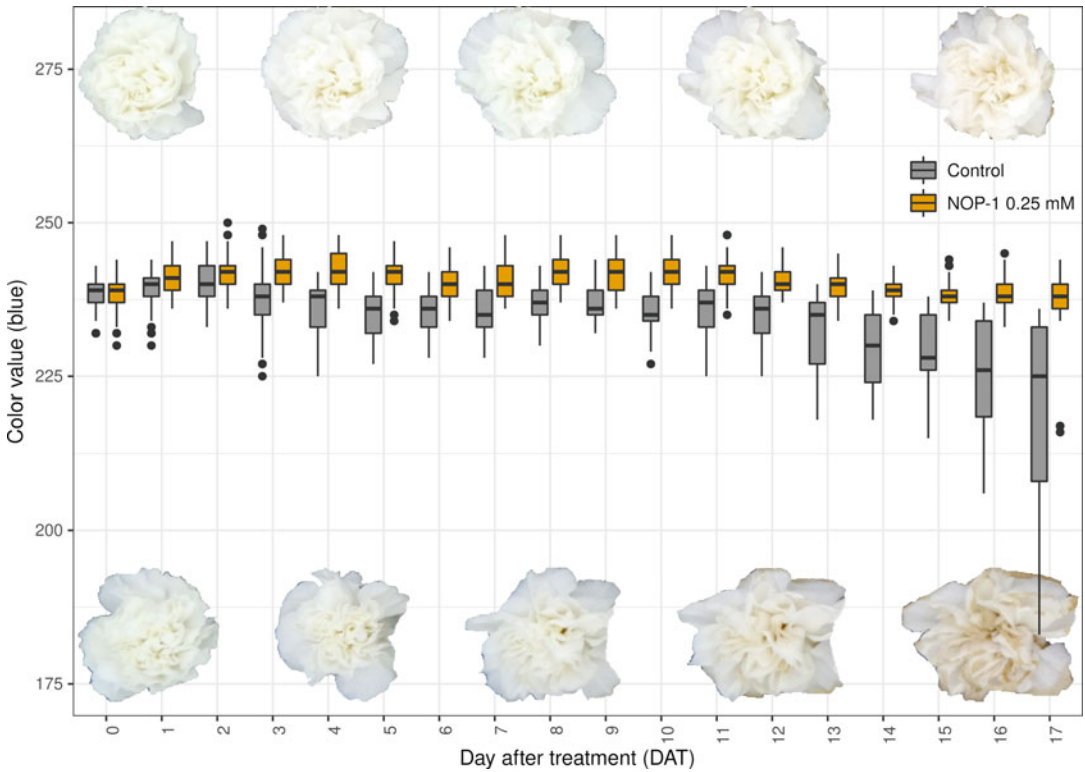


Fig. 2 Time course of senescence tracking in carnation. The most populated bin from the frequency distribution of blue color values extracted from the RGB images is plotted in the course of 17 days. Whisker box plot boxes in gray represent mock-treated triplicate averages and orange represents triplicates treated with one initial dose of 0.25 mM NOP-1. The carnation inflorescences (top row) show representative images from the indicated time point of mock-treated plants. NOP-1-treated plants are shown in the bottom row

4 Notes

1. Any model of Raspberry Pi will work; however, for capturing images at maximum resolution supported by PiCam, a Raspberry Pi 3 or later is recommended. Choose a SD card that is at least 16 GB in size if you intend to use it for image storage in addition to holding the operating system image. Optionally, attach a USB stick to the RPi. External USB hard disks may be used but usually require external power (e.g., via a powered USB hub). Refer to RPi documentation [20] on how to install the Raspbian Linux distribution and set up network connectivity. If you do not intend to use the RPi with network access, a USB keyboard and a screen with HDMI port or appropriate adapters are needed. Screen and keyboard are recommended for the initial setup since this will enable the user to benefit from a live preview for adjusting the view port (*see* Subheading 3.3, step 6). It is recommended to install the necessary

software and test the camera (*see* Subheading 3.3) before installing the hardware in the phyto-chamber. This includes updating the operating system and installed packages to their latest versions. For best compatibility, use a genuine PiCam module and connect it to the CSI port on the RPi. For capturing images at near infrared (NIR), PiCam noIR can be used. This will however result in slight color distortions under visible light conditions.

2. Displacement of plants during watering might introduce distortions in petal area measurements and/or color analysis.
3. PETG is highly recommended for printing as it provides sufficient tolerance to commonly used chemicals. Choose a color that provides minimal contrast to the background and maximum contrast to the petals.
4. To obtain a water-tight setup, print at low speeds and set up the printer to slightly over-extrude: 10–25% of over-extrusion is usually sufficient. Depending on the printer model and the brand of filament used, it may be helpful to reduce the speed of the part cooling fan or even to turn it off.
5. Image processing can be resource demanding, depending on image resolution and processing methods used. Hence, a modern computer running an operating system supported by the processing software stack (GNU/Linux, Mac OS, or Windows) with 4 GB of RAM or more is recommended if processing full-size pictures captured by the PiCam.
6. To import results generated by PlantCV into R, the package `jsonlite` [21] is used. Publication-quality data visualization can be achieved by using the R package `ggplot2` [22].
7. If using an external USB device, you have to mount it at the created folder. Refer to the RPi documentation [20] on how to do that.
8. The choice of appropriate filter combinations and algorithms is an iterative empiric process that is manually done using a small subset of images from the dataset that ideally represent different stages of flower senescence. If no common filter set can be derived that works well for the whole dataset, the dataset needs to be split into batches of similar images (e.g., stages of senescence). This manual step will be performed using Jupyter notebooks, which later can be transformed to Python scripts that can be used to process the whole dataset.
9. If color correction is necessary, load the reference image and derive a color correction matrix. Please refer to the PlantCV documentation on color correction and the example Jupyter

notebook that is distributed with this article [15] on how to do that. Apply the color correction matrix to the test image. This will result in a side-by-side view of the reference image, the original example image, and the color-corrected example image. Make sure that colors do not appear distorted.

10. Python can be obtained from the project website (<https://www.python.org>). Commonly used GNU/Linux distributions either provide Python preinstalled or as packages that can be installed using the respective package manager.
11. When required, the mask can be eroded to eliminate overlaps. However, erosion must be applied to all analyzed images uniformly to ensure comparability. Refer to the PlantCV documentation [17] for instructions on how to use the erode function.
12. To convert a functional Jupyter notebook to a python workflow script that can be applied to the whole dataset of images, refer to the instructions provided within the PlantCV documentation [17].
13. Please refer to the R documentation on detailed usage instructions. A number of graphical user interfaces for R are available (e.g., RStudio [23]).

References

1. Huffaker A, Pearce G, Ryan CA (2006) An endogenous peptide signal in *Arabidopsis* activates components of the innate immune response. *Proc Natl Acad Sci U S A* 103 (26):10098–10103. <https://doi.org/10.1073/pnas.0603727103>
2. Matsubayashi Y (2014) Posttranslationally modified small-peptide signals in plants. *Annu Rev Plant Biol* 65:385–413. <https://doi.org/10.1146/annurev-arplant-050312-120122>
3. Santiago J, Brandt B, Wildhagen M, Hohmann U, Hothorn LA, Butenko MA, Hothorn M (2016) Mechanistic insight into a peptide hormone signaling complex mediating floral organ abscission. *elife* 5. <https://doi.org/10.7554/eLife.15075>
4. Okamoto S, Tabata R, Matsubayashi Y (2016) Long-distance peptide signaling essential for nutrient homeostasis in plants. *Curr Opin Plant Biol* 34:35–40. <https://doi.org/10.1016/j.pbi.2016.07.009>
5. Pu L, Govindaraj RG, Lemoine JM, Wu HC, Brylinski M (2019) DeepDrug3D: classification of ligand-binding pockets in proteins with a convolutional neural network. *PLoS Comput Biol* 15(2):e1006718. <https://doi.org/10.1371/journal.pcbi.1006718>
6. Bisson MM, Groth G (2015) Targeting plant ethylene responses by controlling essential protein-protein interactions in the ethylene pathway. *Mol Plant* 8(8):1165–1174. <https://doi.org/10.1016/j.molp.2015.03.014>
7. Bisson MM, Kessenbrock M, Muller L, Hofmann A, Schmitz F, Cristescu SM, Groth G (2016) Peptides interfering with protein-protein interactions in the ethylene signaling pathway delay tomato fruit ripening. *Sci Rep* 6:30634. <https://doi.org/10.1038/srep30634>
8. Kessenbrock M, Klein SM, Muller L, Hunsche M, Noga G, Groth G (2017) Novel protein-protein inhibitor based approach to control plant ethylene responses: synthetic peptides for ripening control. *Front Plant Sci* 8:1528. <https://doi.org/10.3389/fpls.2017.01528>
9. Klein S, Fiebig A, Noga G, Groth G, Hunsche M (2019) Ripening inhibitory effect of the ethylene signalling protein EIN2 derived octapeptide NOP-1 on tomatoes as influenced by repeated applications and applications at different ripening stages. *Sci Hortic* 254:143–147. <https://doi.org/10.1016/j.scienta.2019.05.011>

10. Hoppen C, Muller L, Albrecht AC, Groth G (2019) The NOP-1 peptide derived from the central regulator of ethylene signaling EIN2 delays floral senescence in cut flowers. *Sci Rep* 9(1):1287. <https://doi.org/10.1038/s41598-018-37571-x>
11. Berry JC, Fahlgren N, Pokorny AA, Bart RS, Veley KM (2018) An automated, high-throughput method for standardizing image color profiles to improve image-based plant phenotyping. *PeerJ* 6:e5727. <https://doi.org/10.7717/peerj.5727>
12. Onozaki T (2018) Breeding of carnations (*Dianthus caryophyllus* L.) for long vase life. *Breed Sci* 68(1):3–13. <https://doi.org/10.1270/jsbbs.17091>
13. Edrisi B, Sadrpoor A, Saffari V (2012) Effects of chemicals on vase life of cut carnation (*Dianthus caryophyllus* L. ‘Delphi’) and microorganisms population in solution. *J Ornamental Horticultural Plants* 2(1):1–11
14. <https://www.freecadweb.org/>. Accessed 12 Jul 2019
15. Minges A (2019) Supplemental data: interfering peptides targeting protein-protein interactions in the ethylene plant hormone signaling pathway as tools to delay plant senescence. <https://doi.org/10.5281/zenodo.3333531>
16. Kluyver T, Ragan-Kelley B, Pérez F, Granger BE, Bussonnier M, Frederic J, Kelley K, Hamrick JB, Grout J, Corlay S (2016) Jupyter Notebooks—a publishing format for reproducible computational workflows. *ELPUB*, pp 87–90
17. <https://plantcv.readthedocs.io/en/stable/>. Accessed 12 Jul 2019
18. Williamson VG, Milburn JA (1995) Cavitation events in cut stems kept in water: implications for cut flower senescence. *Sci Hortic* 64(4):219–232. [https://doi.org/10.1016/0304-4238\(95\)00842-x](https://doi.org/10.1016/0304-4238(95)00842-x)
19. <https://www.putty.org/>. Accessed 12 Jul 2019
20. <https://www.raspberrypi.org/documentation/raspbian/applications/camera.md>. Accessed 12 Jul 2019
21. Ooms J (2014) The jsonlite package: a practical and consistent mapping between json data and r objects. arXiv:14032805
22. Wickham H (2016) ggplot2: elegant graphics for data analysis. Springer, New York
23. RStudio Team (2020). RStudio: Integrated Development for R. RStudio, PBC, Boston, MA, <http://www.rstudio.com>

Part III

Chemical Genomics in Hormone Signaling



The Screening for Novel Inhibitors of Auxin-Induced Ca^{2+} Signaling

Kjell De Vriese, Long Nguyen, Simon Stael, Dominique Audenaert, Tom Beeckman, and Steffen Vanneste

Abstract

Ca^{2+} -based second messenger signaling is used by many signal perception mechanisms to modulate specific cellular responses. The well-characterized phytohormone auxin elicits a very rapid Ca^{2+} signal, but the molecular players involved in auxin-induced Ca^{2+} signaling are still largely unknown. The complicated and often redundant nature of the plant Ca^{2+} signaling machinery makes the use of mutants and transgenic lines a painstaking process, which makes a pharmacological approach an attractive alternative to study these processes. Here, we describe the development and utilization of a screening assay that can be used to probe a compound library for inhibitors of auxin-induced Ca^{2+} entry in plant cell suspensions.

Key words Inhibitors, Auxin signaling, Calcium signaling, Auxin-induced calcium signaling

1 Introduction

The phytohormone auxin plays an important regulatory role in nearly all aspects of plant growth and development and thus has been a major topic of plant research for many decades (reviewed in [1–3]). While much is currently known about the main auxin signaling pathway, namely, the nuclear $\text{SCF}^{\text{TIR1/AFB}}\text{-Aux/IAA}$ -dependent signaling pathway (reviewed in [1, 4]), there are indications that other, non-transcriptional auxin signaling pathways regulate some of the faster auxin responses that have been observed. Surprisingly, a recent report showed that auxin activates the Ca^{2+} permeable cation channel CNGC14 in a TIR1/AFB -dependent manner [5]. However, we currently do not fully understand the inner workings of this activation mechanism.

The green lineage has evolved an expanded set of Ca^{2+} channels in large gene families that has diverged significantly from the metazoan Ca^{2+} toolbox [6–9]. An important testimony of this is the dependence of several Ca^{2+} responses on an intact proton gradient

across the plasma membrane [10, 11]. Therefore, the extensive pharmacology that was established in metazoan systems cannot easily be applied for studying plant Ca^{2+} channels [12]. Instead, plant Ca^{2+} research is currently mostly reliant on Ca^{2+} chelators such as EGTA, or non-specific Ca^{2+} channel blockers like La^{3+} and Gd^{3+} [12]. Therefore, we recently performed a chemical genetic screen for inhibitors of auxin-induced Ca^{2+} signaling as a first step in establishing a plant-tailored Ca^{2+} pharmacology.

Here, we describe the development, setup, and utilization of this screening assay, as well as protocols for transforming and maintaining the transgenic Ca^{2+} sensor BY-2 cell line that was utilized in this screening assay [11].

2 Materials

1. Tobacco BY-2 cells.
2. Falcon tubes (15 mL and 50 mL).
3. Disposable plastic pipettes (10 mL).
4. Aluminum foil.
5. White 96-well plates.
6. Micropipette (200 μL) and disposable tips.
7. Sterile toothpicks.
8. Erlenmeyers (100 mL and 250 mL).
9. Petri dish plates (80 mm \times 20 mm).
10. Surgical tape.
11. Spatula.
12. BY-2 growth media: For 1 L media, add 4.3 g of Murashige and Skoog (MS) basal salt mixture, 0.2 g of KH_2PO_4 , and 30 g of sucrose to a glass bottle. Dissolve in 850 mL of ultrapure water. Adjust pH to 5.8 using KOH. Add ultrapure water up to 1 L. For solid media, add 6.5 g plant culture agar. Autoclave before use.
13. BY-2 vitamins: Add 0.02 g of 2,4-D to a 50-mL Falcon tube and dissolve in 1 mL of ethanol. Add 0.05 g of thiamine and 5 g of myo-inositol. Add ultrapure water up to 50 mL. Filter-sterilize and aliquot 10 mL in 50-mL falcon tubes. Store at $-20\text{ }^\circ\text{C}$.
14. Coelenterazine-h (Ctz-h): Prepare stock solution of 5 mM in methanol. Store at $-20\text{ }^\circ\text{C}$ and protect from light (*see Note 1*).
15. Compound library: Prepare 200 \times concentrated stock solutions of the library compounds in DMSO (*see Note 2*).

16. Negative and positive controls: 100% DMSO (negative control) and GdCl₃ (2 M stock solution in 100% DMSO; positive control).
17. Elicitor solution: Add 11,052 mg of 2,4-D powder into a 50-mL falcon tube. Dissolve in 50 µL of ethanol. Add ultrapure water up to 50 mL.
18. Discharge solution: 0.1 M CaCl₂ and 20% ethanol (v/v) in ultrapure water.
19. Laminar flow hood.
20. Centrifuge capable of holding 50-mL falcon tubes: For our experiments, an Eppendorf 5804R Refrigerated Centrifuge was used.
21. Rotary shaker.
22. Liquid handling robot: For our experiments, a Tecan Freedom EVO200 equipped with a 96-channel head was used.
23. Luminescence imaging system: For our experiments, a NightSHADE LB985 In Vivo Plant Imaging System (Berthold Technologies) carrying a deep-cooled slow-scan CCD camera from Andor Instruments Ltd. (Belfast, UK) was used.
24. Luminescence plate reader: For our experiments, a LUMIstar Galaxy (BMG LABTECH) or GloMax Navigator (Promega) was used.

3 Methods

3.1 *BY-2 Transformation*

Transformation of the BY-2 cells should be done using sterile equipment under a laminar flow hood to avoid contamination of the cells.

1. Dilute 3 mL of wild-type tobacco BY-2 cells in 40 mL of BY-2 medium supplemented with 40 µL of BY-2 vitamins in 250-mL Erlenmeyers and grow for 3 days at 25 °C on a rotary shaker (130 rpm).
2. Grow your recombinant *Agrobacterium* strain (e.g., LBA4404) that expresses a UBQ10::YFP-apoaequorin construct [13] in 5 mL of YEB medium supplemented with the appropriate selection antibiotics in a 15-mL Falcon tube. Partially untie the screwcap and seal with surgical tape to allow aeration of the culture.
3. After 2 days of growth, dilute 1 mL of the *Agrobacterium* culture in 5 mL of YEB medium in a 50-mL Falcon tube. Partially untie the screwcap and seal with surgical tape to allow aeration of the culture.

4. After 3 days of growth (*see Note 3*), transfer 4 mL of the BY-2 culture with a 10-mL pipet to an 80 mm × 20 mm Petri dish plate. Add 300 µL of the *Agrobacterium* culture (OD₆₀₀ = 1) and mix gently. The mixture should cover the full Petri dish plate. Seal with surgical tape one time around. Incubate at 25 °C without shaking or moving for 2 days.
5. After 2 days of growth, spread the mixture on an 80 mm × 20 mm Petri dish plate (*see Note 4*) containing 40 mL of solid BY-2 medium supplemented with 500 µg/mL carbenicillin (Cb), 200 µg/mL vancomycin (Vm), and the appropriate selection antibiotics of your construct (e.g., 100 µg/mL kanamycin (Km) or 30 µg/mL hygromycine (Hyg)) (*see Note 5*). Do not wash the mixture.
6. After 14 days of growth, calli should become visible as tiny opaque dots. Use a sterile toothpick to transfer them to a new 80 mm × 20 mm Petri dish plate with selective BY-2 medium (*see Note 6*). Use a binocular to check at least 100 calli for YFP-expression of the YFP-apoaequorin construct (*see Note 7*).
7. Start a transformed BY-2 liquid culture by transferring a homogeneous appearing callus of approximately 1 cm in diameter to 20 mL of liquid BY-2 medium supplemented with 20 µl of BY-2 vitamins in a 100-mL Erlenmeyer.

3.2 Growing the BY-2 Cells

Subculturing of BY-2 cells should be done using sterile equipment under a laminar flow hood to avoid contamination of the cells.

1. Add 40 mL of liquid BY-2 medium into a 250-mL Erlenmeyer. Add 40 µL of BY-2 vitamins and mix.
2. Transfer 1 mL of a week-old BY-2 culture to the fresh BY-2 medium using a sterile 10-mL plastic pipette (*see Note 8*). Loosen the screw cap one full turn, and seal with surgical tape to allow aeration of the cells.
3. Incubate on a rotary shaker at 25 °C and 130 rpm.
4. Refresh the liquid culture every week by repeating **steps 1–3** (*see Note 9*). To maintain a backup culture, grow the cells on a plate containing solid BY-2 medium supplemented with BY-2 vitamins. This backup culture can be maintained at 25 °C for up to 1 month. Refresh before or when browning of the callus starts to appear.

3.3 Preparation of BY-2 Cells for Ca²⁺ Measurements

Preparation of BY-2 cells should be done using sterile equipment under a laminar flow hood to avoid contamination of the cells.

1. Grow and subculture YFP-apoaequorin-expressing BY-2 cells as described above.

2. Five days after subculturing, gently transfer 10 mL of the BY-2 cells to a 50-mL Falcon tube using a disposable 10-mL plastic pipette with large tip opening (*see Note 10*).
3. Centrifuge the cells at $2800 \times g$ for 5 min at room temperature (*see Note 11*).
4. Carefully remove the supernatant without disturbing the BY-2 cell pellet. Gently add fresh BY-2 medium up to 10 mL (*see Note 10*). Gently resuspend the BY-2 cells (*see Note 12*).
5. Add 5 μM of the Ctz-h stock solution to the BY-2 cells (2.5 μM final concentration) (*see Note 1*). Wrap the falcon tube in aluminum foil to protect the Ctz-h from light degradation. Incubate the cells in a rotary shaker (25 °C, 130 rpm) in the dark for at least 3 h to allow reconstitution of aequorin in the BY-2 cells.
6. Repeat **steps 3** and **4** to remove the excess of Ctz-h. The BY-2 cells are now ready for Ca²⁺ measurements.

3.4 Primary Screen Setup

It is important to evaluate the quality of the assay by calculating its Z-prime (Z') factor (*see Note 13*) (Fig. 1a) before conducting the primary screen (Fig. 1b).

1. Prepare the appropriate amount of BY-2 cells as described above (Subheading 3.3).
2. Distribute 100 μL of the reconstituted BY-2 cell solution into single wells of a white 96-well plate using a 200- μL micropipette (*see Note 14*).
3. Add 0.5 μL of DMSO (negative control; 0.5% final concentration) and 0.5 μL of the GdCl₃ stock solution (positive control; 10 mM final concentration) to alternating wells of the first and last columns of the 96-well plate. Add 0.5 μL of the screening compound stock solutions (50 μM final concentrations) to individual wells of the remaining center columns (*see Note 15*). When adding the controls and compounds, pipet up and down several times to mix. Preincubate the BY-2 cells with the compounds for 30 min in the dark before starting Ca²⁺ measurements (*see Note 16*).
4. Use a liquid handling robot to add 100 μL of the elicitor solution to each well of the plate in rapid succession, and immediately transfer the plate to the luminescence imaging system (*see Note 17*).
5. Measure the induced luminescent signal with the luminescence imaging system. Make sure to capture the entire dynamic Ca²⁺ response, including the initial maximal Ca²⁺ response, until the attenuation phase is reached (*see Note 18*). For our setup,

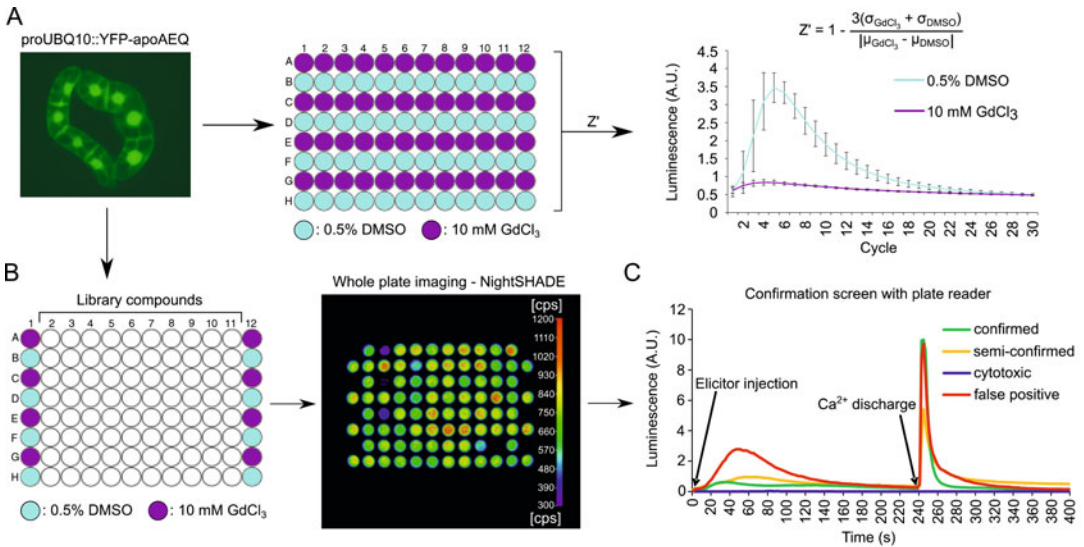


Fig. 1 Schematic representation of primary screen for Ca²⁺ signaling inhibitors. **(a, b)** Multiwell setup for screening inhibitors of auxin-induced Ca²⁺ responses via YFP-*apoaequorin*-expressing BY-2 cells. Based on the means and standard deviations of both the positive (10 mM GdCl₃, purple) and negative (0.5% DMSO, cyan) controls of a test run, a Z' score can be calculated **(a)**. Using this setup, a compound library can be screened for inhibitors of 2,4-D-induced Ca²⁺ signaling **(b)**. The outer columns contain positive (10 mM GdCl₃, purple) and negative (0.5% DMSO, cyan) controls, with the assay compounds in the ten inner columns (50 μM; white). Addition of auxin induces a rapid luminescence-based signal that can be detected with a luminescence imaging system (e.g., NightSHADE LB985 In Vivo Plant Imaging System (Berthold Technologies)). Hit compounds can be retained that lower the maximum signal below a certain threshold (e.g., less than 55% of that of the DMSO-treated control cells). **(c)** Confirmation screen of the primary hit compounds in a multiwell plate reader. After 240 s, 50 μL of the discharge solution (0.1 M CaCl₂ and 20% ethanol) is added and luminescence is measured for the remaining 160 s. Based on their Ca²⁺ response and burst patterns, the tested compounds can be further categorized into four groups: confirmed (green), semi-confirmed (yellow), cytotoxic (blue), and false-positive (red) compounds, for which example patterns are shown. Reproduced from De Vriese et al. [11], www.plantphysiol.org, Copyright American Society of Plant Biologists

luminescence was measured for 30 cycles with an exposure time of 10 s per cycle, resulting in a total measuring time of 5 min per plate.

6. Determine the maximum luminescence signal for each well based on its cycle with the highest luminescence counts per second (cps) that was measured. Calculate the average maximum cps value of the negative control wells of the plate. Normalize the maximum cps values of each well by dividing by the average maximum cps value of the negative control wells.
7. Choose a cutoff of the normalized signal below which the compounds are recognized as primary hits (e.g., compounds that reduced the negative control signal by 45% or more).

3.5 Confirmation Screen Setup

Hit compounds that are discovered with the primary screen can be validated with a follow-up confirmation screen using more sensitive equipment (Fig. 1c).

1. Prepare the appropriate amount of BY-2 cells as described above (Subheading 3.3).
2. Distribute 100 μL of the reconstituted BY-2 cell solution into single wells of a white 96-well plate using a 200- μL micropipette (*see Note 14*).
3. Add 0.5 μL of DMSO (negative control; 0.5% final concentration) and 0.5 μL of the GdCl₃ stock solution (positive control; 10 mM final concentration) to alternating wells of the first and last columns of the 96-well plate. Add 0.5 μL of the screening compound stock solutions (50 μM final concentrations) to individual wells of the remaining center columns (*see Note 15*). When adding the controls and compounds, pipet up and down several times to mix. Incubate the BY-2 cells with the compounds for 30 min in the dark before starting Ca²⁺ measurements (*see Note 16*).
4. Prepare a luminescence plate reader equipped with at least two pipetting channels (e.g., LUMIstar Galaxy (BMG LABTECH) or GloMax Navigator (Promega)). Prime the first pipetting channel with the elicitor solution and the second pipetting channel with the discharge solution (*see Note 19*). Configure the plate reader in a well-per-well measuring setup. Insert the 96-well plate into the plate reader. The following two steps should be performed for each individual well of the 96-well plate consecutively.
5. Automatically add 100 μL of the elicitor solution to the well to induce luminescence and measure the light emission at desired intervals for a desired time period. For our experiments, luminescence was measured every 1.5 s for 200 s.
6. Immediately following this measurement, discharge the remaining reconstituted aequorin by the automated addition of 50 μL of the discharge solution, and measure the light emission at desired intervals for a desired time period. For our experiments, luminescence was measured every 1.5 s for an additional 100 s, resulting in a total measuring time of 5 min per well (*see Note 20*).

4 Notes

1. Coelenterazine is very light-sensitive when not bound to aequorin. Avoid exposure to light whenever possible by working in a low-light environment and wrapping each aliquot in aluminum foil.

2. We used 10 mM stock concentrations for final compound concentrations of 50 μ M. Concentrations can be adjusted according to personal preference.
3. You may have to test the optimal time point for your culture.
4. A sterile spatula can be used for this. Be gentle to avoid damaging the cells.
5. *Agrobacteria* are sensitive to Cb and Vm.
6. Again include Cb and Vm to the medium to eliminate remaining *Agrobacteria*.
7. High variability sometimes occurs, depending on the construct.
8. Release the cells directly into the medium. Do not drop the cells or let them run alongside the glass of the Erlenmeyer as this may damage the cells.
9. We advise keeping at least one additional liquid backup culture, in case of contamination of the culture or damage to the Erlenmeyer.
10. 10 mL is the volume of BY-2 cell suspension required to fill one 96-well plate. Multiply this volume by the desired amount of plates. We recommend preparing some excess of BY-2 cells to account for dead volume during the different handling steps.
11. Avoid centrifuging at higher g , as this may damage the cells.
12. Do not vortex or shake with high force as this may damage the cells.
13. The Z' factor is a commonly used statistical indicator of quality for high-throughput assays [14]. It gives an estimation of the assay quality by discriminating the effect of hit molecules from readout variation based on two parameters: the ‘separation band’ and the dynamic range of the assay. The separation band is the difference between the mean of the negative control (e.g., DMSO) plus three times the standard deviation of the negative control and the mean of the positive control (e.g., $GdCl_3$) minus three times the standard deviation of the positive control. The dynamic range of the assay is the difference between the mean of the positive and negative controls.

$$Z' = 1 - \frac{3(\sigma_{GdCl_3} + \sigma_{DMSO})}{|\mu_{GdCl_3} - \mu_{DMSO}|}$$

To obtain a good Z' factor, the means of the positive and negative controls should differ strongly from each other, while the standard deviations should be kept as low as possible. Ideally, the Z' factor should be as close to 1 as possible. Assays with a Z' factor between 0.5 and 1 are generally being considered to be excellent [14].

14. When distributing the BY-2 cells, cut off the end of the pipette tip to avoid damaging the cells. Avoid precipitation of the cells in the falcon tube by gently rotating the falcon tube while distributing the cells.
15. Concentrations and plate layout listed can be adjusted according to personal preference or need. We recommend keeping the final DMSO concentration after compound addition at 0.5% or lower. Higher DMSO concentrations tend to negatively affect the BY-2 cells.
16. This preincubation allows the compounds to interact with their potential targets and allows recovery of potential touch response signals caused by compound addition back to baseline levels.
17. It is important to start the Ca^{2+} measurements as soon as possible (preferably within 10 s) after elicitor addition. This minimizes the loss of the earliest Ca^{2+} response signal, especially for fast Ca^{2+} responses. Make sure that at least the maximum signal produced in each well can be detected. Therefore, we recommend getting acquainted with the full dynamics of the Ca^{2+} response of your elicitor of interest prior to screening.
18. Calibrate the luminescence imaging system before starting the screen to determine optimal detection settings (measuring time, baseline signal, maximum signal, etc.). For this, a control plate containing positive and negative controls can be used.
19. We recommend using a low pump speed to avoid unwanted touch responses caused by fast addition of the elicitor.
20. The discharge signal is used to assess the viability of the cells after compound treatment. A low discharge signal usually indicates cytotoxicity of the tested compound. The discharge signal can also be used to calculate the absolute cytoplasmic Ca^{2+} concentrations by applying the empirically determined formula $\text{pCa} = 0.332588(-\log k) + 5.5593$ [15]. The rate constant k in this formula equals the elicitor-induced luminescence counts per second divided by the total remaining counts as determined by the discharge signal. The bioluminescent signal of our transgenic BY-2 cell lines could not be converted to absolute $[\text{Ca}^{2+}]_{\text{cyt}}$ values because the total luminescent signal after aequorin discharge could not be completely detected in situ due to saturation of the plate reader detector. Therefore, all treatments were always evaluated relative to controls within each corresponding 96-well plate. This normalization also accounted for day-to-day variation in amplitude and shape of the Ca^{2+} signals.

Acknowledgments

K.D.V. was supported by the Special Research Fund Ghent University (01D25813).

References

1. Salehin M, Bagchi R, Estelle M (2015) SCF^{TIR1/AFB}-based auxin perception: mechanism and role in plant growth and development. *Plant Cell* 27:9–19
2. Vanneste S, Friml J (2009) Auxin: a trigger for change in plant development. *Cell* 136:1005–1016
3. Weijers D, Wagner D (2016) Transcriptional responses to the auxin hormone. *Ann Rev Plant Biol* 67:539–574
4. Lavy M, Estelle M (2016) Mechanisms of auxin signaling. *Development* 143:3226–3229
5. Dindas J, Scherzer S, Roelfsema MRG et al (2018) AUX1-mediated root hair auxin influx governs SCF(TIR1/AFB)-type Ca(2+) signaling. *Nat Commun* 9:1174
6. Edel KH, Kudla J (2015) Increasing complexity and versatility: how the calcium signaling toolkit was shaped during plant land colonization. *Cell Calcium* 57:231–246
7. Jammes F, Hu HC, Villiers F et al (2011) Calcium-permeable channels in plant cells. *FEBS J* 278:4262–4276
8. Marchadier E, Oates ME, Fang H et al (2016) Evolution of the calcium-based intracellular signaling system. *Gen Biol Evol* 8:2118–2132
9. Ward JM, Maser P, Schroeder JI (2009) Plant ion channels: gene families, physiology, and functional genomics analyses. *Annu Rev Physiol* 71:59–82
10. Behera S, Zhaolong X, Luoni L et al (2018) Cellular Ca(2+) signals generate defined pH signatures in plants. *Plant Cell* 30:2704–2719
11. De Vriese K, Himschoot E, Dunser K et al (2019) Identification of novel inhibitors of auxin-induced Ca(2+) signaling via a plant-based chemical screen. *Plant Physiol* 180:480–496
12. De Vriese K, Costa A, Beeckman T, Vanneste S (2018) Pharmacological strategies for manipulating plant Ca(2+) signalling. *Intl J Mol Sci* 19:E1506
13. Mehlmer N, Parvin N, Hurst CH et al (2012) A toolset of aequorin expression vectors for in planta studies of subcellular calcium concentrations in *Arabidopsis thaliana*. *J Exp Bot* 63:1751–1761
14. Zhang JH, Chung TD, Oldenburg KR (1999) A simple statistical parameter for use in evaluation and validation of high throughput screening assays. *J Biomol Screen* 4:67–73
15. Knight H, Trewavas AJ, Knight MR (1996) Cold calcium signaling in *Arabidopsis* involves two cellular pools and a change in calcium signature after acclimation. *Plant Cell* 8:489–503



Identification of ABA Receptor Agonists Using a Multiplexed High-Throughput Chemical Screening

Jorge Lozano-Juste, Irene García-Maquilón, José Brea, Rocío Piña, Armando Albert, Pedro L. Rodriguez, and María Isabel Loza

Abstract

Small molecules that can activate abscisic acid (ABA) receptors represent valuable probes to study ABA perception and signaling. Additionally, these compounds have the potential to be used in the field to counteract the negative effect of drought stress on plant productivity. The PYR/PYL ABA receptors, in their ligand-bound conformation, inactivate protein phosphatases 2C (PP2Cs), triggering physiological responses that are essential for plant adaptation to environmental stresses, including drought. Based on this ligand-induced PP2C inactivation mechanism, we have developed an *in vitro* assay for the identification of ABA-receptor agonists by high-throughput screening of chemical libraries. The assay allows simultaneous use of different ABA receptors, increasing the chances to find new agonists and eliminates the need for parallel screening. In this chapter, we describe detailed procedures for the identification of ABA agonists using this multiplexed assay in a medium- (96-well plates) or a high-throughput (384-well plates) setup.

Key words Abscisic acid, Agonist, Screening, High-throughput, PP2C, Drought, Chemical genomics, Small molecule, Plant

1 Introduction

The sesquiterpenoid hormone abscisic acid (ABA) regulates many aspects of plant growth and development, including the adaptation to stress. ABA biosynthetic and metabolic pathways integrate different stimuli to control ABA levels in the plant cell. Different environmental alterations promote ABA accumulation. Drought stress stimulates ABA biosynthesis in roots, as well as in the aerial parts of the plant, producing an increased amount of around 10- to 40-fold, depending on the species [1–3]. ABA is perceived by a family of nucleocytoplasmic proteins known as pyrabactin resistance (PYR) 1/PYR1-like (PYL)/regulatory component of ABA receptor (RCAR) proteins (PYR/PYL/RCAR) [4, 5]. The

Jorge Lozano-Juste, Irene García-Maquilón, and José Brea contributed equally to this work.

PYR/PYL/RCAR receptors, in their ligand-bound conformation, inhibit the activity of protein phosphatases 2C (PP2C), which are in charge of keeping the ABA signaling pathway “off” under favorable environmental conditions (Fig. 1) [6]. In turn, the enzymatic inactivation of the phosphatase activity of PP2Cs allows the activation of plant-specific serine/threonine kinases of the sucrose-non-fermenting-related kinase subfamily 2 (SnRK2s) (Fig. 1) [7]. SnRK2s phosphorylate a large number of protein targets to contribute to stress adaptation [8]. PYR/PYL/RCAR receptors bind ABA within a hydrophobic pocket surrounded by two flexible loops essential for hormone binding and known as the gate and the latch loops [9, 10]. The ligand-binding process can be broken down into three steps: (1) ABA binding to a latch-closed/gate-open PYR/PYL/RCAR conformation, (2) structural rearrangement into a latch-closed/gate-closed state, and (3) PP2C binding to the ABA receptor in the latch-closed/gate-closed configuration [11]. The formation of the ternary complex, receptor-ABA-PP2C, involves the entrance of the PYR/PYL/RCAR gate loop within the PP2C catalytic core, causing the inactivation of the phosphatase activity of the PP2C [9, 12, 13]. In the last years, the core elements of the ABA signaling pathway have been elucidated in a number of plant species. Consequently, different approaches derived from this knowledge have been pursued to improve plant performance under drought stress. Among them, chemical approaches have been extremely useful in identifying ABA receptor agonists [14]. These compounds receive great interest because they (1) represent molecular probes to better understand the ABA signaling pathway and (2) could potentially be used as agrochemicals to protect crops against drought. In the last years, several ABA receptor agonists have been described. Pyrabactin was the first ABA receptor agonist to be reported, and it was central to identify the PYR/PYL family of ABA receptors [13]. A second agonist, quinabactin, was found in an exhaustive chemical screening using Y2H assays (Fig. 1) [15]. Quinabactin activates several ABA receptors and enhances plant drought tolerance when sprayed on plant leaves [15]. Only a few quinabactin analogs have been reported so far. Among them, AMF4, a four fluorine modification of quinabactin (Fig. 1), showed stronger activity than quinabactin, indicating that halogen substitutions at the 4-methylbenzyl ring of quinabactin improve the interaction with some receptors [16]. Recently, the modification of the toluyl position of quinabactin probed even more effective, increasing compound activity by tenfold in vitro [17]. Based on quinabactin properties and using a medicinal chemistry approach, Aditya et al. synthesized cyanabactin, a new ABA receptor agonist (Fig. 1) [18]. Cyanabactin is more specific toward PYR1 and PYL1 dimeric receptors than quinabactin, and it is able to activate the ABA response and reduce plant leaf transpiration [18]. Both quinabactin and cyanabactin are promising molecules to control plant

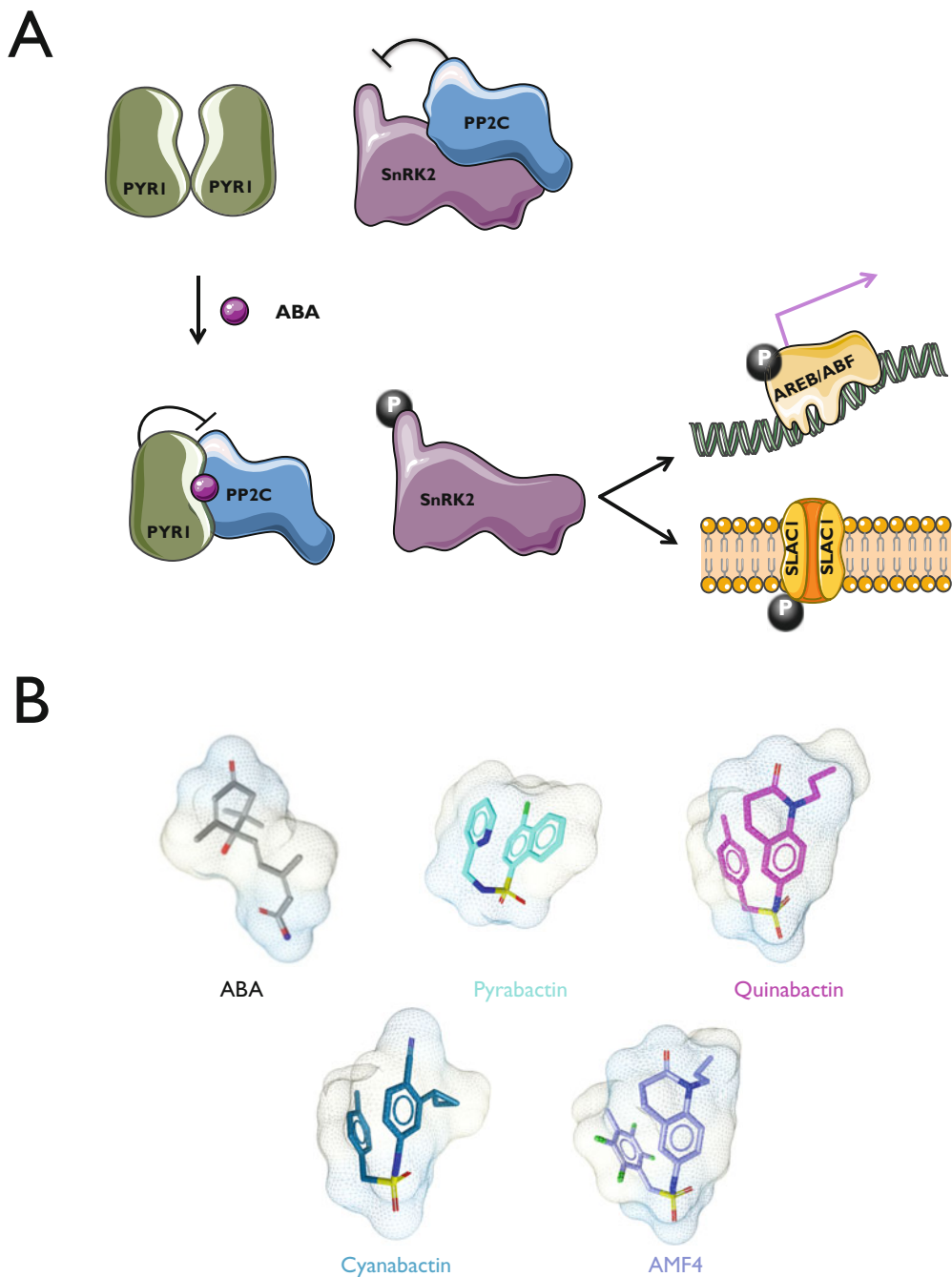


Fig. 1 (a) Schematic representation of the ABA signaling pathway. (b) Structure of ABA and the ABA receptor agonists pyrabactin, quinabactin, cyanabactin, and AMF4

transpiration and drought resistance. However, these molecules are selective toward some ABA receptors [15, 18]. Hence, synthetic molecules able to activate all ABA receptors have not been

described yet. By the other hand, structural information on ABA receptors has led to the design of ABA receptor antagonists like AS6 and PANMe [19, 20].

In this chapter, we describe the use of an in vitro assay to screen chemical libraries for ABA receptor agonists. The procedure is based on a biochemical phosphatase assay. In a first step, the chemical library is assayed in the presence of ABA receptors and PP2C. Compounds able to bind to the receptors and inhibit phosphatase activity are then re-analyzed in a secondary screening using only PP2C, to eliminate those molecules that directly inhibit the phosphatase activity independent of the receptors. The assay allows for multiplexing different ABA receptors in the same reaction, reducing screening time and cost. We have ruled out any interference caused by the simultaneous use of different receptors by using quinabactin. The addition of 3 different receptors does not have a negative effect on the IC_{50} of PYR1 for quinabactin, a good indicator of the absence of interference (Fig. 5).

We have set up the assay for medium- (96-well plates) or high-throughput (384-well plates) screening. This makes the screen suitable for a larger range of plate readers and throughputs. The assay has a good signal-to-background ratio ($S/B \approx 3$) and an excellent reproducibility factor ($Z' \approx 0.85$), thus being amenable for agrochemical drug discovery.

2 Materials

2.1 Protein Purification

1. pETM11 protein expression plasmid.
2. *Escherichia coli* BL21 (DE3) and DH5 α strains.
3. LB medium: 5 g tryptone, 10 g yeast extract, 10 g NaCl, pH 7.0 (final volume adjusted to 1 L). Autoclaved. Add 15 g/L of agar before autoclaving for LB plates.
4. Kanamycin (50 mg/L).
5. Isopropyl-beta-d-thiogalactoside (IPTG) (1 M). Dissolve 2.38 g of IPTG in 10 mL of water. Store at -20°C .
6. Ni-NTA agarose.
7. Imidazole (1 M, pH 8.0). Dissolve 6.8 g of imidazole in 100 mL of water and adjust pH to 8.0 with HCl. Autoclave at 120°C for 20 min.
8. Lysis buffer: 50 mM Tris-HCl (pH 8.0), 250 mM KCl, 0.1% Tween-20, 10% glycerol, 10 mM imidazole, 10 mM β -mercaptoethanol. Adjust pH to 8.0 with HCl.
9. Wash buffer: 50 mM Tris-HCl (pH 8.0), 250 mM KCl, 0.1% Tween-20, 20% glycerol, 30 mM imidazole, 10 mM β -mercaptoethanol. Adjust pH to 8.0 with HCl.

10. Elution buffer: 50 mM Tris-HCl (pH 8.0), 250 mM KCl, 0.1% Tween-20, 20% glycerol, 250 mM imidazole, 10 mM β -mercaptoethanol. Adjust pH to 8.0 with HCl.
11. Gravity-flow plastic columns.
12. Nanodrop ND-1000.

2.2 PP2C

Phosphatase Assay

1. (+)-Abscisic acid. Prepare at 1 mM in DMSO. Keep at -20°C .
2. 1 M MnCl_2 . Dissolve 19.79 g of $\text{MnCl}_2 \cdot 4\text{H}_2\text{O}$ in 100 mL of water. Autoclave at 120°C for 20 min.
3. *p*-Nitrophenyl phosphate (*p*NPP) (50 mM in 10 mM Tris-HCl, pH 8.0): Dissolve 371.14 mg of 4-nitrophenyl phosphate, disodium salt hexahydrate, in 20 mL of 10 mM Tris-HCl (pH 8.0). Aliquot into 5 mL stocks. Store at -20°C .
4. 10 mM Tris-HCl (pH 8.0). Weigh 1.21 g of Tris base and dissolve it in 80 mL of water. Adjust pH to 8.0 with concentrated HCl. Adjust the volume to 100 mL with water. Autoclave at 120°C for 20 min.
5. Plate reader. Read the absorbance during 0.1 s/well at 405 nm for 10–20 min in a 96- or 384-well plate reader.
6. Transparent 96-well or 384-well plates.

3 Methods

3.1 Preparation of Stock Chemical Library Plates

1. Dissolve chemicals to 10 mM concentration with DMSO into 96- or 384-well plates (*see Note 1*). Seal the plates and keep at -20°C (*see Note 2*).

3.2 Protein Purification

1. Clone HAB1 and ABA receptors into protein expression vector pETM11. Transform sequence-validated plasmids into BL21 (DE3) cells and select in LB media plates containing 50 $\mu\text{g}/\text{mL}$ of kanamycin.
2. Grow BL21 (DE3) cells with the corresponding plasmids in 5 mL of LB liquid media containing 50 $\mu\text{g}/\text{mL}$ of kanamycin overnight at 37°C at 220 rpm.
3. Use 500 μL of the saturated cultures to prepare glycerol stocks by mixing with 500 μL of 80% glycerol. Keep at -80°C .
4. Inoculate the remaining 4.5 mL into 500 mL of LB liquid media containing 50 $\mu\text{g}/\text{mL}$ of kanamycin.
5. Incubate at 30°C at 180 rpm until OD_{600} reaches 0.5. Reduce the temperature of the shaker to 16°C .
6. When $\text{OD}_{600} = 0.8$, add 500 μL of 1 M IPTG (final concentration 1 mM). In the case of the HAB1 protein, add also 250 μL of 1 M MnCl_2 (final 0.5 mM). Incubate overnight at 16°C at 180 rpm.

7. Centrifuge cells in 250- or 500-mL sterile bottles at 5000 rpm ($3300 \times g$) at 4 °C for 15 min.
8. Remove supernatant and resuspend the pellets in 10 mL of ice-cold lysis buffer containing 10 mM imidazole (*see Note 3*).
9. Freeze the lysates in 13-mL culture tubes at -80 °C. Thaw the tubes on water and freeze them again at -80 °C. Repeat one more time (*see Note 4*).
10. Thaw the tubes in water and sonicate the lysates on ice. Centrifuge at $48,298 \times g$ at 4 °C for 30 min (*see Note 5*).
11. Apply the supernatant into a gravity column loaded with 1 mL of Ni-NTA beads. Collect the flow-through and apply it to the column again (*see Note 6*).
12. Wash Ni-NTA beads with 60 column volumes of ice-cold wash buffer containing 30 mM imidazole (60 mL).
13. Elute the purified proteins using 500 μ L of ice-cold elution buffer containing 250 mM imidazole 6 times. Collect each elution in a separate tube.
14. Quantify the protein concentration measuring absorbance at 280 nm using a nanodrop. Pool fractions with a protein concentration greater than 0.5 μ g/ μ L. Quantify the concentration of the pooled protein and store at -80 °C (*see Note 7*).
15. For quality control, run 5 μ g of purified protein in a 10% SDS-PAGE gel and stain with Coomassie blue.

3.3 Chemical Screening Using a PP2C Phosphatase Assay in 96-Well Plate Format

1. Thaw the stock chemical library plate and spin it at 2000 rpm for 1 min in a 96-well plate centrifuge.
2. Shake the library in a mixer for 10 min at low speed, for example, 600 rpm (*see Note 8*).
3. Thaw purified recombinant proteins (ABA receptors and PP2C), *p*NPP, and ABA. Once thawed, keep proteins on ice and DMSO, ABA, substrate and chemical plates at room temperature (*see Note 9*).
4. To assay receptor-mediated PP2C inhibition in response to ABA, prepare a reaction mix including 1 μ M PP2C and 2 μ M receptor in water in a volume of 50 μ L per well.
5. Dispense 1 μ L of 1 M MnCl_2 into each well of a 96-well plate (*see Note 10*).
6. Add 1 μ L of DMSO into the first column (from A1 to H8) as a negative control and 1 μ L of 1 mM ABA into the last column (from A12 to H12) as a positive control, as illustrated in Fig. 2 (*see Note 10*).
7. Add 1 μ L of the test compound from stock chemical library to the 96-well chemical screening plate (*see Note 10*).

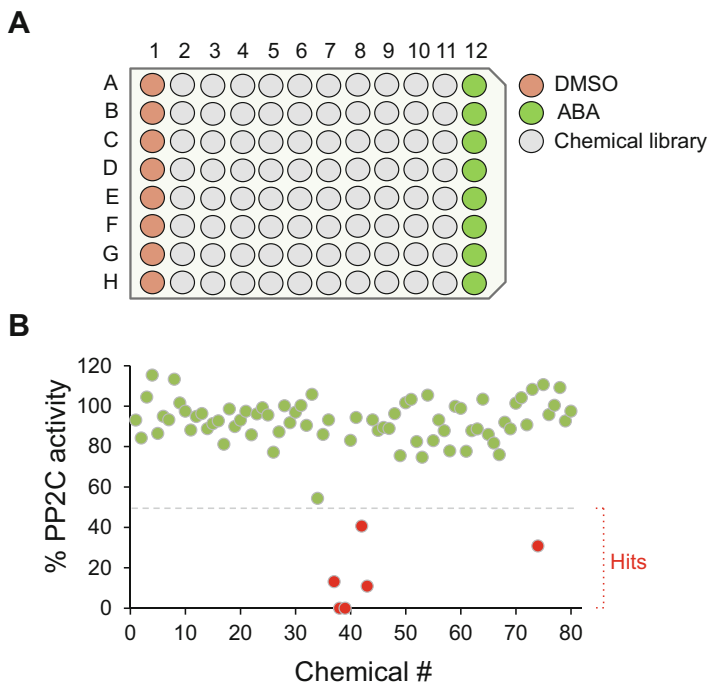


Fig. 2 PP2C enzymatic assay in 96-well plate format. (a) Representative diagram of a 96-well chemical screening plate. The position of DMSO, ABA (negative and positive control, respectively), and the different chemical compounds are indicated. (b) Representative results from one chemical screening plate. Candidate compounds are highlighted in red

8. Transfer the reaction mix containing the recombinant proteins to the 96-well chemical screening plate. Incubate for 10 min at room temperature (*see Note 11*).
9. Add 50 μL of the substrate (50 mM *p*NPP in 10 mM Tris-HCl, pH 8.0) to make the final volume to 100 μL (*see Note 11*).
10. Immediately monitor the absorbance at 405 nm for 20 min in a plate reader.
11. Record the absorbance values for each well.
12. To calculate relative PP2C activity, subtract the absorbance at time = 0 min from the absorbance at time = 20 min. The absorbance of DMSO wells will represent 100% PP2C activity. The percentage of PP2C activity for each well is calculated following the simple equation:

$$\% \text{PP2C activity} = (\Delta \text{Abs}_{(t_{20}-t_0)} \times 100) / \text{Abs}_{\text{DMSO}}$$

13. An example result from a screening plate is shown in Fig. 2. We have defined a threshold of at least 50% reduction of PP2C activity to identify candidate hits.

14. Re-analyze candidate hits in PP2C assays without receptors. Compounds that can inhibit PP2C activity only in the presence of receptors are considered as candidates for future tests (*see Note 12*).

3.4 Chemical Screening Using a PP2C Phosphatase Multiplexed Assay in 384-Well Plate Format

3.4.1 Adaptation of the PP2C Phosphatase Assay to 384-Well Plate Format

To set up conditions for PP2C assay in 384-well plate format, first use only DMSO and ABA controls as depicted in Fig. 3.

1. Dispense 0.5 μL of 1 M MnCl_2 in all the wells of a 384-well plate (*see Note 13*).
2. Add ABA and DMSO controls to the appropriate wells following the diagram shown in Fig. 3 (*see Note 14*).
3. Prepare the receptor + phosphatase mix. For one reaction, use 0.5 μM PP2C and 1 μM PYR/PYL receptor. Add water to adjust the volume to 25 μL . Dispense 25 μL per well (*see Note 13*). Spin briefly to collect the liquid.

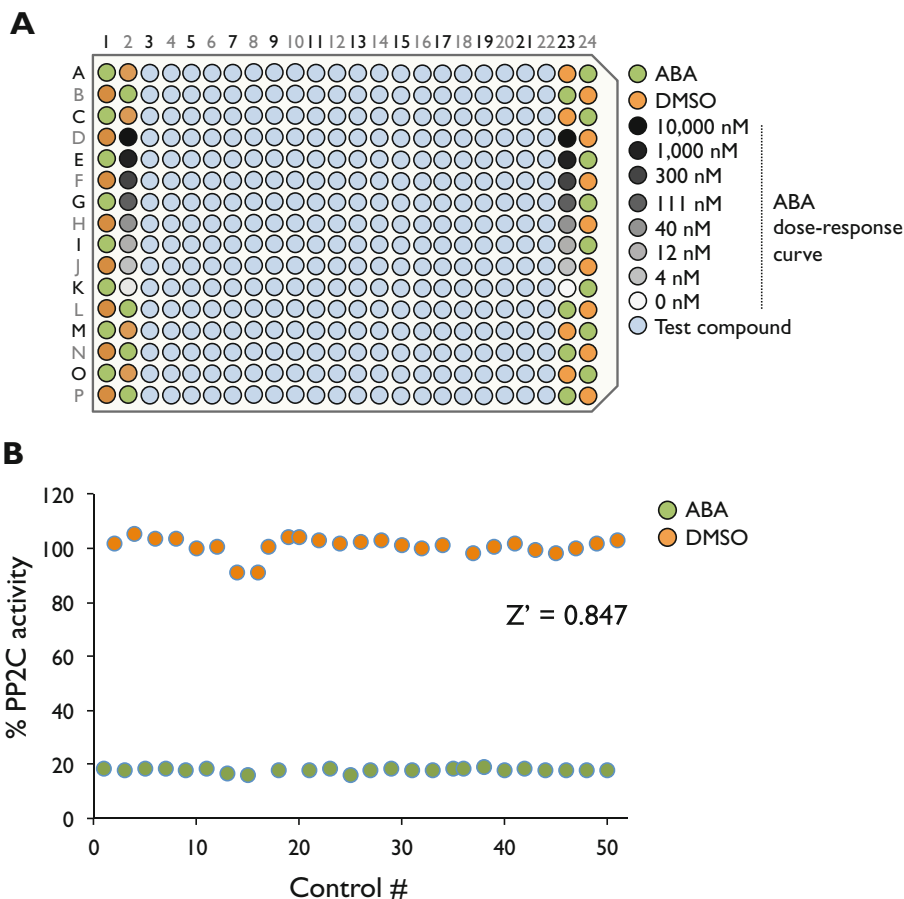


Fig. 3 PP2C enzymatic assay in 384-well plate format. **(a)** Representative diagram of a 384-well chemical screening plate. The position of DMSO, ABA (negative and positive control, respectively), ABA dose–response curve, and the different chemical compounds are indicated. **(b)** Representative control results from one chemical screening plate. The Z' value of the assay is indicated

4. Incubate the reaction at room temperature for 10 min.
5. Add 25 μL of the substrate (50 mM pNPP in 10 mM Tris-HCl, pH 8.0) to each well (*see Note 15*).
6. Immediately read absorbance at 405 nm in a plate reader.
7. Make another measurement 10 min after the addition of the substrate.
8. Calculate the activity of controls and dose–response curves as described in Subheading 3.3.
9. To assess the suitability and reproducibility of the procedure, perform this assay 3 times in 3 different days. Calculate Z' factor [21]. The Z' factor is a measure to quantify the appropriateness of an assay for use in a high-throughput screen. A Z' value greater than 0.5 indicates that the assay conditions are good. Otherwise, optimization should be performed. Z' values were calculated according to the formula [21]:

$$Z' = 1 - ((3SD_{c+} + 3SD_{c-}) / (\mu_{c+} - \mu_{c-}))$$

where SD_{c+} and SD_{c-} are the standard deviation of positive and negative control wells, respectively, and μ_{c+} and μ_{c-} are the mean of positive and negative control wells, respectively.

3.4.2 Assay Multiplexing

The use of multiple receptors in the same reaction reduces screening time and cost. We have performed control experiments to study the possible interference that may be caused by the simultaneous use of different receptors. Quinabactin is an ABA receptor agonist selective for PYR1, PYL1, PYL2, and PYL5 *in vitro* [15]. By performing dose–response curves and calculating IC_{50} for quinabactin using only PYR1 or PYR1 in combination with PYL4 and PYL8, any interference of receptor multiplexing has been ruled out (Fig. 4). We recommend carrying out this kind of interference analysis using the user's receptors of choice.

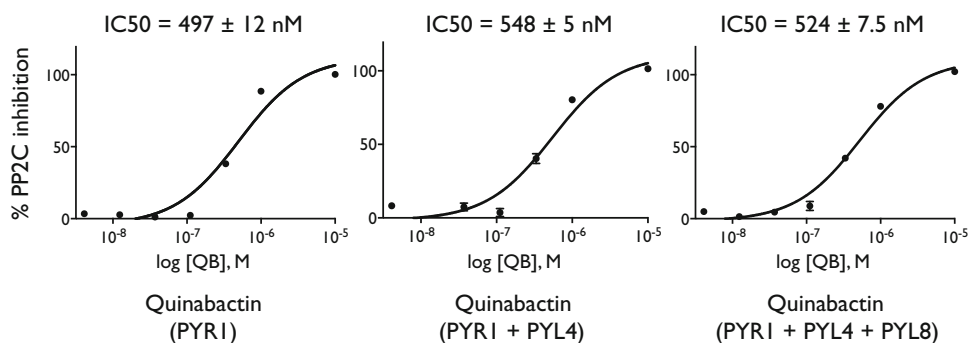


Fig. 4 The PP2C enzymatic assay in 384-well plate format tolerates receptor multiplexing. Quinabactin dose–response curves were performed in the presence of PYR1, PYR1 + PYL4, and PYR1 + PYL4 + PYL8. Note that there is no significant change in the IC_{50} values for quinabactin

1. Prepare three different receptor–PP2C mixes.
 - (a) Only PYR1 + HAB1.
 - (b) PYR1 + PYL4 + HAB1.
 - (c) PYR1 + PYL4 + PYL8 + HAB1.
 (*see Note 16*).
2. Add 0.5 μL of 1 M MnCl_2 in the plate.
3. Dispense the required amount of each protein into each well on the plate.
4. Dispense the required amount of protein for dose–response curves as shown in Fig. 3.
5. Wait for 10 min at room temperature.
6. Add 25 μL of the substrate (50 mM pNPP in 10 mM Tris-HCl, pH 8.0) to each well (*see Note 15*).
7. Immediately read absorbance at 405 nm in a plate reader.
8. Make another measurement in a plate reader after 10 min.
9. Calculate the activity of controls and dose–response curves as in Subheading 3.3.
10. Compare IC_{50} values for the different receptor–PP2C mixes. No difference between IC_{50} values indicates the absence of multiplexing interference in the assay (Fig. 3).

3.4.3 A Screening Example Using the Multiplexed 384-Well Plate Assay

1. Dispense 0.5 μL of 1 M of MnCl_2 in all the wells of a 384-well plate (*see Note 13*).
2. Prepare the receptors (PYR1, PYL4, and PYL8) + phosphatase mix. For one reaction, use 0.5 μM PP2C and 1 μM PYR/PYL of each receptor. Add water to adjust the volume to 25 μL .
3. Add ABA and DMSO controls to appropriate wells following the diagram in Fig. 3 (*see Note 14*).
4. Add the compounds from the chemical library to the appropriate wells following the diagram illustrated in Fig. 3 (*see Note 14*).
5. Dispense 25 μL of receptors + phosphatase mix per well (*see Note 13*). Spin briefly to collect the liquid.
6. Incubate at room temperature for 10 min.
7. Add 25 μL of the substrate (50 mM pNPP in 10 mM Tris-HCl, pH 8.0) to each well (*see Note 15*).
8. Immediately read absorbance at 405 nm in a plate reader.
9. Make another measurement after 10 min.
10. Calculate the activity of chemicals, controls, and dose–response curves as in Subheading 3.3.

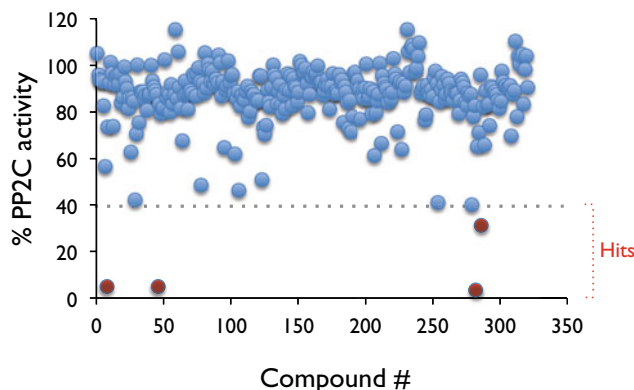


Fig. 5 Identification of ABA agonists using a PP2C phosphatase assay in 384-well plate format. Representative results from one screening plate. Candidate compounds are highlighted in red

11. An example of the result from a screening plate is shown in Fig. 5. A threshold of at least 60% reduction of PP2C activity can be defined to identify candidates.
12. Re-analyze candidates in PP2C assays without receptors. Compounds that can inhibit PP2C activity only in the presence of receptors are considered as candidate hits (*see Note 12*).

4 Notes

1. The use of a liquid handling robot is recommended.
2. Make sure the plates are tightly closed to avoid DMSO–water to mix. Minimize freeze-thawing cycles.
3. Removal of the tip of 5-mL pipette tips can help to resuspend the pellet.
4. The purification procedure can be stopped at this point.
5. Repeat this step to avoid clogging the columns, especially if using an FPLC. Alternatively, pass the extract through 2 layers of Miracloth or filter it with a 0.4- μ M filter.
6. An FPLC column could be used instead.
7. Protein molecular weight and extinction coefficient could be used for a more accurate quantification.
8. Some compounds in the chemical library are hard to dissolve. We recommended this step to improve solubility.
9. DMSO-containing solutions are frozen below 19 °C.
10. The use of a multichannel electronic pipette is recommended.

11. The use of a repeater pipette is recommended. The reaction conditions for a total volume of 100 μL per well are 2 μM recombinant ABA receptor, 1 μM recombinant PP2C phosphatase (receptor:phosphatase ratio 2:1), 10 mM MnCl_2 , 100 μM chemical/10 μM ABA/DMSO, and 25 mM *p*NPP in 5 mM Tris-HCl, pH 8.0, as the substrate.
12. Complementary assays to verify *in vivo* activity will be needed.
13. The use of a Multidrop Combi is recommended to fill the 384-well plate.
14. An Echo 550 acoustic liquid handler was used for the accurate distribution of compounds and to facilitate the configuration of dose–response curves.
15. The use of a Multidrop Combi at low speed to avoid bubbles is recommended to fill the 384-well plate.
16. PYR1, PYL4, and PYL8 were selected to represent the three different clades of ABA receptors [4].

Acknowledgments

This work has received funding from the European Union’s Horizon 2020 research and innovation programme under the Marie Skłodowska-Curie Grant Agreement No. [707477] to J. L.-J.; Xunta de Galicia (ED431C 2018/21) and Ministry of Economy and Competiveness (Innopharma Project) and European Regional Development Fund (ERDF) to M.I.L.; and Ministerio de Ciencia e Innovacion (BIO2017-89523R to A.A. and BIO2017-82503-R to P.L.R.).

References

1. Ikegami K, Okamoto M, Seo M et al (2008) Activation of abscisic acid biosynthesis in the leaves of *Arabidopsis thaliana* in response to water deficit. *J Plant Res* 122:235
2. Ilahi I, Dörffling K (1982) Changes in abscisic acid and proline levels in maize varieties of different drought resistance. *Physiol Plant* 55:129–135
3. Ren H, Gao Z, Chen L et al (2007) Dynamic analysis of ABA accumulation in relation to the rate of ABA catabolism in maize tissues under water deficit. *J Exp Bot* 58:211–219
4. Park S-Y, Fung P, Nishimura N et al (2009) Abscisic acid inhibits type 2C protein phosphatases via the PYR/PYL family of START proteins. *Science* 324:1068–1071
5. Ma Y, Szostkiewicz I, Korte A et al (2009) Regulators of PP2C phosphatase activity function as abscisic acid sensors. *Science* 324:1064–1068
6. Cutler SR, Rodriguez PL, Finkelstein RR et al (2010) Abscisic acid: emergence of a core signaling network. *Annu Rev Plant Biol* 61:651–679
7. Vlad F, Rubio S, Rodrigues A et al (2009) Protein phosphatases 2C regulate the activation of the Snf1-related kinase OST1 by abscisic acid in *Arabidopsis*. *Plant Cell* 21:3170–3184
8. Wang P, Xue L, Batelli G et al (2013) Quantitative phosphoproteomics identifies SnRK2 protein kinase substrates and reveals the effectors of abscisic acid action. *Proc Natl Acad Sci U S A* 110(27):11205–11210
9. Melcher K, Ng L-M, Zhou XE et al (2009) A gate-latch-lock mechanism for hormone

- signalling by abscisic acid receptors. *Nature* 462:602–608
10. Santiago J, Dupeux F, Round A et al (2009) The abscisic acid receptor PYR1 in complex with abscisic acid. *Nature* 462:665–668
 11. Moreno-Alvero M, Yunta C, Gonzalez-Guzman M et al (2017) Structure of ligand-bound intermediates of crop ABA receptors highlights PP2C as necessary ABA co-receptor. *Mol Plant* 10:1250–1253
 12. Yin P, Fan H, Hao Q et al (2009) Structural insights into the mechanism of abscisic acid signaling by PYL proteins. *Nat Struct Mol Biol* 16:1230–1236
 13. Dupeux F, Antoni R, Betz K et al (2011) Modulation of abscisic acid signaling in vivo by an engineered receptor-insensitive protein phosphatase type 2C allele. *Plant Physiol* 156:106–116
 14. Wim D, Okamoto M, Cutler SR (2018) Small molecule probes of ABA biosynthesis and signaling. *Plant Cell Physiol* 59(8):1490–1499
 15. Okamoto M, Peterson FC, Defries A et al (2013) Activation of dimeric ABA receptors elicits guard cell closure, ABA-regulated gene expression, and drought tolerance. *PNAS* 110:12132–12137
 16. Cao M-J, Zhang Y-L, Liu X et al (2017) Combining chemical and genetic approaches to increase drought resistance in plants. *Nat Commun* 8(1):1183
 17. Elzinga D, Sternburg E, Sabbadin D et al (2019) Defining and exploiting hypersensitivity hotspots to facilitate abscisic acid agonist optimization. *ACS Chem Biol* 14(3):332–336
 18. Vaidya AS, Peterson FC, Yarmolinsky D et al (2017) A rationally designed agonist defines subfamily IIIA ABA receptors as critical targets for manipulating transpiration. *ACS Chem Biol* 12(11):2842–2848
 19. Takeuchi J, Okamoto M, Akiyama T et al (2014) Designed abscisic acid analogs as antagonists of PYL-PP2C receptor interactions. *Nat Chem Biol* 10:477–482
 20. Takeuchi J, Mimura N, Okamoto M et al (2018) Structure-based chemical design of abscisic acid antagonists that block PYL-PP2C receptor interactions. *ACS Chem Biol* 13:1313–1321
 21. Zhang J-H, Chung TDY, Oldenburg KR (1999) A simple statistical parameter for use in evaluation and validation of high throughput screening assays. *J Biomol Screen* 4:67–73



A Luciferase Reporter Assay to Identify Chemical Activators of ABA Signaling

Irene García-Maquilón, Pedro L. Rodríguez, Aditya S. Vaidya, and Jorge Lozano-Juste

Abstract

Plant stress tolerance relies on intricate signaling networks that are not fully understood. Several plant hormones are involved in the adaptation to different environmental conditions. Abscisic acid (ABA) has an essential role in stress tolerance, especially in the adaptation to drought. During the last years, chemical genomics has gained attention as an alternative approach to decipher complex traits. Additionally, chemical-based strategies have been very useful to untangle genetic redundancy, which is hard to address by other approaches such as classical genetics. Here, we describe the use of an ABA-inducible luciferase (LUC) reporter line for the high-throughput identification of chemical activators of the ABA signaling pathway. In this assay, seven-day-old *pMAPKKK18-LUC*⁺ seedlings are grown on 96-well plates and treated with test compounds. Next, the activity of the LUC reporter is quantified semiautomatically by image analysis. Candidate compounds able to activate the reporter are thus identified and subjected to a secondary screen by analyzing their effect on ABA-related phenotypes (e.g., inhibition of seed germination). This assay is fast, high-throughput, nondestructive, semiquantitative and can be applied to any other luciferase reporter lines, making it ideal for forward chemical genetic screenings.

Key words Abscisic acid, Reporter, Luciferase, MAPKKK18, Screening, High-throughput, Drought, Chemical genomics, Small molecule, Plant

1 Introduction

Chemical genomics has arisen as an alternative to overcome the limitations of classical genetics, including redundancy and lethality. This recent discipline uses small molecules to study biological systems and to understand protein function, helping to elucidate a biological process in a specific organism [1, 2]. Chemical genomics often involves high-throughput screening (HTS) of large chemical libraries for compounds that cause the desired effect, i.e., phenotype of interest, regulation of the target activity, or reporter activation [2]. Phenotypic screenings are aimed to discover small molecules able to control a particular trait. However, the

identification of the target modulated by the chemical compound is not trivial and represents a bottleneck for this approach [3]. Also, phenotypic-driven chemical screenings make it more laborious to carry out structure–activity relationship (SAR) studies and to use them to rationally design improved chemical analogs. Alternatively, target-based approaches, with the purpose of identifying new small molecules that interact with a specific target and modulate its activity, are also frequently used [4, 5]. In this case, it is preferable to have previous knowledge about the target of choice and about its involvement into the cellular process of interest. In any case, an easy and informative assay needs to be developed in order to study the impact of chemical probes on the target's activity. In addition to phenotypic and targeted approaches, reporter-based screenings have been widely used to evaluate the effects of compounds on a pathway or target of interest. For instance, direct quantification of β -glucuronidase activity (GUS activity) in *Arabidopsis thaliana* (*Arabidopsis*) has been used in HTS of chemical libraries for modulators of salicylic acid signaling [6] and for inducers of plant defense responses [7–9]. Luciferase (LUC) has several advantages over GUS or GFP reporters. It has a relatively short half-life (3 h) compared to GFP (24 h) or GUS (days) [10] and also allows for nondestructive signal detection with virtually no background issues [10]. Additionally, reporter-based screens can provide either quantitative or semiquantitative data, allowing for compound ranking and prioritization.

Understanding the processes of adaptation and tolerance to water stress, especially in plants with agronomic interest, is very important nowadays. Under adverse environmental conditions, such as drought, salinity, and extreme temperatures, plant growth and productivity are severely affected [11]. The plant hormone abscisic acid (ABA) is crucial for plant stress adaptation, with a major relevance in drought resistance [12, 13]. ABA regulates guard cell closure, limiting transpiration under water stress conditions [14, 15]. Additionally, ABA guides root growth toward the water source and also prevents root branching toward the dry soil in two processes called hydropatterning and xerobranching, respectively [16–21]. These traits have been exploited biotechnologically to increase plant resistance to drought stress. For instance, overexpression of the PYL5 ABA receptor in *Arabidopsis* confers hypersensitivity to ABA and a significant tolerance to drought stress [22]. This strategy also works in staple crops where the overexpression of hexaploid wheat, TaPYL4 ABA receptor, increases productivity under water stress [23]. Lately, new components of the ABA signaling pathway have been described; for example, a novel mechanism that protects plants from drought stress has been identified [24]. Under water deficit, plants detect reduced water content of the substrate and synthesize the CLE25 peptide in roots. Then, it is believed that the root-derived CLE25 peptide moves from the root

to the shoot via phloem [24]. Next, CLE25 binding by BAM receptors promotes ABA biosynthesis and stomatal closure in leaves contributing to plant resistance to drought stress [24]. Additionally, application of the CLE25 peptide protects plants from water stress. Altogether, it is clear that activation of the ABA signaling pathway increases plant stress tolerance.

In this chapter, we describe a high-throughput method to identify small molecules able to activate the ABA signaling pathway. The procedure is based on a reporter line that expresses the LUC⁺ protein fused to the promoter of the ABA-responsive gene *MAPKKK18* [4, 25]. First, *pMAPKKK18::LUC⁺* transgenic seeds are germinated and grown in 96-well plates for 7 days. Then, the test compounds are applied along with luciferin, and seedling imaging is performed 6 h after the treatment. Images are then semiautomatically quantified, and compounds able to activate the LUC reporter are identified. Candidate chemical activators are then retested using complementary bioassays (e.g., inhibition of seed germination) to study the activation of ABA-related phenotypes.

2 Materials

2.1 Generation of Transgenic Lines

1. *MAPKKK18* promoter-specific primers pMAPKKK18-F 5'-AAGCGGCGCGTGGAGAGAGA-3'; pMAPKKK18-R 5'-GCTGTCCATCTCTCCGTCGC-3'.
2. pENTR/D-TOPO cloning kit.
3. DH5 α *E. coli* competent cells.
4. *Agrobacterium tumefaciens* strain GV3101 competent cells.
5. Agroinfiltration solution: 5% sucrose, 0.02% Silwet.
6. *Arabidopsis* seeds of Col-0 ecotype.
7. 100 mg/mL gentamicin. Dissolve 1 g of gentamicin in 10 mL of water. Sterilize by filtration through a 0.2- μ m-pore-size membrane filter. Store at -20 °C.
8. Selection plates: Half-strength Murashige and Skoog (MS) media with 0.5% sucrose, 100 μ g/mL gentamicin, and 1% agar. Dissolve 2.15 g of MS salts and 5 g of sucrose in 800 mL of water. Adjust pH to 5.7 with KOH. Bring the volume to 1000 mL with water. Add 10 g agar to the media and then autoclave at 120 °C for 20 min. Cool down the sterilized media to 55 °C and add 1 mL of 100 mg/mL gentamicin. Mix the media with gentamicin and then distribute the mixture into 150 \times 15 mm Petri plates (50 mL per plate). Store at 4 °C.

9. 100 mM D-luciferin. Dissolve 159.21 mg of D-luciferin potassium salt in 5 mL of water. Distribute 0.5 mL aliquots into 1.5-mL test tubes. Store at $-20\text{ }^{\circ}\text{C}$ (*see Note 1*).
10. Charge-coupled device (CCD) camera.

2.2 Chemical Screening

1. Transgenic *pMAPKKK18-LUC⁺* seed.
2. 96-well plates (*see Note 2*).
3. Chemical library, control compounds, and DMSO as a solvent.
4. Half-strength MS media with 0.5% sucrose and 1% agar.
5. 100 mM D-luciferin. *See* previous section.
6. CCD camera.
7. ImageJ (<https://imagej.nih.gov/ij/index.html>) with PlateReader 2.1 plugin installed.
8. 10 mM 2-(N-morpholino)ethanesulfonic acid (MES), pH 5.7: Dissolve 976 mg of MES in 450 mL of water. Adjust pH to 5.7 using HCl. Bring the volume to 500 mL with water and autoclave at $121\text{ }^{\circ}\text{C}$ for 20 min.
9. 96-well PCR plates (14-230-232, Fisher).

3 Methods

3.1 Generate *pMAPKKK18::LUC⁺* Reporter Line

1. Clone the *MAPKKK18* promoter into the pENTR/D-TOPO vector using the cloning kit. Mix 2 μL of the PCR product obtained using the primers pMAPKKK18-F/pMAPKKK18-R with the components provided with the kit: 1 μL salt solution, 1 μL TOPO vector, and 2 μL water. Incubate at room temperature ($21\text{--}22\text{ }^{\circ}\text{C}$) for 5 min. Transform the cloning product to *E. coli* DH5 α competent cells and then verify the clone by sequencing the plasmid DNA.
2. Clone the *MAPKKK18* promoter into the destination vector pFlash, which contains *LUC⁺*, through LR reaction using clonase II enzyme mix following the manufacturer's instructions. In brief, mix 150 ng of the pENTR/pMAPKKK18 plasmid DNA with 150 ng of pFlash plasmid and 1 μL of LR clonase II in a final volume of 4 μL . After 1-h incubation at RT, terminate the reaction with 1 μL of proteinase K (provided with the kit) and incubate at $37\text{ }^{\circ}\text{C}$ for 10 min. Transform the LR reaction product into DH5 α *E. coli* cells to generate pFlash/pMAPKKK18-*LUC⁺*.
3. Transform the verified pFlash/pMAPKKK18-*LUC⁺* plasmid DNA into *Agrobacterium tumefaciens* GV3101 competent cells.

4. Transform pFlash/pMAPKKK18-LUC⁺ into *Arabidopsis thaliana* Col-0 plants using agrobacterium-mediated transformation by floral-dipping [26].
5. Select homozygous single insertion transgenic plants expressing the transgene in T3 generation plants (*see Note 3*).

3.2 Grow Transgenic Plants

1. Fill a 96-well plate with 150 μ L of half-strength MS media (0.5% sucrose, 1% agar) per well.
2. For one screening plate, weigh 50 mg of *pMAPKKK18::LUC⁺ Arabidopsis* seeds (2500 seeds approximately). Sterilize seeds with 30% commercial bleach with 0.02% Tween-20 for 10 min. Remove the bleach solution and wash seeds with sterile water 5 times. Remove the water and suspend the seeds in 2 mL of sterile tap agar (0.12% agarose in water).
3. Dispense 20 μ L of tap agar containing approximately 25 seeds in each well (*see Note 4*).
4. Incubate the plate at 4 °C for 3 days.
5. Place the plates under long-day conditions (18 h light/6 h dark) at 23 °C light/21 °C dark for 7 days.

3.3 Prepare Chemical Plates

1. Thaw stock chemical plates at RT for 10 min.
2. Shake stock chemical plates at 400 r.p.m. for 5 min at RT (*see Note 5*).
3. Transfer compounds from stock chemical plates into working plates. Dilute the compounds in working plates to 2.5 mM with DMSO. Thoroughly seal the plates and store them at -20 °C (*see Note 6*).

3.4 Chemical Screening

The chemical library screening workflow is summarized in Fig. 1. In brief, treat 7-day-old *pMAPKKK18::LUC⁺* seedlings grown under long-day conditions with chemicals at a final concentration of 25 μ M. Apply luciferin with the test chemicals at the same time. Image plates 6 h after chemical and luciferin treatment using a LAS-3000 imager and then quantify acquired images using the ImageJ plugin ReadPlate 2.1. Retest candidate compounds in secondary screening assays by analyzing their effect on ABA-related phenotypes (e.g., inhibition of seed germination).

1. Prepare 10 mL (per plate) of 100 μ M D-luciferin in 10 mM MES (pH 5.7). Add 99 μ L of freshly prepared 100 μ M D-luciferin into each well of the 96-well PCR plate (*see Note 7*).
2. Transfer 1 μ L of the compound from the 2.5 mM working chemical plate and the appropriate controls (DMSO and ABA) into the 96-well PCR plate containing 99 μ L of 100 μ M D-luciferin following the scheme in Fig. 1 (*see Note 8*).

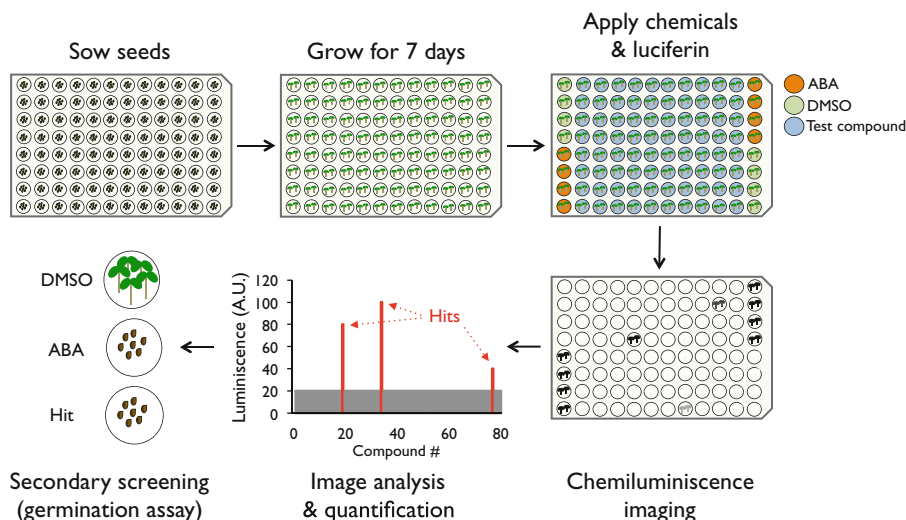


Fig. 1 Schematic representation of the proposed chemical screening

3. Transfer 100 μL of the mixture of D-luciferin and 25 μM test compound into the 96-well plates containing 7-day-old seedlings following the scheme in Fig. 1.
4. Incubate seedlings with the test compound and D-luciferin for 6 h under growing conditions (Fig. 2a).
5. Image luciferase-produced luminescence with the CCD camera (see Note 9).
6. To improve visual results, the grayscale image obtained with the CCD camera can be transformed by modifying the LUTs of the image (ImageJ > Image > Lookup tables > Fire) (Fig. 2b).

3.5 Process the Images and Identify Candidate Compounds

1. Install the ReadPlate plugin (<http://imagej.nih.gov/ij/macros/ReadPlate2.1.txt>) on ImageJ/Fiji [27].
2. Open your .tif image with ImageJ. Plate borders must be aligned parallel to the edges of the image. Export the image as a .jpg file and open it with ImageJ.
3. Identify the x, y coordinates of the first (A1) and last (H12) wells.
4. Invert image colors (ImageJ > Edit > Invert) and transform the image into RGB color (ImageJ > Image > Type > RGB color).
5. Run the ReadPlate2.1 plugin (ImageJ > Plugins > Macros > Run... > readplate.ijm).
6. Select the color channel (Gray) and introduce the x, y coordinates of the first (A1) and last (H12) wells.

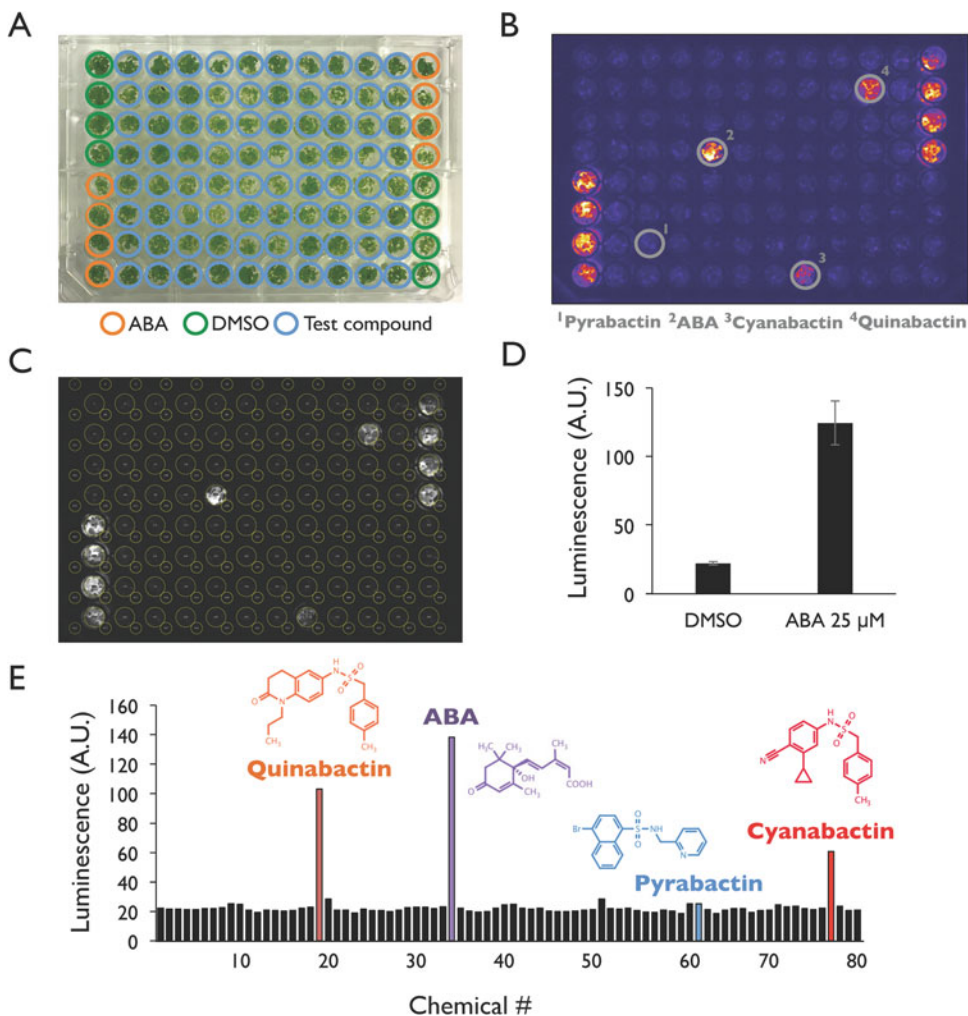


Fig. 2 A luciferase reporter assay to identify chemical activators of ABA signaling. **(a)** 7-day-old pMAPKKK18::LUC⁺ seedlings grown in a 96-well plate. Seedlings in wells that are treated with DMSO, ABA, or the test compound are indicated. **(b)** Visualization of luciferase images after using the Fire LUT (ImageJ). The position of seedlings treated with 25 μ M ABA or the ABA agonists pyrabactin, quinabactin, and cyanabactin are highlighted. **(c)** Semiautomatic image quantification using the PlateReader 2.1 plugin. **(d)** Quantification of fluorescence intensities in seedlings treated with DMSO and ABA controls. **(e)** An example screening result from seedlings treated with 25 μ M ABA and different ABA agonists. 2-D structures of the corresponding compounds used in the treatment are presented on the chart

7. Adjust the circle size diameter to 100 pixels and press OK to proceed with the measurements (Fig. 2c, d). The RGB intensity values are represented in the table as mean.
8. Export results as an Excel spreadsheet file (.xls).
9. Plot quantification results to identify candidate compounds (Fig. 2e).

10. Perform secondary screening with candidate compounds by analyzing their effect on ABA-related phenotypes (e.g., inhibition of seed germination).

4 Notes

1. Luciferin needs to be kept at $-80\text{ }^{\circ}\text{C}$ if long-term storage is required.
2. To minimize plate evaporation and edge effect, we suggest using plates with surrounding built-in reservoirs.
3. It is important to confirm ABA induction of LUC activity from T1 generation and select transgenic lines with low basal levels of LUC activity.
4. We recommend using an electronic pipette to reduce pipetting errors.
5. Because some compounds have low solubility, it is important to shake the compounds to allow them to dissolve better.
6. We suggest using multichannel pipettes or a liquid handling robot in this step for accuracy and saving time.
7. We recommend using a repeater pipette in this step.
8. A multichannel pipette is recommended for this step.
9. The exposure time might vary based on different types of imager. For LAS-3000 imager, an exposure time of 2 min under high-resolution conditions can be used in this step.

Acknowledgments

We thank M.A. Nohales and S. Kay for sharing the pFlash vector. This work has received funding from the European Union's Horizon 2020 research and innovation programme under the Marie Skłodowska-Curie Grant Agreement No. [707477] to J. L.-J. and Ministerio de Ciencia e Innovación (BIO2017-82503-R) to P.L.R.

References

1. Kinoshita T, McCourt P, Asami T et al (2018) Plant chemical biology. *Plant Cell Physiol* 59:1483–1486
2. Dejonghe W, Russinova E (2017) Plant chemical genetics: from phenotype-based screens to synthetic biology. *Plant Physiol* 174:5–20
3. Dejonghe W, Russinova E (2014) Target identification strategies in plant chemical biology. *Front Plant Sci* 5:352
4. Okamoto M, Peterson FC, Defries A et al (2013) Activation of dimeric ABA receptors elicits guard cell closure, ABA-regulated gene expression, and drought tolerance. *PNAS* 110:12132–12137
5. Wim D, Okamoto M, Cutler SR (2018) Small molecule probes of ABA biosynthesis and signaling. *Plant Cell Physiol* 59(8):29

6. Halder V, Kombrink E (2018) High-throughput screening of chemical compound libraries for modulators of salicylic acid signaling by in situ monitoring of glucuronidase-based reporter gene expression. *Methods Mol Biol* 1795:49–63
7. Rodriguez-Salus M, Bektas Y, Schroeder M et al (2016) The synthetic elicitor 2-(5-bromo-2-hydroxy-phenyl)-thiazolidine-4-carboxylic acid links plant immunity to hormesis. *Plant Physiol* 170:444–458
8. Knoth C, Eulgem T (2014) High-throughput screening of small-molecule libraries for inducers of plant defense responses. *Methods Mol Biol* 1056:45–49
9. Knoth C, Salus MS, Girke T et al (2009) The synthetic elicitor 3,5-dichloroanthranilic acid induces NPR1-dependent and NPR1-independent mechanisms of disease resistance in *Arabidopsis*. *Plant Physiol* 150:333–347
10. de Ruijter NCA, Verhees J, van Leeuwen W et al (2003) Evaluation and comparison of the GUS, LUC and GFP reporter system for gene expression studies in plants. *Plant Biol* 5:103–115
11. Pandey P, Irulappan V, Bagavathiannan MV et al (2017) Impact of combined abiotic and biotic stresses on plant growth and avenues for crop improvement by exploiting physiomorphological traits. *Front Plant Sci* 8:537
12. Daszkowska-Golec A (2016) The role of abscisic acid in drought stress: how ABA helps plants to cope with drought stress. In: Hossain MA, Wani SH, Bhattacharjee S et al (eds) *Drought stress tolerance in plants, vol 2: molecular and genetic perspectives*. Springer, Cham, pp 123–151
13. Zhu J-K (2002) Salt and drought stress signal transduction in plants. *Annu Rev Plant Biol* 53:247–273
14. Schroeder JI, Allen GJ, Hugouvieux V et al (2001) Guard cell signal transduction. *Annu Rev Plant Physiol Plant Mol Biol* 52:627–658
15. Kim T-H, Böhmer M, Hu H et al (2010) Guard cell signal transduction network: advances in understanding abscisic acid, CO₂, and Ca²⁺ signaling. *Annu Rev Plant Biol* 61:561–591
16. Takahashi N, Goto N, Okada K et al (2002) Hydrotropism in abscisic acid, wavy, and gravitropic mutants of *Arabidopsis thaliana*. *Planta* 216:203–211
17. Eapen D, Barroso ML, Campos ME et al (2003) A no hydrotropic response root mutant that responds positively to gravitropism in *Arabidopsis*. *Plant Physiol* 131:536–546
18. Antoni R, Gonzalez-Guzman M, Rodriguez L et al (2012) PYRABACTIN RESISTANCE1-LIKE8 plays an important role for the regulation of abscisic acid signaling in root. *Plant Physiol* 161:931–941
19. Bao Y, Aggarwal P, Robbins NE et al (2014) Plant roots use a patterning mechanism to position lateral root branches toward available water. *Proc Natl Acad Sci U S A* 111:9319–9324
20. Dietrich D, Pang L, Kobayashi A et al (2017) Root hydrotropism is controlled via a cortex-specific growth mechanism. *Nat Plants* 3:17057
21. Orman-Ligeza B, Morris EC, Parizot B et al (2018) The xerobranching response represses lateral root formation when roots are not in contact with water. *Curr Biol* 28:3165–3173. e5
22. Santiago J, Rodrigues A, Saez A et al (2009) Modulation of drought resistance by the abscisic acid receptor PYL5 through inhibition of clade A PP2Cs. *Plant J* 60:575–588
23. Mega R, Abe F, Kim J-S et al (2019) Tuning water-use efficiency and drought tolerance in wheat using abscisic acid receptors. *Nat Plants* 5:153–159
24. Takahashi F, Suzuki T, Osakabe Y et al (2018) A small peptide modulates stomatal control via abscisic acid in long-distance signalling. *Nature* 556:235–238
25. Vaidya AS, Peterson FC, Yarmolinsky D et al (2017) A rationally designed agonist defines subfamily IIIA abscisic acid receptors as critical targets for manipulating transpiration. *ACS Chem Biol* 12:2842–2848
26. Clough SJ, Bent AF (1998) Floral dip: a simplified method for *Agrobacterium*-mediated transformation of *Arabidopsis thaliana*. *Plant J* 16:735–743
27. Angelani et al (2018) A metabolic control analysis approach to introduce the study of systems in biochemistry: the glycolytic pathway in the red blood cell. *Biochem Mol Biol Educ* <https://doi.org/10.1002/bmb.21139>



Chapter 11

Identification of Novel Molecular Regulators Modulating Ethylene Biosynthesis Using EMS-Based Genetic Screening

Chanung Park, Dong Hye Seo, Joseph Buckley, and Gyeong Mee Yoon

Abstract

The gaseous hormone ethylene regulates a diverse range of plant development and stress responses. Ethylene biosynthesis is tightly regulated by the transcriptional and posttranscriptional regulation of ethylene biosynthetic enzymes. ACC synthase (ACS) is the rate-limiting enzyme that controls the speed of ethylene biosynthesis in plant tissues, thus serving as a primary target for biotic and abiotic stresses to modulate ethylene production. Despite the critical role of ACS in ethylene biosynthesis, only a few regulatory components regulating ACS stability or ACS transcript levels have been identified and characterized. Here we show a genetic approach for identifying novel regulatory components in ethylene biosynthesis by screening EMS-mutagenized *Arabidopsis* seeds.

Key words *Arabidopsis*, Ethylene biosynthesis, *eto3*, Suppressor screening, Cytokinin

1 Introduction

The plant hormone ethylene regulates plant growth, development, and various stress responses [1]. To operate the diverse roles of ethylene in a different context, a plant needs to possess regulatory mechanisms that stringently control ethylene biosynthesis and response. Biosynthesis of ethylene is mainly regulated by influencing transcript levels of *1-aminocyclopropane-1-carboxylic synthase* (ACS) or its activity/stability of ACS isozymes, rate-limiting enzymes in ethylene biosynthesis [2, 3]. Although the transcriptional regulation of ACS genes has been considered a major regulatory mechanism to modulate ethylene biosynthesis, an increasing number of studies have shown that the posttranslational control of ACS such as protein stability plays a critical role in ethylene biosynthesis regulation [4–7]. Higher plant genome possesses a multi-gene family of ACS genes whose encoded proteins are generally classified into three different types, i.e., type-1, type-2, and type-3, based on the presence or absence of the regulatory sites or motifs in the C-terminus of the ACS proteins [4, 7]. Molecular genetics

studies have revealed that the stability of type-2 ACS proteins is regulated by Ethylene Overproducer 1 (ETO1) and its two paralogs ETO1-like 1 (EOL1) and EOL2 E3 ligases [8, 9]. These E3 ligases contain a BTB (broad-complex, tramtrack, bric-à-brac)/TRP (tetratricopeptide repeat) domain and specifically bind to the C-terminal domain of type-2 ACS, resulting in the degradation of the type-2 ACS proteins through the 26S proteasome pathway.

Several phytohormones have been identified as an internal cue that regulates the stability of ACS protein either positively or negatively, thus controlling ethylene biosynthesis [5, 10]. Cytokinin is one such hormone affecting the stability of ACS proteins. Cytokinin increases ACS protein stability by acting through the C-terminal domain of type-2 ACS. However, several recent studies suggested that cytokinin also controls the stability of ACS proteins via a non-C-terminus-dependent manner; cytokinin increases the protein stability of type-1 ACS, which does not contain the ETO1-binding site [5]. Moreover, cytokinin increases the protein stability of the *eto3*, a mutant of type-2 ACS9 possessing a mutation in the ETO1-binding site [10]. Collectively, these results indicate the existence of an alternative pathway by which cytokinin increases ethylene production without acting through the TOE motif. The *eto3* exhibits a shorter root-length phenotype and constitutive triple response in the light or darkness, respectively, compared to a wild-type seedling due to its higher ethylene production [11]. The cytokinin treatment further accentuates these ethylene-overproduction phenotypes of the *eto3*, displaying significantly reduced root growth and exaggerated triple response. By taking advantage of these distinctive cytokinin-induced phenotypic changes in the *eto3* mutant, ethyl methanesulfonate (EMS)-mutagenized *eto3* can be screened to identify novel molecular components that control ethylene biosynthesis in the TOE-independent manner (Fig. 1).

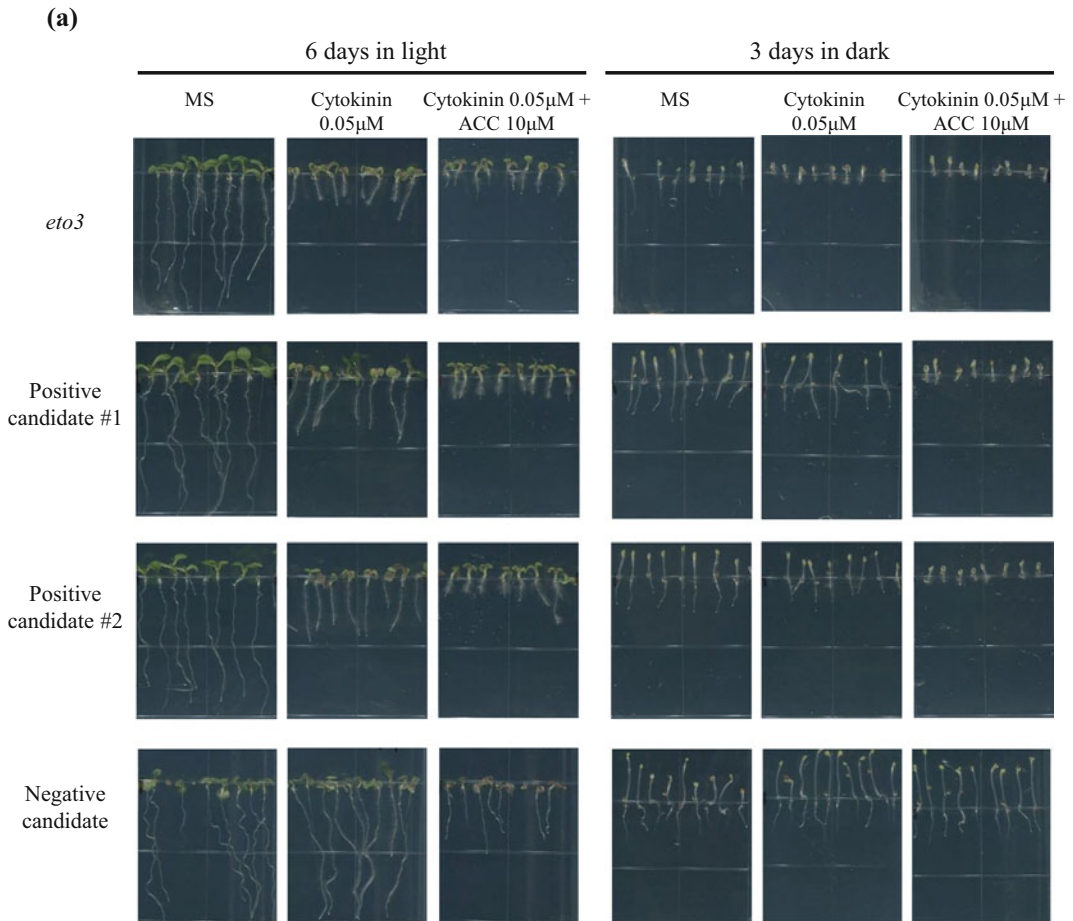
2 Materials

2.1 Seed Sterilization

1. Microcentrifuge tubes.
2. Concentrated HCl.
3. Commercial bleach.
4. Glass desiccator or cake carrier.
5. Sterilized ddH₂O.

2.2 Suppressor Screening, Ethylene Measurement, and Other Physiological Assays

1. EMS-mutagenized *Arabidopsis eto3* seeds.
2. Square Petri dishes.
3. Racks for supporting plates in a vertical position.
4. Pasteur pipette.



(b)

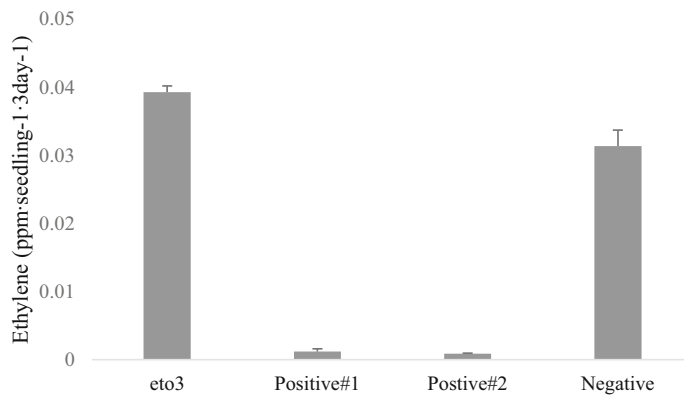


Fig. 1 Identification of *eto3* suppressors with a reduced cytokinin sensitivity and ethylene production. **(a)** EMS-mutagenized *eto3* seeds were screened on cytokinin media both under light and dark conditions. The suppressor mutants displaying longer roots and a reduced triple response in the cytokinin media were further screened for ACC-mediated rescue of triple response (positive candidates #1 and 2). Mutants that did not pass these screens were removed from the further investigation (negative candidate). **(b)** Ethylene measurement of suppressor mutants in **(a)**. Ethylene produced from 3-day-old seedlings grown in MS media was measured using a gas chromatograph

5. Murashige and Skoog (MS) media: MS salt, sucrose, and agar.
6. Cytokinin.
7. 1-Aminocyclopropane-1-carboxylic acid (ACC).
8. Gas chromatograph (GC) (for example, a Shimadzu, GC-2010 plus with HS-20 head sampler).
9. Air, helium, and hydrogen gas with $\geq 99\%$ purity.
10. GC vials, aluminum caps with septa.
11. Crimper and decapper.
12. Commercial aluminum foil.

3 Methods

3.1 Screening for *eto3* Suppressors in Response to Cytokinin

3.1.1 Seed Sterilization

1. Place about 100 μL volume of m2 seeds to microcentrifuge tubes.
2. Open the lids of the tubes and place them in a glass desiccator (or a cake carrier).
3. Place a beaker containing 100 mL of commercial bleach with 3 mL of concentrated HCl alongside the rack with tubes containing seeds in the glass desiccator (*see Note 1*) and close the lid.
4. Incubate the seeds in the desiccator for at least 4 h.

3.1.2 Suppressor Screening

1. Prepare half-strength MS media with 1% sucrose, 0.6% (W/V) agar, and 0.05 μM of cytokinin.
2. Pour about 30 mL of the media to square Petri dishes and let the media solidify for 20 min in a clean bench.
3. Place around 50 m2 seeds on the second and the fifth lines of each plate using a Pasteur pipette.
4. Seal the plates with micropore tape and place the plates for 3 days in a 4 °C dark chamber or refrigerator for stratification.
5. Transfer the plates to a light chamber with constant light and vertically stand them on racks (*see Note 2*).
6. After 6 days in the light chamber, scan the plates and compare the root length of mutant seedlings with that of the *eto3* grown in the same plates.
7. Select the candidate suppressor seedlings with longer roots compared to the *eto3*, transfer them to soil, and let them self-fertilize, and harvest seeds (m3).
8. Repeat **steps 3–6** using m3 seeds to confirm the root phenotypes and segregation.

9. Transfer the mutants displaying longer roots in response to cytokinin to soil and harvest seeds (m4) from the self-fertilized mutant plants.
10. Repeat **steps 3–6** using m4 seeds to select homozygous individuals.

3.2 Observation of Triple Response and Measurement of Ethylene Production in the Selected Suppressor Mutants from the Root Assay

The suppressor mutants that displayed a reduced cytokinin response for root growth were selected for triple response observation and ethylene measurement.

1. Place each homozygous suppressor seeds and *eto3* to square plates with half-strength MS agar with and without 0.05 μ M cytokinin.
2. Place the plates in a 4 °C dark chamber or refrigerator for 3 days and incubate in the light chamber for 1–2 h.
3. Incubate the plates in the dark chamber for 3 days.
4. Identify suppressors that do not show accentuated triple response in cytokinin media.
5. Prepare 3 mL of half-strength MS agar to each GC vials.
6. Place 20–25 seeds of each suppressor candidate that showed a reduced response to cytokinin for triple response (from **step 4**). Prepare *eto3* vials as a control (*see Note 3*).
7. Seal the vials with sterilized aluminum foils and incubate them in a 4 °C dark chamber or refrigerator for 3 days.
8. Cap the vials using a crimper with UV light-sterilized aluminum caps with septa.
9. Incubate the vials in the light chamber for 1–2 h.
10. Subsequently, incubate them in the dark chamber for 3 days.
11. Measure ethylene levels accumulated in each vial using a gas chromatograph (*see Note 4*).
12. Remove the caps using a decapper and count seedlings in the vials (*see Note 5*).
13. Calculate ethylene levels by dividing total ethylene measured with total germinated seedlings. Select suppressors that show lower ethylene levels than *eto3*.

3.3 Identification of Suppressors that Show ACC-Mediated Rescued Triple Responses and Root Phenotype

The mutants that passed through the three rounds of selection steps, i.e., root growth assay, triple response, and ethylene production, were further tested for ACC-mediated rescue of the cytokinin-induced triple response and ethylene production.

1. Prepare three sets of half-strength MS agar plates: MS only, MS with 0.05 μM cytokinin, and MS with 0.05 μM cytokinin and 10 μM ACC.
2. Place selected suppressor seeds on each plate with *eto3* as a control. Make duplicates of each plate for root growth assay and triple response assay.
3. Incubate the plates in a 4 °C dark chamber or refrigerator for 3 days.
4. Incubate the plates in a light chamber for 1–2 h and place them vertically on standing racks.
5. Incubate one set of plates in the dark chamber for 3 days and place another set of duplicated plates in the light chamber for an additional 6 days.
6. Observe if ACC treatment rescues the triple response and root length of suppressors to a similar extent to what is observed for the *eto3* mutant seedlings. Suppressor mutants failing to show comparable triple response and reduced root length to the *eto3* mutants are eliminated (*see Note 6*). Mutants that show ACC-mediated rescued triple response and root length will be selected for mapping to identify the mutations in the genome.

4 Notes

1. Perform chlorine gas-mediated seed sterilization in a fume hood due to its toxicity. Reducing the flow rate of the hood will prevent loss of chlorine gas generated in a cake carrier or desiccator during the sterilization. Furthermore, using a chemical-resistant marker (VWR, Cat. No. 95042-566) will prevent erasing labels on tubes with seeds after the incubation.
2. Tilt the plates slightly (~10–15 °C) to prevent roots from growing toward the air instead of into growth media. This also applies to other physiological assays that require vertical growth of seedlings.
3. Prepare 0.6% top agar and mix with sterilized seeds, which helps seeds to rest in the center of a vial.
4. Prepare at least three empty vials with air before measuring actual sample vials to prevent altering ethylene levels owing to the carryover ethylene from previous runs.
5. Remove seedlings from the vials and place them in a weighing dish with 3–5 mL of water for easy counting.
6. *Arabidopsis* seedlings will exhibit further reduced root length in the presence of additional ACC compared to seedlings in cytokinin-only media.

References

1. Abeles FB, Morgan PW, Saltveit JEM (1992) Ethylene in plant biology. Academic, San Diego, CA
2. Yang SF, Hoffman NE (1984) Ethylene biosynthesis and its regulation in higher plants. *Ann Rev Plant Physiol* 35(1):155–189
3. Adams DO, Yang SF (1979) Ethylene biosynthesis: identification of 1-aminocyclopropane-1-carboxylic acid as an intermediate in the conversion of methionine to ethylene. *Proc Natl Acad Sci U S A* 76(1):170–174
4. Chae HS, Kieber JJ (2005) Eto Brute? Role of ACS turnover in regulating ethylene biosynthesis. *Trends Plant Sci* 10(6):291–296
5. Lee HY, Chen YC, Kieber JJ, Yoon GM (2017) Regulation of the turnover of ACC synthases by phytohormones and heterodimerization in *Arabidopsis*. *Plant J* 91(3):491–504
6. Yoon GM (2015) New insights into the protein turnover regulation in ethylene biosynthesis. *Mol Cells* 38(7):597–603
7. Booker MA, DeLong A (2015) Producing the ethylene signal: regulation and diversification of ethylene biosynthetic enzymes. *Plant Physiol* 169(1):42–50
8. Yoshida H, Nagata M, Saito K, Wang KLC, Ecker JR (2005) *Arabidopsis* ETO1 specifically interacts with and negatively regulates type 2 1-aminocyclopropane-1-carboxylate synthases. *BMC Plant Biol* 5:14
9. Wang KL, Lurin C, Ecker JR (2004) Regulation of ethylene gas biosynthesis by the *Arabidopsis* ETO1 protein. *Nature* 428(6986):945–950
10. Hansen M, Chae HS, Kieber JJ (2009) Regulation of ACS protein stability by cytokinin and brassinosteroid. *Plant J* 57(4):606–614
11. Chae HS FF, Kieber JJ (2003) The *eto1*, *eto2*, and *eto3* mutations and cytokinin treatment increase ethylene biosynthesis in *Arabidopsis* by increasing the stability of ACS protein. *Plant Cell* 15(2):545–559



Investigation of Auxin Biosynthesis and Action Using Auxin Biosynthesis Inhibitors

Kazuo Soeno, Akiko Sato, and Yukihisa Shimada

Abstract

Auxin plays important roles in almost all aspects of plant growth and development. Chemical genetics is an effective approach to understand auxin action, especially in nonmodel plant species, in which auxin-related mutants are not yet available. Among auxin-related chemical tools, we present approaches to utilize auxin biosynthesis inhibitors. The inhibitors are effective not only to understand auxin biosynthesis but also to understand auxin action. The effectiveness of the inhibitors can be assessed based on *in vitro* or *in vivo* assays. The *in vitro* assay employs enzyme inhibition assays. The *in vivo* assay employs UPLC-MS/MS-based analysis of endogenous IAA and its intermediates or metabolites.

Key words Chemical genetics, Arabidopsis, Auxin biosynthesis, Reverse genetics

1 Introduction

Indole-3-acetic acid (IAA) is a natural auxin that regulates almost all aspects of plant growth and development. In classical studies, auxin action was studied mainly with exogenous application of IAA to plants. However, exogenous auxin has been known to be ineffective or less effective, especially when applied to intact plants, e.g., in hypocotyls or stems. The main reason is because the endogenous auxin level necessary to support plant growth is saturated or maximum. Overdose of exogenous auxin also results in inhibition of growth. One of the main reasons is evolution of ethylene in response to exogenous auxin. To solve these problems and to better understand physiological functions of auxin, it is ideal to knock out or knock down the endogenous auxin level or activity using chemical tools.

Chemical genetic approaches using micromolecules have been widely employed to analyze the function of auxin [1, 2]. Auxinole and PEO-IAA were developed as potent inhibitors of auxin signaling [3]. On the other hand, there are several types of auxin efflux transport inhibitors, such as 1-*N*-naphthylphthalamic acid (NPA)

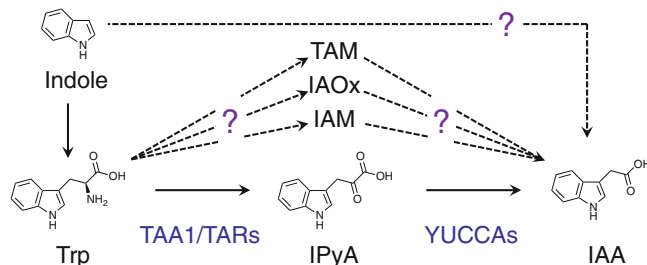


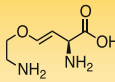
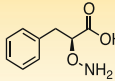
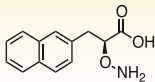
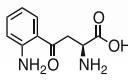
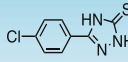
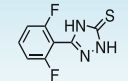
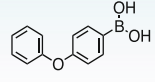
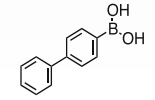
Fig. 1 Auxin biosynthesis pathways

and 2,3,5-triiodobenzoic acid (TIBA). However, specificities of known transport inhibitors to auxin action are questionable. For example, TIBA inhibits vesicle trafficking process [4] and NPA inhibits actin cytoskeleton remodeling [5]. These inhibitors are effective in nonplant species. Among auxin inhibitors, use of auxin biosynthesis inhibitor is advantageous. The specificity to auxin action is well established in recent studies, since these inhibitors directly inhibit auxin biosynthesis enzymes. In addition, it is also advantageous that the specificity of the inhibitor can be confirmed with co-application of the inhibitor with auxin, when growth inhibition can be recovered by the co-treatment.

The indole-3-pyruvic acid (IPyA) pathway has been proposed as the main pathway for IAA biosynthesis in *Arabidopsis*. In the IPyA pathway, TAA1/TARs synthesize IPyA from L-tryptophan [6, 7], and YUCCAs (YUCs) convert IPyA to IAA [8] (see Fig. 1). Evidence from chemical biology approaches supported the function of the IPyA pathway in *Arabidopsis*. The TAA1/TAR inhibitors L- α -aminooxy-phenylpropionic acid (L-AOPP) [9], L-kynurenine (L-Kyn) [10], and pyruvamine (PVM) [11] effectively blocked IPyA production and subsequent auxin biosynthesis in vivo and in vitro. In addition, the YUC inhibitor yucasin [12], YDF [13], and aromatic borate [14] effectively inhibited auxin biosynthesis in vivo and in vitro. The well-established auxin biosynthesis inhibitors are listed in Table 1.

In this chapter, we show the utility of auxin biosynthesis inhibitors. The effectiveness of the inhibitors can be assessed based on in vitro or in vivo assays. The in vitro assay employs enzyme inhibition assay. The in vivo assay employs UPLC-MS/MS-based analysis of endogenous IAA, its intermediates, or metabolites. Specific action of inhibitors can be assessed in recovery tests, in which co-treatment of the inhibitor with auxin results in the recovery of the inhibition either in plant growth assay or in marker gene expression assay. In this chapter, we have omitted methods for plant growth assays, which can be referred to other chapters of *Plant Chemical Genomics* [15].

Table 1
Auxin biosynthesis inhibitors

Target enzymes	Inhibitor	Inhibitor constant (K_i)	Costs /100 mg	Reference	
TAA1/TARs aminotransferase	AVG		8.6 μ M	3,115 USD	9
	AOPP		350 nM	1,950 USD	9
	PVM 1169		76.8 nM	N.A.	11
	Kyn		11.5 μ M	71.3 USD	10
YUCCAs monooxygenase	Yucasin		N.A.	N.A.	12
	YDF		N.A.	N.A.	13
	PPBo		56 nM	2.16 USD	14
	BBo		67 nM	1.34 USD	14

2 Materials

2.1 *E. coli* Strains

1. DH5 α strain as a cloning host.
2. SoluBL21 strain as an expression host.

2.2 Plant Material and Growth Medium

1. *Arabidopsis thaliana*, Columbia-0 (Col-0) ecotype as wild type (WT).
2. Rice (*Oryza sativa*) cultivar Nihonbare.

2.3 Hardware and Software

1. BioTRON (NK system) for plant cultivation for inhibitor treatment experiments.
2. DOUBLE SHAKER NR-30 (TAITEC) with spring shaker table for inhibitor treatment for *Arabidopsis* seedlings.

3. MULTI SHAKER (EYELA) with sheet shaker for inhibitor treatment for rice seedlings.
4. Multi-beads shocker[®] (YASUI KIKAI) for sample homogenization.
5. Disposable Flow Control Disposable Liners for Visiprep[™] DL (SUPELCO) with Visiprep[™] SPE Vacuum Manifold (SUPELCO) is used to carry out solid-phase extraction to prevent contamination. SPE column is used as OASIS HLB SPE cartridge column (1 cc, 30 mg, Waters) and OASIS MCX SPE cartridge (1 cc, 30 mg, Waters).
6. UPLC-MS/MS. UPLC-MS/MS (ACQUITY Ultra-performance Liquid Chromatography-TQ Detector, Waters) in multiple reaction monitoring (MRM) mode is used as analyses for IAA-related compounds.

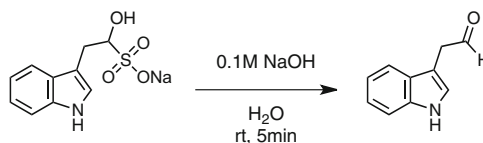
The settings for the UPLC section are as follows: ACQUITY UPLC BEH C₁₈ Column (1.8 μm, 2.1 × 100 mm; Waters) connected to an ACQUITY UPLC BEH C₁₈ VanGuard Pre-Column (1.7 μm, 2.1 × 5 mm; Waters) with column temperature at 35 °C.

The settings for the TQ Detector section are as follows: capillary voltage 3 kV, extractor voltage 3 V, RF lens 0.1 V, source temperature 150 °C, desolvation temperature 350 °C, desolvation gas flow 600 L/h, and cone gas flow 50 L/h.

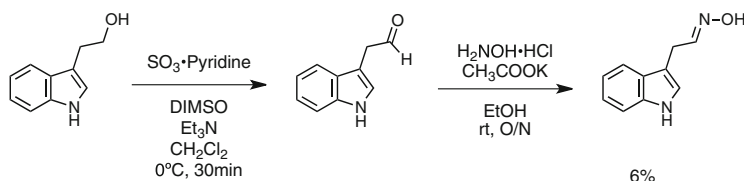
The quantification of endogenous compounds is obtained by MRM of the precursor and the appropriate product ion, with the optimal fragmenting voltage and collision energy determined using the MassLynx[™] Quan Optimize software ver. 4.0 (Waters), for the various diagnostic transitions. Chromatograms were analyzed using the QuanLynx[™] software ver. 4.0 (Waters).

2.4 Standard and Internal Standard

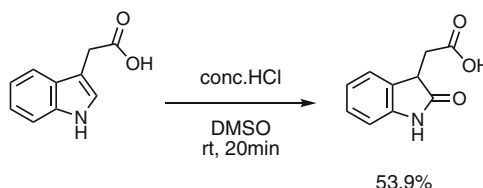
Standards for L-tryptophan (Trp), indole-3-acetamide (IAM), and IAA: Wako Chemicals (Osaka, Japan, <http://www.wako-chem.co.jp>). Standards for tryptamine (TAM) and IPyA: Sigma-Aldrich Co. (St. Louis, MO, USA, <http://www.sigmaaldrich.com/japan.html/>). The standard for indole-3-acetaldehyde (IAAld) was also purchased from Sigma-Aldrich as indole-3-acetaldehyde sodium bisulphite addition compound, and free IAAld was prepared from this product according to a previous report (*see* Scheme 1) [16]. Indole-3-acetyl-L-alanine (IAAla), indole-3-acetyl-L-leucine (IALeu), indole-3-acetyl-L-aspartic acid (IAAsp), and indole-3-acetyl-L-glutamic acid (IAGlu): OlChemim s.r.o. (Slechtitelu, Olomouc, Czech Republic, <http://www.olchemim.cz/Default.aspx>). Standards for *cis/trans*-indole-3-acetaldoxime (IAOx) are synthesized according to a previous report (*see* Scheme 2) [17]. The standard for 2-oxindole-3-acetic acid (oxIAA) is synthesized from IAA according to a previous report (*see* Scheme 3) [18].



Scheme 1 Preparation of free indole-3-acetaldehyde (IAAld)



Scheme 2 Synthesis of *cis/trans*-indole-3-acetaldoxime (IAOx)



Scheme 3 Synthesis of 2-oxindole-3-acetic acid (oxIAA)

Internal standards, [$^2\text{H}_5$]-Trp and [$^2\text{H}_5$]-IAA: Cambridge Isotope Laboratories (Tewksbury, MA, USA, <http://www.isotope.com>). The internal standards, [$^2\text{H}_4$]-TAM and [$^2\text{H}_5$]-IAM: C/D/N Isotopes (Pointe-Claire, QC, Canada, <https://www.cdnisotopes.com>).

3 Methods

3.1 Prepare Recombinant Protein

1. Clone the target gene of your interest into an *E. coli* expression vector. For example, insert the DNA fragment of the target gene into the multicloning site of pCold I vector, in-frame with the *N*-terminal His₆-coding sequence.
2. Transform the expression vector into SoluBL21, in which the chaperone vector pG-Tf2 (Takara) has been introduced.
3. Inoculate the transformant into 15 mL of LB medium containing 50 $\mu\text{g}/\text{mL}$ of carbenicillin and 20 $\mu\text{g}/\text{mL}$ of chloramphenicol, and incubate with shaking at 37 °C for overnight.

4. Starter culture is transferred to a fresh 1 L of terrific broth with 50 $\mu\text{g}/\text{mL}$ of carbenicillin, 20 $\mu\text{g}/\text{mL}$ of chloramphenicol, and 5 ng/mL of tetracycline for continued growth under the same conditions. When the OD_{600} of the culture reaches 0.8–2.0, cool the culture to 15 $^{\circ}\text{C}$, and let it stand for 30 min. After cooling, add isopropyl- β -D-thiogalactopyranoside (0.2 mM) and incubate with shaking at 15 $^{\circ}\text{C}$ for 1 day.
5. Harvest cells by centrifugation at $3500 \times g$ for 10 min at 4 $^{\circ}\text{C}$. Store harvested cells at -80°C until use.
6. Re-suspend in 5 mL of extraction buffer (50 mM Tris-HCl, 0.5 M NaCl, 40 mM imidazole, 10% glycerol, 1% Tween 20, pH 8.0 with 0.5 mg/mL lysozyme chloride) per gram wet cell volume, and sonicate the suspension on ice.
7. Centrifuge at $20,400 \times g$ for 20 min at 4 $^{\circ}\text{C}$ and keep the supernatant.
8. Load the supernatant into 5 mL of the HisTrap HP column equilibrated with wash buffer (50 mM Tris, 0.5 M NaCl, 100 mM Imidazole, 10% Glycerol, pH 8.0). Wash the resin with the same buffer and elute the bound protein with elution buffer (50 mM Tris-HCl, 0.5 M NaCl, 0.5 M imidazole, 10% glycerol, pH 8.0).
9. Replace the eluted sample with 50 mM Tris-HCl, 0.5 M NaCl, and 10% glycerol, pH 8.0, using a PD-10 column. Quantify the protein concentration of the sample by methods such as the Bradford assay (Bio-Rad), and divide into aliquots, immediately frozen in liquid nitrogen, and stock at -80°C until use.

3.2 Enzyme Inhibition Assay of TAA1

1. In vitro TAA1 activity assay is performed as previously described for the borate buffer assay [7] with minor modifications. The reaction mixture is prepared in 500 μL of 0.5 M borate (pH 8.5) containing 300 μL Trp, 1 mM sodium pyruvate, 10 μM pyridoxal phosphate, 1 μg of purified TAA1 recombinant protein, and 1–100 μM inhibitors. The inhibitors are usually dissolved in dimethyl sulfoxide (DMSO) at 100 times the target concentration, and 5 μL is added to the reaction mix. For control experiment, add 5 μL of DMSO. The reaction is initiated by adding a mixture of Trp and the inhibitor and then incubated at 35 $^{\circ}\text{C}$ for 30 min, and the reaction is stopped by the addition of 20 μL of 6 M HCl.
2. Absorbance at 330 nm is measured to monitor the amount of IPyA–borate complex. Reaction mixtures without TAA1 or heat-inactivated TAA1 are used as control.

3.3 Enzyme Inhibition Assay of YUCCA

1. In vitro YUCCA enzyme assay is performed as described in Mashiguchi et al. [9], with minor modifications. The reaction mixture is prepared in 200 μL of 50 mM Tris (pH 8.0)

containing 3 μM IPyA (*see Note 1*), 1 mM NADPH, 30 μM FAD, 1 μg of purified YUCCA, and 1–100 μM inhibitor. The inhibitor is dissolved in DMSO at 100 times the target concentration, and 2 μL is added to the reaction mix. The reaction is started by adding a mixture of IPyA and inhibitor and then incubated at 30 °C for 5 min, and the reaction is stopped by the addition of 10 μL of 1 M HCl.

2. Reaction products (IAA) are analyzed by high-pressure liquid chromatography (HPLC) system (HITACHI) with COSMOSIL 5C18-MS-II (Nacalai Tesque) with fluorescence detection ($\lambda_{\text{ex}}/\lambda_{\text{em}} = 280/355 \text{ nm}$). The sample is eluted at a flow rate of 1.0 mL/min with 0.1% acetic acid/water (solvent A) and 0.1% acetic acid/methanol (solvent B) by using 50% solvent B (0–2 min), a gradient from 50% to 75% solvent B (2–12 min), 98% solvent B (12–14 min), and 50% solvent B (13–20 min). The IAA elutes around 4.3 min and IPyA elutes broadly thereafter. Because IPyA is unstable and is nonenzymatically converted to IAA, it is important to always prepare a control without YUCCA enzyme and subtract the amount of nonenzymatically produced IAA from the other measured IAA amounts.

3.4 Inhibitor Treatment for Arabidopsis Seedlings

1. Sterilize Arabidopsis seeds with 1 mL of 70% ethanol (EtOH) with vortex mixing for 5 min twice and then 1 mL of sterilized ion exchange water containing 1.5% sodium hypochlorite solution and 0.05% of Tween-20 with vortex mixing for 5 min twice. Rinse with sterilized ion exchange water ten times and then suspend in sterilized 1 mL of 0.1% agar twice.
2. Sow sterilized Arabidopsis seeds on sterilized solid half-strength Murashige and Skoog ($\frac{1}{2}$ MS) media containing 1% sucrose and 0.8% agar (pH 5.8) plate and incubate at 22 °C for 4 days under continuous light in BioTRON (light setting: pattern 2).
3. Transfer 25 Arabidopsis seedlings to 5 mL of sterilized liquid $\frac{1}{2}$ MS media containing 1% sucrose in a centrifuge tube (50 mL) and pre-incubation rotational shaking (120 rpm) with a DOUBLE SHAKER NR-30 shaker for 1 day under the same conditions in BioTRON (*see Note 2*).
4. Add the inhibitor dissolved in 5 μL of DMSO to liquid $\frac{1}{2}$ MS medium so that the inhibitor is finally at the appropriate concentration and then continue shaking for 3 h (*see Note 3*).
5. Transfer Arabidopsis seedlings to a 50-mL centrifuge tube, which has packed with the Kimwipe at the bottom, and centrifugation for 30 s at $1250 \times g$ for dehydration of the seedlings. The procedures from **steps 2 to 5** are illustrated in Fig. 2.

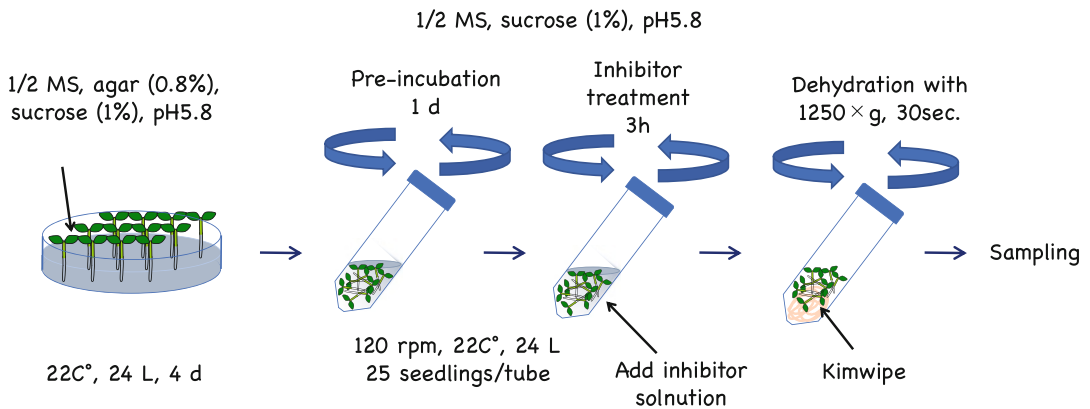


Fig. 2 Growth and inhibitor treatment of *Arabidopsis* seedlings

6. Transfer *Arabidopsis* seedlings to a 2-mL screw cap conical tube containing zirconia beads (*see Note 4*).
7. Freeze samples in liquid nitrogen after weighing. Store at -80°C until analyses.

3.5 Inhibitor Treatment for Rice Seedlings

1. Wash and sterilize rice seeds with a series of treatments with 30 mL of sterilized ion exchange water with shaking twice in a centrifuge tube (50 mL), 30 mL of 70% EtOH with shaking for 1 min once, 30 mL of sterilized ion exchange water with shaking for four times, and 40 mL of sterilized ion exchange water containing 50% sodium hypochlorite solution with mixing for 25 min once.
2. Transfer rice seedlings to a 500-mL beaker and rinse with 200 mL of sterilized ion exchange water five times and then immerse 300 mL of sterilized ion exchange water for 1 h three times.
3. Transfer rice seedling to large Petri dish (22 cm in diameter, 6 cm height) and soak with sterilized ion exchange water and then incubate at 25°C for 3 days under continuous light in BioTRON (light setting: pattern 4) for germination.
4. Transplant rice seedlings to 0.8% agar plate with the young leaf sheath on top and incubate for 2 days under the same conditions in BioTRON (*see Note 5*).
5. Transfer 20 rice seedlings to 30 mL of sterilized ion exchange water in centrifuge tubes (50 mL) and pre-incubation rotational shaking (60 rpm) with a MULTI SHAKER MMS-3010 shaker for 1 day under the same conditions in BioTRON.
6. Add the inhibitor dissolved in DMSO (15 μL) to sterilized ion exchange water so that the inhibitor is finally at the appropriate concentration; continue shaking for 3 h (*see Note 6*).

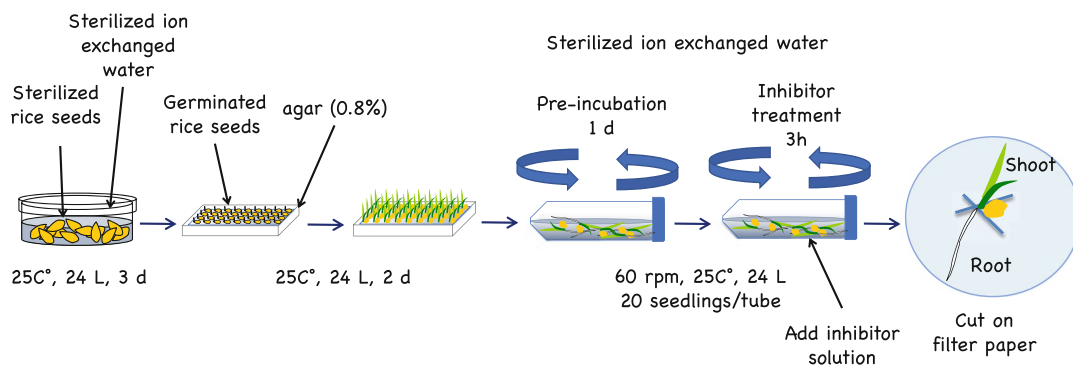


Fig. 3 Growth and inhibitor treatment of rice seedlings

7. Cut into shoot, root, and seed with a scalpel on filter paper, and then place them in 2-mL screw cap conical tubes containing stainless beads (*see Note 7*). The procedures from **steps 2 to 7** are illustrated in **Fig. 3**.
8. Freeze samples in liquid nitrogen after weighing. Store at -80°C until analyses.

3.6 Analyzing IAA-Related Compounds except for IPyA and IAAla

1. Homogenize the frozen plant samples (fresh weight (FW), ~ 130 mg) using a Multi-beads shocker[®] (*see Note 8*).
2. For analyses of IAA-related compounds except for IPyA and IAAla, add $[^2\text{H}_5]$ -Trp (16 ng/mg FW), $[^2\text{H}_4]$ -TAM (80 pg/mg FW), $[^2\text{H}_5]$ -IAM (24 pg/mg FW), and $[^2\text{H}_5]$ -IAA (40 pg/mg FW) as internal standards and dissolve in 800 μL of 50% acetonitrile (MeCN) on ice, and then mix by vortexing.
3. Add 260 mg of QuEChERS extraction mixture powder and mix it by vortexing, followed by partition by centrifugation at $16,100 \times g$ for 10 min at 4°C (*see Note 9*).
4. Recover the supernatant of the MeCN layer (~ 400 μL) and adjust to 80% MeCN by adding 100 μL of ultrapure water, load on a conditioned OASIS HLB SPE cartridge column, and elute with 500 μL of 80% methanol (MeOH).
5. Combine the eluates and evaporate to dryness in vacuo, and then dissolve in ultrapure water (500 μL) with vortex mixing and load on a conditioned OASIS MCX SPE cartridge.
6. Wash the column with ultrapure water (500 μL) and elute using 500 μL of MeOH; accordingly, total IAA, IAM, IAox, oxIAA, IAAla, IALeu, IAGlu, and IAAsp are obtained (MeOH Fr.).
7. Elute with 500 μL of MeOH containing 1 M NH_4OH ; accordingly, total Trp and TAM are obtained ($\text{NH}_4\text{OH}/\text{MeOH}$ Fr.).

8. Evaporate each fraction to dryness in vacuo and dissolve in 5% MeCN (90 μ L). For the total Trp analyses, further dilute the 1 M $\text{NH}_4\text{OH}/\text{MeOH}$ fraction to 300-fold with 5% MeCN (1/300 $\text{NH}_4\text{OH}/\text{MeOH}$ Fr.).
9. Filtrate each fraction of 5% MeCN solution with a 0.22- μ m filter.
10. Fifty microliters of each fraction (MeOH, 1 M $\text{NH}_4\text{OH}/\text{MeOH}$, and 1/300 $\text{NH}_4\text{OH}/\text{MeOH}$ Fr.) is analyzed by UPLC-ESI-MS/MS in MRM mode.
11. Injected samples are eluted using a 15-min gradient of 0.05% formic acid in ultrapure water (A) and 0.05% formic acid in MeCN (B) at a flow rate of 0.2 mL/min. The following gradient is used: 5% B (0–5 min), 5–85% B (5–9 min), 85–100% B (8–9 min), and 100% B (9–15 min). Then, the column is re-equilibrated to the initial conditions (10 min).
12. The compounds are quantified using a standard curve generated from the ion chromatogram response of standards versus internal standards (*see* **Note 10**).

3.7 Analyses for IPyA and IAAlD

1. Frozen plant samples are homogenized in liquid nitrogen and extracted using a QuEChERS method without adding internal standards, as described in Subheading 3.6 (steps 1–3).
2. Recover the supernatant of the MeCN layer (~400 μ L) to a screw cap tube (1.5 mL), and then add 1 mL of 50% methanol solution containing 200 μ L of 350 mM imidazole (pH 7.0), 0.2 mg sodium diethyldithiocarbamate, and 0.1 mg 2,6-di-*tert*-butyl-4-methylphenol on ice.
3. Add 100 μ L of 2% methoxyamine-HCl in pyridine (*see* **Note 11**) and lightly stir up and down (app. 20 times), followed by incubation for 30 min at 60 °C for methoximation in the dark.
4. The reaction mixture is evaporated to dryness in vacuo, then dissolved in ultrapure water (500 μ L) with vortex mixing, and loaded on a conditioned OASIS HLB SPE cartridge column.
5. Wash the column with ultrapure water (500 μ L) and elute with 500 μ L of 80% MeOH.
6. The eluates are evaporated to dryness in vacuo, then dissolved in ultrapure water (500 μ L) with vortex mixing, and loaded on a conditioned OASIS MCX SPE cartridge.
7. Wash the column with ultrapure water (500 μ L) and then IPyA-methoxime and IAAlD-methoxime (containing IAox-methoxime) are eluted with 500 μ L of MeOH (IPyA/IAAlD-methoxime fraction).

8. IPyA/IAAld-methoxime fraction is evaporated to dryness in vacuo, dissolved in 5% MeCN (90 μ L), and then filtrated using a 0.22- μ m filter.
9. Fifty microliters of the IPyA/IAAld-methoxime fraction is analyzed by UPLC-ESI-MS/MS in MRM mode as described above using the same conditions (*see* Subheading 3.6, **step 11**).
10. The contents of IPyA and IAAld are determined from the response of MRM transition intensity obtained by the precursor and the appropriate production of the respective methoxime compounds (*see* **Note 12**).

4 Notes

1. Since IPyA is unstable, dissolve in ethanol and store at -20°C or less when making stock, and use it as soon as possible (at least in a few months).
2. Insert the centrifuge tube diagonally (app. $60\text{--}70^{\circ}$) into the spring shaker table.
3. The amount of DMSO is less than 0.1% of the culture medium to avoid growth inhibition by DMSO. Without inhibitor treatment, add an appropriate amount of DMSO as mock treatment.
4. Weigh 2-mL screw cap conical tubes containing 3 zirconia beads before sampling Arabidopsis seedlings.
5. To prevent drying, the agar tray is put in a container wrapped with plastic film with a small amount of water.
6. Lay the centrifuge tube sideways on the sheet shaker table.
7. Weigh 2-mL screw cap conical tubes containing stainless 3 beads before frozen in liquid nitrogen.
8. Homogenization conditions when using Multi-beads shocker[®] are summarized in Table 2. The samples can also be subjected to auxin-responsive marker gene expression analysis using qRT-PCR after RNA extraction.
9. Constitution of QuEChERS extraction mixture powder: NaCl (40 mg), MgSO₄ anhydrous (160 mg), sodium citrate tribasic dehydrate (40 mg), and sodium dihydrogen citrate (20 mg). Preparation of QuEChERS extraction mixture powder stock: homogenize NaCl (3.0 g) and sodium citrate tribasic dehydrate (3.0 g) in a centrifuge tube (50 mL) with metal cone (MC-1315, YASUI KIKAI, Japan) using a Multi-beads shocker[®] at 1800 rpm for 90 s twice. Add MgSO₄ anhydrous (12.0 g) and sodium dihydrogen citrate (1.5 g) and homogenize at 1800 rpm for 90 s twice.

Table 2
Conditions for Multi-beads shocker[®] homogenization

Plant sample	Beads				Pattern for Multi-beads shocker [®]				
	Tube	Material	Diameter	Number	Speed meter (rpm)	On time (s)	Off time (s)	Cycle (times)	Pattern repeat times ^a
Arabidopsis seedlings	2mL ^b	zirconia	4 mm	3	1800	90	0	1	0
Rice seedlings	2mL ^b	stainless	4 mm	3	1500	15	3	5	3

^aBetween pattern repeat, sample were re-frozen in liquid nitrogen

^bScrew cap conical tube: ST-0250 (YASUI KIKAI)

10. Standard curve generated from the ion chromatogram response of standards versus internal standards: Trp/[²H₅]-Trp (0.05–2 ng/0.5 ng, $R^2 = 0.9997$), IAM/[²H₅]-IAM (12.5–400 pg/500 pg, $R^2 = 0.9987$), TAM/[²H₄]-TAM (12.5–500 pg/500 pg, $R^2 = 0.9997$), IAOx/[²H₅]-IAA (25–400 pg/500 pg, $R^2 = 0.9998$), IAA/[²H₅]-IAA (12.5–400 pg/500 pg, $R^2 = 0.9997$), oxIAA/[²H₅]-IAA (12.5–400 pg/500 pg, $R^2 = 0.9994$), IAAla/[²H₅]-IAA (12.5–400 pg/500 pg, $R^2 = 0.9984$), IALeu/[²H₅]-IAA (12.5–400 pg/500 pg, $R^2 = 0.9997$), IAAsp/[²H₅]-IAA (12.5–400 pg/500 pg, $R^2 = 0.9978$), and IAGlu/[²H₅]-IAA (12.5–400 pg/500 pg, $R^2 = 0.9999$). The retention times, MS/MS transitions, and MRM conditions of the cone voltage and collision energy are summarized in Table 3.
11. 2% methoxyamine-HCl in pyridine is commercially available as MOX[™] Reagent (Thermo Scientific, USA); however, it can be prepared from methoxyamine-HCl and pyridine and stored at room temperature.
12. For the endogenous amounts of IPyA and IAAla, labeled IPyA and IAAla are not used as internal standards in this protocol. Thus, the contents of these compounds are roughly estimated. If quantitative analysis is required, the absolute calibration curve method should be conducted. Because part of IAOx is methoxylated to the same structure as methoxime of IAAla, the amount of IAAla must be corrected, taking the effect of endogenous IAOx into account in Arabidopsis.

Table 3
Diagnostic MRM transitions and optimized instrument settings (cone voltage and collision Energy, CE) and retention times of authentic compounds of the UPLC-MS/MS method

Compound	Ion mode	MRM transition	Cone/CE (V)	Retention time ^a (min)
Trp	EI+	205.1 > 188.1	20/9	5.84 ± 0.02
[² H ₅]-Trp	EI+	210.3 > 192.2	20/9	5.82 ± 0.02
IAM	EI+	175.5 > 129.8	25/14	7.12 ± 0.01
[² H ₅]-IAM	EI+	180.2 > 134.1	25/15	7.07 ± 0.00
TAM	EI+	161.1 > 144.1	15/9	6.43 ± 0.06
[² H ₄]-TAM	EI+	165.2 > 148.1	20/12	6.42 ± 0.02
<i>cis</i> -IAOx	EI+	175.1 > 158.1	25/15	8.56 ± 0.01
<i>trans</i> -IAOx	EI+	175.1 > 158.1	25/15	8.45 ± 0.01
IAA	EI+	176.1 > 130.1	30/21	8.12 ± 0.01
[² H ₅]-IAA	EI+	181.2 > 134.1	25/15	8.09 ± 0.00
oxIAA	EI-	190.0 > 146.0	25/12	6.91 ± 0.00
IAAIa	EI+	247.1 > 129.8	25/24	7.56 ± 0.00
IALeu	EI-	287.1 > 129.8	35/18	8.93 ± 0.01
IAAsp	EI-	289.0 > 131.8	30/15	6.98 ± 0.01
IAGlu	EI+	305.1 > 129.8	25/24	7.01 ± 0.01
IPyA-methoxime	EI+	233.2 > 130.2	20/20	9.08 ± 0.01
IAAId-methoxime	EI+	189.1 > 129.8	25/27	10.13 ± 0.01

^aMeans ± SD (*n* = 6)

References

- De Rybel B, Audenaert D, Beeckman T, Kepinski S (2009) The past, present, and future of chemical biology in auxin research. *ACS Chem Biol* 4:987–998. <https://doi.org/10.1021/cb9001624>
- Ma Q, Robert S (2014) Auxin biology revealed by small molecules. *Physiol Plant* 151:25–42. <https://doi.org/10.1111/ppl.12128>
- Hayashi K, Joshua N, Hirose M et al (2012) Rational design of an Auxin antagonist of the SCF^{TIR1} auxin receptor complex. *ACS Chem Biol* 7:590–598. <https://doi.org/10.1021/cb200404c>
- Dhonukshe P, Grigoriev I, Fischer R et al (2008) Auxin transport inhibitors impair vesicle motility and actin cytoskeleton dynamics in diverse eukaryotes. *Proc Natl Acad Sci U S A* 105:4489–4494. <https://doi.org/10.1073/pnas>
- Zhu J, Bailly A, Zwiewka M et al (2016) TWISTED DWARF1 mediates the action of auxin transport inhibitors on actin cytoskeleton dynamics. *Plant Cell* 28:930–948. <https://doi.org/10.1105/tpc.15.00726>
- Stepanova AN, Robertson-Hoyt J, Yun J et al (2008) TAA1-mediated auxin biosynthesis is essential for hormone crosstalk and plant development. *Cell* 133:177–191. <https://doi.org/10.1016/j.cell.2008.01.047>
- Tao Y, Ferrer J-L, Ljung K et al (2008) Rapid synthesis of auxin via a new tryptophan-dependent pathway is required for shade avoidance in plants. *Cell* 133:164–176. <https://doi.org/10.1016/j.cell.2008.01.049>

8. Soeno K, Goda H, Ishii T et al (2010) Auxin biosynthesis inhibitors, identified by a genomics-based approach, provide insights into auxin biosynthesis. *Plant Cell Physiol* 51:524–536. <https://doi.org/10.1093/pcp/pcq032>
9. Mashiguchi K, Tanaka K, Sakai T et al (2011) The main auxin biosynthesis pathway in Arabidopsis. *Proc Natl Acad Sci U S A* 108:18512–18517. <https://doi.org/10.1073/pnas.1108434108>
10. He W, Brumos J, Li H et al (2011) A small-molecule screen identifies L-kynurenine as a competitive inhibitor of TAA1/TAR activity in ethylene-directed auxin biosynthesis and root growth in Arabidopsis. *Plant Cell* 23:3944–3960. <https://doi.org/10.1105/tpc.111.089029>
11. Narukawa-Nara M, Nakamura A, Kikuzato K et al (2016) Aminoxy-naphthylpropionic acid and its derivatives are inhibitors of auxin biosynthesis targeting l-tryptophan aminotransferase: structure–activity relationships. *Plant J* 87:245–257. <https://doi.org/10.1105/tpc.111.089029>
12. Nishimura T, Hayashi K, Suzuki H et al (2014) Yucasin is a potent inhibitor of YUCCA, a key enzyme in auxin biosynthesis. *Plant J* 77:352–366. <https://doi.org/10.1105/tpc.111.089029>
13. Tsugafune S, Mashiguchi K, Fukui K et al (2017) Yucasin DF, a potent and persistent inhibitor of auxin biosynthesis in plants. *Sci Rep* 7:13992. <https://doi.org/10.1105/tpc.111.089029>
14. Kakei Y, Yamazaki C, Suzuki M et al (2015) Small-molecule auxin inhibitors that target YUCCA are powerful tools for studying auxin function. *Plant J* 84:827–837. <https://doi.org/10.1111/tpj.13032>
15. Doyle SM, Robert S (2014) Using a reverse genetics approach to investigate small-molecule activity. *Methods Mol Biol* 1056:51–62. https://doi.org/10.1007/978-1-62703-592-7_6
16. Bower PJ, Brown HM, Purves WK (1978) Cucumber seedling indoleacetaldehyde oxidase. *Plant Physiol* 61:107–110. https://doi.org/10.1007/978-1-62703-592-7_6
17. Sugawara S, Hishiyama S, Jikumaru Y et al (2009) Biochemical analyses of indole-3-acetaldoxime-dependent auxin biosynthesis in Arabidopsis. *Proc Natl Acad Sci U S A* 106:5430–5435. https://doi.org/10.1007/978-1-62703-592-7_6
18. Takase S, Uchida I, Tanaka H, Aoki H (1986) Synthesis of debromo-8,8a-dihydroflustramine C1, a model synthesis toward amauromine. *Tetrahedron* 42:5879–5886. [https://doi.org/10.1016/S0040-4020\(01\)96069-7](https://doi.org/10.1016/S0040-4020(01)96069-7)

Part IV

Target Identification and Confirmation Approaches



Target Profiling of an Anticancer Drug Curcumin by an In Situ Chemical Proteomics Approach

Dan-dan Liu, Chang Zou, Jianbin Zhang, Peng Gao, Yongping Zhu, Yuqing Meng, Nan Ma, Ming Lv, Chengchao Xu, Qingsong Lin, and Jigang Wang

Abstract

Interdisciplinary chemical proteomics approaches have been widely applied to the identification of specific targets of bioactive small molecules or drugs. In this chapter, we describe the application of a cell-permeable activity-based curcumin probe (Cur-P) with an alkyne moiety to detect and identify specific binding targets of curcumin in HCT116 colon cancer cells. Through click chemistry, a fluorescent tag or a biotin tag is attached to the probe-modified curcumin targets for visualization or affinity purification followed by mass spectrometric identification. A quantitative proteomics approach of isobaric tags for relative and absolute quantification (iTRAQ)TM is applied to distinguish specific curcumin targets from nonspecific binding proteins.

Key words Chemical proteomics, Curcumin, Activity-Based probe, Target identification, Mass spectrometry

1 Introduction

Chemical proteomics approaches, such as activity-based protein profiling (ABPP), are compound-centric approaches, which combine drug affinity chromatography with mass spectrometry (MS). They have been established as powerful and prevalent tools for the analysis of specific subcellular proteomes [1, 2]. They have been widely used to determinate protein-binding profiles and reveal mechanisms of small-molecule drugs and detect active sites and sites of posttranslational modification of various proteins [3–6]. ABPP employs synthesized small-molecular probes containing biotin, fluorescent tags such as rhodamine, or clickable tags such as alkyne to covalently attack a distinct class of proteins. Coupled with

Dan-dan Liu, Chang Zou and Jianbin Zhang contributed equally to this work.

LC-MS/MS analysis, it has been applied to the detection of interactions of small molecules with proteins, enzyme activity profiling, drug discovery, and target validation [7–9]. Various quantitative proteomics approaches have been established to determine the abundance of proteins. These include the metabolic labeling approaches such as the stable isotope labeling by amino acids in cell culture (SILAC), chemical labeling approaches such as ICAT, tandem mass tag (TMT), bio-orthogonal noncanonical amino acid tagging (BONCAT), and isobaric tag for relative and absolute quantitation (iTRAQ), as well as label-free approaches [10, 11]. Quantitative proteomics approaches have been applied in conjunction with chemical proteomics studies for improved specificity of target identification, such as the profiling of *de novo* protein synthesis during starvation-mediated autophagy [12, 13], target identification of natural and traditional medicines [10], and exploring the specificity of protein–protein or protein–drug interactions [14–16].

The detailed protocol for target identification that we describe in this chapter is based on *in situ* proteomic profiling of curcumin targets in HCT116 colon cancer cell line [17]. Briefly, a cell-permeable curcumin probe (Cur-P) with an alkyne moiety, which fully retained the curcumin activity, was synthesized and used to react with the protein targets in live cells, and click chemistry was applied to ligate biotin tags to the protein targets through the alkyne moiety for affinity enrichment and target identification and quantitation, or to ligate a fluorescent dye to the target proteins for visualization *in situ*. This protocol mainly includes two parts: (1) Unlike the bulky biotin tag, the tiny alkyne group has little effect on the plasma membrane penetration ability of curcumin; thus, the Cur-P can directly target the proteins *in vivo*. The biotin tag conjugated to the probe by click chemistry after cell lysis. The proteins were then enriched and purified with the streptavidin beads. Subsequently, the captured protein targets of curcumin were digested by trypsin and identified with mass spectrometry and bioinformatics tools. (2) A quantitative proteomics approach of isobaric tags for relative and absolute quantification (iTRAQ)TM was applied to distinguish specific binding targets from nonspecific binding proteins (including endogenously biotinylated proteins), thus enhancing the reliability of the curcumin targets identified.

2 Materials

2.1 Cell Culture and Extraction of Cellular Proteins

1. HCT116 colon cancer cell line.
2. Dulbecco's modified Eagle's medium (DMEM, containing 4500 mg/L D-glucose, without L-glutamine, sodium pyruvate, L-methionine, and L-cystine). Store at 4 °C.

3. L-Glutamine.
4. Heat inactivated fetal bovine serum (FBS). Store at $-20\text{ }^{\circ}\text{C}$.
5. $1\times$ antibiotic/antimycotic.
6. Cell incubator, $37\text{ }^{\circ}\text{C}$, 5% (v/v) CO_2 .
7. Corning six-well microplates.
8. Thermo Scientific Nunc Cell Culture/Petri Dishes 150 mm Dish.
9. $1\times$ PBS, pH 7.2–7.4. Store at $4\text{ }^{\circ}\text{C}$.
10. Dimethyl sulfoxide (DMSO).
11. Trypsin ($10\text{ ng}/\mu\text{L}$; sequencing grade). Store at $-20\text{ }^{\circ}\text{C}$ for up to 1 month. Avoid repeated freeze–thaw cycles.
12. Centrifuge tubes with screw caps, 15 mL.
13. Refrigerated centrifuge.
14. Ultrasonic water bath cleaner.
15. Refrigerators, $4\text{ }^{\circ}\text{C}$.
16. Freezers, $-20\text{ }^{\circ}\text{C}$ and $-80\text{ }^{\circ}\text{C}$.
17. Biological safety level 2 tissue culture hood.
18. Water bath, $37\text{ }^{\circ}\text{C}$.
19. Increasing concentrations of Cur-P ($5\text{--}60\text{ }\mu\text{M}$) in 2 mL of medium.

2.2 Click Chemistry

1. Coomassie Plus Assay Kit.
2. $1\times$ PBS, pH 7.2–7.4. Store at $4\text{ }^{\circ}\text{C}$.
3. Centrifuge tubes with screw caps, 15 mL.
4. Rhodamine B-azide.
5. Biotin-azide.
6. Rhodamine B-alkyne.
7. Tris (2-carboxyethyl) phosphine hydrochloride, $\geq 98\%$ purity (TCEP).
8. Tris [(1-benzyl-1*H*-1, 2, 3-triazol-4-yl) methyl] amine (TBTA).
9. Copper sulfate, $\geq 99.99\%$ purity (CuSO_4).
10. Dimethyl sulfoxide (DMSO).
11. Refrigerators, $4\text{ }^{\circ}\text{C}$.
12. Freezers, $-20\text{ }^{\circ}\text{C}$ and $-80\text{ }^{\circ}\text{C}$.
13. Vortex mixer.
14. Thermo shaker.
15. Acetone.
16. Refrigerated centrifuge.

17. Sodium dodecyl sulfate (SDS). Prepare SDS stock: 10% (wt/vol) SDS solution in water. This solution can be stored at room temperature for up to 1 year.
18. Ultrasonic water bath cleaner.
19. Water bath, 80–90 °C.

2.3 SDS-PAGE and Fluorescence Scanning

1. 4–20% SDS-PAGE gel.
2. Typhoon 9410 laser scanner.
3. Image Quant software.

2.4 Protein Affinity Enrichment Using Streptavidin Beads

1. Streptavidin beads.
2. 1× PBS, pH 7.2–7.4. Store at 4 °C.
3. Centrifuge tubes with screw caps, 15 mL.
4. Refrigerated centrifuge.
5. Sodium dodecyl sulfate (SDS).
6. Urea. Urea buffer should be prepared fresh: 6 M urea, 25 mM ammonium bicarbonate buffer.
7. Ultrapure water. Unless otherwise specified, all reagents are prepared with 18.2 MΩ ultrapure water.
8. Triethylammonium bicarbonate buffer, 1 M (TEAB).
9. Tris (2-carboxyethyl) phosphine hydrochloride, ≥98% purity (TCEP).
10. Vortex mixer.
11. Thermo shaker.
12. Methyl methanethiosulfonate (MMTS).
13. Trypsin (sequencing grade). Store at –20 °C for up to 1 month. Avoid repeated freeze–thaw cycle. Trypsin solution: 10 ng/μL.
14. Parafilm.
15. MicroSpin columns.
16. Freezer, –80 °C.

2.5 iTRAQ Labeling of the Tryptic Peptides

1. SpeedVac.
2. iTRAQ Method Development Kit.
3. Freezer, –80 °C.
4. Triethylammonium bicarbonate buffer, 1 M (TEAB).
5. Vortex mixer.
6. Sodium hydroxide (NaOH).
7. Isopropanol.

8. Phosphoric acid.
9. Chemical fume hood.
10. Centrifuge tubes with screw caps, 15 mL.

2.6 Strong Cation Exchange (SCX) Chromatography to Clean Up Samples

1. Refrigerated centrifuge.
2. 50-mL Falcon tube.
3. Cation Exchange Buffer Pack, containing individual 100-mL bottles of loading buffer, elution buffer, cleaning buffer, and storage buffer. The Buffer Pack also includes one 0.2-mL cation exchange cartridge. All SCX buffers should be stored at 4 °C.
4. Chemical fume hood.
5. Phosphoric acid.
6. Microcentrifuge tubes, 1.5 mL.
7. Shaker for microcentrifuge tubes with temperature control.
8. Refrigerators, 4 °C.
9. Cation exchange column.

2.7 Desalting of Labeled Samples by C18 Column

1. C18 Sep-Pak column.
2. Centrifuge tubes with screw caps, 15 mL.
3. C18 buffer A: 98% H₂O, 2% ACN, 0.05% FA. Acetonitrile (ACN). Formic acid (FA). The solution is prepared directly before use.
4. Elution buffer E1: 50% ACN, 50% H₂O; elution buffer E2: 75% ACN, 25% H₂O. The solution is prepared directly before use.
5. 5-mL syringe.
6. 50-mL Falcon tube.
7. Freezer, -80 °C.
8. Parafilm.
9. Lyophilizer machine.
10. Mobile phase A/weak wash: 2% ACN, 0.1% FA. This solution can be stored at room temperature for up to 1 month.
11. 2-mL Eppendorf tube.
12. SpeedVac.

2.8 Nano-LC Electrospray Ionization MS

1. C18 buffer A: 98% H₂O, 2% ACN, 0.05% FA.
2. Eksigent nano-liquid chromatography (nano-LC)-Ultra system coupled to the ChiPLC-nanoflex system (Eksigent). The trap (sizes: 200 μm × 0.5 mm) and analytical columns (sizes: 75 μm × 150 mm) are packed with ChromXP C18-CL, 3 μm.

3. Mobile phase B/strong wash: 98% ACN, 0.1% FA. This solution can be stored at room temperature for up to 1 month.
4. TripleTOF 5600 system (AB SCIEX, Foster City, CA) (*see Note 1*).

2.9 Protein Identification and iTRAQ Quantification

1. ProteinPilot™ Software 4.5 (AB SCIEX) (*see Note 2*).
2. SwissProt (2013_09, total 540958 sequences) as the database.

3 Method

3.1 Profiling of Curcumin-Specific Target Proteins with Fluorescence Labeling

3.1.1 Cell Culture and Extraction of Cellular Proteins

1. Culture HCT116 cells in 2 mL of modified McCoy's 5A medium with L-glutamine supplemented with 10% FBS, and 1× antibiotic/antimycotic at 37 °C in the presence of 5% (v/v) CO₂ to achieve 80–90% confluence in six-well plates.
2. Discard the original medium and wash the cells with 1× PBS three times.
3. Treat HCT 116 cells with increasing concentrations of activity-based curcumin probe (Cur-P) (5–60 μM) in 2 mL of medium and continue to incubate at 37 °C with 5% CO₂ for 4 h. For control treatment, use 2 mL of medium containing 1% DMSO instead.
4. Following treatment, discard the medium, and wash the cells three times with 1× PBS and then add trypsin to detach the cells from the plate. Then, collect the cell suspension into a 15-mL centrifugal tube.
5. Pellet the cells at 1200 × *g* in a centrifuge. Discard the supernatant and resuspend the cells in 100 μL of 1× PBS.
6. Sonicate the cell suspension with 1-s pulses for 60 s to lyse the cells, and then pellet the cells in a centrifuge (10,000 × *g*, 45 min) to remove the insoluble fraction. The protein-containing supernatant can be stored at –80 °C until use.

3.1.2 Click Chemistry Tagging with Rhodamine B-Azide

1. Quantify the protein concentration for each sample from [3.1.1 step 6](#) (e.g., Bradford assay). Conduct fluorescence labeling subsequently with an equal amount (50 μg) of extracted proteins for each sample.
2. Top up the volume of each sample to 2 mL with 1× PBS in a 5-mL centrifuge tube.
3. The following chemicals are needed to prepare the click reaction: rhodamine B-azide (10 μM), TCEP (1 mM), TBTA (100 μM), and CuSO₄ (1 mM) (*see Note 3*).

4. Successively add 20 μL of rhodamine B-azide, 20 μL of TCEP, 20 μL of TBTA, and 20 μL of CuSO_4 to each sample and vortex, respectively.
5. Incubate the prepared samples at room temperature and protect them from light for 2 h with constant gentle mixing.
6. Transfer each sample to a 15-mL centrifuge tube and top up with precooled (-20°C) acetone to a total volume of 10 mL to precipitate proteins and remove free rhodamine B-azide from the mixture.
7. Incubate the samples at -20°C for 4 h, and then centrifuge (30 min, $4000 \times g$, 4°C) to pellet the proteins.
8. Remove the supernatant carefully without disturbing the protein pellet, and then moderately air-dry the pellet to remove the remaining acetone at room temperature (*see Note 4*).
9. Dissolve the pellets with 100 μL of $1 \times$ SDS loading buffer and sonicate at 0.5-s pulses for 60 s. Heat the samples for 5 min at $80\text{--}90^\circ\text{C}$ to ensure complete protein dissolution.

3.1.3 SDS-PAGE and Fluorescence Scanning

1. Separate 50 μL of the sample with 4–20% gradient SDS-PAGE gel.
2. Following one-dimensional gel separation, use Typhoon 9410 laser scanner (GE Healthcare) to obtain the gel images, and analyze the images by Image Quant software. Normalize the fluorescence contrast against the DMSO control to minimize the background.

3.2 Identifying the Targets of Curcumin with iTRAQ-Based Quantitative Chemical Proteomics Approach

3.2.1 Cell Culture and Extraction of Cell Protein

1. Culture HCT116 cells in 20 mL of DMEM (10% FBS, 5% CO_2 incubation at 37°C) media to achieve 80% confluence in 150-mm culture dishes.
2. Discard the original media and wash the cells with $1 \times$ PBS three times.
3. Treat HCT 116 cells with Cur-P (30 μM) in 20 mL of media with a final DMSO concentration of 1% and continue to incubate at 37°C with 5% CO_2 for 4 h. For control treatment, use 20 mL of media containing 1% DMSO.
4. Following the treatment, discard the media, and wash the cells three times with $1 \times$ PBS and then add trypsin to detach the cells from the plate. Then, collect the cell suspension into a 15-mL centrifuge tube.
5. Pellet the cells at $1200 \times g$ in a centrifuge. Discard the supernatant and resuspend the cells in 100 μL of $1 \times$ PBS.
6. Sonicate the cells suspension with 1-s pulses for 60 s to lyse the cells, and then pellet the cells in a centrifuge ($10,000 \times g$, 45 min) to remove the insoluble fraction. Store the protein-containing supernatant at -80°C until use.

3.2.2 *Click Chemistry Tagging with Biotin-Azide Tag*

1. Quantify the protein concentration for each sample from **3.2.1 step 6** (e.g., Bradford assay). Conduct subsequent click chemistry for biotin tagging with equal amounts (4 mg) of extracted proteins for each sample (two Cur-P-treated and two DMSO-treated samples).
2. Top up the volume of each sample to 2 mL with 1× PBS in a 5-mL centrifuge tube.
3. Need the following chemicals to prepare the click reaction: biotin-azide (10 μM), TCEP (1 mM), TBTA (100 μM), and CuSO₄ (1 mM) (*see Note 3*).
4. Successively add 20 μL of biotin-azide, 20 μL of TCEP, 20 μL of TBTA, and 20 μL of CuSO₄ to each sample and vortex, respectively.
5. Incubate the prepared samples at room temperature and protect the samples from light for 4 h with constant gentle mixing.
6. Transfer each sample to a 15-mL centrifuge tube and top up with precooled (−20 °C) acetone to a total volume of 10 mL to precipitate proteins and remove free biotin-azide from the mixture.
7. Incubate the samples at −20 °C for 4 h, and then centrifuge (30 min, 4000 × *g*, 4 °C) to pellet the protein.
8. Pour out the supernatant carefully without disturbing the protein pellet. Then, moderately air-dry the pellet to remove the remaining acetone at room temperature (*see Note 4*).
9. Redissolve the pellets with 1 mL of PBS containing 0.1% SDS and sonicate at 0.5-s pulses for 60 s. The samples are heated for 5 min at 80–90 °C to ensure complete protein dissolution.

3.2.3 *Affinity Enrichment Using Streptavidin Beads*

1. Add 40 μL of suspended streptavidin beads and 5 mL of 1× PBS into a 15-mL centrifuge tube to wash the beads, and then centrifuge to collect the beads (700 × *g*, 3 min, room temperature). Repeat the washing step three times (*see Note 5*).
2. Add the protein sample obtained from **3.2.2 step 9** to the washed beads and incubate with gentle rotation using a rotator (room temperature, 2 h).
3. Centrifuge the mixture (700 × *g*, 3 min) and gently pour out the supernatant without disturbing the beads.
4. Add 10 mL of 1% SDS in 1× PBS into the centrifuge tube, and carefully mix for 10 min with a rotator to wash the beads, and then pellet the beads in a centrifuge (700 × *g*, 5 min, room temperature) and discard the supernatant. Repeat the washing procedure three times.
5. Repeat **3.2.3 step 4**, except that 10 mL of 1% SDS in 1× PBS is replaced with 10 mL of 6 M urea to wash the beads three times.

6. **3.2.3 step 4** is repeated, except that 10 mL of 1% SDS in 1× PBS is replaced with 10 mL of 1× PBS to wash the beads three times.
7. Finally, use 10 mL of ultrapure water to wash the beads one time, following the procedure described in **3.2.3 step 4**.
8. Resuspend the beads in 150 μL of 20 mM TEAB and then add 2 μL of TCEP (100 mM stock solution) to each sample.
9. Vortex the mixtures and incubate in a Thermo shaker (50 min, 60 °C, 800 rpm), and then cool the samples at room temperature.
10. For cysteine blocking, add 1 μL of MMTS (200 mM stock solution) to each sample in a chemical fume hood to avoid the toxicity of MMTS. Then, vortex the mixtures and incubate at room temperature for 20 min.
11. Prepare the trypsin solution (10 ng/ μL , sequencing grade modified trypsin) in water in advance.
12. To digest the proteins captured on the beads, add 10 μL (100 ng) of trypsin solution to each sample and incubate at 37 °C for 16 h (*see Note 6*).
13. Separate digested peptides from the beads with a filter spin column and collect sample solutions containing digested peptides.
14. The samples are ready for the subsequent iTRAQ labeling step, or they can be stored at -80 °C until required.

3.2.4 iTRAQ Labeling of the Tryptic Peptides

1. Use a vacuum concentrator (SpeedVac™) device to evaporate the samples obtained from **3.2.3 step 14**. It may take several hours for the samples to dry completely. The dried peptide samples can be stored up to 1 year at -80 °C if not used immediately.
2. Add 30 μL of TEAB (0.5 M) to reconstitute the dried samples, followed by vortexing, rotating, or sonicating to ensure that the solution is clear.
3. Adjust the pH value of the samples to 8 (alkaline) with NaOH to ensure the best labeling efficiency.
4. Prepare the 8-plex iTRAQ reagents (SCIEX; Foster City, CA) according to the manufacturer's instructions. Bring the reagents to room temperature and add 50 μL of isopropanol to each reagent (8-plex).
5. React the digested peptides with respective iTRAQ reagents according to the manufacturer's instructions (2 h, room temperature) for the 8-plex kit. Use iTRAQ reagents 117 and 118 to label negative control samples 1 and 2 and use iTRAQ reagents 119 and 121 to label Cur-P pull-down samples 1 and 2 (*see Note 7*).

6. Pool together the labeled iTRAQ samples in a single new tube and subject to LC-MS/MS analysis to identify and quantify the target proteins.

3.3 LC-MS/MS

Procedures

3.3.1 Strong Cation Exchange (SCX) Chromatography to Clean Up Samples

1. Centrifuge ($14,000 \times g$, 10 min) the pooled iTRAQ sample (from 3.2.4, step 6) and transfer the supernatant to a 50-mL Falcon tube. Dilute the sample about ten times with SCX loading buffer.
2. Adjust the pH of the sample to 2.5–3.3 in a fume hood with phosphoric acid.
3. Inject 1 mL of cleaning buffer into the SCX cartridge to clean and condition the cartridge. Divert the flow-through to waste.
4. Inject 2 mL of loading buffer into the SCX cartridge. Divert the flow-through to waste.
5. Inject the diluted sample from 3.3.1 step 1 slowly (1 drop/s) into the SCX cartridge without introducing any air bubbles and collect the flow-through with a new 50-mL Falcon tube.
6. For removing excess reagents from the SCX cartridge, such as TCEP, SDS, and iTRAQ reagents, inject 1 mL of loading buffer into the SCX cartridge and collect the flow-through into a 50-mL Falcon tube. Keep this flow-through fraction until the MS/MS analysis, verifying the success of the sample loading into the SCX cartridge. Repeat loading if necessary.
7. Inject 500 μ L of elution buffer and gather the eluate in a new 1.5-mL sample tube.
8. Wash the cartridge by injecting 1 mL of cleaning buffer. Divert the flow-through to waste.
9. Inject 2 mL of storage buffer into the SCX cartridge. Divert the flow-through to waste. Disassemble the cartridge and store it at 4 °C.

3.3.2 Desalting of Labeled Samples by C18 Column

1. Transfer the sample collected from 3.3.1 step 7 into a 15-mL centrifuge tube and rinse the original 1.5-mL tube several times with 3–4 mL of C18 buffer A (98% H₂O, 2% ACN, 0.05% FA) and transfer the liquid into the 15-mL centrifuge tube to dilute the sample.
2. Rinse a fresh 5-mL syringe with 100% ACN and connect the syringe to the short end of a Sep-Pak C18 cartridge column. Inject 10 mL of 100% ACN and then 10 mL of C18 buffer A (98% H₂O, 2% ACN, 0.05% FA) into the column to condition the column (*see Note 8*).
3. Inject the diluted sample from 3.3.2 step 1 slowly into the column and collect the flow-through. Reinject the flow-through slowly into the column and collect the secondary flow-through.

4. Inject 5 mL of C18 buffer A into the column to flush the column.
5. Inject 5 mL of elution buffer E1 (50% ACN, 50% H₂O) and 5 mL of elution buffer E2 (75% ACN, 25% H₂O) sequentially into the column and collect the flow-through with a new 50-mL Falcon tube.
6. Add equal volume (10 mL) of Milli-Q water into the 50-mL Falcon tube, swirl the tube gently, and freeze it overnight at -80°C .
7. Substitute the cap of the 50-mL Falcon tube with parafilm, tightly wrap several times, and punch 5–10 holes in the parafilm with a needle gently.
8. Place the tube in a lyophilizer overnight to lyophilize the sample.
9. Add 1.5 mL of mobile phase A (2% ACN, 0.1% FA) to reconstitute the lyophilized sample, and then transfer the sample into a 2-mL Eppendorf tube.
10. The sample can be dried with a SpeedVac concentrator and stored for several months at -80°C if not used immediately.

3.3.3 Nano-LC Electrospray Ionization MS

1. Add 80 μL of C18 buffer A to redissolve the dried sample from **3.3.2, step 10**.
2. Perform the nano-LC separation of iTRAQ-labeled peptides by injecting 4 μL of the reconstituted sample into the LC system. Recommended equipment: Eksigent nano-LC Ultra and ChiPLC-nanoflex (Eksigent, Dublin, CA) system with Trap-Elute configuration. The trap (sizes: 200 $\mu\text{m} \times 0.5$ mm) and analytical columns (sizes: 75 $\mu\text{m} \times 150$ mm) are packed with ChromXP C18-CL, 3 μm (Eksigent, Germany). Other suitable nano-LC systems can also be used instead.
3. For the gradient elution step, prepare mobile phase B (98% ACN, 0.1% FA) in advance. Set a flow rate to 300 nL/min and use the parameters in Table 1 successively for peptide separation.
4. It is recommended that the SCIEX TripleTOF 5600 or 6600 series mass spectrometers are used for the analysis of iTRAQ-labeled peptides. If other types of mass spectrometers are to be used, make sure that the collision energy is optimized to fragment iTRAQ-labeled peptides and the reporter ions of m/z 113–121 can be detected with sufficient sensitivity and resolution. For SCIEX TripleTOF 5600 or 6600 series mass spectrometers, the parameters can be set as follows: For acquiring MS spectra, high-resolution mode ($>30,000$) is used with a mass range of 400–1250 m/z and an accumulation time of 250 ms for each spectrum. For acquiring MS/MS spectra, high-

Table 1
HPLC-MS/MS mobile phase gradient elution condition

Gradient composition of mobile phase B	Time (min)	Purpose
5–12%	20	Gradient elution
12–30%	90	Gradient elution
30–90%	2	Gradient elution
90%	5	Regeneration of the column
90–5%	3	Equilibration
5%	13	Equilibration

sensitivity mode (resolution > 15,000) is used with a mass range of 100–1800 m/z and a dynamic exclusion of 15 s. Rolling collision energy and iTRAQ reagent collision adjustment settings for MS/MS analyses should be turned on. Up to 20 precursors per duty cycle are selected for MS/MS analysis, with an accumulation time of 100 ms for each spectrum.

3.4 Protein Identification and iTRAQ Quantification

1. For protein identification and iTRAQ quantification, the ProteinPilot™ software (SCIEX) is recommended. If using other software, only unique peptides should be used to calculate the iTRAQ ratios of identified proteins. Peptides with incomplete iTRAQ labeling, trypsin miscleavage, or methionine oxidation should be excluded for protein quantification. For the curcumin target identification, SwissProt (2013_09, total 540958 sequences) was used as the database with the following search parameter settings: cysteine alkylation with MMTS; trypsin digestion; TripleTOF 5600; biological modifications. A decoy database search strategy was applied to estimate the false discovery rate (FDR) (*see Note 9*).
2. For data analysis, export the protein summary file into a suitable tool, such as Microsoft Excel.
3. For protein identification, apply the cutoff threshold of unused score > 1.3, corresponding to >95% protein confidence interval, with an FDR of 0.33% (in the case of curcumin target identification).
4. iTRAQ ratios can be calculated for all the treatment vs control samples. For the labeling described in Subheading 3.2.4 (step 5), the ratios will thus be 119:117, 119:118, 121:117, and 121:118. The iTRAQ ratios can then be converted to log₂ values for statistical analysis.
5. A one-sample *t*-test can be performed to check whether the mean of the iTRAQ ratios is truly different from 0 (*see Note 10*).

6. Use $p \leq 0.05$ as the significant cutoff.
7. Get rid of proteins with results of 118/117 or 121/119 iTRAQ ratio ≥ 1.3 or ≤ 0.77 , which are unreliable due to their inconformity between replicates.
8. To improve the reliability and robustness of the data, proteins with only one unique peptide identified could also be removed, or else, further experiments would need to be performed to validate for such identification.
9. Proteins with a mean iTRAQ ratio (treatment over control) of < 2 are excluded (*see Note 11*). The remaining proteins are considered as the true targets of the drug.

4 Notes

1. iTRAQ analysis has been optimized with SCIEX mass spectrometers such as the 4800 and 5800 MALDI-TOF/TOF, as well as the 5600 and 6600 series TripleTOF mass spectrometers. Mass spectrometers from other vendors may also be used, such as the Orbitrap mass spectrometers with the capability of high-energy collision dissociation (HCD). However, optimization of collision energy would be required to ensure effective dissociation of reporter ions.
2. Besides ProteinPilot (all different versions), most of the commonly used search engines (MASCOT, PEAKS, MaxQuant, etc.) are capable of analyzing the iTRAQ dataset.
3. Rhodamine B-azide, Biotin-azide and TBTA reserves are dissolved in DMSO and can be prepared in advance and stored at $-20\text{ }^{\circ}\text{C}$ for 2 months for future use. CuSO_4 and TCEP are dissolved in water and should be freshly prepared.
4. Care should be taken to avoid excessive drying of the sample, which will simplify the following dissolving step.
5. The centrifugation speed should be controlled no more than $1000 \times g$ for the streptavidin beads are fragile.
6. During incubation, the centrifuge tubes are sealed with parafilm to avoid evaporation.
7. Attention should be paid to ensure that the iTRAQ reagents are completely transferred to the samples and that the volumes between the samples are equal.
8. To ensure the binding efficiency of the column, try to avoid the introduction of air bubbles into the column as much as possible during the whole procedure.
9. Do not normalize the iTRAQ ratio. If ProteinPilot is used, background correction is not recommended.

10. In Excel, for each set of four log₂ ratios associated with each protein, create four 0 values and then perform a two-tailed paired *t*-test. This is equivalent to a 1-sample *t*-test.
11. This is the cutoff threshold to distinguish specific drug target from nonspecific binding proteins. This is an arbitrarily defined value, suggesting that the specific drug targets are significantly enriched with the drug analog probe compared to the control.

Acknowledgments

We acknowledge the support from the National Natural Science Foundation of China (81841001) and the Major National Science and Technology Program of China for Innovative Drug (2017ZX09101002-001-001-05).

References

1. Zhu H, Tamura T, Hamachi I (2019) Chemical proteomics for subcellular proteome analysis. *Curr Opin Chem Biol* 48:1–7
2. Activity-Based Protein Profiling, in eLS.1-9
3. Bantscheff M, Scholten A, Heck AJ (2009) Revealing promiscuous drug-target interactions by chemical proteomics. *Drug Discov Today* 14(21–22):1021–1029
4. Rix U, Superti-Furga G (2009) Target profiling of small molecules by chemical proteomics. *Nat Chem Biol* 5(9):616–624
5. Borne AL, Hung T, McCloud RL et al (2019) Deciphering T cell Immunometabolism with activity-based protein profiling. In: Cravatt BF, Hsu K-L, Weerapana E (eds) Activity-based protein profiling. Springer International Publishing, Cham, pp 175–210
6. Bennis HJ, Tate EW, Child MA (2019) Activity-based protein profiling for the study of parasite biology. In: Cravatt BF, Hsu K-L, Weerapana E (eds) Activity-based protein profiling. Springer International Publishing, Cham, pp 155–174
7. Strmiskova M, Desrochers GF, Shaw TA, Powdermill MH, Lafreniere MA, Pezack JP (2016) Chemical methods for probing virus–host proteomic interactions. *ACS Infect Dis* 2(11):773–786
8. Wang S, Tian Y, Wang M, Wang M, Sun G-B, Sun X-B (2018) Advanced activity-based protein profiling application strategies for drug development. *Front Pharmacol* 9:353
9. Wijeratne A, Xiao J, Reutter C, Furness KW, Peon R, Zia-Ebrahimi M, Vacitt RN, Strewlow JM, Van Horn RD, Peng S-B, Barda DA, Engler TA, Chalmers MJ (2018) Chemical proteomic characterization of a covalent KRASG12C inhibitor. *ACS Med Chem Lett* 9(6):557–562
10. Wang J, Gao L, Lee YM, Kalesh KA, Ong YS, Lim J, Jee J-E, Sun H, Lee SS, Hua Z-C, Lin Q (2016) Target identification of natural and traditional medicines with quantitative chemical proteomics approaches. *Pharmacol Ther* 162:10–22
11. Wright MH, Sieber SA (2016) Chemical proteomics approaches for identifying the cellular targets of natural products. *Nat Prod Rep* 33(5):681–708
12. Wang J, Zhang J, Lee Y-M, Koh P-L, Ng S, Bao F, Lin Qm Shen H-M (2016) Quantitative chemical proteomics profiling of de novo protein synthesis during starvation-mediated autophagy. *Autophagy* 12(10):1931–1944
13. Wong YK, Zhang J, Hua Z-C, Lin Q, Shen H-M, Wang J (2017) Recent advances in quantitative and chemical proteomics for autophagy studies. *Autophagy* 13(9):1472–1486
14. West GM, Tucker CL, Xu T, Park SK, Han X, Yates JR, Fitzgerald MC (2010) Quantitative proteomics approach for identifying protein-drug interactions in complex mixtures using protein stability measurements. *Proc Natl Acad Sci U S A* 107(20):9078–9082

15. Tate S, Larsen B, Bonner R, Gingras A-G (2013) Label-free quantitative proteomics trends for protein-protein interactions. *J Proteome* 81:91–101
16. Miguel M, Juan Pablo A (2013) Quantitative proteomics: a strategic ally to map protein interaction networks. *IUBMB Life* 65(1):9–16
17. Wang J, Zhang Z, Zhang C-J, Wong YK, Lim TK, Hua Z-C, Liu B, Tannenbaum SR, Shen H-M, Lin Q (2016) In situ proteomic profiling of curcumin targets in HCT116 colon cancer cell line. *Sci Rep* 6:22146



Label-Free Target Identification and Confirmation Using Thermal Stability Shift Assays

Cecilia Rodriguez-Furlan and Glenn R. Hicks

Abstract

Target identification presents one of the biggest challenges to chemical genomic approaches. In recent years, several methods have been applied for target identification and validation in plant cells. Here, we describe a label-free method based on the thermodynamic stabilization of a protein by interaction with a small-molecule ligand. With increasing temperature, proteins undergo thermal denaturation resulting in irreversible aggregation and precipitation. The binding of a small molecule to its target can enhance protein stability resulting in an increased temperature of aggregation (T_{agg}). This distinct increase in the temperature of aggregation known as a thermal shift can identify a compound–target protein interaction in high-throughput assays or, validate a predicted interaction.

Key words Small-molecule inhibitors, Target protein, Label-Free Target Identification, Thermal Stability Shift Assay

1 Introduction

Chemical genomics has proven invaluable to study dynamic processes in plant cells. In the past few years, a growing number of publications have reported successful target identification for several small molecules [1–4]. In each case, it was essential to detect small molecule-protein interactions to validate potential targets. Several *in vitro* and *in vivo* techniques can assist researchers in the identification of small-molecule protein targets. Amongst the successful approaches are techniques dependent on the tagging of bioactive molecules with moieties for detection or the use of reporter systems [5]. While effective and valuable, these approaches have experimental limitations, such as conformational restrictions, which complicate small-molecule tagging while maintaining biological activities. Label-free approaches potentially address issues of bioactivity while yielding a system more representative of cell physiology. These approaches are based on changes in protein stability due to direct interaction with a small molecule [6]. One of

these methods denoted as a thermal shift assay is described in this protocol. The assay relies on the principle that as temperature increases, proteins lose their native conformation and become denatured. Denaturation causes proteins to adopt a random coil conformation, which leads to aggregation. The distinct temperature at which aggregation occurs for a given protein is defined as the temperature of aggregation (T_{agg}). T_{agg} is determined by a complex balance between the number and energies of intraprotein hydrogen bonds and salt bridges and interactions with other molecules [7]. Ligand binding results in increased thermal stability of the protein, causing a positive shift in T_{agg} , also described as a thermal shift [8]. The thermal shift assay generates a thermal denaturation curve and monitors the curve for a shift in T_{agg} upon binding of a bioactive compound (Fig. 1). A shift in T_{agg} is evidence of a protein–small molecule direct interaction.

In this chapter, we describe the application of the thermal shift assay in a high-throughput target identification setting named thermal proteome profiling (TPP) [9]. We also describe a qualitative approach for target validation that requires prior knowledge of potential candidate targets known as a cellular thermal shift assay (CETSA) [10]. This technique can be performed in live plants and utilizes an antibody-based readout to measure stability shifts of target proteins in a protein mixture. Finally, we describe a protocol denoted isothermal dose–response fingerprint (ITDRF), where T_{agg} is used to analyze the stability of a target protein as a function of increasing ligand concentration to determine the affinity of the small molecule for the target [10].

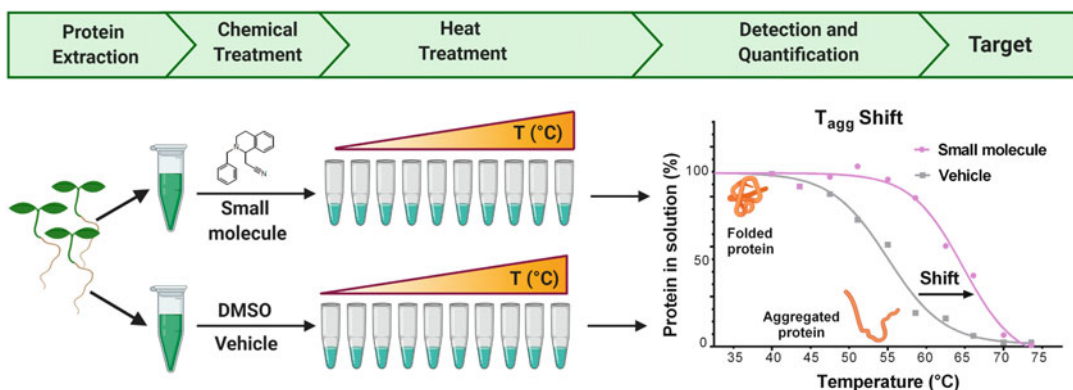


Fig. 1 Schematic representation of the experimental setup of a general thermal shift assay. *Arabidopsis* protein extracts are treated with a small molecule of interest or a vehicle control. Protein extracts are aliquoted and heated to ten different temperatures. Aggregated proteins are subsequently precipitated by centrifugation. The remaining protein in solution is detected via mass spectrometry or immunoblotting. Detected proteins are quantified, and thermal profile curves are constructed to calculate the temperature of aggregation (T_{agg}) for vehicle and treated samples. The T_{agg} shift is calculated by finding the difference in temperature at the inflection point between vehicle and treated samples. Shift in the T_{agg} of a protein indicates interaction with the small molecule and therefore is useful to identify or validate a target

2 Materials

2.1 Protein Extraction

1. Extraction buffer (50 mM Tris-HCl at pH 7.5, 150 mM NaCl, 0.4% (v/v) NP40, complete protease inhibitor mixture EDTA free (Roche)).
2. 2-mL tubes prefilled with beads (we recommend stainless steel beads).
3. Liquid nitrogen.
4. Tissue grinder (Mini-Beadbeater-96) or vortex (Cell disruptor).
5. 2D Quant Kit (GE Healthcare UK Ltd.) to determine protein concentration.

2.2 Thermal Shift

1. Bioactive small molecule: 10 mM stock solution in dimethylsulfoxide (DMSO).
2. PCR tubes (0.2 mL) (*see Note 1*).
3. Protein low-binding tubes (1.5 mL) (Eppendorf).
4. Protein low-binding pipette tips (Sigma-Aldrich).
5. Lysis buffer (*see Subheading 2.1, item 1*)
6. PCR mastercycler (temperature gradient necessary, *see Note 2*)
7. Refrigerated microcentrifuge (Eppendorf Microcentrifuge 5430 R).

2.3 TPP

2.3.1 Protein Digestion and TMT Labeling

1. Proteolytic enzyme (e.g., chymotrypsin, trypsin, LysC, or AspN).
2. TMT 16-plex Mass Tag Labeling Kit (Thermo Fisher Scientific).
3. 100 mM triethyl ammonium bicarbonate (TEAB)
4. 200 mM Tris(2-carboxyethyl)phosphine hydrochloride (TCEP)
5. 375 mM iodoacetamide
6. Acetone.
7. Hydroxylamine solution 50% w/v.
8. C18 spin tips or columns (Thermo Fisher Scientific).
9. Column equilibration/rinse solution: 0.1% trifluoroacetic acid (TFA) in ultrapure water.
10. Column elution solution: 0.1% TFA in 5% acetonitrile (ACN) with ultrapure water.
11. High-resolution Orbitrap LC-MS/MS mass spectrometer.

2.4 CETSA and ITDRF

1. e-PAGEL (Atto) or similar precast polyacrylamide gels for SDS-PAGE.
2. Sample buffer (1×): 50 mM Tris-HCl, pH 6.8, 4% (w/v) SDS, 10% (w/v) glycerol, 0.02% (w/v) BPB, 10% (v/v) 2-mercaptoethanol. Store at room temperature.
3. Running Buffer (10×): 250 mM Tris-HCl, pH 8.3, 1920 mM glycine, 1% (w/v) SDS. Store at room temperature.
4. Prestained molecular weight markers: Kaleidoscope markers (Bio-Rad).

2.5 Western Blot

1. Trans-Blot Turbo Mini PVDF Transfer Packs (Bio-Rad).
2. Trans-Blot Turbo Transfer System (Bio-Rad).
3. Tris-buffered saline (TBS) (1×): prepare 1 L of 20 mM Tris-HCl, pH 7.4, 150 mM NaCl.
4. Washing buffer: TBS (1×) containing 0.05% (w/v).
5. Blocking solution: TBS-T (1×) with 5% nonfat dry milk.
6. First antibody, for example, anti-His (Thermo Fisher Scientific).
7. Secondary antibody, for example, anti-mouse antibody-Horse radish peroxidase (Abcam).
8. Enhanced chemiluminescence (ECL) detection reagent (Pierce).
9. X-ray film or imaging system (Bio-Rad).

3 Methods
3.1 Protein Extraction

1. Weigh the Arabidopsis tissue of choice and place it into 2-mL low-binding microcentrifuge tubes.
2. Freeze by immersing the tubes in liquid nitrogen.
3. Grind the tissue with a mechanical homogenizer or vortex using stainless steel beads.
4. Add two volumes of extraction buffer per mg of fresh tissue (Subheading 2.1) and allow it to thaw on ice.
5. Clear the homogenate by centrifugation at $5000 \times g$ for 10 min at 4 °C.
6. Place the supernatant in a new tube and centrifuge again at $14,000 \times g$ for 20 min at 4 °C. The supernatant can be used directly for the subsequent experiments.
7. Quantify protein concentration using a commercial kit such as 2D Quant Kit (GE Healthcare) according to the manufacturer's instructions using bovine serum albumin as the standard. Dilute your protein extract to a final concentration of 2 mg/mL.

3.2 General Thermal Shift Protocol

The protein extract is treated with either the small molecule of interest or the vehicle (e.g., DMSO) and afterward split in aliquots, each treated with one of 10 different temperatures within a certain temperature range (*see Note 3*). The treatment with the small molecule can be instead performed in live plants before protein extraction. Alternatively, sequential thermal denaturation can be performed using purified proteins.

1. Prepare two protein low-binding 1.5-mL tubes and fill each with 1.0 mL of protein extract.
2. Add the appropriate amount of compound to the protein extract to achieve the desired final concentration. Depending upon the potency of the small molecule, this is typically in the micromolar range of 1–100 μM (*see Note 4*).
3. As a control, add an equal volume of vehicle (e.g., DMSO) to the other protein extract.
4. Incubate for 1 h at 4 °C with constant mixing by inversion.
5. Create a temperature gradient thermocycler program to incorporate temperature points from 37 to 68 °C. Set the heated lid at 100 °C (*see Note 3*).
6. Divide each protein extract into 8–10 aliquots in 0.6 ml tubes (50 μL each) (*see Note 5*). Spin the tubes for 30 s at 4 °C, and then keep them at 4 °C prior to use (less than 10 min).
7. Set the thermocycler program to run for a total of 10 min and start to preheat the block for a minimum of 5 min (*see Note 3*). During preheating, remove the tubes from 4 °C and place them at room temperature for 3 min. Place the tubes in the thermocycler with the heated lid closed for 3 min.
8. Rapidly remove the tubes from the thermocycler and place them into 1.5-mL adaptor tubes, and centrifuge at $14,000 \times g$ for 30 min at 4 °C to pellet the aggregated protein.
9. Remove the supernatant from each tube. Strictly avoid touching the pellet with the pipette tip to avoid false results. Place each supernatant into a clean, low-protein retention 1.5-mL tube.

3.3 TPP

TPP incorporates high-throughput mass spectrometry (MS) for protein identification and quantification. Additionally, after proteolysis, peptides are covalently labeled with stable (isobaric) isotope tags of varying mass introduced at the N-terminus and side-chain amines of peptides [11]. Isobaric tags are designed such that differentially labeled peptides appear as single peaks in MS scans, reducing the probability of peak overlap. The use of isobaric labeling methods in MS/MS allows the identification of proteins from different sources in a single experiment. TMT-16 labeling (Thermo Fisher Scientific) enables the monitoring of different temperature

points simultaneously to draw a complete melting curve and thereby allows the determination of the thermal shift for each protein in the mixture quantitatively (*see* **Notes 6** and **7**).

1. Adjust the volume of supernatant in each tube to 100 μL with 100 mM TEAB.
2. Add 5 μL of a 200 mM reducing reagent (TCEP) stock and incubate samples at 55 $^{\circ}\text{C}$ for 1 h.
3. Add 5 μL of the 375 mM iodoacetamide to the sample and incubate for 30 min. Protect samples from light at room temperature.
4. Add 50 μL of trypsin/Lys-C protease mix (Thermo Fisher Scientific) protein sample solution.
5. Incubate with shaking at 37 $^{\circ}\text{C}$ for 1–3 h to digest the protein sample.
6. Proceed with the TMT labeling according to the manufacturer's instructions. Briefly, add 40 μL of TMT reagent dissolved in 100% acetonitrile to each tube and incubate for 30–60 min at room temperature. To quench the reaction, add 50 μL of 5% hydroxylamine and 20% formic acid solution to each labeling reaction.
7. Clean up the peptides by using C18 spin tips or columns according to the manufacturer's instructions (Thermo Fisher Scientific). Briefly, equilibrate the columns with the column equilibration/rinse solution and centrifuge at $1000 \times g$ for 1 min. Transfer the C18 spin tip and adapter to a new microcentrifuge tube. Add 10 μL of the sample to the tip and centrifuge at $1000 \times g$ for 2 min. Wash the tip by adding 20 μL of column equilibration/rinse solution and centrifuge at $1000 \times g$ for 1 min. Repeat. Add 20 μL of column elution solution and centrifuge at $1000 \times g$ for 1 min. Repeat. Dry the samples in a Speed Vac and then resuspend with column elution solution for LC-MS analysis.
8. Run the samples on a high-resolution Orbitrap mass spectrometer capable of MS/MS fragmentation.
9. After the LC-MS/MS analysis, fold protein changes must be calculated relative to protein abundance at the lowest temperature in the vehicle samples or drug-treated samples. The fold changes indicate the relative amount of nondenatured protein at the corresponding temperature. A melting curve for each protein must be generated (*see* **Note 8**). A change in the thermal stability of a protein is indicated by a compound-induced shift of its melting curve. This is apparent for a given protein as a difference between the T_{agg} derived from untreated or vehicle controls and, compound-treated conditions.

3.4 CETSA

The principles of thermal shift are retained for CETSA assays, notwithstanding the complex environment of intact cells. Heat treatments can be performed *in vivo* or in protein extracts in the presence of a small molecule then, unfolded and aggregated proteins are removed by centrifugation, and the thermal stability of individual proteins that remain in solution can be monitored by a protein detection method such as immunoblotting [12]. This method verifies the association of small molecules with their candidate targets and their potency. Detection by immunoblot requires specific antibodies against the protein of interest or version of the protein fused to a fluorescent protein or epitope tag. Following detection, the quantification of band intensities is required to generate a melting curve. The immunoblot-based analysis can, for example, be used after TPP and mass spectrometry (or other target identification methods) as a follow-up experiment with an antibody directed against the identified target protein or predicted off targets to confirm these results [3, 4].

1. SDS-PAGE: Samples can be separated by denaturing acrylamide gel electrophoresis. Use the supernatant recovered in Sub-heading 3.1 (step 7) and dilute it to 1:1 with SDS-PAGE sample buffer. If not recommended otherwise (*see Note 9*), the samples are heated at 95 °C for 10 min using a thermal block. Let the samples cool down for at least 5 min and spin down the condensate before proceeding with gel loading. Load 40 µL of compound-treated sample and 40 µL of each vehicle-treated sample for all the tested temperatures. Load 5 µL of prestained molecular weight markers in each gel. Place the gel into the holder and place it into the tank. Fill the tank with running buffer and run at 80 V until the Coomassie Blue dye front reaches the bottom of the gel.
2. Blot transfer: Using the Trans-Blot Turbo Mini PVDF Transfer Packs (Bio-Rad), assemble the transfer sandwich according to the manufacturer's instructions. Choose a preset transfer program on the Trans-Blot Turbo Transfer System (Bio-Rad) considering the predicted molecular mass of the protein of interest, and the thickness and size of the SDS gel to be transferred.
3. Immunoblot: Block the blot with blocking solution for 1 h at room temperature with constant rocking. Dilute the primary antibody as recommended in blocking solution. Rock overnight at 4 °C. Remove the primary antibody solution and add washing buffer. Incubate for 10 min shaking vigorously. Repeat two times. Use the blocking solution to incubate with the secondary antibody (raised against the species source of the primary antibody) coupled to a detection enzyme or

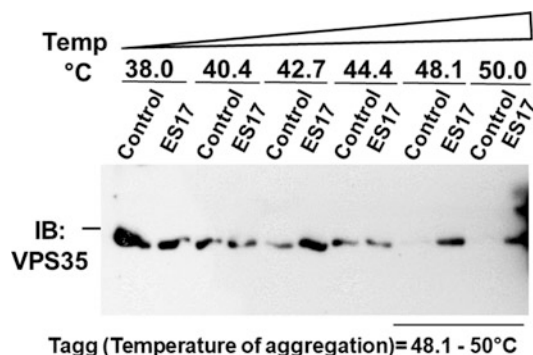


Fig. 2 Example of a CETSA assay for ES17 to validate VPS35 as a protein target. *Arabidopsis* plants were treated with 100 μ M ES17 or DMSO. Protein extracts were treated with increasing temperatures. Immunodetection by Western blot indicates that the T_{agg} of VPS35 treated with DMSO is 48–50 °C. In the presence of ES17, protein is stabilized, shifting the T_{agg} . (Images reproduced from Rodriguez-Furlan et al. Proc Natl Acad Sci, USA 116.42 (2019): 21291–21301)

fluorophore for 1–2 h with gentle rocking. Remove the secondary antibody solution and add washing buffer. Incubate for 10 min shaking vigorously. Repeat two times.

4. Detection: For enzyme-coupled secondary antibodies, add ECL reagent, wait for 5 min, and then wash the membrane (*see Note 10*). Image the blot using X-ray film or a chemiluminescence imaging system (Bio-Rad).
5. Quantification: Use suitable software for densitometric analysis (e.g., Image J, Bio-Rad Gel Doc, ChemiDoc) to quantify the band intensities on the blot. Plot the intensity against the temperature values to generate a melting curve (e.g., GraphPad Prism or Excel). Determine the T_{agg} of the candidate target protein in untreated or vehicle-treated samples. Use this information to determine whether the thermal shift, if any, exists in the treated samples (*see Note 11*).
6. Figure 2 highlights an example of the validation of small-molecule (ES17) target protein (VPS35A) interaction using CETSA.

3.5 ITDRF

In this approach, protein extracts are aliquoted and serial concentrations of the small molecule are added to each tube. In the presence of the small molecule, the temperature and heating time are kept constant at T_{agg} (determined, for example, by CETSA). After detection by immunoblotting, densitometric analysis can indicate the concentration of ligand at which 50% of the total stabilizing effect has been observed. This concentration is denoted as the half-maximal effective concentration (EC_{50}) and is an indicator of the affinity of the small molecule for the target.

1. Divide each protein extract obtained in Subheading 3.1 (step 7) into 10 aliquots and place them into 0.6 ml tubes (50 μ L each).
2. Add serially increasing concentrations of the small molecule to each tube and, in parallel, add equivalent amounts of the vehicle solvent and incubate for 1 h at 4 °C with occasional shaking (*see* **Note 12**).
3. Centrifuge the tubes at $300 \times g$ for 30 s at 4 °C and then keep at 4 °C prior to use (less than 10 min).
4. Create a thermocycler program for a constant temperature ($\geq T_{agg}$) and with the lid heated at 100 °C. Set the program to run for a total of 10 min, preheating the block for a minimum of 5 min.
5. Remove the tubes from 4 °C and place them at room temperature for 3 min.
6. Place the tubes in the thermal cycler for 3 min.
7. Remove the tubes, and using adapters, place them in a microcentrifuge and centrifuge at $14,000 \times g$ for 30 min at 4 °C.
8. Recover the supernatant from each tube and transfer it to a new 1.5-mL tube.
9. For detection by immunoblotting, follow the instructions in Subheading 3.4.
10. Perform densitometric analysis of the band detected on the immunoblot using suitable software (e.g., Image J, Bio-Rad Gel Doc, ChemiDoc,). To quantify the fold protein changes across the different concentrations of compound, use as a reference the sample treated with the lowest compound concentration or buffer-only condition (100% stable protein) (*see* **Note 13**).
11. Sigmoidal curve fitting and EC_{50} can be calculated with Graph-Pad Prism software using nonlinear regression. The curve can help to estimate the minimum dose threshold, which is the lowest compound concentration required to confidently work over the baseline level (*see* **Note 14**).

As an example, in Fig. 3 we can observe the percentage of the signal corresponding to the ES17 concentration at which maximum stabilization of its target VPS35A is achieved and as well as the EC_{50} of 0.9 μ M. IDRTF allows the ranking of small-molecule affinities for a single protein target. Therefore, it is useful not only as a target validation approach but more detailed structure–activity relationship (SAR) studies. Accordingly, we can *see* in Fig. 3 that an inactive analog of ES17 (iES17) fails to stabilize the target because it interacts weakly or fails to interact with the target.

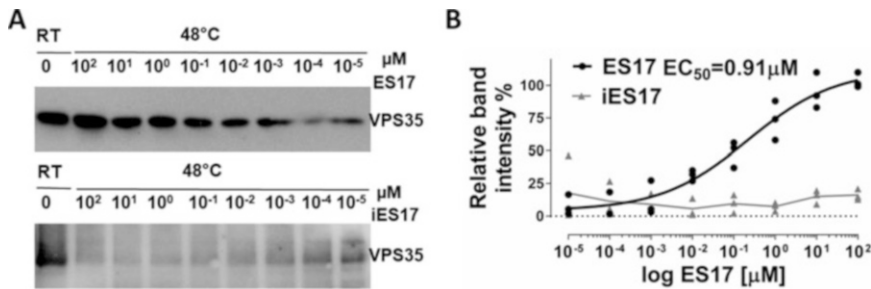


Fig. 3 Representative IDTRF result for protein extracts treated with increasing concentrations of ES17 or iES17 (inactive analog ES17). Using the T_{agg} of VPS35, samples were treated with increasing concentrations of ES17 or iES17. ES17 stabilizes VPS35, preventing its aggregation in a concentration-dependent manner. On the contrary, iES17 does not stabilize VPS35 from thermal aggregation. The graph is based on raw data from immunoblot chemiluminescence readings for three independent experiments for ES17 (dots) or iES17 (triangles). ES17 results indicate a half-maximal effective concentration (EC_{50}) of approximately 1 μM . (Images reproduced from Rodriguez-Furlan et al. Proc Natl Acad Sci, USA 116.42 (2019): 21291–21301)

4 Notes

1. PCR tubes (0.2 mL) that are suitable for ultracentrifugation are necessary at maximum $14,000 \times g$.
2. Use a PCR mastercycler that allows heating different tubes at different temperatures, suitable for gradient temperature increase.
3. Temperature range is usually set between 37 and 68 °C. Some PCR thermocyclers may be limited in the number of temperatures steps. Therefore, to cover the full range of desired temperatures, it may be necessary to use two thermocyclers (and two programs) in parallel.
4. As plant lysates have a high concentration of proteins, we recommend using the small molecule at a higher concentration compared to the ones used for *in planta* assays.
5. Heat the thermocycler lid to 100 °C to avoid sample evaporation/condensation in PCR tubes.
6. Thermal shift assays should be performed at least in triplicate. TTP experiments should be ideally performed as quadruplicate to obtain high-confidence MS data to calculate protein melting curves.
7. iTRAQ 8-plex isobaric labels (AB Sciex Pte. Ltd) are an alternative product that allows the multiplexing of up to 8 different samples.
8. The package TPP for R provides executable workflows that conduct all necessary data analysis steps (<http://bi conductor.org/packages/release/bioc/html/TPP.html>) [13].

9. To preserve membrane proteins, the extracts should not be heated above 50 °C because it can cause protein aggregation.
10. CETSA experiments must be replicated at least three times in order to confirm a shift in the thermal stability of a target protein.
11. If using secondary antibodies coupled to fluorophores, we suggest preventing desiccation of the membrane by keeping the humid membrane between the sides of a transparent plastic bag or between two sides of plastic film.
12. ITDRF treatments *in planta* can be performed by incubating with increasing concentrations of the small molecule or the vehicle prior to protein extraction.
13. For any proteins to be confidently considered stabilized or destabilized by the compound, we suggest a cutoff were the fold-change value at any of the highest three compound concentration points represents at least a 30% change when compared to the minimum responsive level or the minimum dose threshold.
14. Determine the EC₅₀ with GraphPad Prism software using nonlinear regression of the type [Inhibitor] vs. Response (three parameters) with the function $Y = \text{Bottom} + (\text{Top} - \text{Bottom}) / (1 + (X / \text{IC}_{50}))$.

References

1. Zhang C, Brown MQ, van de Ven W et al (2016) Endosidin2 targets conserved exocyst complex subunit EXO70 to inhibit exocytosis. *Proc Natl Acad Sci U S A* 113(1):E41. LP-E50
2. Li R, Rodriguez-Furlan C, Wang J et al (2017) Different endomembrane trafficking pathways establish apical and basal polarities. *Plant Cell* 29(1):90–108
3. Dejonghe W, Sharma I, Denoo B et al (2019) Disruption of endocytosis through chemical inhibition of clathrin heavy chain function. *Nat Chem Biol* 15(6):641–649
4. Rodriguez-Furlan C, Domozych D, Qian W et al (2019) Interaction between VPS35 and RABG3f is necessary as a checkpoint to control fusion of late compartments with the vacuole. *Proc Natl Acad Sci U S A* 116(42):21291–21301
5. Lee J, Bogyo M (2013) Target deconvolution techniques in modern phenotypic profiling. *Curr Opin Chem Biol* 17(1):118–126
6. Lyu J, Wang K, Ye M (2020) Modification-free approaches to screen drug targets at proteome level. *TrAC Trends Anal Chem* 124:115574. ISSN 0165-9936, <https://doi.org/10.1016/j.trac.2019.06.024>
7. Rees DC, Robertson AD (2001) Some thermodynamic implications for the thermostability of proteins. *Protein Sci* 10(6):1187–1194
8. Lo M-C, Aulabaugh A, Jin G et al (2004) Evaluation of fluorescence-based thermal shift assays for hit identification in drug discovery. *Anal Biochem* 332(1):153–159
9. Savitski MM, Reinhardt FB, Franken H et al (2014) Tracking cancer drugs in living cells by thermal profiling of the proteome. *Science* 346(6205):1255784
10. Molina DM, Jafari R, Ignatushchenko M et al (2013) Monitoring drug target engagement in cells and tissues using the cellular thermal shift assay. *Science* 341(6141):84–87
11. Rauniyar N, Yates JR (2014) Isobaric labeling-based relative quantification in shotgun proteomics. *J Proteome Res* 13(12):5293–5309
12. Jafari R, Almqvist H, Axelsson H et al (2014) The cellular thermal shift assay for evaluating drug target interactions in cells. *Nat Protoc* 9(9):2100–2122
13. Childs D, Bach K, Franken H et al (2019) Nonparametric analysis of thermal proteome profiles reveals novel drug-binding proteins. *Mol Cell Proteomics* 18(12):2506–2515



Drug Affinity Responsive Target Stability (DARTS) Assay to Detect Interaction Between a Purified Protein and a Small Molecule

Lei Huang, Diwen Wang, and Chunhua Zhang

Abstract

Drug affinity responsive target stability (DARTS) assay is used to detect the interaction between a ligand and a protein based on the observation that some ligands can protect the target protein from degradation by proteases when mixed in a solution. To set up the assay, a ligand is first mixed with a purified candidate target protein or a total cell lysate that contains a candidate target protein. Then, different amounts of protease are added to the mixture to allow the enzyme to digest the protein in the mixture. After protease digestion, the candidate target protein is detected by assays such as western blot, silver staining, or Coomassie blue staining. In theory, the candidate protein should be protected by the ligand from protease digestion, which is reflected by higher abundance of the candidate protein in mixtures containing the ligand compared with the control treatment. There are a few significant advantages of DARTS: (a) the ligand does not need to be modified so the native ligand could be used; (b) the candidate target protein could be either purified protein or protein that is present in the total cell lysate; and (c) the assay can be used together with proteomics analysis to identify an unknown target protein. The assay is especially valuable to test the interaction between the ligand and membrane proteins that are often challenging to purify. In this chapter, we use Endosidin2 (ES2) and its target protein *Arabidopsis thaliana* EXO70A1 (AtEXO70A1) as an example to show the step-by-step procedure of the DARTS assay.

Key words DARTS, Ligand, Target protein, Endosidin2, AtEXO70A1

1 Introduction

Small molecules are useful and indispensable tools in biology research to understand growth, disease, stress response, etc. [1]. Most of the drugs used in disease control are bioactive small molecules that target endogenous proteins [2, 3]. Small molecules are especially valuable in cell biology research because they allow the manipulation of dynamic cellular processes in a transient, reversible, and dose-dependable manner. For example, multiple bioactive small molecules have been identified to affect plant endomembrane trafficking, and these molecules have been valuable tools

in understanding the mechanisms of dynamic protein transport in plants [4]. The identification of small molecules of interest often starts with chemical library screening. Upon completion of the screening, candidate small molecules need to be further characterized, and the endogenous target protein(s) needs to be identified to better use the small molecule. The process of target identification can be quite challenging and time-consuming. Nowadays, there are various approaches available for the target identification of small molecules [5]. One of the widely used approaches is affinity chromatography combined with mass spectrometry analysis [6]. This approach begins with structure–activity relationship analysis of the small molecule to identify nonessential site so that an affinity tag can be added to the molecule without disrupting the bioactivity of the molecule. A modified small molecule with an affinity tag can be used for affinity chromatography to pull out the endogenous target protein, and the identity of the endogenous target protein can be characterized using mass spectrometry [6]. The most challenging step for affinity chromatography can be to find a way to modify the small molecules without disturbing its activity, and the identified interaction between the small molecule and the candidate target protein often requires further confirmation by other assays [6].

Drug affinity responsive target stability (DARTS) assay contains a few steps [7]. First, the purified protein or cell lysate is mixed with the small molecule of interest. The solvent molecule or the inactive analog molecule will be mixed with the protein as well as necessary controls for the DARTS assay. Then, incubate the mixture of the protein and the small molecule with gentle shaking. The mixture is then aliquoted into small volumes, and the same volume of different concentrations of protease is added to the aliquots of the mixture. After a certain time of protease digestion, stop the digestion reaction by deactivating the protease [7]. The next step is to separate the protease-digested samples on SDS-PAGE and use different approaches to detect the candidate target protein. The protection of protein degradation can be quantified by comparing the abundance of candidate protein in samples incubated with an active molecule with that of solvent or inactive analog control molecules. If the ligand molecule binds to the candidate protein, higher protein abundance is expected in the sample mixed with the ligand molecule.

Similar to affinity chromatography, the DARTS assay could also be used as an initial approach to identify the potential target of small molecules of interest when combined with quantitative proteomic analysis [8, 9]. In this case, cell lysate will be incubated with the small molecule or the solvent control molecule. Then, the mixture will be digested with a mixture of different types of proteases. After protease digestion, the protein will be separated on SDS-PAGE, and protein bands that show higher intensity in the test small molecule than the negative control molecule will be

identified and dissected to proceed for mass spectrometry analysis. The identified candidate target protein will further be tested for direct interaction with the small molecule of interest.

Compared with affinity chromatography, the DARTS assay does not require modification on small molecules of interest. The assay is straightforward and does not require special facilities, which makes it an easy access approach for most of the biology labs [10]. However, DARTS is a qualitative assay, which means that it does not provide the binding affinity between the protein and small molecule of interest and it is also not applicable for proteins that show little susceptibility to proteolysis due to the protein properties. The DARTS assay is often combined with a more quantitative binding assay, such as microscale thermophoresis (MST), to better characterize the interaction between the small molecule and the target protein.

ES2 is a small molecule that targets the EXO70 subunit of the conserved exocyst complex to inhibit exocytosis in plants, mammals, and fungi [11, 12]. The direct interaction between ES2 and AtEXO70A1 has been confirmed using DARTS assay, MST assay, differential scanning fluorimetry assay, and saturation transfer difference (STD) nuclear magnetic resonance (NMR) spectroscopy assay [4, 11, 12]. In this chapter, we use ES2 and AtEXO70A1 as an example to show how to set up the DARTS assay to test the interaction of a small molecule with a purified candidate target protein.

2 Materials

1. AtEXO70A1 expression construct: pRSF-Duet-AtEXO70A1.
2. LB medium (tryptone 10 g/L, yeast extract 5 g/L, and NaCl 10 g/L).
3. 1.5-mL microcentrifuge tubes.
4. Dimethyl sulfoxide (DMSO).
5. ES2 stock solution in DMSO (20 mM).
6. AKTA pure FPLC system (GE Healthcare, Pittsburgh, PA).
7. Nanodrop 2000.
8. Lysis buffer (50 mM Tris-HCl, pH 8.0, 0.5 M NaCl, 40 mM imidazole).
9. Elution buffer (50 mM Tris-HCl, pH 8.0, 0.5 M NaCl, 250 mM imidazole).
10. Dialysis buffer (50 mM Tris-HCl, pH 8.0, 0.5 M NaCl, 5% glycerol).
11. Ultrapure water (*see Note 1*).

12. Protease (*see Note 2*).
13. Timer.
14. Acetic acid (1% (v/v) and 5% (v/v)).
15. Silver staining developing solution (2% (w/v) sodium carbonate and 0.04% (v/v) formaldehyde).
16. Silver staining fixing solution (50% (v/v) methanol and 5% (v/v) glacial acetic acid).
17. Methanol (50%).
18. Silver nitrate (0.1% (w/v)) (*see Note 3*).
19. Sodium thiosulfate (0.02% (w/v)).
20. 5× SDS loading buffer (DTT 0.25% (w/v), bromophenol blue 0.25% (w/v), glycerol 50% (v/v), SDS 10% (w/v), and 0.25 M Tris-HCl, pH 6.8).
21. Bovine serum albumin.
22. Scanner.

3 Method

3.1 Purification of AtEXO70A1 Protein

1. Clone AtEXO70A1 full-length coding sequence into pRSF-Duet vector and transform the plasmid into BL21(DE3) competent cell for protein expression [7]. Take glycerol stock of AtEXO70A1 from $-80\text{ }^{\circ}\text{C}$ freezer and thaw on ice. Streak the culture on LB kanamycin agar plate and culture at $37\text{ }^{\circ}\text{C}$ overnight to obtain a single colony. Pick a single colony to inoculate 5 mL of LB liquid medium with kanamycin and culture at $37\text{ }^{\circ}\text{C}$ overnight with shaking. The next morning, inoculate 1 L of LB liquid medium with kanamycin with 2.5 mL of the overnight culture and shake at $37\text{ }^{\circ}\text{C}$ till OD_{600} reaches 0.6. Cool down the culture on ice and add isopropyl β -D-1-thiogalactopyranoside (IPTG) to a final concentration of 0.1 mM to induce protein expression and let the culture grow at $16\text{ }^{\circ}\text{C}$ overnight with shaking. After overnight culture, collect the cells by centrifugation at $4000 \times g$ for 15 min and add 50 mL of lysis buffer to resuspend the cells. Lyse the resuspended cells by sonication and spin the lysed cells at $20,000 \times g$ for 1 h. Collect the supernatant and apply to the equilibrated HisTrap HP column to purify His-tagged AtEXO70A1 using an AKTA pure FPLC system (GE Healthcare, Pittsburgh, PA) (*see Note 4*). Dialyze the protein in dialysis buffer overnight to remove imidazole and measure protein concentration by measuring OD_{280} using Nanodrop 2000. Aliquot the protein into different tubes and store at $-80\text{ }^{\circ}\text{C}$ for future usage.

3.2 Protein Proteolysis by Pronase

1. Take an aliquot purified AtEXO70A1 protein from $-80\text{ }^{\circ}\text{C}$ refrigerator and put on ice for several minutes until the protein thaws completely.
2. Take two Eppendorf tubes and add $2.5\text{ }\mu\text{g}$ of AtEXO70A1 protein and $2.5\text{ }\mu\text{g}$ of BSA to each tube. Add dialysis buffer to make the volume in each tube to $200\text{ }\mu\text{L}$ in total (*see Note 5*).
3. Add DMSO to one tube of protein mixture to a final concentration of 2% and add an equal volume of ES2 stock to the other tube of protein mixture to make the final concentration of ES2 to $400\text{ }\mu\text{M}$. Incubate the protein and DMSO/ES2 mixture at room temperature for 1 h with gentle rotating (*see Note 6*).
4. After 1 h incubation, aliquot the mixture of protein with DMSO and protein with ES2 into 3 separate tubes, with $60\text{ }\mu\text{L}$ in each tube. In each tube, add $1\text{ }\mu\text{L}$ of pronase that has been diluted at 1:3000 or 1:10000 from 10 mg/mL stock or $1\text{ }\mu\text{L}$ of water (*see Note 7*).
5. After proteolysis for 30 min, terminate the reaction by adding $15\text{ }\mu\text{L}$ of $5\times$ SDS loading buffer and boil for 5 min. The boiled samples can be used immediately for SDS-PAGE or can be stored at $-20\text{ }^{\circ}\text{C}$ for long-term storage (*see Note 8*).
6. Load boiled samples on SDS-PAGE and run for electrophoresis.
7. After electrophoresis, the gel is ready for further protein detection analysis.

3.3 Protein Detection by Silver Staining

There are different methods to detect protein after electrophoresis, and we choose to use silver staining (Fig. 1) because of its high sensitivity.

1. Submerge the gel with fixing solution in a plastic container and shake gently for 20 min.
2. Replace fixing solution with sufficient 50% methanol solution and shake gently for 10 min.
3. Remove 50% methanol and add enough ddH₂O, and shake the gel gently for 10 min.
4. Remove ddH₂O.
5. Submerge the gel in 0.02% sodium thiosulfate for 1 min.
6. Wash the gel twice with ddH₂O for 30 s each time.
7. Place the gel in chilled 0.1% silver nitrate solution and incubate at $4\text{ }^{\circ}\text{C}$ for 20 min with gentle shaking.

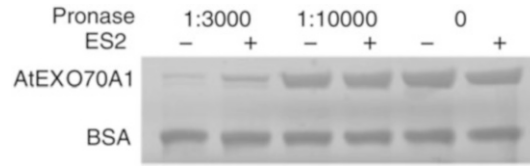


Fig. 1 ES2 protects AtEXO70A1 from digestion by pronase. Representative images of DATRS assay to test the binding between ES2 and AtEXO70A1. AtEXO70A1 protein together with BSA was treated with ES2 (400 μ M) and DMSO (2%) and detected by silver staining. At 1:3000 dilution of pronase, ES2-treated AtEXO70A1 showed an obvious higher band intensity compared with DMSO treatment while the BSA band intensity between ES2 and DMSO was comparable

8. Remove 0.1% silver nitrate and add developing solution with slight vigorously shaking. When the staining intensity is reached to the desired level, stop the reaction by replacing the developing solution with 5% acetic acid (*see Note 9*).
9. Scan the protein gel with a scanner to convert the gel to an image.
10. Open the scanned gel image with ImageJ and convert the image to grayscale.
11. Invert the image so that the protein bands show positive values.
12. Draw a box that includes the protein band using the rectangle tool and measure the integrated density for the selected region. Move the box to an area that contains the background of the gel and measure the integrated density in this background region. Subtract the background density from the protein band density to obtain the real integrated density of the protein band. Perform the same measurement for each protein band of AtEXO70A1 and BSA.
13. For each protein at specific pronase concentration, calculate the protein band intensity ratio of samples incubated with ES2 against samples incubated with DMSO. A higher intensity AtEXO70A1 band should be detected in samples incubated with ES2 compared with samples incubated with DMSO. The intensity of BSA should not be affected by ES2.
14. Perform at least three independent repeats to obtain statistical analysis for possible differences in samples incubated with ES2 compared with samples treated with DMSO.

4 Notes

1. Impurities in the water would interfere with the silver staining and double-distilled water (ddH₂O) with a resistivity of 18.2 M Ω -cm is preferred for the preparation of all the reagents.
2. Pronase is a mixture of different types of proteases. Prepare 10 mg/mL pronase stock solution using ddH₂O water, aliquot, and store at -20 °C.
3. Silver nitrate reagent needs to be stored at 4 °C and wrapped with aluminum foil to keep from light.
4. In case when the HPLC protein purification system is not available, purify protein manually with a specific column or other protein purification equipment.
5. BSA is a loading control that could be used as a reference for the calculation of relative band intensity of AtEXO70A1 between ES2 treatment and DMSO treatment.
6. The drug concentration that is used in the DARTS assay is often much higher than the concentration of the drug that causes biological phenotypes. For example, ES2 causes about 50% plant growth inhibition at 40 μ M. However, we found that ES2 can significantly protect AtEXO70A1 from proteolysis at concentrations of 200 to 400 μ M.
7. The pronase concentration is very important for the DARTS assay; using too high or too low concentration of pronase may not be able to distinguish the band intensity difference between small molecule and solvent control treatment, and different proteins also show different susceptibility to pronase. A pretest experiment with a series dilution of pronase is needed in order to know what range of pronase is suitable for a specific protein.
8. The pronase digestion time for all the samples needs to be strictly controlled at 30 min. Add pronase to one sample and mix it well by pipetting and wait for 30 s before adding to another sample. Thus, a 30-s interval is kept between each sample. In order to avoid mistakes that may occur when adding pronase, it is better to write down the time of adding pronase and terminating the reaction for each individual sample before the experiment.
9. During the developing process, the developing solution will turn yellow quickly. It is critical that the development solution remains transparent. Discard the yellow color developing solution and replace it with a fresh developing solution. To save the gel for a longer term, keep the silver-stained gel in 1% acetic acid.

Acknowledgments

This work was supported by Purdue University Provost start-up fund to C.Z.

References

1. Kang C, Keller TH (2020) Probing biological mechanisms with chemical tools. *Pharmacol Res* 153:104656. <https://doi.org/10.1016/j.phrs.2020.104656>
2. Solier S, Muller S, Rodriguez R (2020) Whole-genome mapping of small-molecule targets for cancer medicine. *Curr Opin Chem Biol* 56:42–50. <https://doi.org/10.1016/j.cbpa.2019.12.005>
3. Li F, Ma C, Wang J (2015) Inhibitors targeting the influenza virus hemagglutinin. *Curr Med Chem* 22(11):1361–1382. <https://doi.org/10.2174/0929867322666150227153919>
4. Huang L, Li X, Zhang C (2019) Progress in using chemical biology as a tool to uncover novel regulators of plant endomembrane trafficking. *Curr Opin Plant Biol* 52:106–113. <https://doi.org/10.1016/j.pbi.2019.07.004>
5. Hu Y, Zhao T, Zhang N, Zhang Y, Cheng L (2019) A review of recent advances and research on drug target identification methods. *Curr Drug Metab* 20(3):209–216. <https://doi.org/10.2174/1389200219666180925091851>
6. Lomenick B, Olsen RW, Huang J (2011) Identification of direct protein targets of small molecules. *ACS Chem Biol* 6(1):34–46. <https://doi.org/10.1021/cb100294v>
7. Lomenick B, Hao R, Jonai N, Chin RM, Aghajan M, Warburton S, Wang J, Wu RP, Gomez F, Loo JA, Wohlschlegel JA, Vondriska TM, Pelletier J, Herschman HR, Clardy J, Clarke CF, Huang J (2009) Target identification using drug affinity responsive target stability (DARTS). *Proc Natl Acad Sci U S A* 106(51):21984–21989. <https://doi.org/10.1073/pnas.0910040106>
8. Hwang HY, Kim TY, Szasz MA, Dome B, Malm J, Marko-Varga G, Kwon HJ (2020) Profiling the protein targets of unmodified bio-active molecules with drug affinity responsive target stability and liquid chromatography/tandem mass spectrometry. *Proteomics* 20:e1900325. <https://doi.org/10.1002/pmic.201900325>
9. Park YD, Sun W, Salas A, Antia A, Carvajal C, Wang A, Xu X, Meng Z, Zhou M, Tawa GJ, Dehdashti J, Zheng W, Henderson CM, Zelazny AM, Williamson PR (2016) Identification of multiple Cryptococcal fungicidal drug targets by combined gene dosing and drug affinity responsive target stability screening. *MBio* 7(4):e01073–e01016. <https://doi.org/10.1128/mBio.01073-16>
10. Pai MY, Lomenick B, Hwang H, Schiestl R, McBride W, Loo JA, Huang J (2015) Drug affinity responsive target stability (DARTS) for small-molecule target identification. *Methods Mol Biol* 1263:287–298. https://doi.org/10.1007/978-1-4939-2269-7_22
11. Zhang C, Brown MQ, van de Ven W, Zhang ZM, Wu B, Young MC, Synek L, Borchardt D, Harrison R, Pan S, Luo N, Huang YM, Ghang YJ, Ung N, Li R, Isley J, Morikis D, Song J, Guo W, Hooley RJ, Chang CE, Yang Z, Zarsky V, Muday GK, Hicks GR, Raikhel NV (2016) Endosidin2 targets conserved exocyst complex subunit EXO70 to inhibit exocytosis. *Proc Natl Acad Sci U S A* 113(1):E41–E50. <https://doi.org/10.1073/pnas.1521248112>
12. Huang L, Li X, Li Y, Yin X, Li Y, Wu B, Liao CJ, Mo H, Mengiste T, Guo W, Dai M, Zhang C (2019) Endosidin2-14 targets the exocyst complex in plants and fungal pathogens to inhibit exocytosis. *Plant Physiol* 180(3):1756–1770. <https://doi.org/10.1104/pp.18.01457>



Using Differential Scanning Fluorimetry (DSF) to Detect Ligand Binding with Purified Protein

Xiaohui Li and Chunhua Zhang

Abstract

Differential scanning fluorimetry (DSF) can be used to detect the binding of a small molecule ligand to a purified target protein. Upon binding with certain ligands, the protein can be stabilized from thermal denaturation. DSF uses a fluorescent dye and Real-Time PCR instrument to detect the unfolding process of proteins during thermal denaturation. The experiment can be set up and finished in 1 day once the purified protein is available.

Key words Differential scanning fluorimetry, Ligand binding, Purified protein, Real-Time PCR instrument

1 Introduction

Ligand–protein interaction is of interest for many researchers, including those looking for inhibitors of target proteins. So far, many methods have been developed to study the ligand–protein interaction, for example, microscale thermophoresis (MST) [1], cellular thermal shift assay (CETSA) [2], drug affinity responsive target stability (DARTS) [3], and saturation transfer difference (STD) NMR spectroscopy (STD-NMR) [4]. Among these methods, differential scanning fluorimetry (DSF) has its advantages as an inexpensive method to detect ligand binding as it is typically performed with a Real-Time PCR instrument, which is easy to get access for most labs. Instead, MST and STD-NMR need special equipment that might not be available. DSF can also be used as a high-throughput method to screen for the ligand of the target protein.

Most proteins will become unstable and unfold upon the increase of temperature. The hydrophobic regions can be exposed when the protein unfolds. Some fluorescent dyes, for example, SYPRO Orange, can get a fluorescence quantum yield when bound to hydrophobic regions. The fluorescence change can be

detected and quantified by a Real-Time PCR instrument. The thermal stability of proteins can be increased upon binding with its ligand [5, 6]. T_m value can be used to represent the thermal stability of a protein. If incubation of a protein with a ligand introduces a “thermal shift” or T_m change, when compared to incubation with DMSO, it provides evidence for the binding of the ligand with the protein. DSF has been successfully used as a method to detect ligand binding for many target proteins, for example, inhibitor VIII with human AKT1 [7], rigosertib with human RAS effectors [8], and Endosidin9 with *Arabidopsis* clathrin heavy chain (CHC) [9].

2 Materials

2.1 Reagents

1. Purified protein stock (*see Note 1*).
2. Small molecule stock, including the small molecule of interest and another small molecule as a negative control.
3. Reaction buffer I: 150 mM NaCl, 50 mM Tris-HCl (pH 8.0); reaction buffer II: 150 mM NaCl, 50 mM Tris-HCl (pH 8.0), 2% DMSO (*see Note 2*).
4. Fluorescence dye for protein quantification: SYPRO Orange dye (5000 \times stock) (*see Note 3*).

2.2 Instrument

1. Real-Time PCR instrument, for example, BioRad CFX Connect or Roche LightCycler 480.
2. White bottom 96-well PCR plate with optical seals.

3 Methods

3.1 Prepare Reaction Mix

1. Dilute the purified protein stock to 2 μ M with reaction buffer I.
2. Prepare the small molecule serial gradient dilution in a white-well Real-Time PCR plate. Add 15 μ L of reaction buffer II to well 2 to well 8. Mix 1.6 μ L of the 40 mM small molecule stock with 38.4 μ L of reaction buffer I to get 1.6 mM dilution. Add 15 μ L of small molecule dilution to well 1 and well 2. Mix well 2 to get a 1:1 dilution of small molecule. Take 15 μ L from well 2 and add to well 3 and continue to make the 1:1 serial dilution to get 8 concentration gradients in total. Prepare the serial gradient dilution of the negative control molecule in the same way.
3. Prepare the reaction mix. Calculate the volume of protein stock needed to get 260 μ L of 2 μ M protein master mix (protein stock volume needed = 2 μ M \times 260 μ L/protein stock concentration). Add 0.52 μ L of SYPRO Orange dye (5000 \times) to the calculated volume of protein stock and then add reaction buffer I until getting a final volume of 130 μ L.

Mix 15 μ L of protein dilution with the small molecule dilution in each well. Mix the protein dilution with the negative

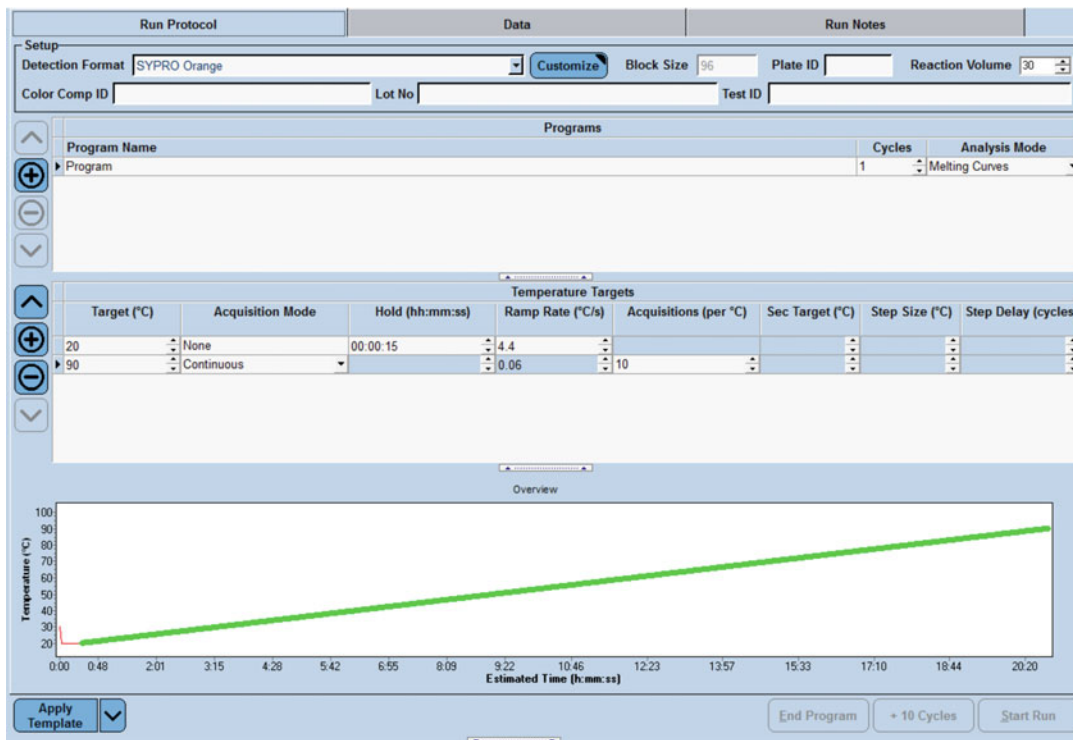


Fig. 1 Parameter settings for DSF assay on Roche LC480 instrument

control molecule dilution in the same way. Seal the plate with optical seals.

4. Centrifuge the PCR plate at 500 rpm to remove air bubbles.

3.2 Setting Up the Thermal Shift Program

For Roche LightCycler 480 Real-Time PCR instrument System II, set the filter combination of excitation and emission as 465 nm and 580 nm. Under the “Selected Filter Combination List,” change the name to “SYPRO Orange,” “Melt Factor” as 1, “Quant Factor” as 10, and “Max Integration Time” as 1 s. In the “Run Protocol” page, set the “Detection Format” to SYPRO Orange, “Block Size” to 96, and “Reaction Volume” to 30. Select protein melting as the “Program Name,” set “Cycles” as 1, and “Analysis Mode” as melting curve. In the “Temperature Targets” menu, set the parameters as in Fig. 1. Click the down arrow near the “Apply Template” button and click “Save As Template.” Next, place the PCR plate in a Roche LightCycler 480 Real-Time PCR instrument and start the experiment with a saved template.

3.3 Data Analysis

For data analysis, use the T_m calling analysis to find the temperature correlates to the peak of $-(d/dT)$ fluorescence (see Note 4).

If T_m shift can be detected with the presence of a ligand, and not with the presence of negative control, then the results will indicate that there’s binding between the target protein and the small molecule of interest (see Note 5).

4 Notes

1. Purified proteins should be dialyzed before being used in DSF experiments to get rid of imidazole or glutathione.
2. Alternative buffer can also be used, for example, PBS or HEPES buffer.
3. If SYPRO Orange does not perform well with the target protein, other fluorescent dyes can also be used.
4. The (d/dT) fluorescence is the first derivative of the melting curve. The peak of $-(d/dT)$ fluorescence is the minimum of $-(d/dT)$ fluorescence, or the maximum of (d/dT) fluorescence.
5. If T_m shift cannot be detected, it does not necessarily mean that there is no binding between the target protein and the small molecule of interest. It is possible that the binding of the ligand cannot protect the protein against thermal denaturation. In this case, another method needs to be employed to study the interaction.

Acknowledgments

Research in Zhang laboratory was supported by Purdue University Provost's start-up to C. Zhang.

References

1. Wienken CJ, Baaske P, Rothbauer U, Braun D, Duhr S (2010) Protein-binding assays in biological liquids using microscale thermophoresis. *Nat Commun* 1:100
2. Molina DM, Jafari R, Ignatushchenko M, Seki T, Larsson EA, Dan C, Nordlund P (2013) Monitoring drug target engagement in cells and tissues using the cellular thermal shift assay. *Science* 341(6141):84–87
3. Lomenick B, Hao R, Jonai N, Chin RM, Aghajan M, Warburton S, Wohlschlegel JA (2009) Target identification using drug affinity responsive target stability (DARTS). *Proc Natl Acad Sci U S A* 106(51):21984–21989
4. Mayer M, Meyer B (1999) Characterization of ligand binding by saturation transfer difference NMR spectroscopy. *Angew Chem Int Ed* 38(12):1784–1788
5. Niesen FH, Berglund H, Vedadi M (2007) The use of differential scanning fluorimetry to detect ligand interactions that promote protein stability. *Nat Protoc* 2(9):2212
6. Vivoli M, Novak R, Littlechild JA, Harmer NJ (2014) Determination of protein-ligand interactions using differential scanning fluorimetry. *J Vis Exp* 91:e51809
7. Wu WI, Voegtli WC, Sturgis HL, Dizon FP, Vigers GP, Brandhuber BJ (2010) Crystal structure of human AKT1 with an allosteric inhibitor reveals a new mode of kinase inhibition. *PLoS One* 5(9):e12913
8. Athuluri-Divakar SK, Vasquez-Del Carpio R, Dutta K, Baker SJ, Cosenza SC, Basu I, Vogt PK (2016) A small molecule RAS-mimetic disrupts RAS association with effector proteins to block signaling. *Cell* 165(3):643–655
9. Dejonghe W, Sharma I, Denoo B, De Munck S, Lu Q, Mishev K, Savatin D (2019) Disruption of endocytosis through chemical inhibition of clathrin heavy chain function. *Nat Chem Biol* 15(6):641–649



Microscale Thermophoresis (MST) to Detect the Interaction Between Purified Protein and Small Molecule

Lei Huang and Chunhua Zhang

Abstract

Microscale thermophoresis (MST) is a biophysical assay to quantify the interaction between molecules, such as proteins and small molecules. In recent years, the MST assay has been used to detect protein–protein and protein–drug interactions. The assay detects the interaction between molecules by quantifying the thermophoretic movement of fluorescent molecules in response to a temperature gradient. In practice, the fluorescent molecule is mixed with different concentrations of the nonfluorescent ligand, and the mixture of molecules in solution is loaded to capillaries. A temperature gradient is applied to samples in the capillaries, and the movement of the fluorescent molecule in the temperature gradient is detected and recorded. The effect of different concentrations of the nonfluorescent ligand on the movement of the fluorescent molecule is quantified to test for the interaction between molecules. If the fluorescent molecule interacts with the ligand, the molecular properties of the molecules, such as charge, size, and hydration shell, will influence the molecular motility. MST has the advantages of being quantitative and robust. In this chapter, we will use Endosidin2 and its target protein *Arabidopsis thaliana* EXO70A1 (AtEXO70A1), as an example to show the procedure of using MST to test the interaction between a GFP-tagged protein and a small molecule.

Key words Microscale thermophoresis (MST), Endosidin2 (ES2), AtEXO70A1

1 Introduction

Bioactive small molecules allow transient manipulation of biological processes and serve as a useful tool to study cell activities. In recent years, small molecules have been identified to affect different steps of plant endomembrane trafficking pathways [1]. However, the endogenous target protein(s) for some of these molecules are still unknown, which limits our interpretation of observations obtained from using these small molecules. There are different assays available nowadays to test the interaction between small molecule and protein, such as drug affinity responsive target stability (DARTS), thermal shift assay, and isothermal calorimetry [2]. MST is a relatively new approach but has been widely used as a quantitative assay for target identification

[3, 4]. MST instrument uses an infrared laser objective to produce a temperature gradient in samples loaded in the capillaries and monitors the motility of the fluorescent molecule in capillaries in real time by exciting fluorophore and collecting emitted fluorescence over time. The thermophoretic properties of the fluorescence-labeled molecule are determined by charge, size, and hydration shell, and some of these properties would change once the molecule binds to the ligand. When using MST to test the interaction between a protein and a small molecule, the protein is often labeled with fluorescence by creating a green fluorescence fusion protein or through a covalent labeling by a fluorescence dye. The covalent labeling kit is available through the Nonotemper company that commercialized the technology. For proteins with aromatic residues, fluorescence labeling is not necessary and the inherent fluorescence can be used to detect protein motility. In this case, a label-free MST instrument is required to detect the interaction. Besides testing the interaction between a protein and a small molecule, MST has been used to analyze other biomolecular interactions, such as oligonucleotide interactions, protein–DNA interactions, protein–protein interactions, and protein–liposome interactions [3].

ES2 inhibits exocytosis by targeting the EXO70 subunit of the exocyst complex [5, 6]. ES2 has been used as a tool to understand the exocytosis process [1]. Here, we use ES2 and AtEXO70A1 as an example to show how to set up MST assay to identify the interaction between a small molecule and a candidate target protein. The manufacturer provides a detailed guideline for the experiment setup as well.

2 Materials

1. AtEXO70A1 expression construct.
2. LB medium (tryptone 10 g/L, yeast extract 5 g/L, and NaCl 10 g/L).
3. PCR tubes.
4. 1.5-mL microcentrifuge tubes
5. Dimethyl sulfoxide (DMSO) (*see Note 1*).
6. ES2 stock solution in DMSO (24 mM).
7. AKTA pure FPLC system (GE Healthcare, Pittsburgh, PA).
8. Nanodrop 2000.
9. Monolith NT.115 standard capillaries.
10. MST buffer (50 mM Tris–HCl, pH 7.5, 150 mM NaCl, 10 mM MgCl₂, 0.05% (v/v) Tween 20).
11. Monolith NT.115 system.
12. MO.Control and MO.Affinity Analysis software.

3 Methods

3.1 Purification of AtEXO70A1 Protein

Amplify AtEXO70A1 coding sequence using the primers AtEXO70A1-F: AAAACTGCAGATGGCTGTTGATAGCA-GAAT and AtEXO70A1-R: AAAAAGCGGCCGCTTACCGGCG TGGTTCATTCA and purify the product using a Gel DNA Recovery kit. Double digest the AtEXO70A1 fragment with PstI and NotI and at the same time double digest the modified pRSF-Duet-GFP vector with the same enzymes. Ligate the digested PCR product and the vector to obtain the pRSF-Duet-GFP-AtEXO70A1 construct. Verify the recombinant vector by sequencing the insert.

The procedures for protein expression and purification are as follows: Transform the verified pRSF-Duet-GFP-AtEXO70A1 construct into BL 21(DE3) competent cells; pick a single colony and inoculate 5 mL of LB liquid medium with kanamycin; and grow the culture at 37 °C overnight with shaking. Inoculate 2.5 mL of overnight culture to 1 L of LB medium with kanamycin and let the cells grow at 37 °C with shaking till OD₆₀₀ reaches 0.6. Allow the culture to cool down on ice and add isopropyl β-D-1-thiogalactopyranoside (IPTG) to a final concentration of 0.05 mM. Allow the cells to grow at 16 °C with shaking overnight. Collect the cells by centrifugation at 4000 × *g* for 15 min at 4 °C and purify the fusion protein using Ni-NTA column; remove the His6-SUMO tag using ULP1 (*see Notes 2 and 3*).

3.2 Pretests for Protein Quality, Fluorescence Intensity, and Possible Ligand-Induced Effects

The purpose of the pretests is to make sure the protein has sufficient fluorescence to allow the instrument to detect the motility and has an expected single-peak spectrum. The pretests also allow the detection of any possible fluorescence from the ligand.

1. For protein quality evaluation, mix 10 μL of 100 nM GFP-AtEXO70A1 protein with an equal volume of MST buffer in a PCR tube, allow the mixture to enter the Monolith NT.115 standard capillaries, and put the capillaries in positions 1 and 2 of the sample tray in the MST device. Set up the laser level and detection time through the software and get the measurement of the fluorescence profile. The protein can be used for the next step only when the scanned samples show a smooth curve with a single peak (*see Note 4*) and normal MST traces (*see Note 5*) (Fig. 1).
2. For the ligand-induced effect test, add 1 μL of ES2 to 9 μL of MST buffer and mix well by pipetting. Then add 10 μL of MST buffer. The test procedure is the same as the protein quality evaluation. The ligand produced autofluorescence should be less than 10% of average fluorescence from the protein (*see Note 6*).

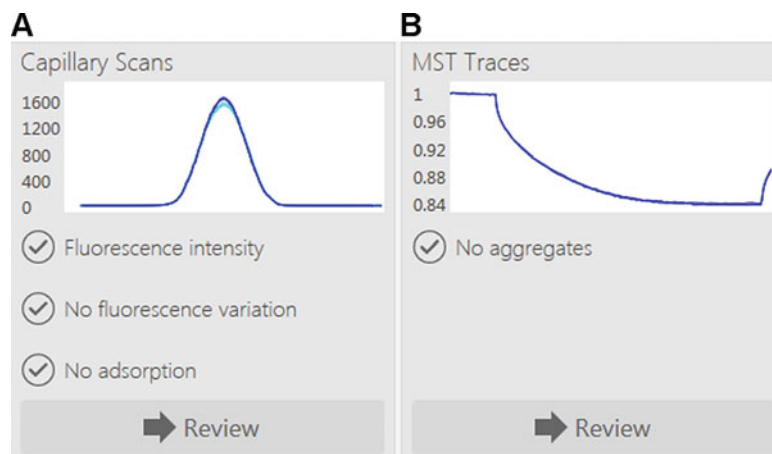


Fig. 1 Prescanning of GFP-AtEXO70A1 in capillaries to check protein quality. GFP-AtEXO70A1 protein shows normal capillary fluorescence shape (a) and normal MST traces (b)

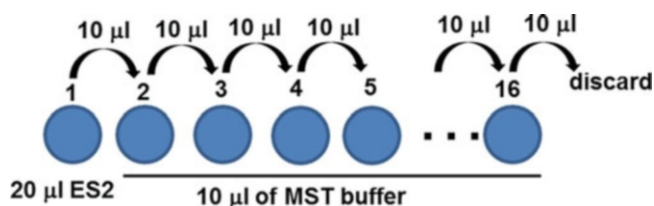


Fig. 2 Preparation of ES2 series dilution solutions. 10 μL of ES2 from tube 1 was transferred to tube 2; mix well and further transfer to tube 3 and so on. After mixing the ligand in tube 16, get rid of the 10 μL leftover solution. All of the 16 tubes have equal volume and the same amount of DMSO solvent

3.3 Binding Affinity Test

After pretests, titrate GFP-AtEXO70A1 protein with ES2. It is important to keep the same concentration of the solvent in different reactions through the serial dilution. An example for the serial dilution is shown in Fig. 2. Before setting up the reaction, make sure to set up the software for desired laser power.

1. Prepare 25 μL of $2 \times$ ES2 solution by adding 2.5 μL of ES2 stock and 22.5 μL of MST buffer into a PCR tube and mix well.
2. Add 18 μL of DMSO and 162 μL of MST buffer into a 1.5-mL microcentrifuge tube and mix well.
3. Add 10 μL of mixed MST buffer into PCR tubes 2–16.
4. Add 20 μL of prepared $2 \times$ ES2 into PCR tube 1.
5. Transfer 10 μL of $2 \times$ ES2 from PCR tube 1 to PCR tube 2 with a pipette and mix well by pipetting up and down several times; transfer 10 μL of diluted ES2 from PCR tube 2 to PCR tube 3 and mix. Repeat the procedure for PCR tubes 4–16. Discard the leftover 10 μL after adding to PCR tube 16 (Fig. 2).

6. Add 10 μL of 100 nM GFP-AtEXO70A1 protein into each PCR tube and mix well by pipetting.
7. Put a Monolith NT.115 standard capillary into each PCR tube and allow the solution to enter the capillary.
8. Put the capillaries in positions 1 to 16 in the sample tray of the MST device and start the program (*see Note 7*).
9. After running the samples, check the fluorescence intensity from the capillaries scan window. For different capillaries, the fluorescence intensities among different capillaries need to be as equal as possible and the variations of $\pm 10\%$ of overall fluorescence can be tolerated. Variations higher than 10% of the overall fluorescence are considered as outliers and should not be used for further analysis. Sometimes, there are huge variations among several tubes, and this might be caused by protein aggregates (*see Note 8*).

3.4 Data Analysis

The binding affinity test can be repeated independently at least three times, and the results could be combined and analyzed using Mo. Affinity Analysis software (Fig. 3). The software could provide K_D value, K_D confidence, response amplitude, and signal to noise value (*see Note 9*).

4 Notes

1. If DMSO or DMF is used as a solvent to dissolve ligand, the final concentration of the solvent needs to be considered. High concentrations of the solvent cause a negative effect on protein stability, and the concentration should be less than 5%.
2. We are not putting a lot of details about the protein purification procedure because this step will vary depending on the protein and the affinity tag that is used for protein purification. The goal is to obtain high purity protein without an affinity tag.
3. The protein labeled with fluorophore could also be used for the MST assay by the protein labeling kit provided by NanoTemper Technologies. For more detailed information, see the manual of Monolith Protein Labeling Kit.
4. The maximum fluorescence intensity is about 2400 counts, and the optimal intensity is between 200 and 1500 counts. If at first the protein intensity exceeds 2400, one needs to decrease the protein concentration until the fluorescence intensity reaches the range of required. Sometimes, the hydrophobic residues of protein could attach to the capillary surface and cause unspecific adsorption, which will reflect on the irregular capillary scan shape. Adding detergent or BSA may help to reduce the effect of protein adsorption to capillary.

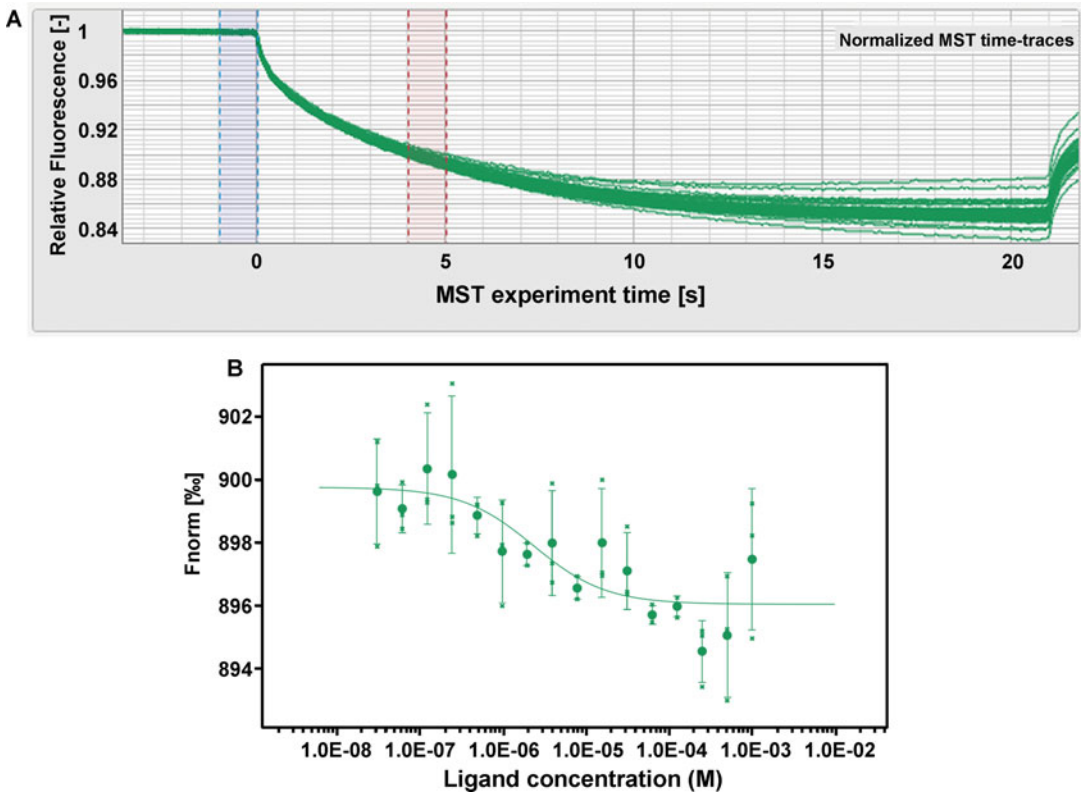


Fig. 3 ES2 interacts with AtEXO70A1. The binding curve from the MST experiment shows the interaction between ES2 and AtEXO70A1. (a) The relative fluorescence chart indicates the fluorescence change of mixed ES2 and AtEXO70A1 samples at different time points. (b) The MST dose–response curve shows the interaction between ES2 and AtEXO70A1

5. Protein aggregation causes irregular MST traces and fluctuation of fluorescence intensity that does not reflect the real motility of the protein. Centrifuge the protein at $16,000\text{--}20,000 \times g$ for 5 min to get rid of the aggregated protein. Adding detergents such as 0.05% Tween 20 could solve the problem in some cases.
6. In the case when ligand autofluorescence exceeds 10% of the average target fluorescence, ligand could be used as the target instead of the fluorescence protein. In this case, titrate the unlabeled protein instead.
7. Do not discard the remaining mixed samples in case you need to re-run the samples.
8. In such a case, centrifugation of the protein, to get rid of aggregates in the pellet, adding detergents such as 0.05% Tween 20 may help. Sometimes, when ligand and protein mix together, the protein fluorescence decreases dramatically. In such a case, the SDS denatured test needs to be done, which

could distinguish fluorescence changes caused by an interaction between ligand and protein or by nonspecific effects. For more detailed information, see the MST operation manual.

9. The signal to noise is an indicator of the quality of binding data, and it is equal to response amplitude divided by the noise. A signal to noise of more than 5 is desirable. Since the Monolith system is quite sensitive to the motility of fluorescence protein, it is necessary to use different ligands and proteins as negative controls to exclude the false-positive interaction between the ligand and tested protein, and also other ligand-protein binding test assays such as DARTS and thermal shift assay could be used to verify the binding conclusion obtained from MST assay.

Acknowledgments

This work was supported by Purdue University Provost start-up fund to C.Z.

References

1. Huang L, Li X, Zhang C (2019) Progress in using chemical biology as a tool to uncover novel regulators of plant endomembrane trafficking. *Curr Opin Plant Biol* 52:106–113
2. Futamura Y, Muroi M, Osada H (2013) Target identification of small molecules based on chemical biology approaches. *Mol Biosyst* 9 (5):897–914
3. Jerabek-Willemsen M, André T, Wanner R, Roth HM, Duhr S, Baaske P, Breitsprecher D (2014) MicroScale thermophoresis: interaction analysis and beyond. *J Mol Struct* 1077:101–113
4. Entzian C, Schubert T (2016) Studying small molecule–aptamer interactions using MicroScale thermophoresis (MST). *Methods* 97:27–34
5. Zhang C, Brown MQ, van de Ven W, Zhing Z-M, Wu B, Young MC, Synek L, Borchardt D, Harrison R, Pan S, Luo N, Huang Y-MM, Ghang Y-J, Ung N, Li R, Isley J, Morikis D, Song J, Guo W, Hooley R, Chang C-E, Yang Z, Zarsky V, Muday G, Hicks GR, Raikhel NV (2016) Endosidin2 targets conserved exocyst complex subunit EXO70 to inhibit exocytosis. *Proc Natl Acad Sci U S A* 113(1):E41–E50
6. Huang L, Li X, Li Y, Yin X, Li Y, Wu B, Mo H, Liao C-J, Mengiste T, Guo W, Dai M, Zhang C (2019) Endosidin2-14 targets the exocyst complex in plants and fungal pathogens to inhibit exocytosis. *Plant Physiol* 180(3):1756–1770

INDEX

A

- Abscisic acid (ABA)..... 4, 62, 99–110,
113–119
Agonists 62, 99–110
Arabidopsis thaliana 4, 13, 18, 25,
51, 61, 62, 64, 67, 114, 117, 133
Arabidopsis thaliana EXO70A1
(AtEXO70A1) 177–181,
188, 189
Auxin biosynthesis 131–143

C

- Chemical genetic screens 29–36, 90
Chemical genetics 4, 15, 29–32, 131
Chemical genomics 61–70, 113,
132, 163
Chemical proteomics 147–160
Chemotherapeutics 49, 50, 54
Cryptochromes 17–26
Curcumin 147–160
Cytokinins 124, 126–129
Cytoskeleton 50–54, 132

D

- Differential scanning fluorimetry
(DSF) 177, 183, 184
Drought 69, 99–101,
114, 115
Drug affinity responsive target stability
(DARTS) 175–181, 183,
187, 193

E

- Endomembranes 4, 49, 50, 52–54,
175, 187
Endosidin2 (ES2) 177, 179, 180, 181,
188–190, 192
Ethylene biosynthesis 123–128
Eto3 124, 126–128

F

- Fatty acid amide hydrolase (FAAH) 4

G

- Growth inhibition 50, 132, 141, 181

H

- High-throughput 18, 29, 31, 96, 99–110,
113, 115, 164, 167, 183

I

- Image processing 22, 74, 83
Immunodetection 170
In vitro inhibitory test 42

L

- Ligand binding 72, 100, 164,
183, 184
Ligands 62, 72, 164, 170, 176,
183–185, 188, 189, 191–193
Lipids 3, 15
Luciferase 113–119

M

- MAPKKK18 115, 116
Mass spectrometry (MS) 5, 6, 8, 10,
12, 18, 19, 31, 34–36, 52, 65, 90, 115–117,
126–128, 134, 137, 140–142, 147, 148, 151,
152, 156–158, 165, 167–169, 172, 176, 177
Microscale thermophoresis (MST) 177, 183,
187–193

N

- N-acylethanolamines (NAEs) 3, 4
N-lauroylethanolamide (NAE) 3–6, 8–10, 12

P

- Phenotypic screen 17–27, 113
Photomorphogenesis 18
Photoreceptor 62
Plants 3–15, 18, 20, 21, 23, 26,
31, 32, 35, 36, 39–47, 49–57, 61–63, 67–84,
89–91, 99, 100, 114, 115, 117, 123, 127,
131–133, 139, 140, 163, 164, 167, 172,
175–177, 181, 187

Protein phosphatases 2C (PP2Cs)	100	Small molecule libraries	29, 31, 34
Protocols	31, 32, 35, 40, 46, 66, 90, 142, 148, 164, 167, 185	Small molecules	29, 31, 34, 35, 39, 49, 50, 61, 72, 113–115, 147, 148, 163–165, 167, 169–173, 175–182, 184, 185, 187–193
Purified proteins	104, 167, 175–181, 183–193	Suppressor screen	126
Q			
QPCR instrument	183–185	T	
R			
<i>Ralstonia solanacearum</i>	39, 40, 42, 44–46	Target identification	24, 148, 158, 163–173, 176, 187
Random DNA sequences	62	Target proteins	17, 18, 148, 152, 153, 156, 163, 164, 169, 170, 173, 176, 177, 183–185, 187, 188
Random peptides	69	Transgenic plants	50–52, 117
Reporters	31, 40, 42, 50, 113–119, 157, 159, 163	Type 3 secretion system (T3SS)	39, 40, 42, 46
S			
Screenings	4, 5, 13–15, 17–26, 29, 31–32, 35, 42, 49–57, 63, 68, 69, 89–110, 113, 114, 117, 120, 123–129, 176		